c.1

CARBANION REACTIONS OF METHYLPHOSPHAZENES AND METAL COMPLEXES OF 1-PYRAZOLYLPHOSPHAZENES

by

KEITH DONALD GALLICANO

B.Sc. (Majors), University of British Columbia, 1976

A THESIS SUBMITTED IN PARTIAL FULFILLMENT OF

THE REQUIREMENTS FOR THE DEGREE OF

DOCTOR OF PHILOSOPHY

in the Department of

Chemistry

We accept this thesis as conforming to the

required standard

THE UNIVERSITY OF BRITISH COLUMBIA

December, 1980

In presenting this thesis in partial fulfilment of the requirements for an advanced degree at the University of British Columbia, I agree that the Library shall make it freely available for reference and study. I further agree that permission for extensive copying of this thesis for scholarly purposes may be granted by the Head of my Department or by his representatives. It is understood that copying or publication of this thesis for financial gain shall not be allowed without my written permission.

Department of Chemistry

The University of British Columbia
2075 Wesbrook Place
Vancouver, Canada
V6T 1W5

Date January 5 1981

ABSTRACT

The reaction of Me_2PCl_3 with the linear phosphazene $[NH_2(Ph_2)PNP(Ph_2)NH_2]^+Cl^-$ in chlorobenzene gives not only the expected cyclic product gem-$N_3P_3Ph_4Me_2$, but also significant amounts of $(NPPh_2)_4$, $(NPMe_2)_4$ and the new mixed derivative 1,1,3,3-tetramethyl-5,5,7,7-tetraphenylcyclotetraphosphazene $N_4P_4Me_4Ph_4$. The methylphosphazenes, gem-$N_3P_3Ph_4Me_2$ and $N_4P_4Me_8$, along with $N_3P_3Me_6$, can be deprotonated by alkyllithiums. The resulting carbanions, gem-$N_3P_3Ph_4Me(CH_2^-)$, $N_4P_4Me_4(CH_2^-)_4$ and $N_3P_3Me_3(CH_2^-)_3$ respectively, react with monofunctional electrophiles to form phosphazenes carrying the groups PCH_2R (R = Br, I, PhC(O), and $AsMe_2$). Two phosphazenyl groups have also been joined by the use of a difunctional halide Me_2SiCl_2, yielding the bridged compound $(N_3P_3Ph_4MeCH_2)_2SiMe_2$.

The reaction of the tetracarbanion $N_4P_4Me_4(CH_2^-)_4$ with ethyl benzoate is unique, in that it goes no further than di-substitution. Moreover, the ^1H and ^{31}P n.m.r. spectra of the dibenzoyl derivative indicate vicinal substitution, and depend on both solvent and time. By contrast, a tribenzoyl derivative is formed from the tricarbanion $N_3P_3Me_3(CH_2^-)_3$. These results are explained by the aid of simple Hückel molecular orbital theory, and are informative about conjugation.

The preparation of phosphazenes in which the ring is joined to a pyrazole nucleus by a P-N bond has also been undertaken. The chemical, spectroscopic and structural properties of the homogeneously substituted pyrazolylphosphazenes $[NP(Pz)_2]_{3-6}$, $[NP(Mepz)_2]_{3-5}$ and $[NP(Me_2pz)_2]_{3,4}$ (where Pz denotes the 1-pyrazolyl group, Mepz the 3-methyl-1-pyrazolyl group and Me_2pz the 3,5-dimethyl-1-pyrazolyl group) show that the pyrazolyl groups

act as strongly electron withdrawing substituents on the phosphazene ring, with at most a minor conjugative contribution to the bonding.

These pyrazolylphosphazenes have an added feature, in that the pyridine-type nitrogen in the pyrazole ring is expected to be basic. Thus, their ability to act as donors to transition metal ions, either via the nitrogen atoms in the pyrazole ring or in the phosphazene ring, is an important part of their chemistry. Consequently, the formation of complexes with Mo(0), Co(II), Pd(II), Pt(II), Ag(I), Zn(II) and Cd(II) has been investigated using as ligands $N_3P_3(Me_2pz)_6$, gem-$N_3P_3Ph_2(Me_2pz)_4$ and gem-$N_3P_3Ph_4$-$(Me_xpz)_2$ (x = 1, 2).

Reaction of $N_3P_3(Me_2pz)_6$ with an excess of anhydrous $CoCl_2$ in THF precipitates the di-cobalt complex $N_3P_3(Me_2pz)_6 \cdot 2CoCl_2 \cdot THF$, the crystal structure of which shows the cobalt atoms to be situated in different coordination geometries: tetrahedral and trigonal bipyramidal. The latter configuration involves two Me_2pz groups each on different phosphorus atoms and a nitrogen atom in the phosphazene ring, and is also found in the structure of gem-$N_3P_3Ph_2(Me_2pz)_4 \cdot ZnCl_2$. The former configuration incorporates two Me_2pz groups on the same phosphorus atom, similar to that found in the structure of gem-$N_3P_3Ph_4(Me_2pz)_2 \cdot CoCl_2$. As a comparison, the reaction of $N_3P_3(Me_2pz)_6$ with an excess of $PdCl_2(PhCN)_2$ in CH_2Cl_2 gives the tri-palladium complex $N_3P_3(Me_2pz)_6 \cdot 3PdCl_2$, the ^1H and ^{31}P n.m.r. spectra of which indicate that only bonding to Me_2pz groups on the same phosphorus atom is present.

TABLE OF CONTENTS

LIST OF TABLES

LIST OF FIGURES

LIST OF ABBREVIATIONS, SYMBOLS AND COMMON NAMES

Å	Angstrom
Anal. calcd. .	analysis calculated
br	broad
B.M.	Bohr Magneton
Bu	butyl
ca.	circa
cf	compare
cm^{-1}	wave numbers in reciprocal centimeters
dec	decompose
Et	ethyl
Et_2O	diethyl ether
eq.	equivalent(s)
ev	electron volts
gem	geminal
HMO	Hückel molecular orbital
Hz	Hertz, cycles per second
J	magnetic resonance coupling constant
L(A-B)	length of bond A-B
M	molecular ion in mass spectrometry, metal or moles/liter
Me	methyl
MepzH	3-methylpyrazole
Me_2pzH	3,5-dimethylpyrazole
mg	milligrams
ml	milliliter

mmol	millimole	π	pi
M.pt.	melting point	<	less than
$\hat{N}$	angle at atom N	>	greater than
nm	nanometers		
n.m.r.	nuclear magnetic resonance		
Ph	phenyl		
PN ring	phosphazene ring		
Pr^i	isopropyl		
pzH	pyrazole		
sh	shoulder		
sp	sharp		
T or temp	temperature		
TBP	trigonal bipyramidal		
THF	tetrahydrofuran		
tip	temperature independent paramagnetism		
tlc	thin layer chromatography		
X_m	molar magnetic susceptibility		
xs	excess		
α	Coulomb integral		
β	resonance integral or nephelauxetic ratio		
ϵ	molar extinction coefficient		
Λ_M	molar conductance		
μ	magnetic moment		
ν	wavenumber		
σ	sigma		
δ	n.m.r. chemical shift		

ACKNOWLEDGEMENTS

I would like to express my appreciation to my supervisor, Professor N.L. Paddock, for his support, advice and patience during the course of my graduate studies. His many enlightening discussions and optimistic approach have been a constant source of encouragement.

I am indebted to Drs. R.T. Oakley, T.N. Ranganathan and R.D. Sharma for their helpful suggestions and technical assistance. A special thanks goes to Dr. S. Rettig for his excellent crystallographic work, on which many of the ideas developed in this thesis are based. I also wish to thank Mrs. J. Pulley for her skill and perseverance in the typing of this thesis, Mr. P. Borda for the microanalyses, and the technical staff of the Chemistry Department for their efforts on my behalf.

Finally, I would like to thank my family and friends for their interest and curiosity in room 455.

CHAPTER 1

GENERAL INTRODUCTION

Of the many inorganic systems known today, only the phosphazenes, characterized by the unsaturated repeating unit $(-N=PX_2-)_n$, have been studied intensively over a large range of ring sizes and ligand types; and as such are an important class of compounds for studying the bonding properties of pentavalent phosphorus. Mixed substitution is also possible, where X can be a halogen or a wide variety of organic groups such as amino, alkoxy, aryloxy, alkyl and aryl. Some of these compounds (I-III) are illustrated below.

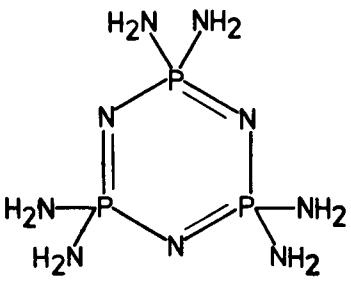

I

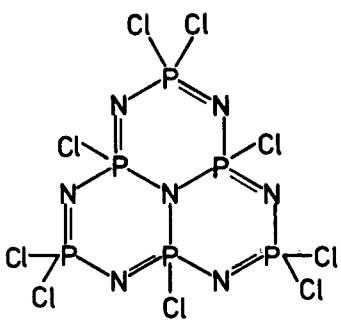

II

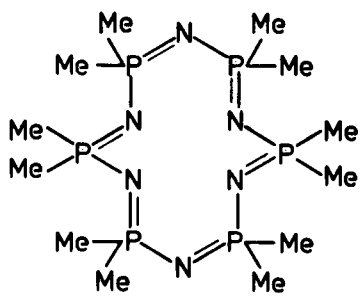

III

The most important phosphazene compounds are the chlorophosphazenes $(NPCl_2)_n$. They are the precursors of many phosphazene derivatives and are the building blocks for phosphazenes of large ring size ($n > 4$). Although replacement of the chlorines by nucleophiles is a vital part of their chemistry, basic nucleophilic substitution reactions in phosphoryl chemistry $R_2(Cl)P=O$, applied to chlorophosphazenes, sometimes proceed with difficulty,

or not at all. They are generally slower on account of the greater steric bulk of phosphazenes and the lower electronegativity of nitrogen compared to oxygen; and are more prone to by-products because of the multiple functionality, both phosphorus and nitrogen being capable of participating. For example, the chlorophosphazenes are less susceptible to hydrolysis than phosphoryl chlorides; the trimeric chloride can even be distilled in steam[1]. A part of this thesis is concerned with the effect of substituents, more precisely the pyrazole group, on the physical and chemical properties of the phosphazene ring, a trend that has been the subject of much research in phosphazene chemistry.

The reactions of the substituents themselves, however, have been little studied, and are the main theme of this work. More specifically, this thesis deals with two topics, the preparation and chemistry of 1-pyrazolylphosphazenes and the carbanion reactions of methylphosphazenes. The ligands attached to phosphorus can be divided into two groups: those whose properties can be significantly influenced by conjugation to the phosphazene ring, such as amino and alkoxy groups, and those which do not donate electron density by resonance to the ring, such as halogeno or methyl ligands. Both pyrazole and CH_2^- ligands fall into the former class, but only for carbanions is conjugation to the phosphazene ring expected to be substantial. Thus, the particular properties of the phosphazenyl carbanions are mainly a result of the acceptor properties of the phosphazene ring and the presence in it of a delocalized π- system. On the other hand, any involvement of the phosphazene ring in the chemistry of the pyrazole ligand is expected to be related only to steric or electrostatic factors.

The purpose of this chapter is to give a brief summary of the

background chemistry of phosphazenes, in particular their methods of preparation and donor and acceptor properties, and to introduce some of the chemistry of phosphoryl and pyrazolyl compounds, to which the derivatives made in this work are related.

1.1 Preparation of Phosphazenes

1.1.1 Historical Background

The birth of phosphazene chemistry, in 1834, commenced with the isolation of $(NPCl_2)_3$ from the interaction of phosphorus pentachloride with ammonia[2]. However, a cyclic structure was suggested only after Stokes, in 1895, had prepared and characterized the chlorophosphazenes $(NPCl_2)_{3-7}$. In 1924, Schenck and Römer[3] developed a much improved direct synthetic (ring closure) route to chlorophosphazenes according to Equation 1.1. The first direct synthesis of several organophosphazenes $(NPR_2)_n$

$$nPCl_5 + nNH_4Cl \xrightarrow[120°C]{\text{Solvent}} (NPCl_2)_n + 4nHCl \qquad \ldots (1.1)$$

was not described until around 1960[4-8].

A large number of cyclic phosphazenes have been mentioned in the literature, of which some are prepared by substitution reactions performed on suitable precursors. Since the mid-1950's there has been a tremendous amount of research employed on the substitution reactions of halophosphazenes, usually of the chlorophosphazenes. Fluorination, alcoholysis, phenolysis and in particular aminolysis have all been studied in considerable detail. The two major synthetic routes, direct synthesis and substitution, are both used in this work, and will be discussed in greater detail below.

1.1.2 Direct Methods

Many direct synthetic routes to cyclic phosphazenes have been described in the literature (for a good review see reference 9), the most extensively studied being the ammonolysis of halogeno derivatives of pentavalent phosphorus according to Equation 1.2. The reaction is

$$X_2PCl_3 + NH_4Cl \longrightarrow \frac{1}{n}(NPX_2)_n + 4HCl \quad \ldots (1.2)$$

usually carried out in either tetrachloroethane, chlorobenzene or other suitably inert solvents. The chlorophosphazenes $(NPCl_2)_n$ are prepared according to Equation 1.1 above, but the simple equation is deceptive. Initially the linear derivatives $PCl_4(NPCl_2)_nCl$ and $H(NPCl_2)_nCl$ are formed followed by cyclisation. Both types of linear derivatives have been isolated[10,11]. Furthermore, alkyl [$(NPMe_2)_n$[4] and $(NPEt_2)_n$[5]] and aryl [$(NPPh_2)_n$[6,7] and [$(NP(Ph)Cl)_n$[8]] derivatives can be prepared in a similar fashion. Cyclisation of linear alkylphosphazenes requires either heat[5] or the use of a tertiary amine[4].

In order to develop and extend the carbanion chemistry of methylphosphazenes, efficient methods for the preparation of $(NPMe_2)_{3,4}$ and gem-$N_3P_3Ph_4Me_2$ were required. An improved synthesis of $(NPMe_2)_{3,4}$ has already been developed in our laboratory by using chlorobenzene as the solvent in Equation 1.2. Furthermore, the relative yields of trimer to tetramer can be increased if $MeNH_2 \cdot HCl$ is substituted for NH_4Cl[12], the separation of the two compounds being aided by the solubility of the salts $(NPMe_2)_3 \cdot RCl$ (R=Me or H) in acetonitrile. Phosphazenes of the type gem-$N_3P_3Ph_4X_2$ are usually formed by the interaction of Bezman's

reagent $[NH_2P(Ph_2)NP(Ph_2)NH_2]^+ Cl^-$ with X_2PCl_3 [13-15] (Equation 1.3), but

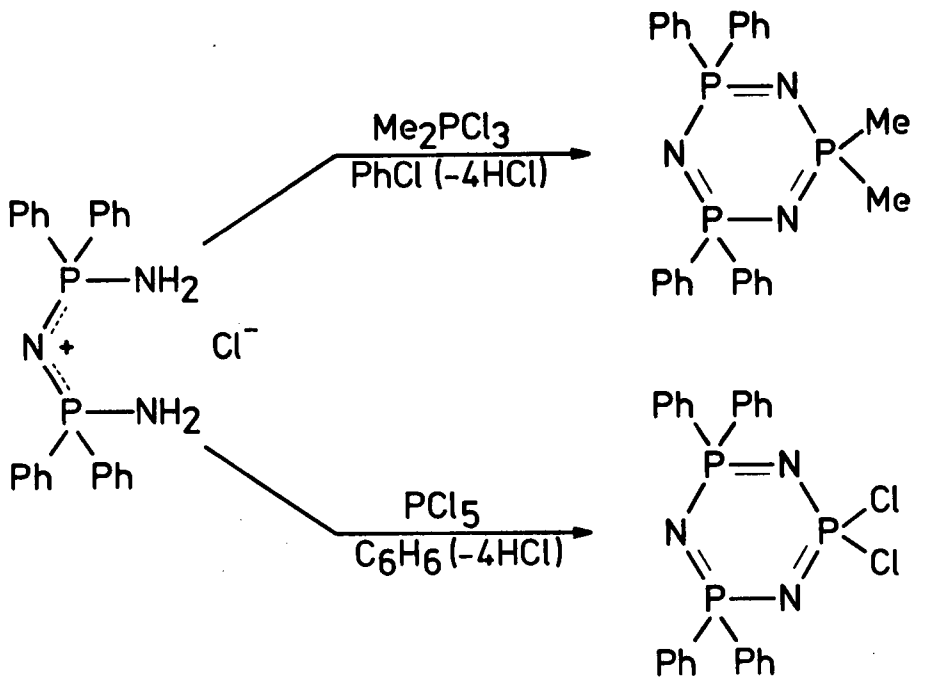

... (1.3)

the yields of the methyl derivative[13] are low and side reactions are dominant. However, the method has recently afforded gem-$N_3P_3Ph_4Me_2$ in relatively good yield in addition to other phosphazene compounds[16]. A full description of the reaction is given in the following chapter.

1.1.3 Substitution Reactions

Nucleophilic substitution reactions in phosphazene chemistry provide an alternative to the ring closure methods for the smaller cyclic polymers, trimer and tetramer, but are the only means possible for preparing phosphazenes of large ring size. This is because only the ammonolysis of PCl_5 produces significant amounts of the higher cyclic

polymers. Thus, ligand substitution of a corresponding chlorophosphazene is the basis for the synthesis of other large ring sizes, from pentamer upwards.

The range and versatility of substitution reactions is discussed below with emphasis only on the compounds related to this work.

1.1.3A Fluorophosphazenes

Ammonolysis of PCl_5 by NH_4F produces mainly ammonium hexafluorophosphate together with small amounts of mixed chlorofluorophosphazenes[17]. The completely fluorinated phosphazenes have only been prepared by fluorination of the corresponding chloride or bromide. Various fluorinating agents such as potassium fluorosulphite[18,19], lead difluoride[20], silver monofluoride[20], sodium fluoride[21] and antimony trifluoride[22] have all been used to prepare partially or fully fluorinated derivatives.

The preparation of the trimeric and tetrameric fluorides $(NPF_2)_{3,4}$ from the corresponding chlorides was first reported by Seel and Langer[18], in which KSO_2F was used as the fluorinating agent (Equation 1.4). Also the reaction appears to be independent of ring size, since the fluorophosphazenes $(NPF_2)_{3-20}$ have all been prepared by this method.

$$(NPCl_2)_n + 2nKSO_2F \longrightarrow (NPF_2)_n + 2nKCl + 2nSO_2 \quad \ldots (1.4)$$

1.1.3B Amino Derivatives

Primary or secondary amines react with halophosphazenes to eliminate hydrogen halide and form an amino substituted phosphazene,

the largest single class of phosphazene derivatives (Reference 9 p.175) (Equation 1.5). Usually an excess of the amine, or triethylamine if the

$$(NPX_2)_n + 4nR_2NH \xrightarrow[(X=Br,F,Cl)]{} [NP(NR_2)_2]_n + 2nR_2NH\cdot HX \qquad \ldots (1.5)$$

nucleophile is a weak base, serves as the hydrohalide acceptor. In this manner, cyclic amino derivatives such as $[NP(N\langle\rangle)_2]_3$[23] and $[NP(N\langle\rangle)_2]_3$[24] have been prepared. Furthermore, the preparation of the dimethylamino-phosphazenes $[NP(NMe_2)_2]_n$ by this method appears to be independent of ring size, for they are known from n=3-9. This preparative technique can also be modified by the use of an alkali metal salt of the amine. For example, the potassium salt of pyrrole reacts with either $(NPCl_2)_3$ or $(NPCl_2)_4$ in benzene to replace all the chlorine atoms[25] (Equation 1.6), but the authenticity of the compound is uncertain. Trialkylsilyl- and trialkyl-stannylamines have also been employed as reactive aminating agents, but

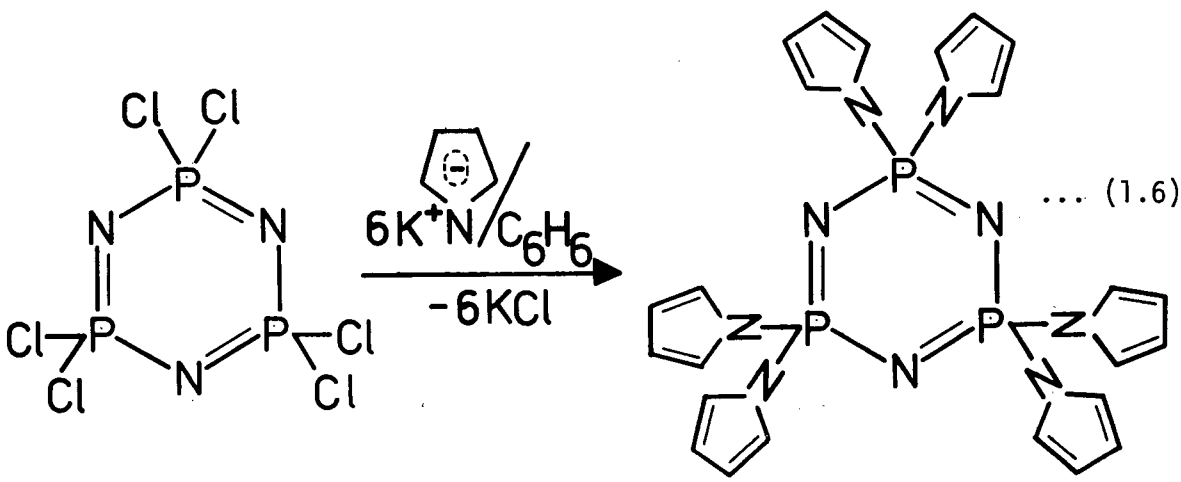

... (1.6)

their use has been mainly confined to the synthesis of partially substituted phosphazenes[26] (Equation 1.7).

$$(NPF_2)_3 + Me_3MNMe_2 \xrightarrow[(M=Si,Sn)]{} N_3P_3F_5(NMe_2) + Me_3MF \quad \ldots (1.7)$$

1.1.3C Aryl and Alkyl Derivatives

Phosphazenes containing carbon-based ligands joined by a P-C bond can be synthesized either by a Friedel and Crafts reaction, or by the reaction of organometallic compounds with halophosphazenes.

The Friedel and Crafts reaction, using $AlCl_3$ as a catalyst, has been used to prepare partially phenylated derivatives (Equation 1.8),

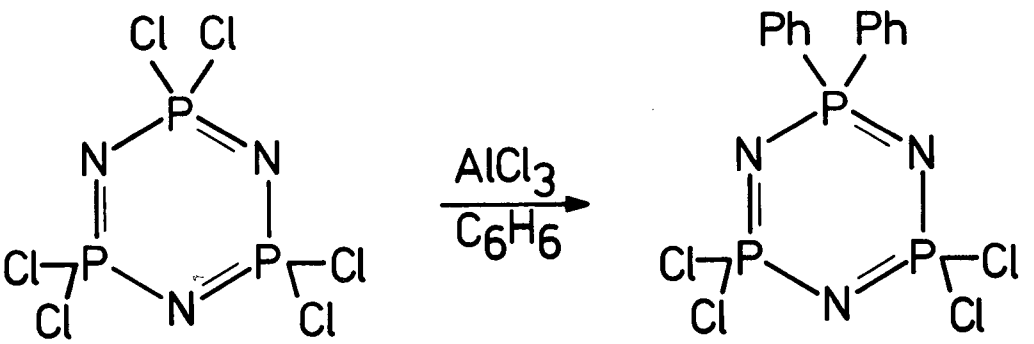

... (1.8)

but the introduction of more than two phenyl groups requires drastic reaction conditions[27]. A more advantageous route involves the use of organometallic reagents, such as organolithium (Equation 1.9) or Grignard reagents (Equation 1.10).

Unfortunately chlorophosphazenes are unsuited for reactions with these reagents. Organolithium compounds, such as phenyl lithium (PhLi)[28] or methyl lithium (MeLi)[29], decompose the products rather than

$$(NPX_2)_n + 2nRLi \longrightarrow (NPR_2)_n + 2nLiX \quad \ldots (1.9)$$

$$(NPX_2)_n + 2nRMgX \longrightarrow (NPR_2)_n + 2nMgX_2 \quad \ldots (1.10)$$

(X=halogen, R=aryl or alkyl)

form organophosphazenes, and Grignard reagents, such as phenylmagnesium bromide (PhMgBr)[30] and methylmagnesium bromide (MeMgBr)[31], yield predominantly open-chain phosphazenes via addition of the nucleophile across the PN bond followed immediately by ring cleavage (IV) and halogen replacement (V). Nonetheless, approximately 5% of the fully phenylated

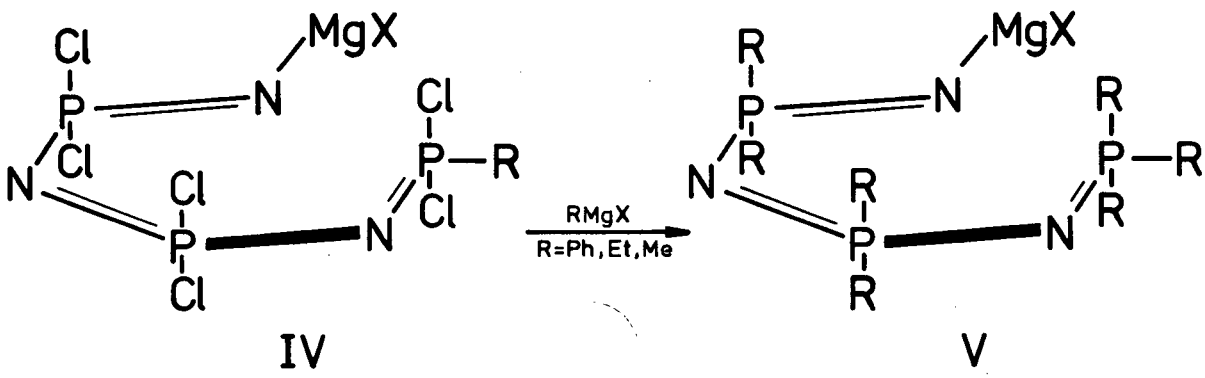

IV V

phosphazene $(NPPh_2)_3$ has been isolated.

However, substitution is favored over addition when chlorophosphazenes are replaced by fluorophosphazenes, probably because the more electronegative fluorine groups strengthen the PN ring system. In this way, good yields of the phenylphosphazenes $(NPPh_2)_{4-6}$[32] and methylphosphazenes $(NPMe_2)_{4,5}$[33] have been achieved by the interaction of PhLi and MeLi, respectively, with the appropriate fluoride. Methylation of $(NPF_2)_{6-12}$ using MeMgBr has afforded $(NPMe_2)_{6-10}$[34], and more recently $(NPMe_2)_{11,12}$[35]. However, the completely substituted trimer $(NPMe_2)_3$ has not been isolated by the substitution method, but is most easily prepared, in addition to small quantities of $(NPMe_2)_4$, by the

ammonolysis of Me_2PCl_3, using $MeNH_2 \cdot HCl$ instead of NH_4Cl.

1.2 Bonding in Phosphazenes

1.2.1 Endocyclic π-Bonding

In addition to the basic σ-framework, using sp^3 hybridization at phosphorus and sp^2 hybridization at nitrogen, there is the formal necessity for the existence of π-bonding in phosphazenes. The first reasonable theories of π-bonding were reported between 1958 and 1961[36-38]. These theories invoked the existence of dπ-pπ bonding between a singly occupied $2p_z$ orbital on nitrogen and a 3d-orbital on phosphorus. Later, it was found that certain properties (such as base strength[39-41]) were dependent on ring size, and thus the π-bonding theory was completed by the inclusion of a second π-system, utilizing the lone pair of electrons on nitrogen for donation into empty 3d-orbitals on phosphorus.

The occurrence of the double π-system is strongly supported by structural evidence: 1) the PN bond lengths in homogeneously substituted phosphazenes are usually equal in length even when ring puckering exists. This contrasts sharply to pπ-pπ systems, such as cyclooctatetraene, where ring puckering produces alternating long and short bonds. 2) The PN bond lengths vary from 1.50-1.60 Å, considerably shorter than the value of 1.77 Å found in the phosphoramidate ion (VI)[42], in which π-bonding is absent; and slightly shorter than the value of 1.68 Å found in tetrametaphosphimate (VII)[43], in which only two electrons contribute to the π-bonding. Additional experimental evidence comes from the structure of $[N_4P_4Me_9]^+[Cr(CO)_5I]^-$. Quaternization causes substantial redistribution of π-electron density within the

ring, resulting in changes in bond lengths which are large enough to be measured. If localization is complete, simple Hückel molecular orbital calculations predict that the lengths of the ring bonds to the quaternized nitrogen should correspond to a single π-component, the second bonds should be the shortest, and the third bonds should be intermediate between the first two; and indeed this is what is found (VIII)[44]. As a comparison, protonation of methylpyridines shows no

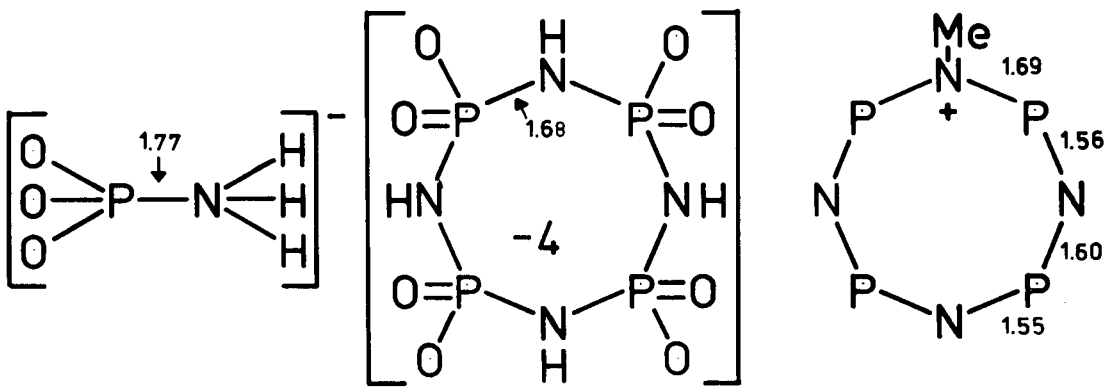

VI VII VIII

significant change in the bond distances connecting the ring atoms[45], consistent with the fact that the lone pair of electrons on nitrogen is not formally involved in the π-system.

Although σ- and π- interactions cannot be completely separated by symmetry, the following approximate description is useful. There are two types of delocalization possible. In one of the π-systems the participating orbitals are antisymmetric with respect to reflection in the local molecular plane (π_a-system or out-of-plane π-system), and in the other they are symmetric (π_s-system or in-plane π-system) (Figure 1.1). In the π_a- system both $3d_{xz}$ and $3d_{yz}$ orbitals on phosphorus are involved, together with the $2p_z$ orbital of nitrogen.

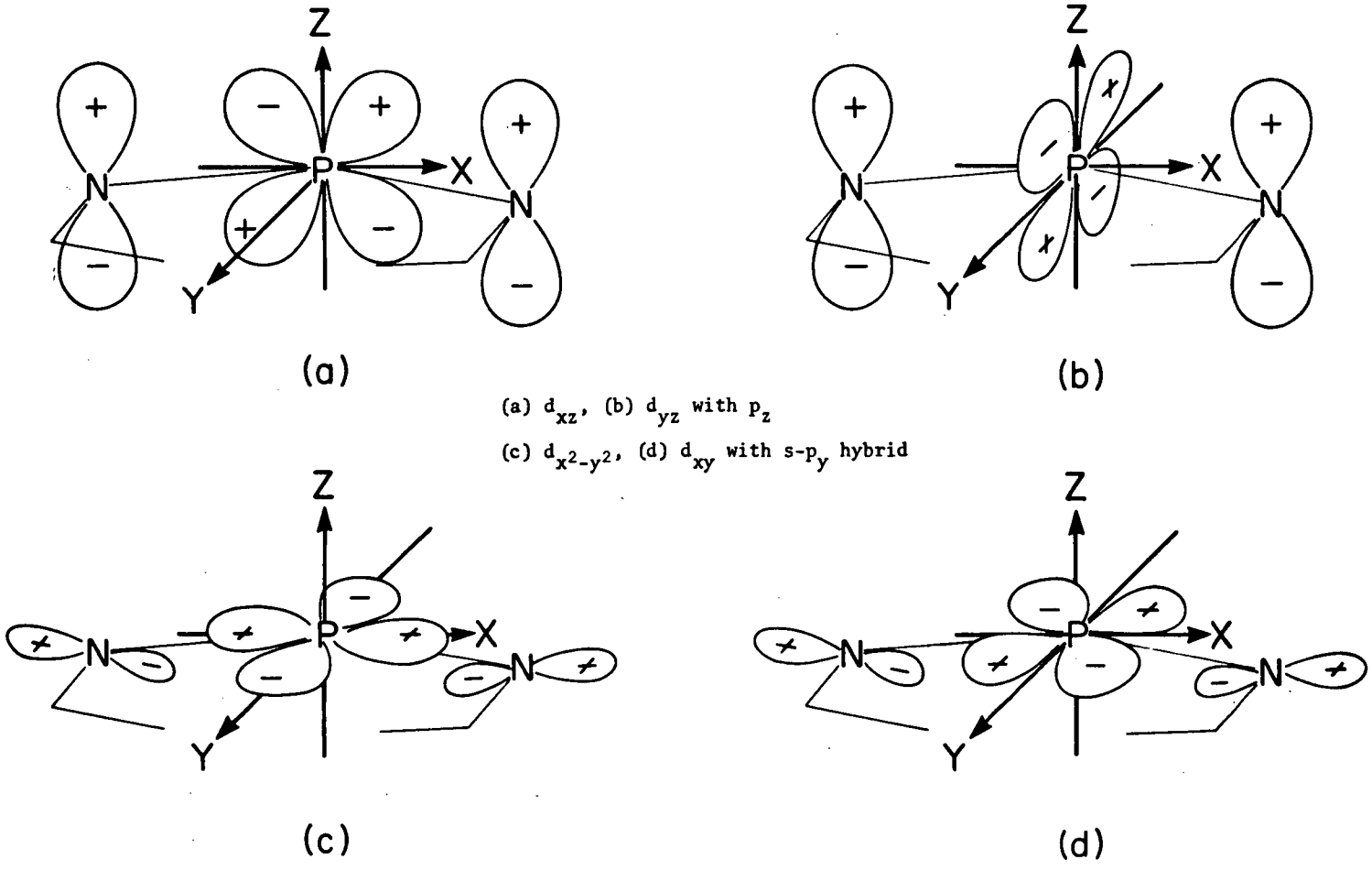

(a) d_{xz}, (b) d_{yz} with p_z

(c) $d_{x^2-y^2}$, (d) d_{xy} with s-p_y hybrid

Figure 1.1. Endocyclic π-system

For a π_s-system the $3d_{xy}$, $3d_{x^2-y^2}$ and $3d_{z^2}$ are allowed to participate, together with the s and p_y orbitals of nitrogen. However, overlap calculations suggest that the two d-orbitals mainly involved in the $d\pi$-$p\pi$ interaction are $d_{x^2-y^2}$ (π_s) and d_{xz} (π_a). It is important to note that the π_s-bonding exists only insofar as lone pair delocalization is present, and supplements the π_a-system which has been proposed to satisfy the formal valence requirement.

The two types of π-interactions can be further distinguished as either homomorphic or heteromorphic. The interaction is homomorphic if the participating orbitals are of the same symmetry species as in $p\pi$-$p\pi$ systems such as benzene, and heteromorphic if they are of different species in the local molecular site group. For planar molecules the molecular site symmetry of the phosphorus and nitrogen atoms is at most C_{2v}. Thus, interactions of the phosphorus $d_{xz}(\pi_a)$ orbital and the nitrogen p_z orbital (π_a) are of the heteromorphic type since they belong to different representations A_2 and B_2, respectively, of the site symmetry group C_{2v}. On the other hand, the π_s-system can be of the homomorphic type, as in $p\pi$-$p\pi$ systems such as benzene, since both the $d_{x^2-y^2}$ orbital of phosphorus and the s-p_y hybrid of nitrogen are of the same symmetry species (A_1) under C_{2v} symmetry.

The π_s-system and the π_a- system are both important stereochemically for two reasons. In the absence of the π_a-system, delocalization of the nitrogen lone pair from the sp_y hybrid into the π_s-system would constrict the molecule in a planar conformation. However, in the presence of the π_a-system, an increase in the use of the π_s-system to the limit of equal contributions produces an analogous situation to that in

acetylene and phosphorus oxychloride ($Cl_3P{=}O$), where the equivalent double π-system introduces rotational symmetry about the internuclear axis. Thus, because of the presence and equality of two π-systems, the geometry of the PN skeleton is not restricted to a particular conformation, and in practice many different molecular shapes are found for phosphazene structures.

1.2.2 Exocyclic π-Bonding

Phosphazenes which show structural and spectroscopic evidence of exocyclicπ-bonding are those which contain ligands capable of conjugating to the ring, either by lone pair delocalization from donor atoms, as in the amino (Figure 1.2A) and alkoxy derivatives, or by interaction of organic π-systems, as in the fluorophenyl compounds (Figure 1.2B). Only the canonical forms (b) and (f) do not have counterparts in carbon chemistry, since it depends on the ability of phosphorus to accommodate twelve electrons in its valence shell. Therefore, the positive charge on the ligand can be neutralized locally.

Electron release to phosphorus in the dimethylaminophosphazenes $[NP(NMe_2)_2]_{4,6,8}$[46-48] is indicated both by the near planarity of the PNC_2 groups (sum of the bond angles around the exocyclic nitrogen ∿ 350°C) and by the shortness of the exocyclic PN bonds (1.67Å average compared to 1.77Å for a single PN bond). The d-orbitals on phosphorus principally involved in exocyclic π-bonding are the d_{xz}, $d_{x^2-y^2}$ and d_{z^2} orbitals, the first one common to the ring π_a- and the exocyclic π_a-systems, and the latter two common to the ring π_s- and the exocyclic π_s-systems (the defining plane for the exocyclic π-system is the XPX plane, assumed

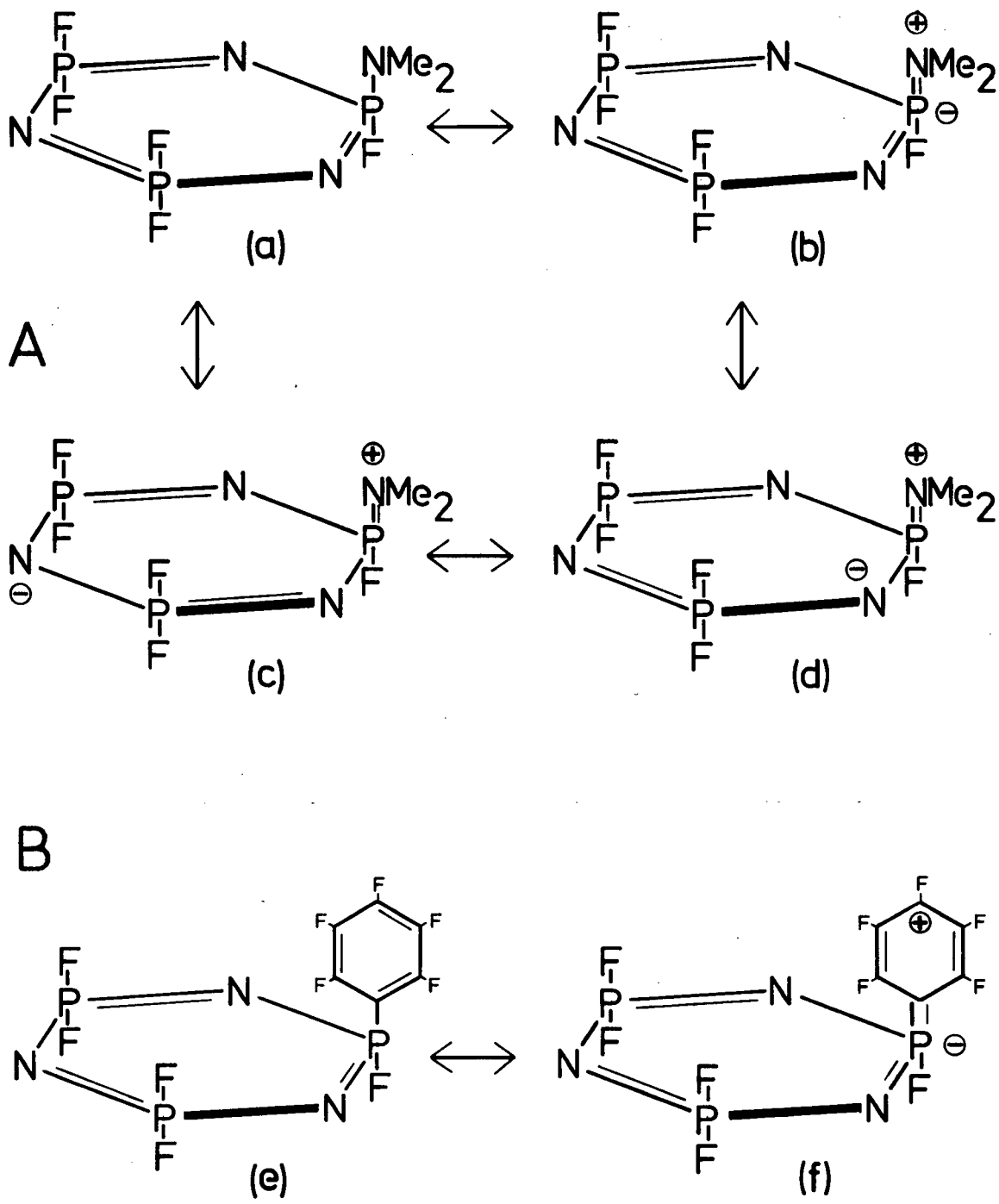

Figure 1.2. Typical canonical forms of $N_3P_3F_5(NMe_2)$ (A) and $N_3P_3F_5(C_6F_5)$ (B).

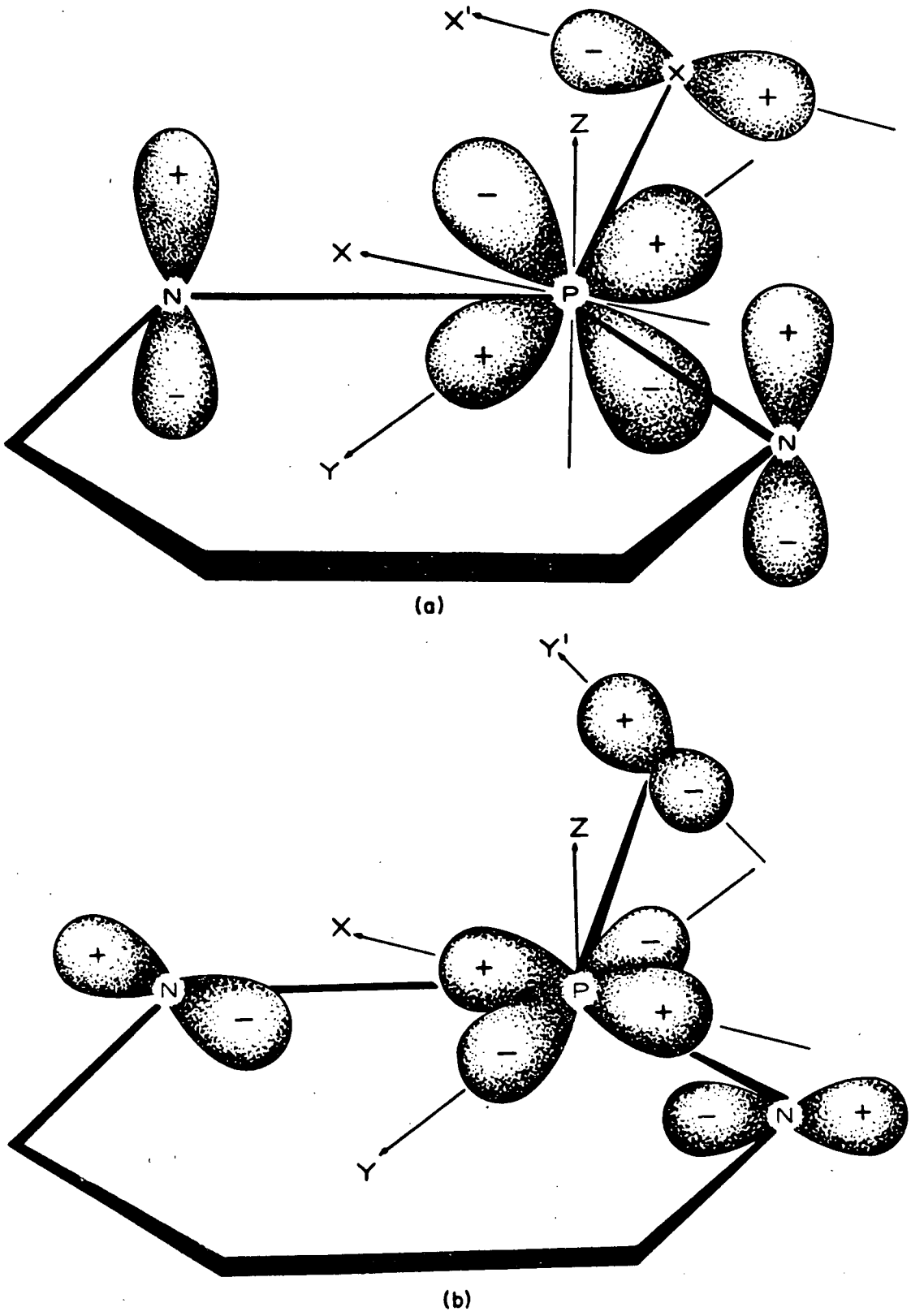

Figure 1.3. Exocyclic π-system: (a) conjugation of an exocyclic $p\pi_a$-orbital with a heteromorphic (d_{xz}) ring π_a-system, and (b) an exocyclic $p\pi_s$-orbital with a homomorphic ($d_{x^2-y^2}$) ring π_s-system.

perpendicular to the NPN plane, Figure 1.3). Further analysis of the structures of the dimethylaminophosphazenes has shown that the two NMe_2 groups are differently aligned for steric reasons, and within each monomer unit $\{N=P(NMe_2)_2\}$, the more strongly bound NMe_2 group is the one that is better oriented to the π_s- orbitals on phosphorus. However, the orientation of the NMe_2 groups in the structure of $[NP(NMe_2)_2]_3$[49] is such that neither is suitably aligned for a strong interaction with the π_s- orbitals on phosphorus, and the exocyclic PN bonds become approximately equal in length, 1.652 Å being the average value. Additional evidence that the π_s-orbitals are more important and more dominant comes from the structures of gem-$N_3P_3Ph_2Cl_4$[50] and gem-$N_3P_3Ph_2F_4$[51] in which the orientation of the phenyl groups is not restricted by steric interactions from neighboring $PF_2(Cl_2)$ units. In the fluoro derivative both phenyl groups can best conjugate to the phosphazene ring through the π_s-orbitals, while in the chloro compound some overlap with the π_a-orbitals is indicated. That exocyclic conjugation does actually occur in phenylphosphazenes has also been demonstrated by ^{19}F n.m.r. spectroscopy of fluorophenyl groups attached to the phosphazene ring: the large deshielding of the para fluorine atom, relative to the meta fluorine atom, in the series $N_nP_nF_{2n-1}(C_6F_5)$ (n=3-8)[52], is an indication of the build up of partial positive charge within the phenyl ring (see Figure 1.2B) caused by donation of π-electron density to the phosphazene ring.

1.3 Donor and Acceptor Properties of Phosphazenes

The ability of the phosphazene ring to accept π-charge from exocyclic groups has important consequences concerning both the chemistry

of the attached ligand and of the ring itself. In aminophosphazenes, the primary effect of exocyclic conjugation is to lower the basicity of the amino nitrogen atoms with concurrent build up of electron density on the ring nitrogens. Thus, protonation generally occurs on an endocyclic nitrogen, and is confirmed by the X-ray crystal structure of the compound gem-$N_3P_3Cl_2(NHPr^i)_4 \cdot HCl$ (IX)[53]. Consistent with this, transition metal nitrates and chlorides bond solely to the ring nitrogens of the fully substituted tetramer $[NP(HNMe)_2]_4$ (X)[54] and hexamer $[NP(NMe_2)_2]_6$ (XI)[55]. Exclusive exocyclic coordination by a metal* is

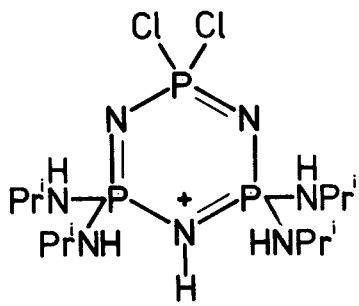

IX

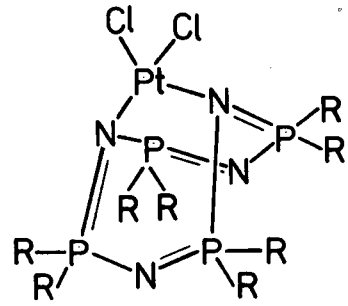

X

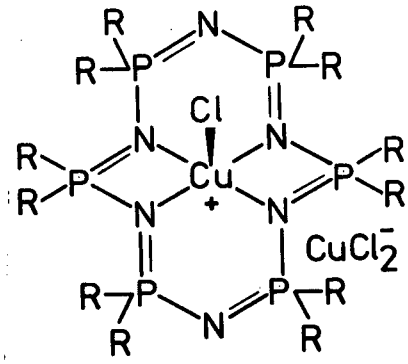

XI

not known for $[NP(NMe_2)_2]_{3-6}$, but there is at least one reported example of a metal complexing to both an endocyclic and an exocyclic nitrogen (in $[NP(NMe_2)_2]_4 \cdot W(CO)_4$)[57], suggesting that the donor properties of the amino group have not been drastically reduced. In relation to this thesis, the chemical and structural properties of the dimethylaminophosphazenes are important, and will constantly serve as a comparison to the results obtained for 1-pyrazolylphosphazenes.

---

*Methylation of $[NP(NMe_2)_2]_3$ with $Me_3O^+BF_4^-$ occurs at the exocyclic nitrogen atoms[56].

Other stable complexes are formed when the substituents on phosphorus are groups of low electronegativity, such as methyl. In methylphosphazenes, the good Lewis base character of the ring nitrogens is a result of inductive effects transmitted through the π-system. Quaternization and protonation occur easily, and crystalline 1:1 adducts such as $(NPMe_2)_3 \cdot TiCl_4$[58] and $(NPMe_2)_3 \cdot I_2$[59] have been isolated. Various transition metal nitrates and chlorides have been made: $(NPMe_2)_4$ reacts with anhydrous $CoCl_2$ and HCl in methyl ethyl ketone to yield a phosphazonium ion complex $[(NPMe_2)_4H^+]_2\ [CoCl_4^{-2}]$, in which one protonated ring occupies a saddle and the other a tub conformation (XII)[60]. In a similar reaction using

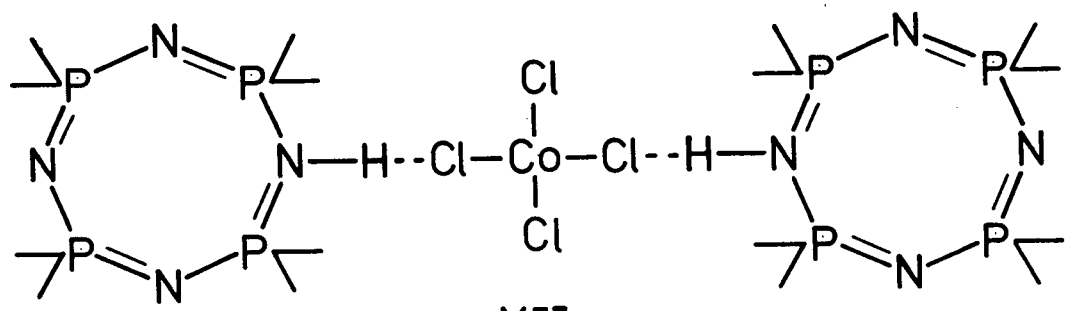

XII

instead anhydrous $CuCl_2$, both the copper ion and the proton bond to a ring nitrogen. The crystal structure (XIII)[61] shows that electron localization

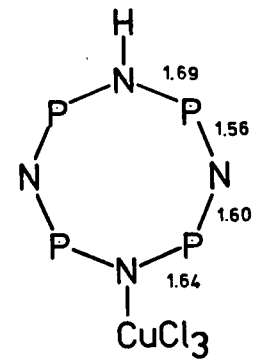

XIII

is less complete on coordination to the metal, since the ring bonds nearest to the coordinated nitrogen are shorter. The recent crystal structures of $(NPMe_2)_6 \cdot PdCl_2$ (XIV)[62] and $(NPMe_2)_8 \cdot Co(NO_3)_2$ (XV)[62] have shown that, at least for large ring sizes, the metal prefers to bond to one end of the ring, and not to the middle. Finally, the methylphosphazenes $(NPMe_2)_{4,5}$ react almost quantitatively with either $Mo(CO)_6$ or $W(CO)_6$ in the solid state to produce yellow solids $L \cdot M(CO)_3$, which are unstable in common organic solvents[63].

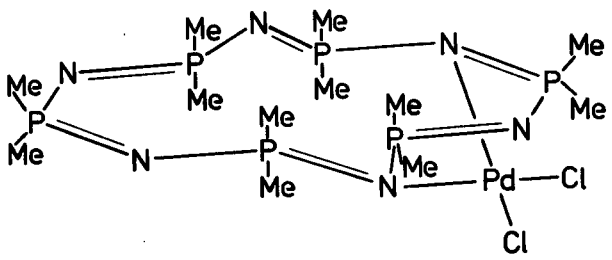

XIV

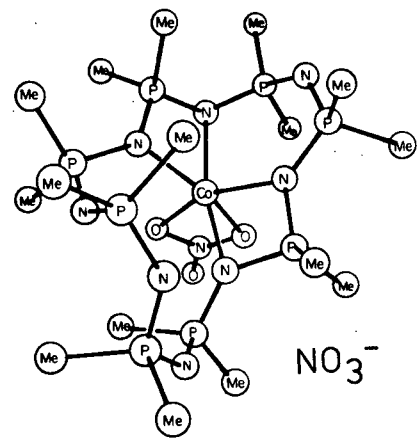

XV

All the complexes discussed above have been shown either crystallographically or spectroscopically to be of the σ-type, coordination to the metal involving the lone pair of electrons on the ring nitrogen and sometimes on the exocyclic amino nitrogen. There has only been one brief report[64] of a π-complex, a compound suggested to be π-$(NPCl_2)_3 \cdot Mo(CO)_3$, but the structure has not been confirmed by X-ray crystallography.

Methylphosphazenes, in addition to behaving as donors, can be deprotonated by strong bases, and the resulting carbanion stabilized by the acceptor properties of the ring as shown by the resonance forms XVI, XVII and XVIII. Previous work[65] has shown that methyl lithium and

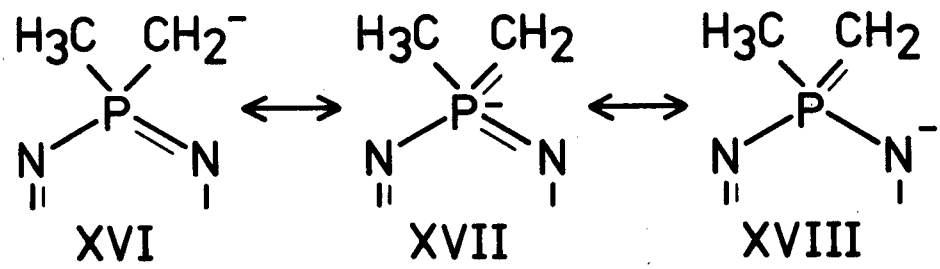

XVI XVII XVIII

n-butyl lithium are able to abstract a proton from a number of methyl groups in $(NPMe_2)_4$, and from a single methyl group in gem-$N_3P_3Ph_4Me_2$, giving stable carbanion intermediates from which novel phosphazene derivatives have been made. Chapter II of this thesis is devoted to an extension of this work as well as to the preparation and reactions of the tricarbanion $N_3P_3Me_3(\bar{C}H_2)_3$.

1.4 Pyrazolyl Compounds

The pyrazole ring system consists of a doubly unsaturated five-membered ring containing two adjacent nitrogen atoms. Pyrazole itself (XIX) is a weaker Lewis base (pK_{BH^+} 2.47[66], Equation 1.11) than its isomer imidazole (XX) (pK_{BH^+} 6.95[66]), and can easily be deprotonated (pK_{HA} 14[66]) by suitable bases (Equation 1.12). Both pyrazole and imidazole form many N(1) substituted derivatives as well as metal complexes via the pyridine-type

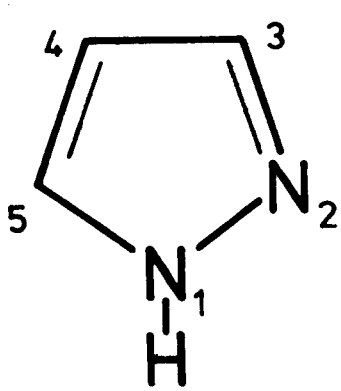

XIX

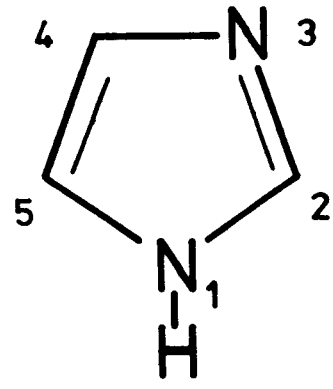

XX

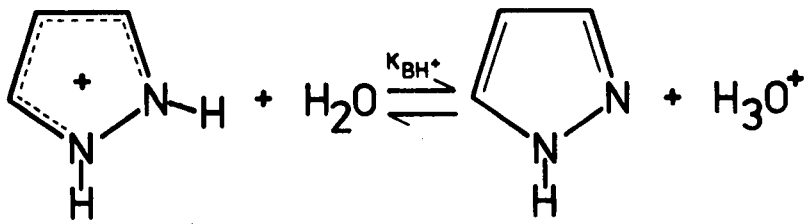

... (1.11)

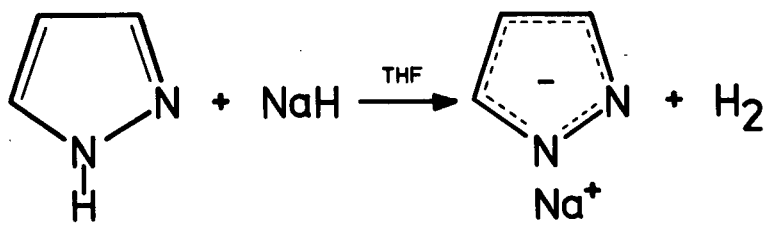

... (1.12)

nitrogen, N(2) on pyrazole and N(3) on imidazole. However, it is not the intention in this section to give a detailed account of the chemistry of pyrazole, of which many books[67,68] and reviews[69] have been written, but rather to help understand the relation between the pyrazole and the phosphazene ring. This will be done through an analysis of the chemical and spectroscopic properties of heterocyclic amides (azolides), and N,N-dimethylformamide.

Table 1.1 shows that both the values of ν(C=O) and the rate of hydrolysis increase with an increasing number of nitrogen atoms in the ring. These trends are also complemented by the decreasing charge density on the carbonyl carbon and on the amide nitrogen, and by the increasing carbonyl bond order, as calculated by simple Hückel M. O. theory. All these facts, taken together, can be explained by assuming that the lone pair of electrons on the amide nitrogen would much rather be connected with

Table 1.1. Values of $\tau_{1/2}$[a], $\nu(C=O)$[b] and Hückel molecular orbital[c] parameters for acetaldehyde[d], N,N-dimethylformamide[e] and N-acetylazoles[f].

Compound	$\tau_{1/2}$ (min)	$\nu(C=O)$ (cm^{-1})	$q(N_3)$	$q(C_1)$	$p(CO)$	$-E_\pi$ (ev)
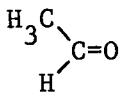	-	1725	-	.4000	.8000	4.0000
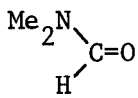	-	1673	1.6265	.6091	.5724	6.8595
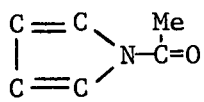	∞	1732	1.4208	.5307	.6574	12.4141
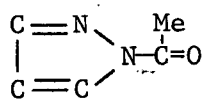	908	1742	1.3831	.5373	.6576	13.6917
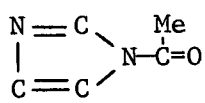	41	1747	1.4006	.5142	.6718	13.7079
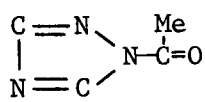	6.4	1765	1.3706	.5264	.6669	14.9759
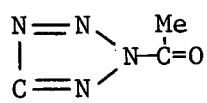	<0.5	1779	1.2388	.5031	.7018	15.9314

(a) Half-lives for the hydrolysis in water at 25°C at pH 7.0. (b) Infrared carbonyl stretching frequencies measured in chloroform, except for N-acetylpyrazole in nujol mull. (c) Calculations based on the molecular framework $C_1{=}O_2$ for acetaldehyde, $N_3{-}C_1{=}O_2$ for N,N-dimethylformamide, and

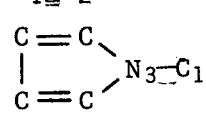 for the N-acetylazoles, nitrogens being substituted for carbons where required. $\alpha_C = 0$, $\alpha_N = -1.0$, $\alpha_O = -1.5$ and $\beta = -1.0$. p = total bond order, q = total charge density and E_π = total π-electron energy. (d) Ref. for $\nu(C=O)$: N.S. Bayliss, R.H. Cole, and L.H. Little, Aust. J. Chem., 8, 26 (1955). (e) Ref. for $\nu(C=O)$: L.J. Bellamy and R.L. Williams, Trans. Faraday Soc., 55, 14 (1959). (f) All data pertaining to the N-acetylazoles are taken from H.A. Staab, Angew. Chem. Int. Ed., 1, 351 (1962); except for N-acetylpyrazole which was taken from W.L. Driessen and P.L.A. Everstijn, Inorganica Chimica Acta, 41, 179 (1980).

the aromatic character of the azole ring. Therefore, the extent to which conjugation to the carbonyl group occurs is reduced compared to formamide, where no competitive delocalization of the amide lone pair is possible. Hence, pyrazole is expected mainly to act inductively as an electron withdrawing substituent on the phosphazene ring, with at most a minor conjugative contribution to the bonding. However, it should be noted that conjugative interactions are more important for phosphorus than for carbon, since phosphate esters and phosphonamides are more stable to hydrolysis than the corresponding carbonyl compounds[70].

The extent of exocyclic conjugation and its effect on the donor properties of 1-pyrazolylphosphazenes is discussed in chapters III and IV.

1.5 Phosphoryl Compounds

The basic chemistry of phosphazenes is in many respects similar to that of the mononuclear phosphoryl compounds. The methyl and methylene protons adjacent to a phosphoryl group (P=O) can easily be removed to give phosphoryl carbanions, the stability of which is due to the acceptor properties of the d-orbitals on phosphorus. Carbanions formed from phosphonate esters $(RO)_2P(O)CH_2R$[71-73], phosphonamides $(Me_2N)_2P(O)CH_2R$[74,75] and phosphine oxides $R_2P(O)CH_2R$[76] have all found particular application as Wittig type intermediates for the synthesis of alkenes.

P-N bonded phosphine oxides can be made from $Cl_3P{=}O$ and amines. In this manner, both tris(pyrazolyl) and tris(3,5-dimethylpyrazolyl) derivatives have been prepared[77,78]. Some of the carbanion reactions of phosphoryl compounds and the substitution reactions of $Cl_3P{=}O$, related to this work, are illustrated in Figure 1.4.

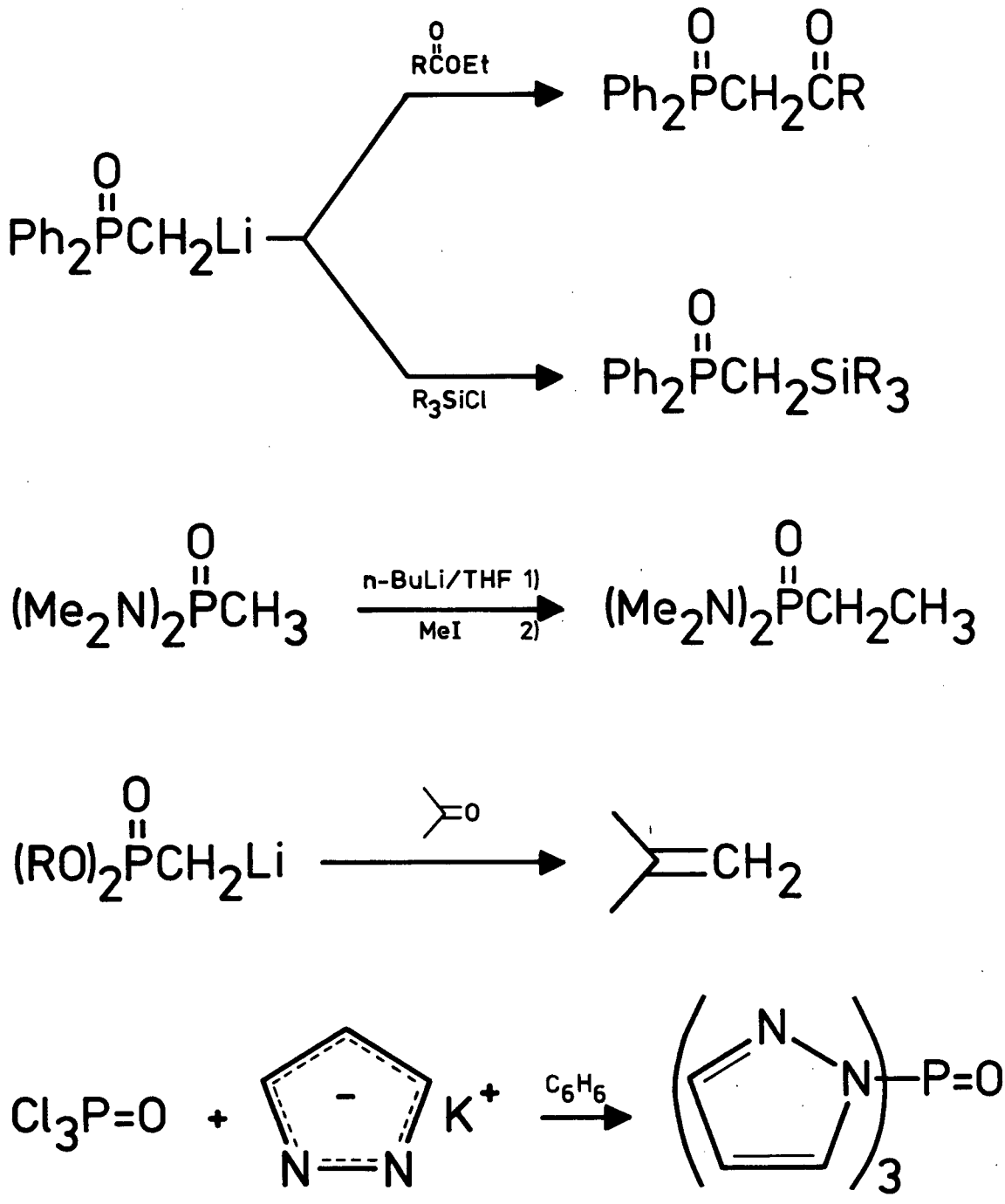

Figure 1.4. Typical reactions of some phosphoryl compounds.

1.6 Summary

This thesis comprises two areas of research: (1) the synthesis and reactions of methylphosphazene carbanions, and (2) the preparation and metal complexes of 1-pyrazolylphosphazenes. Both are basically concerned with the reactions of the substituents themselves; they differ in the degree of conjugation of the substituent with the phosphazene ring. The results are presented in the following three chapters, the final chapter being concerned with the structural parameters of some of the compounds described in earlier chapters.

CHAPTER 2

CARBANION REACTIONS OF METHYLPHOSPHAZENES

The development of the chemistry of the cyclic methylphosphazenes has been limited mainly due to difficulties encountered in their preparation. This thesis is concerned with the two fully methylated phosphazenes $(NPMe_2)_{3,4}$ and the partially methylated derivative gem-$N_3P_3Ph_4Me_2$. The advances that have been made in the preparation of $(NPMe_2)_{3,4}$ have been mentioned in the introductory chapter, while an improved method for the synthesis of gem-$N_3P_3Ph_4Me_2$ is described in Section 2.1 of this chapter.

Methyl substituents on the phosphazene ring increase the electron density at the ring nitrogen atoms, and, as a consequence, the chemistry of methylphosphazenes has been directed towards their behaviour as donors to organic and inorganic acceptors. However, the synthetic possibilities of the acceptor properties of the ring have received little attention, though they can be directly seen in the reactions of the phosphazenyl anion (II) formed from a hydridophosphazene[79] (I) (Equation 2.1).

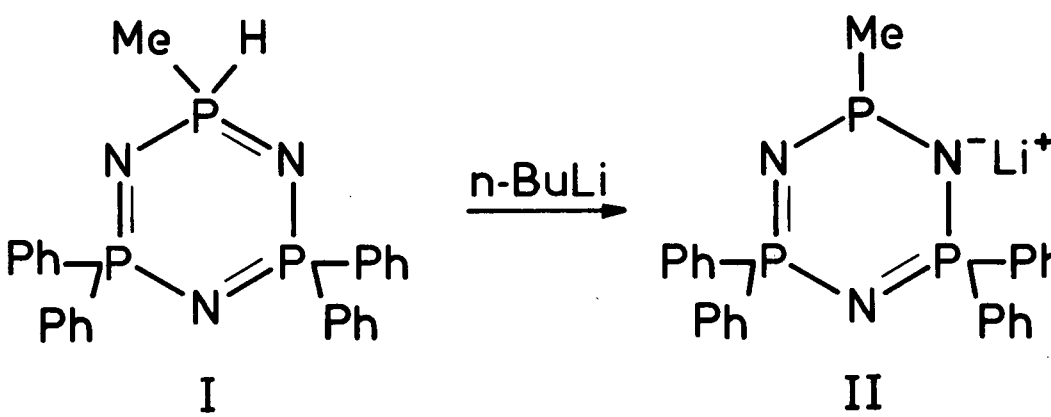

I II ... (2.1)

The results presented in this chapter are from a study of the

reaction of the methylphosphazenes (III) with strong bases (e.g. alkyllithiums) to give carbanion intermediates (IV), which in turn can react with various electrophiles, yielding novel phosphazenes (V) of both synthetic and theoretical interest (Equation 2.2). The synthetic possibilities

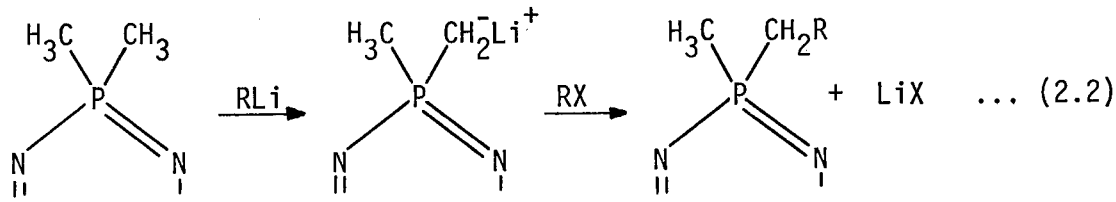

III IV V

of the monocarbanionic derivative gem-$N_3P_3Ph_4Me(CH_2Li)$ have already been explored[80] and are extended in this work. In similar reactions of $N_3P_3Me_6$ and $N_4P_4Me_8$, the formation of polyfunctional carbanions, the orientational pattern of the substituents and the relative reactivities of the trimeric and tetrameric carbanions are discussed, in Sections 2.2, in terms of electronic structure.

2.1 Preparation of Gem-$N_3P_3Ph_4Me_2$

Of the three different methods[13,81,82], all involving ring closure reactions, reported for the preparation of gem-dimethyltetraphenylcyclotriphosphazene, the simplest, at least in principle, is the reaction of dimethyltrichlorophosphorane with the linear phosphazene bis-(aminodiphenylphosphine)-iminium chloride (Equation 2.3). The product is isolated as its hydrochloride, which upon treatment with a suitable base (e.g. Et_3N) is converted into the neutral compound. However, the reported yields are very low (3.4%[81], as the hydrochloride, based on the amount of Me_2PCl_3 used), partly because the boiling point of the solvent, benzene,

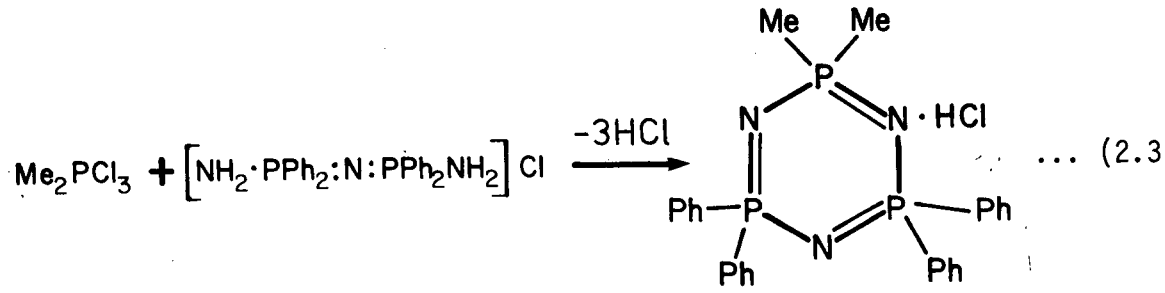

... (2.3)

is not high enough to ensure complete reaction. We have re-examined the preparation by using a higher boiling solvent, chlorobenzene, and have found that the yield is improved to ∿20%, and that other phosphazenes are formed.

Although the yield is still low, it can be attributed, in part, to the competing reactions which are also present in similar ring closure reactions involving $[NH_2(Ph_2)PNP(Ph_2)NH_2]^+Cl^-$ and phosphorus (V) chlorides (PCl_5[14,15], $PhPCl_4$[15] and Ph_2PCl_3[15]). The reaction of the linear phosphazene with PCl_5 in the absence of solvent[15] gives the expected product gem-$N_3P_3Ph_4Cl_2$ (in 25% yield) and, in addition, the tetrameric derivative $N_4P_4Ph_4Cl_4$ (in 6% yield). Similarly, 24% of the tetrameric phosphazene $(NPPh_2)_4$ and 34% of the trimeric compound $(NPPh_2)_3$ are formed when the ring closure is attempted using Ph_2PCl_3. In the present case, it has been found that the reaction of $[NH_2(Ph_2)PNP(Ph_2)NH_2]^+Cl^-$ and Me_2PCl_3 gives not only the desired product gem-$N_3P_3Ph_4Me_2$, but also significant amounts of $(NPPh_2)_4$, $(NPMe_2)_4$ and the new mixed derivative 1,1,3,3-tetramethyl -5,5,7,7 -tetraphenylcyclotetraphosphazene (X). All four compounds can easily be separated (see Section 2.3).

The formation of these tetrameric and trimeric phosphazenes provides a helpful insight into the reaction mechanism, which can be viewed as a result of a ligand exchange reaction[83] of the type shown in Equation 2.4. For the methyl derivatives, either pair of compounds,

$$\underset{\text{VI}}{Me_2PCl_3} + \underset{\text{VII}}{[NH_2(Ph_2)PNP(Ph_2)NH_2]^+Cl^-} \longrightarrow \underset{\text{VIII}}{[Me_2P(NH_2)Cl]^+Cl^-} + \underset{\text{IX}}{NH_2P(Ph)_2NP(Ph)_2Cl_2} \quad \ldots (2.4)$$

VI and VII, or VIII and IX (which were not isolated in this investigation) can condense to form gem-$N_3P_3Ph_4Me_2$. Compounds VIII and IX can also react with either themselves or together to give the range of products shown in the scheme below.

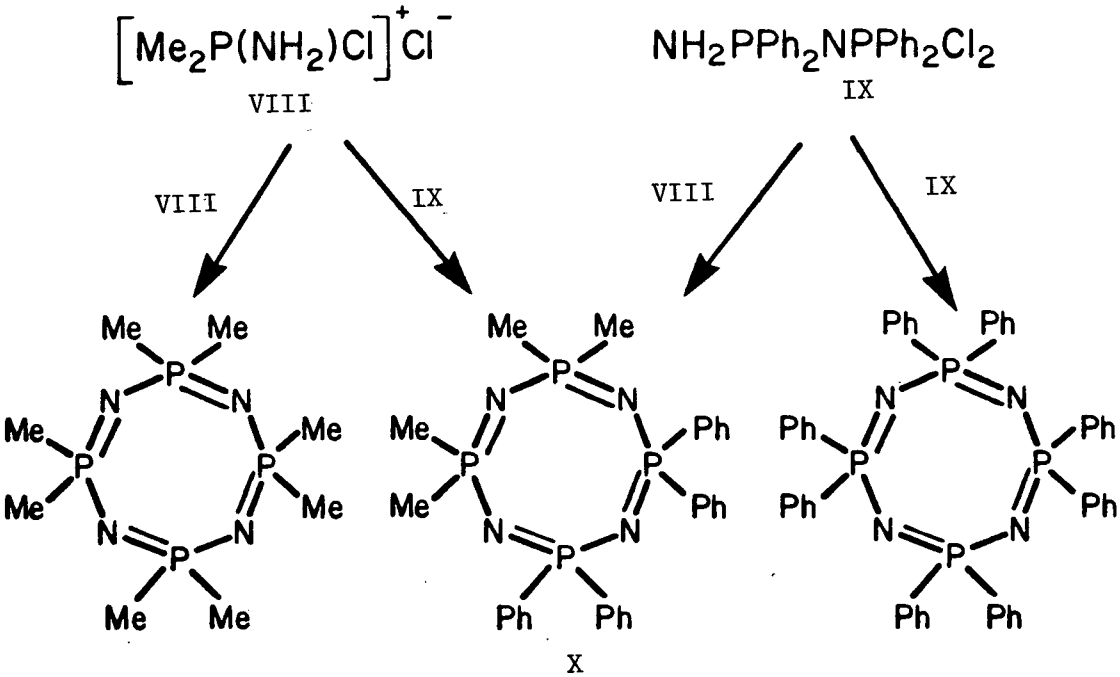

X

The structure of $N_4P_4Me_4Ph_4$ (X) is implied by the method used for its preparation, and is uniquely consistent with the two doublets in its ^{31}P n.m.r. spectrum. Compound X is quaternized by methyl iodide to 1,1,2,3,3 -pentamethyl -5,5,7,7 -tetraphenylcyclotetraphosphazenium

Table 2.1. Infrared[a], ^{1}H[b] and ^{31}P[c] n.m.r. parameters of N-methyl methylphenylphosphazenium iodides and their parent compounds.

Compound	ν(P=N) cm^{-1}	ν(C-N) cm^{-1}	δ_H(MeN)	δ_H(Me_2P)	$-\delta_P$(PPh_2)	$-\delta_P$(PMe_2)
$N_3P_3Ph_4Me_2$[d]	1164 1187 1199	-	-	6H,1.58 d,(14.0)[e]	2P,98.2	1P,85.2
$N_3P_3Ph_4Me_2$·MeI[f]	1220 1260	1070	3H,3.07 t,(11.0)	6H,2.22 d,(14.0)	1P,81.0[g] 1P,93.5[h]	1P,64.1
$N_4P_4Me_4Ph_4$	1240 1260	-	-	12H,1.41 d,(12.5)	2P,108.9 d,(4.9)	2P,96.4 d,(4.1)
$N_4P_4Me_4Ph_4$·MeI	1256 1266sh	1092	3H,2.90 t,(11.4)	12H,1.88 d,(13.3)	2P,103.8	2P,73.3

(a) From nujol mull spectra, assignments tentative. (b) Dilute solutions in $CDCl_3$, δ(ppm) reference internal TMS. PH coupling constants (in Hertz) in parenthesis. δ(Phenyl) ∿7.0-8.0 ppm. Abbreviations: d-doublet, t-triplet, sh-shoulder. (c) Dilute solutions in $CDCl_3$, δ(ppm) reference external P_4O_6. PP coupling constants (in Hertz) in parenthesis. (d) See also R. Appel and G. Saleh, Chem. Ber., 106, 3455 (1973). (e) J(PH) (long range) =1.5Hz. (f) Data from R.T. Oakley, Ph.D. Thesis, University of British Columbia, 1976. (g) PPh_2 atom adjacent to N(Me) atom. (h) PPh_2 atom remote from N(Me) atom.

iodide. Its structure (XI) follows from the equivalence of the four methyl groups and the symmetry of the N-methyl triplet in the ^{1}H n.m.r. spectrum, and from the two-line ^{31}P spectrum. The phosphorus shifts of the Me_2P and the Ph_2P groups are assigned by comparison with those of gem-$N_3P_3Ph_4Me_2$ and its methiodide[13,84,85] (Table 2.1). The comparison also excludes the alternative structure of XI, in which an NMe unit bridges two Ph_2P groups.

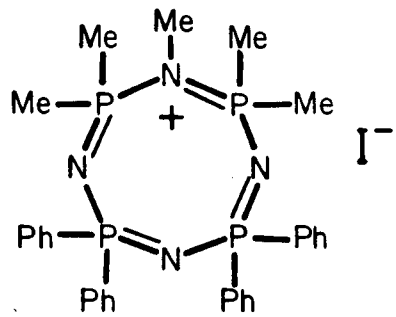

XI

2.2 Formation and Reactions of Methylphosphazenylcarbanions

2.2.1A Formation and Reactions of Gem-$N_3P_3Ph_4Me(CH_2Li)$

Gem-$N_3P_3Ph_4Me_2$ reacts rapidly with salt-free solutions of n-butyl lithium (n-BuLi) or methyl lithium (MeLi)[80] in diethyl ether to precipitate, after an induction period of a few minutes, the lithio-derivative gem-$N_3P_3Ph_4Me(CH_2Li)$. Although the carbanion was not isolated, its existence has been confirmed by its reaction with a number of electrophiles, such as bromine (Br_2), ethyl benzoate ($PhCO_2Et$) and trimethylstannyl chloride (Me_3SnCl), to form new organophosphazenes of the type gem-$N_3P_3Ph_4Me(CH_2R)$[80] (Equation 2.5). Other derivatives prepared in a similar manner include

$$N_3P_3Ph_4Me_2 \xrightarrow{R'Li} N_3P_3Ph_4Me(CH_2Li) \xrightarrow{RX} N_3P_3Ph_4Me(CH_2R) + LiX \quad \text{... (2.5)}$$

R=Br, $SnMe_3$, PhCO

X=Br, Cl , OEt

the carboxylic acid (R=COOH)[80], and the bridged compound XII[86], prepared from the lithio-intermediate by an oxidative coupling reaction involving

$CuCl/O_2$. Only one additional compound was prepared for this thesis because the products are sometimes difficult to separate from the starting material. This was the new bridged phosphazene (XIII) made by joining the two phosphazenyl groups by the use of the difunctional halide Me_2SiCl_2.

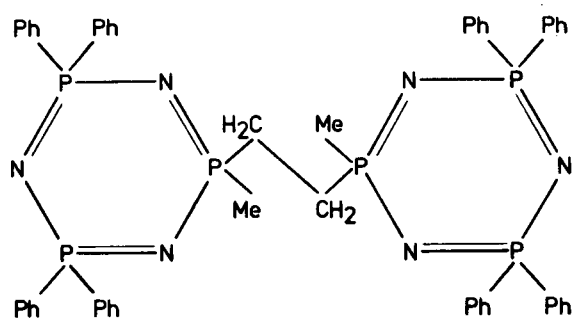

XII

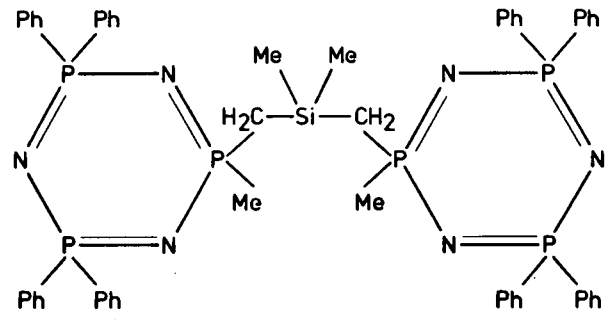

XIII

The fact that small amounts of $N_3P_3Ph_4Me_2$ were recovered in this and most of the previous reactions is probably not a result of incomplete carbanion formation, but is instead due to the enhanced acidity of the methylene hydrogens in the product. Competing reactions such as that illustrated by Equation 2.6 thus become more probable.

$$N_3P_3Ph_4Me(CH_2^-) + N_3P_3Ph_4Me(CH_2R) \longrightarrow N_3P_3Ph_4Me_2 + N_3P_3Ph_4Me(CHR^-) \quad \ldots (2.6)$$

The n.m.r. parameters of the silicon compound are given in Table 2.2. They are broadly similar to those of previously prepared compounds, in that the ^{31}P spectrum consists of two singlets of relative intensity 1:2 ($PMeCH_2R$: $2PPh_2$), and the ^{31}P decoupled ^1H spectrum shows two singlets in the methyl region of relative intensity 3:2 ($3MeP$: $2CH_2P$). Relative to $N_3P_3Ph_4Me_2$, the methylene protons are shielded by the electropositive $SiMe_2$ group. Since electropositive groups disperse π-electron density away from phosphorus, the chemical shift of the $\underline{P}CH_2Si$ atom decreases

with respect to $\underline{PMe_2}$.

The synthetic applications of this monocarbanion are numerous, but, as will be seen, the chemistry of the polyfunctional carbanions is much more influenced by the substituent and the acceptor properties of the ring.

Table 2.2. Infrared[a], ^1H n.m.r.[b] and ^{31}P n.m.r.[c] parameters of $N_3P_3Ph_4Me_2$ and $(N_3P_3Ph_4MeCH_2)_2SiMe_2$.

Compound	ν(P=N) cm^{-1}	δ_H(MeP)	$\delta_H(CH_2P)$	$-\delta_P(PPh_2)$	$-\delta_P(PMeCH_2R)$
$N_3P_3Ph_4Me_2$[d]	1164 1187 1199	6H,1.58 d,(14.0)	-	2P,98.2	1P,85.2
$(N_3P_3Ph_4MeCH_2)_2$ $\cdot SiMe_2$[e]	1170 1182 1195	6H,1.40 d,(13.6)	4H,1.15 d,(16.1)	4P,99.4	2P,83.2

(a) From nujol mull spectra, assignments tentative. (b) Dilute solutions in $CDCl_3$, δ(ppm) reference internal TMS. PH coupling constants (in Hertz) in parenthesis. Abbreviations: d-doublet. (c) Dilute solutions in $CDCl_3$, δ(ppm) reference external P_4O_6. (d) See also R. Appel and G. Saleh, Chem. Ber., 106, 3455 (1973). (e) $\delta_H(Me_2Si)$=-0.17ppm.

2.2.2A Formation and Reactions of $N_3P_3Me_3(CH_2Li)_3$

Hexamethylcyclotriphosphazene, $N_3P_3Me_6$, is deprotonated with three equivalents of n-BuLi in diethyl ether to immediately precipitate the tricarbanion $N_3P_3Me_3(CH_2Li)_3$ (XIV) (Equation 2.7). Successive deprotonation of the PMe groups occurs on different phosphorus atoms, and electrostatically the most stable configuration is the cis-trans-trans* form (XV). The

*Nomenclature refers to the configuration about successive bonds, only the relative order of terms being important. For example, cis-trans-trans, trans-trans-cis and trans-cis-trans are identical terminology.

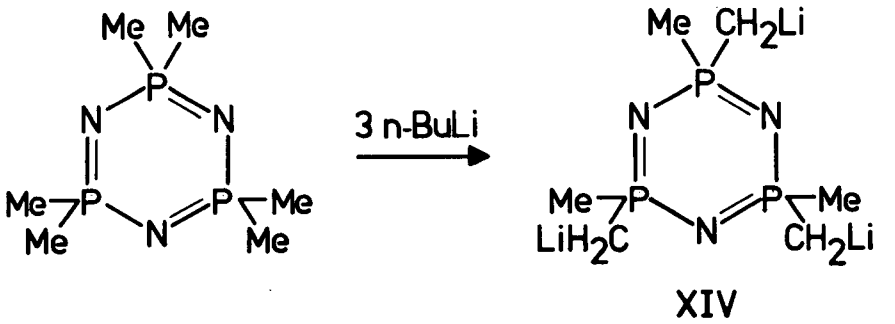

... (2.7)

XIV

alternative cis-cis-cis form (XVI) is also possible. Thus reaction of XIV with electrophiles can give at most two diastereomers. Accordingly,

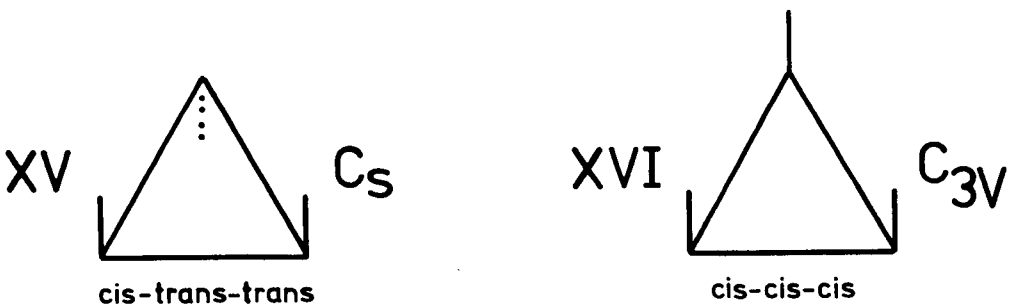

the tricarbanion reacts with pentafluorobromobenzene (C_6F_5Br) via a metal-halogen exchange to produce both tribromo isomers (Equation 2.8a), the

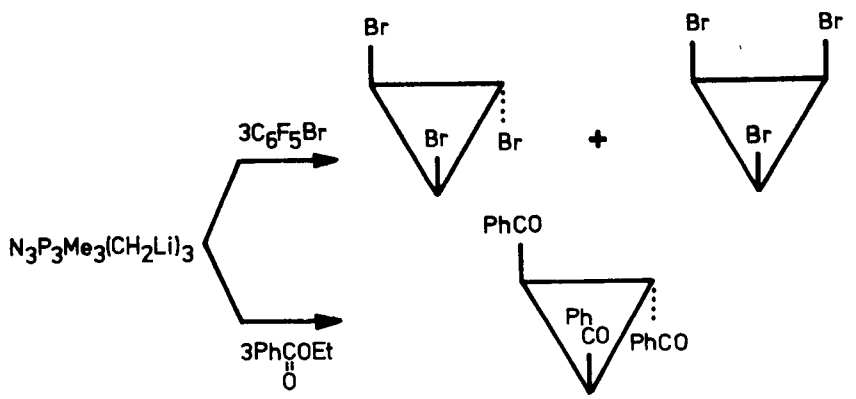

... (2.8a)

... (2.8b)

relative yields being 3:1 in favor of the cis-trans-trans configuration. However, from repeated experiments only the cis-trans-trans form of the tribenzoyl derivative was isolated from reactions of XIV with ethyl benzoate (Equation 2.8b). If both types of tricarbanions XV and XVI are formed on the addition of n-BuLi, then only a proton transfer, of the type shown in Equation 2.9, can account for the one tribenzoyl product.

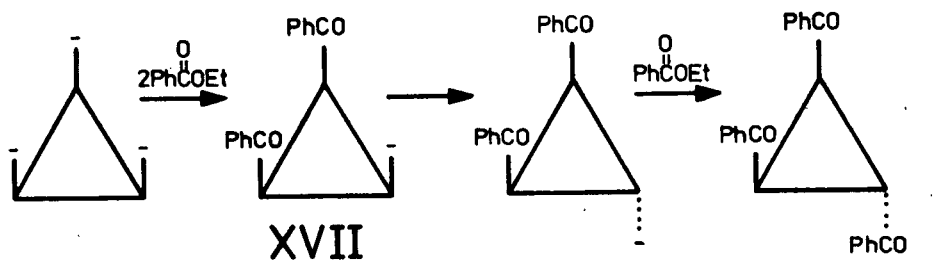

XVII

... (2.9)

Otherwise the dibenzoyl carbanion (XVII) would be expected to give some cis-cis-cis isomer, or if steric hindrance is a factor, a disubstituted derivative upon workup (e.g. addition of H_2O), neither of which was detected. On the other hand, if only the more electrostatically stable carbanion XV is formed, then a similar proton transfer (Equation 2.10) must occur to account for the two tribromo derivatives. Hence, the exact mechanism of deprotonation and product formation remains unclear.

Metal-halogen exchange offers a clean method for the introduction of halogen atoms onto the alkyl substituents of the phosphazene ring. With polyhalogenobenzenes, the electron withdrawing effect of the neighboring halogen atoms is sufficient to promote lithium-halogen exchange. For example, $C_6F_5Br(Cl)$ react with n-BuLi at $-70^{\circ}C$ in Et_2O to give C_6F_5Li and n-BuBr(Cl) in 85% yields[87,88], but C_6F_6 undergoes only alkylation with

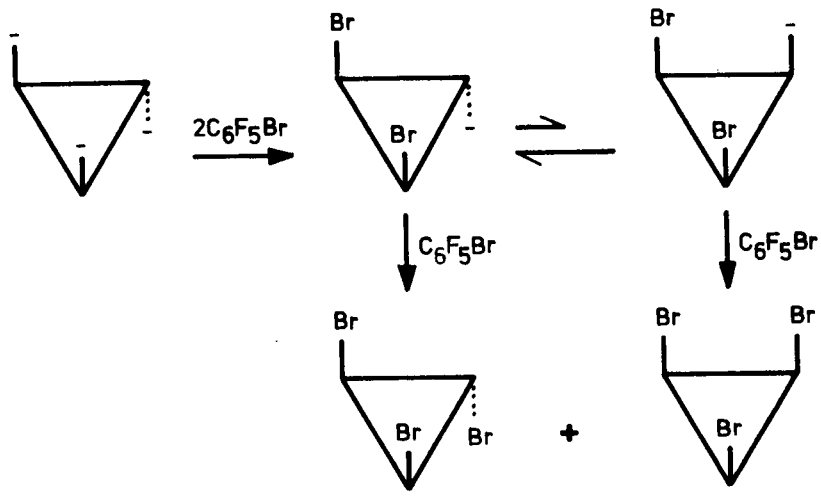

... (2.10)

methyl lithium[89]. Bromine and iodine exchange in preference to chlorine and in preference to displacement of fluorine. Good yields of products via metal-halogen exchange usually occur when the reactions are done at low temperatures and for short reaction times.

2.2.2B Spectra and Structure of $N_3P_3Me_3(CH_2R)_3$ Derivatives

The most useful means for determining the configuration of the tribenzoyl- and tribromo-compounds is by the aid of n.m.r. spectroscopy, both ^{1}H and ^{31}P n.m.r. being equally valuable. The n.m.r. data are given in Table 2.3. One of the advantages of studying compounds which contain a phenyl group is that the benzene ring is a source of a large internal anisotropic magnetic field. Therefore, hydrogen or phosphorus atoms that are geometrically non-equivalent are usually also magnetically non-equivalent. Such is the case for the tribenzoyl derivative. The ^{31}P-decoupled ^{1}H spectrum consists of a pair of singlets, intensities 1:2, for the methyl protons, and a singlet for one methylene group superimposed on an AB pattern

Table 2.3. ^{1}H [a] and ^{31}P [b] n.m.r. parameters of phosphazenes $N_3P_3Me_3(CH_2R)_3$

Compound	$\delta_H(CH_3P)$	$\delta_H(CH_2P)$	$-\delta_P$
$N_3P_3Me_6$	18H,1.46(13.0)	-	3P,87.0
$N_3P_3Me_3[CH_2C(O)Ph]_3$ [c]	6H,1.34(14.0) 3H,1.13(14.6)	[d] 2H ,A,3.56(13.5) 2H ,B,3.40(14.0) J_{AB}=13.0 Hz 2H ,C,3.46(14.9)	2P,A,89.30 1P,B,89.85
$N_3P_3Me_3(CH_2Br)_3$ (cis-cis-cis)	9H,1.67,(12.6) [e]	6H,3.38(5.4)	3P,88.2
$N_3P_3Me_3(CH_2Br)_3$ (cis-trans-trans)	6H,1.72(12.6) [f] 3H,1.69(12.4) [g]	2H,3.35 [h,i] 4H,3.38(3.8)	3P,87.1

(a) Dilute solutions in $CDCl_3$,δ(ppm) reference internal TMS. All methyl and methylene signals are split into a doublet by coupling with phosphorus, PH coupling constants (in Hertz) in parenthesis. (b) Dilute solutions in $CDCl_3$,δ(ppm) reference external P_4O_6. (c) δ_H(Phenyl)=7.4-7.6 and 7.95-8.15. (d) The chemical shifts for H_A and H_B are calculated from the method given by R.A. Hoffman, in "NMR, Basic Principles and Progress", Vol.5, p.56; Springer-Verlag,N.Y., 1971. See Figure 2.1 for an explanation of the symbols A,B and C. (e)-(h) Long range J(PH)≈1.5,1.4,1.5 and 1.6 Hz, respectively. (i) Coupling not measureable (obscured bands).

(Figure 2.1) characteristic of two equivalent methylene groups each containing diastereotopic protons. Only the cis-trans-trans configuration of the benzoyl groups is consistent with this spectrum, and is further supported by the two singlets of relative intensity 1:2 in the ^{31}P spectrum.

The AB pattern for the four methylene protons on the same side of the ring can be realized because there is no symmetry element connecting protons H_A and H_B in each pair of methylene groups (XVIII). Thus, they

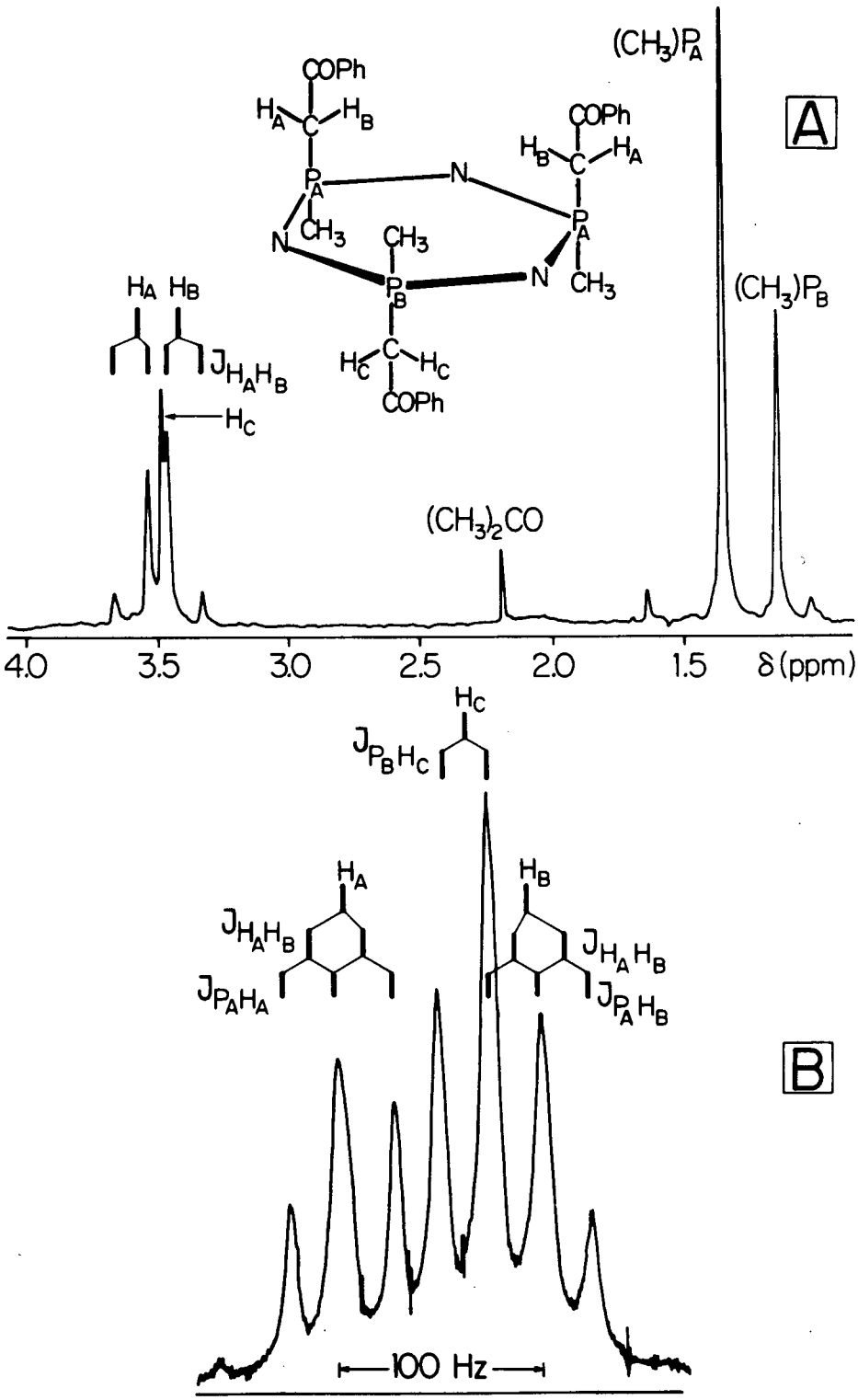

Figure 2.1. ^{31}P-decoupled 100 MHz ^{1}H n.m.r. spectrum (A) of the methylene and methyl regions of $N_3P_3Me_3[CH_2C(O)Ph]_3$, and 400 MHz ^{1}H n.m.r. spectrum (B) of just the methylene region (both on samples in $CDCl_3$ solution).

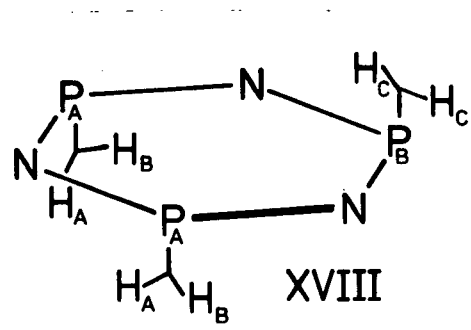

XVIII

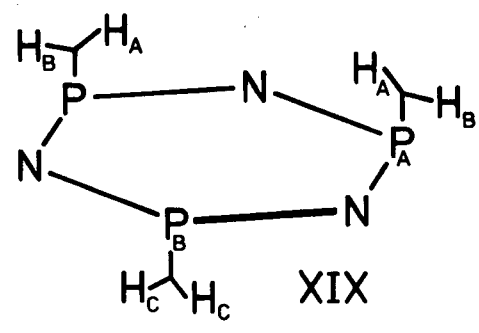

XIX

are non-equivalent by symmetry alone, but only the anisotropy of the benzene ring allows them to be differentiated magnetically. On the other hand, the methylene protons (CH_2P_B or H_C) are connected by a mirror plane (XIX) and are therefore equivalent by symmetry. Hence, only the singlet in the ^1H spectrum. A similar argument can be used to show that P_B is distinct from P_A, consistent with the fact that two singlets of relative intensity 1:2 are present in the ^{31}P spectrum. If the cis-cis-cis isomer was isolated then all the benzoyl groups would be equivalent on the n.m.r. time scale. Thus, the methyl and methylene, and phosphorus signals should appear in the ^{31}P-decoupled ^1H spectrum and the ^{31}P spectrum, respectively, as singlets, as they do for the tribromo derivative of the same configuration. For the cis-trans-trans tribromo isomer, although the differently situated methyl and methylene groups are distinguished, the ^{31}P signal is apparently a singlet and the AB pattern expected for the methylene protons on the same side of the ring is absent. Though the ^1H and ^{31}P spectra are expected to be similar in appearance to those of the tribenzoyl derivative, the small anisotropy of the bromine atom probably causes protons H_A and H_B, and phosphorus atoms P_A and P_B to be in

approximately the same magnetic field; thus producing the observed equivalence in the n.m.r. spectra.

Regarding the infrared spectra of these compounds, assignments can only be made with certainty for the ν(C=O) frequencies in $N_3P_3Me_3[CH_2C(O)Ph]_3$, the superposition of phenyl vibrations, and those of the CH_2Br group, with skeletal modes making detailed assignments difficult. For example, in $(NPMe_2)_3$, ν_{asym}(P=N) occurs at 1180 cm^{-1}, but in $N_3P_3Me_3(CH_2Br)_3$ the strong CH_2Br wagging mode interferes, so preventing the accurate assignment of the two peaks at 1167 and 1209 cm^{-1}. The spectra of the two tribromo isomers are identical.

In the C=O stretching region, two peaks at 1673 and 1659 cm^{-1} of approximate relative intensity 2:1 are observed, and coincide with the three peaks at 1675 (26.5), 1669 (27.1) and 1656 cm^{-1} (33.2) (% intensity of the base peak in brackets) in the Raman spectrum.

2.2.3A Formation and Reactions of $N_4P_4Me_4(CH_2Li)_4$

Like $N_3P_3Me_6$, octamethylcyclotetraphosphazene, $N_4P_4Me_8$, undergoes multiple deprotonation with n-BuLi or MeLi in diethyl ether to produce, in the limit of four equivalents of base, a tetracarbanion $N_4P_4Me_4(CH_2Li)_4$ (XX) (Equation 2.11). Its formation takes considerably longer than the trimeric analogue, precipitation occurring after ~30-45 minutes of heating under reflux. In some cases, using MeLi as the base, no precipitation has been observed[80], but reaction with a number of Group IV metal chlorides Me_3MCl (M=Si,Ge and Sn) has given near quantitative yields of the tetra-substituted phosphazenes $N_4P_4Me_4(CH_2MMe_3)_4$ (M=Si,Ge and Sn)[65]. Tetraethyltetramethylphosphazene ($N_4P_4Me_4Et_4$) has also been prepared by reacting XX with an excess of methyl iodide[65].

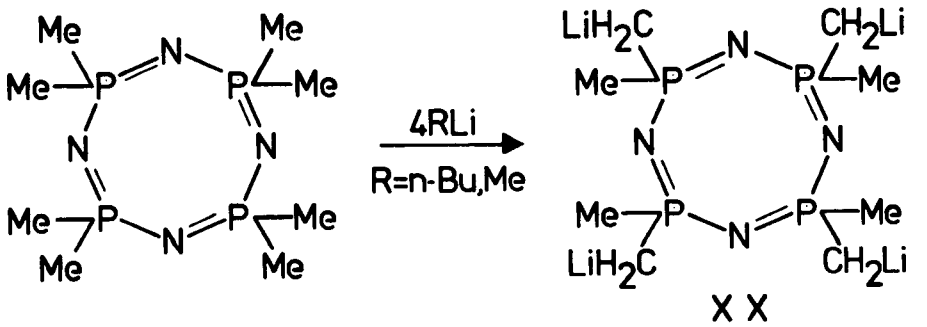

... (2.11)

$N_4P_4Me_8$ also reacts with two equivalents of MeLi followed by two equivalents of Me_3MCl (M=Si,Ge and Sn) to give the antipodally disubstituted phosphazene derivatives $N_4P_4Me_6(CH_2MMe_3)_2$ (M=Si,Ge and Sn) in high yields (Equation 2.12)[80]. However, the existence of a dicarbanion has

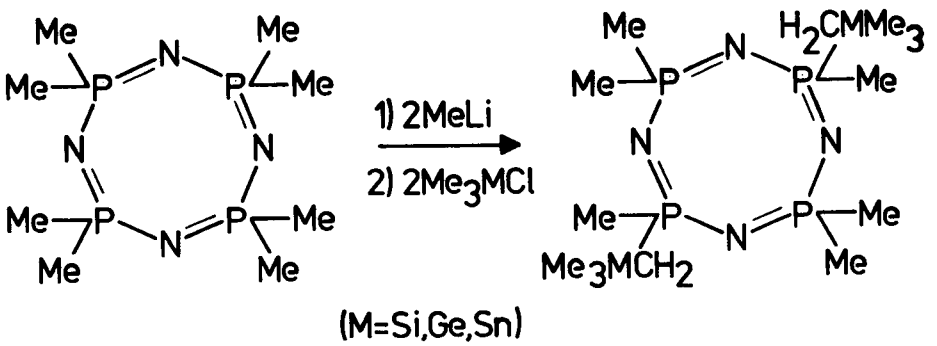

... (2.12)

not yet been confirmed because the formation of a tetracarbanion can also account for the good yields of disubstituted products, if proton abstraction from $N_4P_4Me_8$ is energetically more favorable than trisubstitution (Equations 2.12a-c). Equation 2.12b is plausible because the reaction

$$N_4P_4Me_8 \xrightarrow{2MeLi} \tfrac{1}{2}N_4P_4Me_4(CH_2Li)_4 + \tfrac{1}{2}N_4P_4Me_8 \quad \ldots (2.12a)$$

$$\tfrac{1}{2}N_4P_4Me_4(CH_2Li)_4 \xrightarrow{RX} \tfrac{1}{2}N_4P_4Me_4(CH_2Li)_2(CH_2R)_2 \quad \ldots (2.12b)$$

$$\tfrac{1}{2}N_4P_4Me_4(CH_2Li)_2(CH_2R)_2 \xrightarrow{\tfrac{1}{2}N_4P_4Me_8} \tfrac{1}{2}N_4P_4Me_6(CH_2R)_2 + \tfrac{1}{4}N_4P_4Me_8 + \tfrac{1}{4}N_4P_4Me_4(CH_2Li)_4 \quad \ldots (2.12c)$$

etc.

of excess methyl iodide with the tetracarbanion has given a small amount of the diethyl derivative, obtained as its dihydrochloride[65].

As in the case of $N_3P_3Me_6$, successive deprotonation occurs on different phosphorus atoms, giving a total of four possible diastereomers (XXI-XXIV). However, reaction of XX with pentafluorobromobenzene (C_6F_5Br),

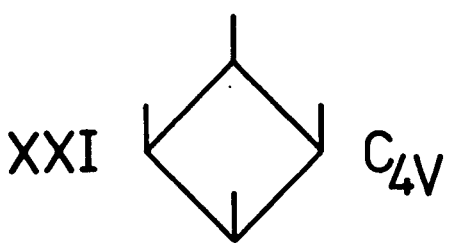

cis-cis-cis-cis

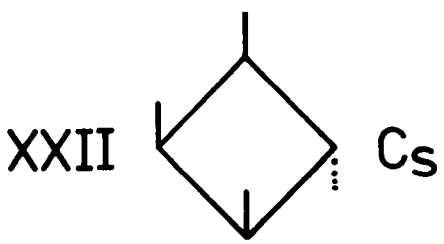

cis-cis-trans-trans

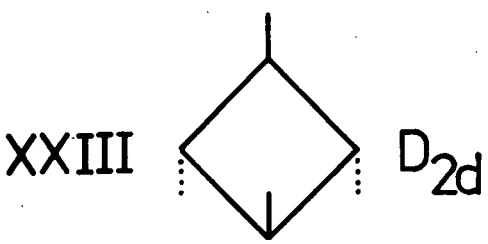

trans-trans-trans-trans

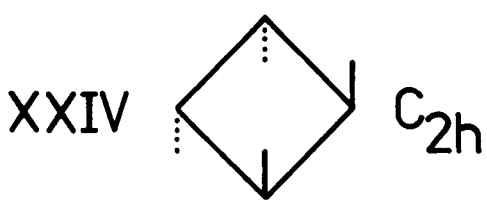

trans-cis-trans-cis

iodine (I_2) and dimethyliodoarsine (Me_2AsI) apparently gives only one isomer (Equation 2.13). The cis-cis-trans-trans structure XXII can be

$$N_4P_4Me_4(CH_2Li)_4 \xrightarrow{RX} N_4P_4Me_4(CH_2R)_4 + 4LiX \quad \ldots (2.13)$$

$R = Br, I, AsMe_2$

$X = C_6F_5, I, I$

excluded on n.m.r. grounds, but no configurational choice can be made between the three more symmetrical possibilities. Structure XXIV could be distinguished if the R groups contain a benzene ring, since an AB pattern would be expected for the methylene hydrogens; but the reaction of the tetracarbanion with ethyl benzoate is significantly different, in that it goes no further than di-substitution. Moreover, n.m.r. spectroscopy indicates vicinal, and not antipodal substitution. The reaction is not controlled by steric factors because both ethyl acetate (CH_3CO_2Et) and ethyl trifluoroacetate (CF_3CO_2Et) react to give di-substituted products (confirmed by mass spectroscopy)[90]. These results were rather surprising, and are explained in Section 2.2.4 in terms of conjugative and electrostatic effects.

Also, $N_4P_4Me_4(CH_2AsMe_2)_4$ reacts with an excess of methyl iodide to give the tetramethiodide salt $N_4P_4Me_4(CH_2AsMe_2)_4 \cdot 4MeI$. Quaternization occurs only on the four arsenic atoms, in agreement with the better nucleophilicity of the heavier Group V elements.

2.2.3B Spectra and Structure of $N_4P_4Me_{8-x}(CH_2R)_x$ Derivatives

The n.m.r. spectra of all the tetrasubstituted derivatives are qualitatively similar, in that the ^{31}P spectrum of each consists of a

singlet, and the ^{1}H spectrum shows two doublets, one each for the four equivalent methyl and methylene groups. This is exactly the pattern predicted for structures XXI and XXIII, and XXIV if the R group does not affect the magnetic field gradient about the methylene protons.

Quaternization on all four arsenic atoms in $N_4P_4Me_4(CH_2AsMe_2)_4 \cdot 4MeI$ is confirmed by the singlet in the ^{31}P spectrum, and by the large downfield shift in the ^{1}H spectrum of the $AsMe_3^+$ methyl singlet (from 1.04 to 2.36δ, Δ=1.32δ) and the CH_2As methylene doublet (from 1.76 to 3.33δ, Δ=1.57δ). The lack of a NMe triplet in the proton spectrum and the absence of a ν(C-N) stretching mode around 1070-1100 cm^{-1} in the infrared further supports exocyclic quaternization.

The interpretation of the chemical shift variations of the methylene protons (Table 2.4) in terms of a σ-inductive effect is broadly consistent with the relative electronegativities of the R groups (Br>I>$AsMe_2$). However, the ^{31}P chemical shifts indicate that I is more electronegative than Br. Generally electronegative ligands concentrate π-electron density onto phosphorus such that the shifts increase with increasing electronegativity of the substituent. Thus, at least for $N_4P_4Me_4(CH_2X)_4$ (X=Br and I), the π-inductive effect is not particularly successful in explaining the difference in chemical shifts, possibly because the difference is small and the ligands are similar.

The di-substituted derivatives are generally more informative. Of the two possible structural isomers, vicinal (XVa-b) and antipodal (XVIa-b), only the latter (XVIa) has been confirmed by X-ray crystallography, that being the structure of $N_4P_4Me_6Et_2 \cdot 2HCl$[91]. Antipodal substitution is also found in the MMe_3 derivatives (M=Si,Ge and Sn), whose

Table 2.4. ^{1}H [a] and ^{31}P [b] n.m.r. parameters of $N_4P_4Me_{8-x}(CH_2R)_x$ derivatives

Compound	$\delta_H(PMe_2)$	$\delta_H(PMe)$	$\delta_H(PCH_2R)$	$\delta_H(R)$	$-\delta_P(PMe_2)$	$-\delta_P(PMe)$
$N_4P_4Me_8$	1.51(11.5)	-	-	-	94.4	-
$N_4P_4Me_4(CH_2Br)_4$	-	1.62(12.5)	3.35(5.8)	-	-	99.61
$N_4P_4Me_4(CH_2I)_4$	-	1.69(12.3)	3.17(5.9)	-	-	102.20
$N_4P_4Me_4(CH_2AsMe_2)_4$	-	1.53(11.6)	1.76(11.1)	1.04	-	96.53
$N_4P_4Me_4(CH_2AsMe_2)_4$ * ·4MeI	-	2.10(11.6)	3.33(10.2)	2.36	-	99.68
$N_4P_4Me_6[CH_2C(O)Ph]_2$ [c] (i)	6H,1.37(12.6) 6H,1.40(12.7)	6H,1.44(13.2)	2H,H_A [d] 3.46(17.0) 2H,H_B 3.57(17.4)	7.35-7.60 7.98-8.07	95.38	101.30
$N_4P_4Me_6[CH_2C(O)Ph]_2$ [c] (ii)	12H,1.47(13.1)	6H,1.44(12.6)	2H,H_A [d] 3.50(16.6) 2H,H_B 3.61(17.0)	7.35-7.60 7.96-8.06	96.57 (11.2)	101.61 (10.6)

(a) δ(ppm), in $CDCl_3$, reference internal TMS, except * in D_2O, reference external TMS. All PH couplings are doublets; J(PH), in Hertz, in parenthesis. (b) δ(ppm) reference external P_4O_6; all in $CDCl_3$, except * in D_2O. J(PP), in Hertz, in parenthesis. (c) (i), fresh solution in $CDCl_3$; (ii), equilibrated solution in $CDCl_3$ (see Figure 2.2). (d) The chemical shifts are calculated from the method given by R.A. Hoffman, in "NMR, Basic Principles and Progress", Vol.5, p.56; Springer-Verlag, N.Y., 1971. Assignments for H_A and H_B are shown in Figure 2.2. J_{AB}=12.4 Hz.

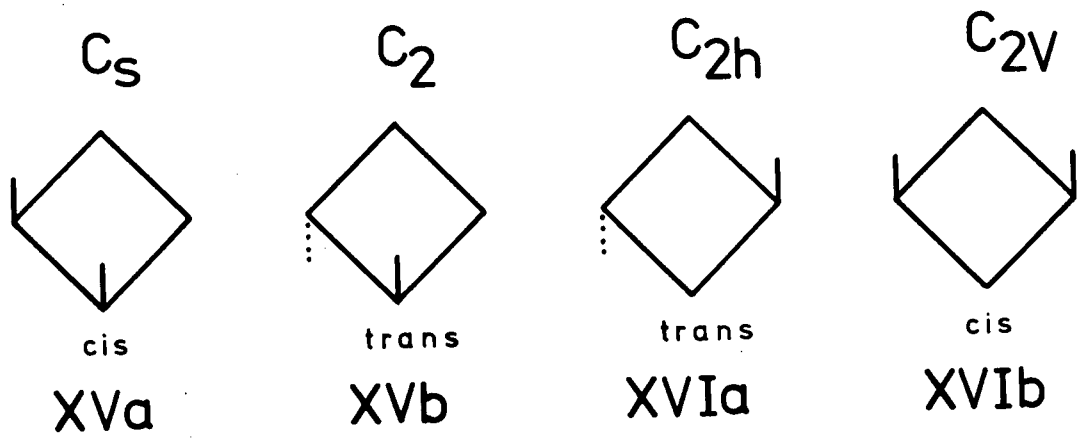

^{31}P spectra consist of a pair of 1:2:1 triplets[80]; the ^{1}H methylene spectrum is a simple doublet and the ^{1}H methyl spectrum displays two doublets of intensity ratio 1:2 ($P(Me)CH_2R$: $2PMe_2$). These compounds probably constitute the trans-configuration (XVIa) since the geminal methyl groups PMe_2 should be distinguished magnetically in the cis-form (XVIb). The ^{1}H and ^{31}P spectra of the dibenzoyl derivative are quite different from those of the antipodally substituted derivatives, and depend on both solvent and time. The ^{31}P-decoupled ^{1}H spectrum of a fresh solution in $CDCl_3$ (Figure 2.2A) exhibits a single AB pattern for the two methylene groups, and three singlets of a relative intensity 1:1:1 in the methyl region, the two methyl groups of the PMe_2 group now being distinguished. The most downfield methyl resonance is assigned to the $P(Me)CH_2R$ group because of the different PH coupling constant. The ^{31}P spectrum shows only two broadened singlets of intensity ratio 1:1, and, together with the proton spectrum, indicates vicinal substitution. (In the antipodal configuration the two protons in each equivalent methylene group are connected by a mirror plane. Thus, they are equivalent by symmetry, and will not show an AB pattern, only a singlet in the ^{31}P-decoupled ^{1}H spectrum.) If the solution is allowed to stand, a slow change occurs

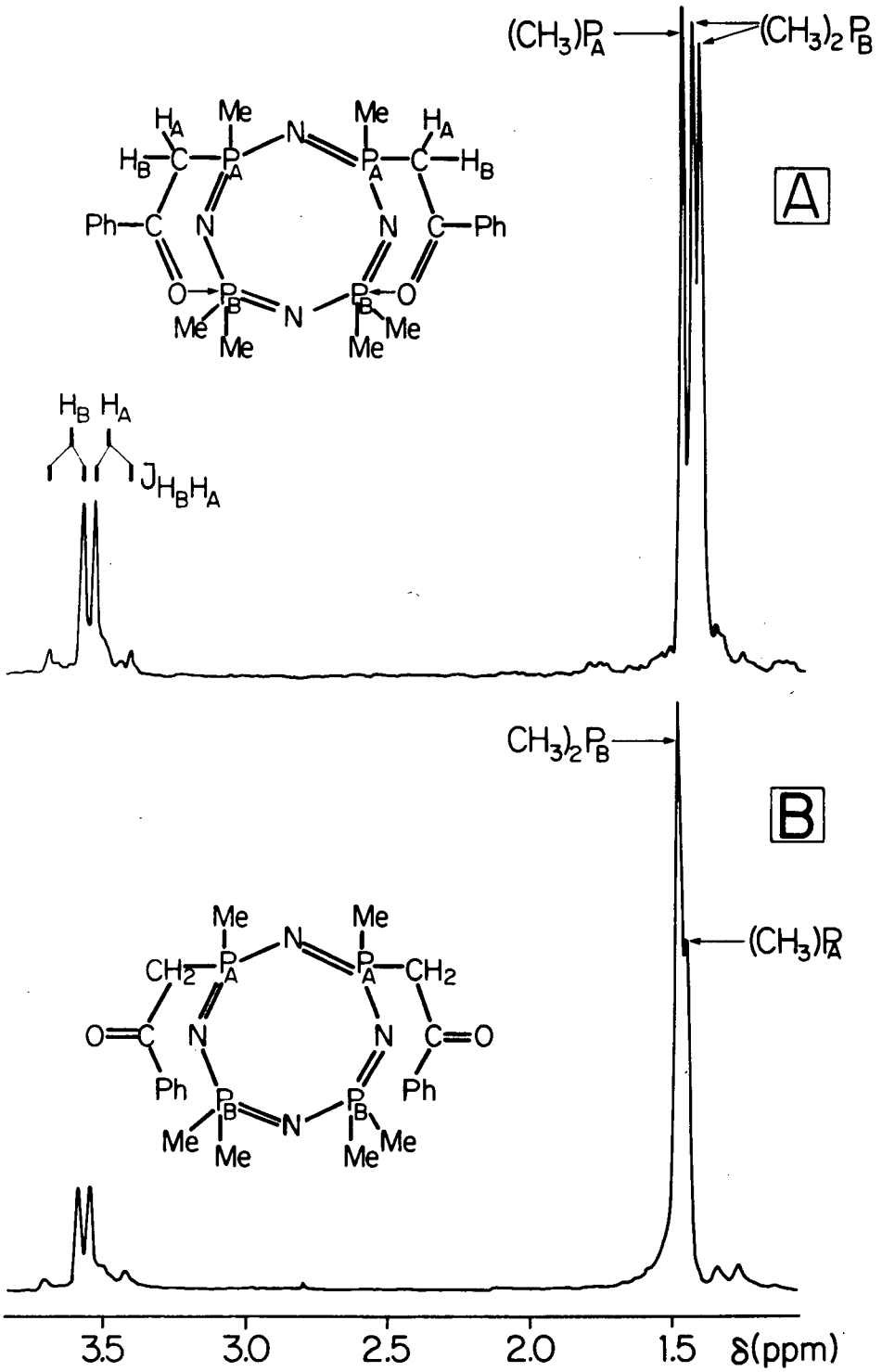

Figure 2.2. ^{31}P-decoupled 100 MHz ^{1}H n.m.r. spectrum of $N_4P_4Me_6[CH_2C(O)Ph]_2$ in a fresh solution of $CDCl_3$ (A), and after sitting in $CDCl_3$ for seven days (B).

(Figure 2.2B), and a similar but immediate change takes place in CD_3OD. The methyl signals become two singlets of relative intensity 2:1, and ^{31}P-^{31}P coupling is observed in the ^{31}P spectrum, each signal now being split into a doublet which shows virtual coupling. The AB pattern of the two equivalent methylene groups remains unchanged, even at 55°C ($CDCl_3$), thereby confirming the diastereotopic nature of the methylene protons in vicinal positions. The benzoyl groups evidently form weak intramolecular bonds possibly similar to those in a Wittig intermediate[92], as shown in XVII, which are broken by competitive hydrogen bonding of the carbonyl

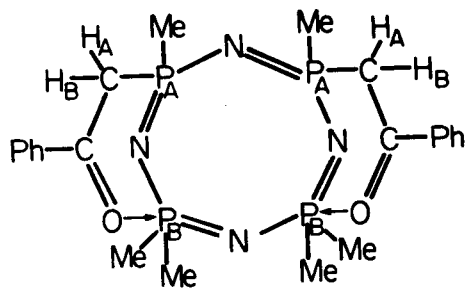

XVII

oxygen atom, slowly with $CDCl_3$, rapidly with CD_3OD. The two methyl groups of the PMe_2unit thereby become equivalent, although they are not required to be so by symmetry. Other small changes in the n.m.r. parameters reflect the altered electron distribution, the greatest of which is the upfield shift of the $Me_2\underline{P}$ phosphorus signal. Not surprisingly, the methylene protons exchange with CD_3OD. Interaction between a ring nitrogen atom and the carbon atom of a carbonyl group may also occur, as it does in $N_3P_3F_5[CH_2C(O)Ph]$[93], but the evidence is inconclusive.

The infrared spectra of the tetrahalo compounds in the PN region,

like that of the tribromo derivative, are largely uninterpretable because of interfering CH_2X (X=I,Br) wagging modes[94]. However, in the tetra-arsine derivatives, the single broad bands at ∿ 1234 and 1206 cm^{-1} can be easily assigned to ν_{asym} (P=N) for $N_4P_4Me_4(CH_2AsMe_2)_4$ and its tetramethiodide salt, respectively. Only one strong carbonyl stretching mode is observed at 1663 cm^{-1} in the infrared, and at 1661 cm^{-1} in the Raman spectrum. The infrared value of ν(C=O) is decreased from 1687 cm^{-1} in acetophenone (PhC(O)Me)[95], and is higher than 1640 cm^{-1} in $N_3P_3F_5[CH_2C(O)Ph]$[93], where intramolecular interactions lower the frequency.

2.2.4 Electronic Effects

The reaction of methylphosphazenes $(NPMe_2)_{3,4}$, metaphosphoric acids $(HPO_3)_{3,4}$ (XXVIII)[96,97] and tetrathiane $(SCH_2)_4$ (XXIX)[98] with bases is

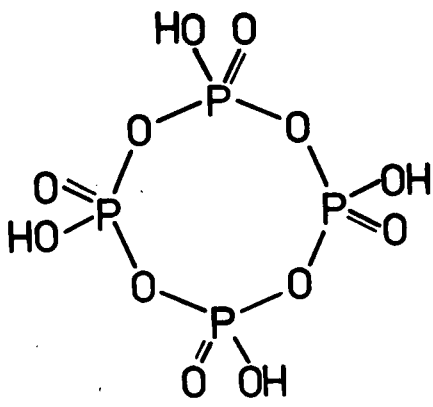

XXVIII

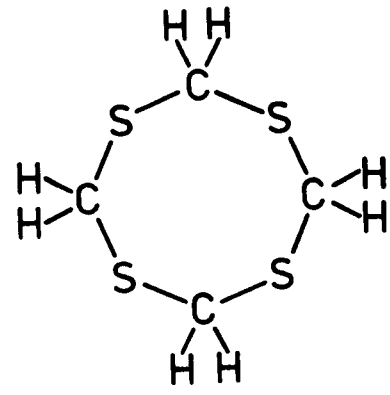

XXIX

similar in that multiple deprotonation occurs with relative ease. Normally removal of one proton would disfavor a second deprotonation by the electrostatic repulsion in the di-anion. However, two chemically significant effects both serve to reduce repulsion: cation-anion association and conjugation. For methylphosphazenes, lithium can coordinate to the ring

nitrogen atoms, as shown in XXX, thereby reducing the effective negative

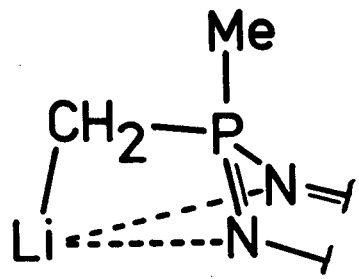

XXX

charge on carbon. Furthermore, the partial localization of the nitrogen lone pair would make an adjacent phosphorus atom more electronegative such that deprotonation of an attached methyl proton is enhanced. More important, conjugation of a carbanionic methylene group with the ring can take place, with consequent charge delocalization and stabilization of the π-electron levels. This effect provides a basis for understanding not only the occurrence of multiple deprotonation, but also the relative reactivities of the trimeric and tetrameric carbanions and the orientation pattern of the substituents.

A model Hückel molecular orbital (HMO) calculation on the N_4P_4 ring shows that the conjugation energy increases, but decreasingly so, with successive deprotonation. The calculations shown in the scheme on the following page, and throughout this section, unless specified otherwise, are based on the homomorphic π-system where $\alpha_N = \alpha_P + 2.5\beta$, $\beta_{endo} = -1.0$, $\alpha_N = -1.25$ and $\alpha_C = \alpha_P = 1.25$. $\beta_{exo} = -1.0$ for these particular calculations, which are for 16 electrons. Electron pairs localized on C are shown as dots ($\beta_{exo} = 0$) and changes in conjugation energy are shown above the arrows (in units of β).

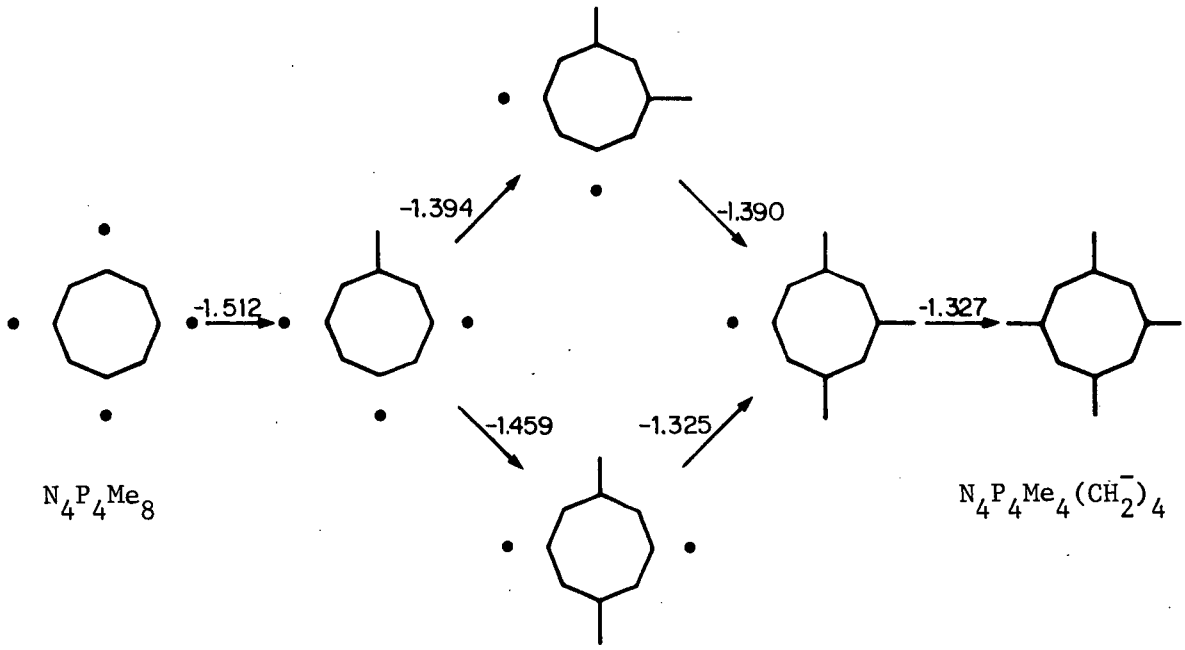

The effect of a substituent on the π-system has important consequences concerning both reactivity and orientation. In the Hückel model, the substituent is assumed to act inductively, that is it affects only the Coulomb parameter of the atom to which it is attached. One effect of an electronegative substituent such as benzoyl is to concentrate π-electron density on that phosphorus atom to which the substituent is bonded, with concurrent withdrawal of π-electron density from the nearest atoms. The positive charge induced on the neighboring phosphorus atoms, like the π-electron energy per electron, is an oscillating function of ring size[99] (Figure 2.3). The positive charge is greatest for the eight-membered ring and least for the six-membered ring, and much greater at P(2) than P(3) for any ring size. Thus, electron transfer to the ring from a carbanion function is more probable in the tetramer than in the trimer, thereby lowering the nucleophilicity of the carbanion in an eight-membered ring.

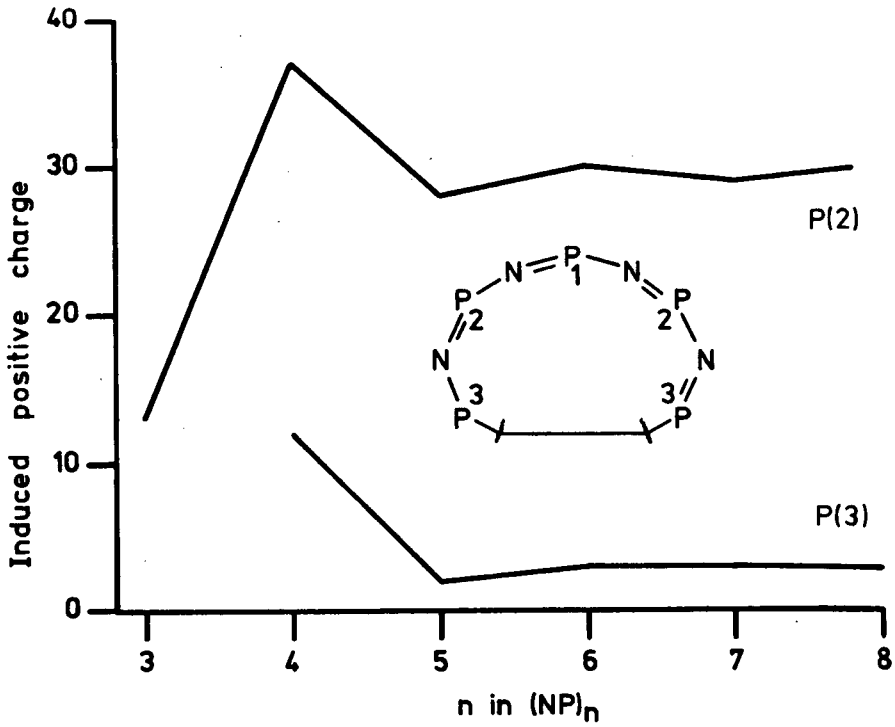

Figure 2.3. Positive charge (x 10^4) induced at P(2) and P(3) by a perturbation of 0.5β at P(1), relative to the unperturbed system. $\alpha_N = \alpha_P + 2.5\beta$. On the same scale, the charge at P(1) is -790 to -752, and at N(1) is +348 to +323.

As the exo-charge decreases towards zero, tri-substitution becomes harder, and we can understand why the reaction of the tetracarbanion with ethyl benzoate stops at di-substitution, even with an excess of the reagent, while benzoylation of the trimer goes to completion. For electropositive substituents, such as CH_2^- , the opposite effect occurs. The induced negative charge on the neighboring phosphorus atom is least in the trimer and greatest in the tetramer. Hence, successive deprotonation of $N_3P_3Me_6$ is more likely to occur faster than for $N_4P_4Me_8$, as observed qualitatively by the relative rates of precipitation.

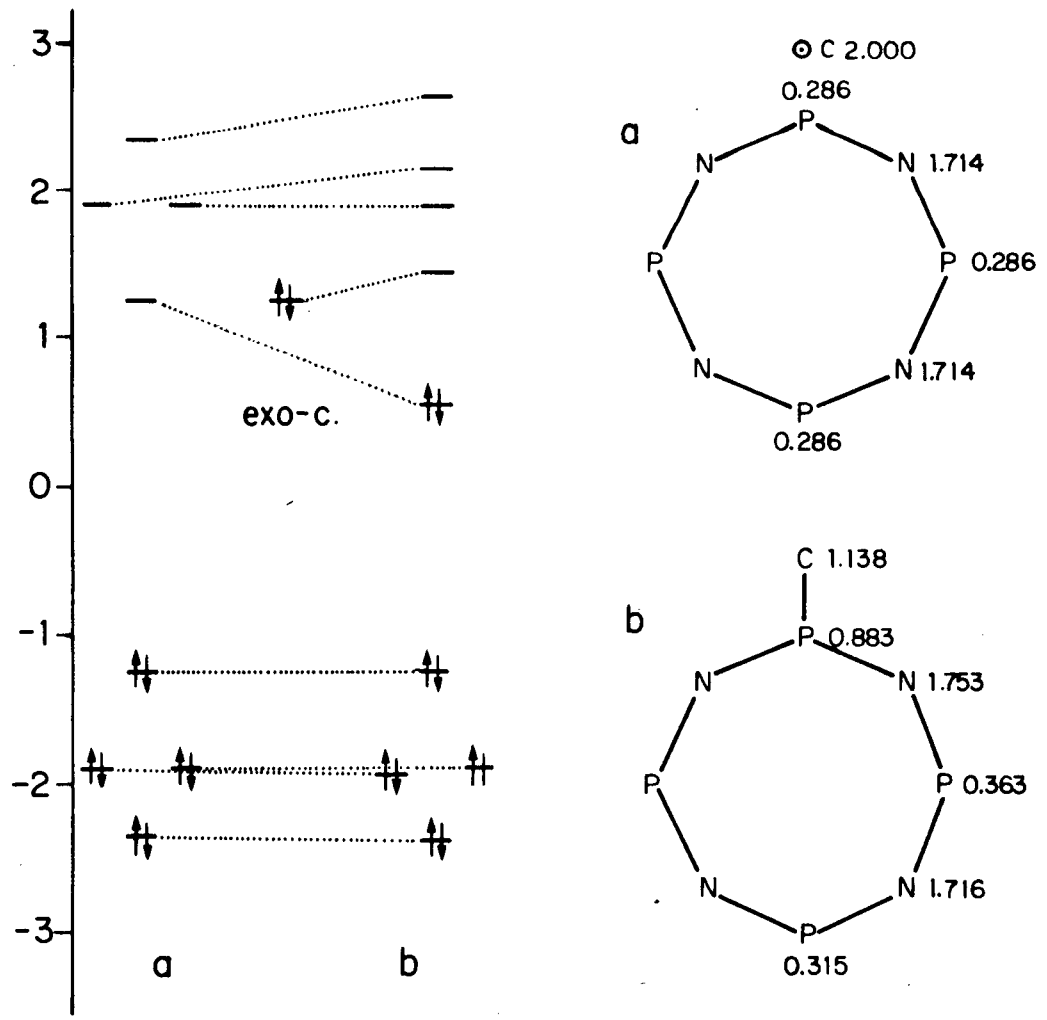

Figure 2.4. Energy levels (ev) and π-charge densities of a) an 8-membered N_4P_4 ring (α_N = -1.25, α_P = +1.25, β_{endo} = -1 ev) and b) the same, but with exocyclic conjugation to form a mono-carbanion, β_{exo} = -1 ev.

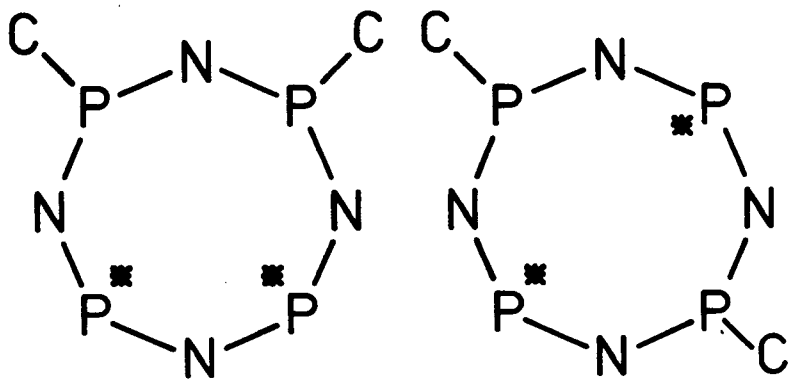

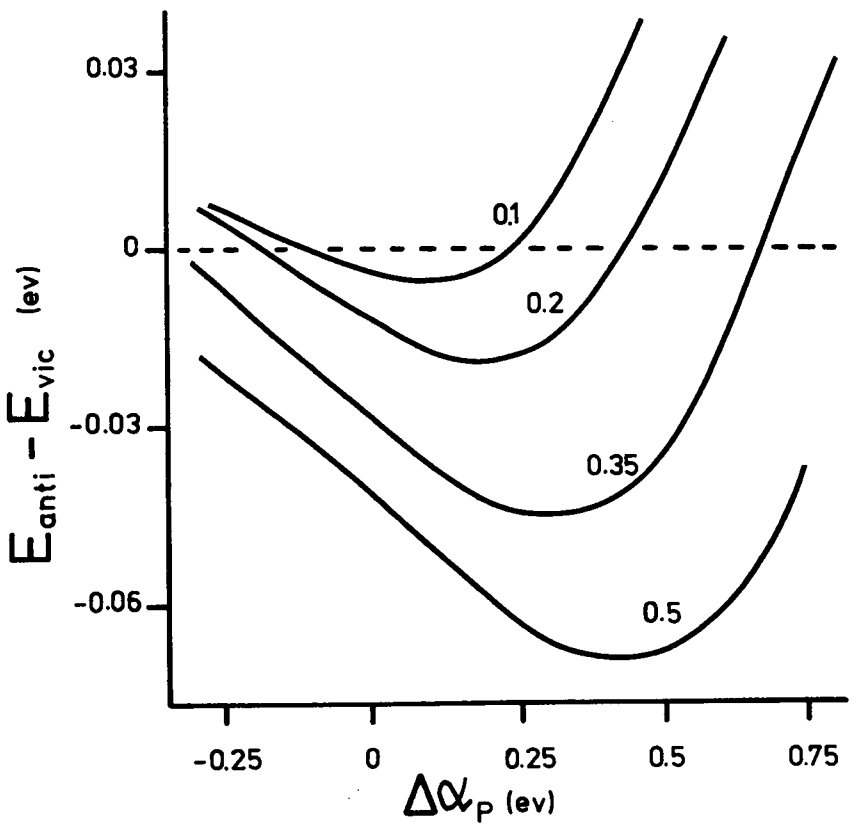

Figure 2.5. π-Energy difference between the vicinal and antipodal disubstituted dicarbanions $E_{anti} - E_{vic}$, as a function of $\Delta\alpha_P$, applied at the phosphorus atoms marked with an asterisk, for various values of $\beta_{exo} / \beta_{endo}$. $\alpha_N = \alpha_P + 2.5\beta$, $\alpha_C = \alpha_P = 1.25$, $\beta_{endo} = -1.0$. A negative value of $E_{anti} - E_{vic}$ corresponds to stability of the antipodal isomer.

The general problem of substituent orientation is more complex. The other major effect of an electronegative substituent is to stabilize the π-system by lowering the energies of the bonding and antibonding orbitals, more so for the latter. The energy effects are greatly increased if the perturbed molecule is conjugated, especially if the Coulomb parameters of C and P are assumed to be equal (Figure 2.4). In detail, the energy preference for a vicinal or an antipodal di-substituted dicarbanion differs somewhat, depending on the values of $\Delta\alpha_P$ and β_{exo}. Figure 2.5 shows the energy preference for the antipodal isomer as a function of the pertubation for various values of β_{exo}. If, for instance $\beta_{exo} = -0.35$, probably sufficient to ensure multiple deprotonation, then the vicinal isomer is more stable if $\Delta\alpha_P > 0.65$. Electropositive substituents increase the negative charge on carbon, so that such substituents will both provide additional stabilization for the antipodal isomer, and encourage tri- and tetra-substitution. In this way, we can understand why the strongly electronegative benzoyl group leads to vicinal substitution, while the methyl and Me_3M (M=Si,Ge and Sn) groups substitute antipodally. It is possible that, if the products could be isolated, more electropositive substituents might substitute vicinally.

Since electron repulsion is particularly important, the numerical conclusions will be altered by the use of better theoretical models, but Hückel theory provides a useful framework for correlating and extending experimental work.

2.3 Experimental

The reaction of $[NH_2(Ph_2)PNP(Ph_2)NH_2]^+Cl^-$ with Me_2PCl_3 was carried out in an atmosphere of dry nitrogen. Dimethyltrichlorophosphorane was

prepared by the chlorination of tetramethyldiphosphine disulphide[99a], and the bis-(aminodiphenylphosphine)-iminium chloride by the ammonolysis of diphenyltrichlorophosphorane[7,81]. Chlorobenzene was dried by distillation from calcium hydride.

The phosphazenes $(NPMe_2)_{3,4}$, which are hygroscopic, were purified and dried by sublimation in vacuo, and $N_3P_3Ph_4Me_2$ by recrystallization from ether/hexane and heating it at 100°C/24 hours. The various electrophiles (MeI, Me_2SiCl_2, $PhCO_2Et$, C_6F_5Br and I_2) which were reacted with the phosphazenyl carbanions were good quality commercial products, purified, if necessary, by distillation or sublimation. Dimethyliodoarsine was prepared according to the method used by Roberts, Turner, and Bury[100]. Diethyl ether was dried by distillation from sodium/benzophenone. n-BuLi in hexane solution, available commercially, was standardized by quenching an aliquot of it in water and titrating it against normal sulphuric acid. Because of the sensitivity of organolithium reagents to oxygen and moisture, the preparations and reactions of the carbanions were all done in an atmosphere of dry nitrogen.

2.3.1 Reaction of Me_2PCl_3 with $[NH_2(Ph_2)PNP(Ph_2)NH_2]^+Cl^-$

A slurry of Me_2PCl_3 (18.7 g, 111 mmol) and $[NH_2(Ph_2)PNP(Ph_2)NH_2]^+Cl^-$ (50.3 g, 111 mmol) in 200 ml chlorobenzene was heated under reflux for ninety minutes. The solvent was removed by distillation, and the residue heated at 120°C/0.1 Torr for forty-five minutes. The remaining glassy, light brown solid was extracted with 4 x 250 ml boiling acetonitrile. The white insoluble residue (3.43 g) of $(NPMe_2)_4 \cdot 2HCl$ was heated with triethylamine and the product extracted with hot hexane to yield 1.93 g $(NPMe_2)_4$ (6.4 mmol, 23%), identified by its melting point and infrared

spectrum. The solvent was removed from the combined extracts, and the residual light brown oil dissolved in 350 ml chloroform and 75 ml triethylamine. After stirring the solution for twelve hours, the mixture was filtered and washed with 2 x 200 ml water. The organic layer was dried over anhydrous Na_2SO_4 and the solvent removed in vacuo. The remaining brown oil was dissolved in 70 ml acetonitrile and concentrated to 30 ml. The white precipitate which formed was filtered off and extracted with diethyl ether, leaving, as the insoluble part, 1.15 g (1.4 mmol, 2.6%) of $(NPPh_2)_4$, identified by its melting point and infrared spectrum. Evaporation of the ether extract yielded long, thick, colourless needles of gem-$N_3P_3Ph_4Me_2$, which were recrystallized from ether/hexane. Yield: 6.10 g (12.9 mmol, 12%). M.pt. 142-144°C (Reference (13): 140-142°C). Anal. calcd. for $P_3N_3C_{26}H_{26}$: C, 65.96; H, 5.54; N, 8.88. Found: C, 65.89; H, 5.66; N, 8.81.

The acetonitrile filtrate was evaporated under reduced pressure and the residue extracted with 2 x 250 ml hot hexane. Evaporation of the hexane extracts yielded a pale yellow oil, which was dissolved in 1:1 ether/hexane. This solution was passed through a column of Silicar CC-7, and evaporated to give a crystalline mixture. Blocks of $N_4P_4Me_4Ph_4$ were separated manually. Yield: 2.50 g (4.6 mmol, 8.2%). M.pt. 132.5-133.5°C. Anal. calcd. for $P_4N_4C_{28}H_{32}$: C, 61.32; H, 5.88; N, 10.21. Found: C, 61.44; H, 5.95; N, 10.29. From the remainder (10.51 g), a further 4.2 g of gem-$N_3P_3Ph_4Me_2$ was isolated by recrystallization, the total yield being 18.2%, based on the Me_2PCl_3.

2.3.2 Preparation of $N_4P_4Me_4Ph_4 \cdot MeI$

A sample of $N_4P_4Ph_4Me_4$ (0.296 g, 0.54 mmol) was dissolved in 20 ml methyl iodide and the solution heated under reflux for twelve hours. The

addition of 150 ml diethyl ether precipitated $N_4P_4Me_4Ph_4 \cdot MeI$, which was recrystallized from toluene/acetonitrile as colourless needles of a toluene adduct. The powdered crystals were heated at 95°C/0.1 Torr for three hours to give $N_4P_4Me_4Ph_4 \cdot MeI$. Yield: 0.328 g (88%). M.pt. 232.5-233°C. Anal. calcd. for $P_4N_4C_{29}H_{35}I$: C, 50.45; H, 5.11; N, 8.11; I, 18.38. Found: C, 50.41; H, 5.09; N, 7.98; I, 18.20.

2.3.3 Preparation of $(N_3P_3Ph_4MeCH_2)_2SiMe_2$

A solution of n-butyl lithium in hexane (0.55 ml, equivalent to 1.21 mmol) was added dropwise from a syringe, to a stirred solution of gem-$N_3P_3Ph_4Me_2$ (0.551 g, 1.16 mmol) in 75 ml diethyl ether. Precipitation of the lithio-derivative gem-$N_3P_3Ph_4Me(CH_2Li)$ occurred after one minute. The mixture was heated under reflux for one hour and then cooled to -50°C. Dimethyldichlorosilane (0.090 g, 0.70 mmol, 20% xs) in 10 ml ether was slowly added resulting in an immediate lessening of turbidity in the reaction mixture, which was then allowed to warm slowly to room temperature. After twenty-four hours the lithium chloride was filtered off and the solvent removed. The residual oil was dissolved in ether and eluted with 500 ml ether on a column of silicar CC-7. The clear, pale yellow oil remaining after evaporation of the solvent contained some $N_3P_3Ph_4Me_2$, which was partially removed by distillation at 200°C/0.03 Torr. The resulting brown gummy residue was extracted with 4 x 50 ml hexane to give, after evaporation of the combined hexane extracts, a white solid identified by its ^1H n.m.r. spectrum and by tlc (chloroform) as a mixture $N_3P_3Ph_4Me_2$ and $(N_3P_3Ph_4MeCH_2)_2SiMe_2$. The product was freed from traces of starting material by repeated crystallization, as tiny needles, from hexane. Yield: 0.260 g (45%).

M.pt. 163-164.5°C. Anal. calcd. for $P_6N_6C_{54}H_{56}Si$: C, 64.67; H, 5.63; N, 8.38. Found: C, 64.53; H, 5.78; N, 8.20.

2.3.4 Preparation and Reactions of $N_xP_xMe_x(CH_2Li)_x$ (x=3,4)

2.3.4A Preparation of $N_xP_xMe_x(CH_2Li)_x$

In a typical preparation, a slight molar excess (∿ 5-10% xs) of n-butyl lithium in hexane was added dropwise from a syringe, to a stirred solution of $(NPMe_2)_{3 \text{ or } 4}$ in diethyl ether. A heavy white precipitate of $N_3P_3Me_3(CH_2Li)_3$ was formed immediately, while ∿ 30-45 minutes of heating under reflux was required to precipitate $N_4P_4Me_4(CH_2Li)_4$. To ensure completion of the reactions, the mixtures were gently heated under reflux for two hours before reacting them with an electrophile.

2.3.4B Preparation of $N_3P_3Me_3(CH_2Br)_3$

A solution of bromopentafluorobenzene (2.322 g, 9.40 mmol, 5% deficit) in 60 ml ether was added, over a period of fifteen minutes, to a cold slurry (-78°C) of $N_3P_3Me_3(CH_2Li)_3$ prepared from the reaction of $N_3P_3Me_6$ (0.743 g in 75 ml ether, 3.30 mmol) and n-butyl lithium (4.15 ml in hexane, 10.13 mmol). The turbidity decreased, and the reaction mixture became yellow and finally dark brown on being allowed to warm to -20°C over a period of 3.5 hours; the addition of 50 ml aqueous HCl (10.2 mmol) removed most of the colour. The ether layer was washed with 2 x 25 ml water and dried over Na_2SO_4. After removal of the solvent, the light brown residue was washed with acetone. The remaining white solid was identified by its ^1H and ^{31}P n.m.r. spectra and by tlc (50/50 acetone/hexane) as a mixture of two isomers of $N_3P_3Me_3(CH_2Br)_3$. Yield: 0.152 g (10.5%). Anal. calcd. for $C_6H_{15}N_3P_3Br_3$:

C, 15.60; H, 3.27; N, 9.10; Br, 51.91. Found: C, 15.89; H, 3.10; N, 9.00; Br, 51.50. The isomers (cis-cis-cis:cis-trans-trans - 1:3) were partly separated by crystallization from acetone, in which the latter is the more soluble. If n-butyl lithium and bromopentafluorobenzene are both used in 10% excess, some tetrabromo derivatives are formed.

2.3.4C Preparation of $N_3P_3Me_3[CH_2C(O)Ph]_3$

A solution of ethyl benzoate (1.107 g, 7.37 mmol) in 60 ml ether was added, over a period of ten minutes, to a cold slurry (-35°C) of $N_3P_3Me_3(CH_2Li)_3$ prepared from the reaction of $N_3P_3Me_6$ (0.500 g in 125 ml ether, 2.22 mmol) and n-butyl lithium (3.00 ml in hexane, 7.29 mmol). Midway through the addition the turbidity rapidly decreased. The solution was almost clear at -35°C but became more turbid with time and increase in temperature. The temperature was allowed to rise to room temperature, and 75 ml aqueous potassium fluoride (0.5 M) was added after sixteen hours to precipitate the lithium as its fluoride. The ether layer was separated, washed with 50 ml water and dried over Na_2SO_4. Removal of the ether left a pale yellow oil, which was distilled under reduced pressure to give 0.301 g unreacted ethyl benzoate. The residual white solid was recrystallized twice from acetone as colourless flakes of $N_3P_3Me_3[CH_2C(O)Ph]_3$. Yield: 0.070 g (7.3%, based on the amount of ethyl benzoate that reacted). M.pt. 173-177°C. Anal. calcd. for $N_3P_3C_{27}H_{30}O_3$: C, 60.34; H, 5.63; N, 7.82. Found: C, 60.06; H, 5.59; N, 7.89.

2.3.4D Preparation of $N_4P_4Me_4(CH_2Br)_4$

A solution of bromopentafluorobenzene (5.391 g, 21.83 mmol) in 50 ml ether was added, over a period of ten minutes, to a cold slurry (-78°C) of

$N_4P_4Me_4(CH_2Li)_4$ prepared from the reaction of $N_4P_4Me_8$ (1.500 g in 90 ml ether, 5.00 mmol) and n-BuLi (8.30 ml in hexane, 21.83 mmol). The temperature was raised to -10°C over two hours, the solution washed with 60 ml H_2O, and the golden brown ether layer dried over Na_2SO_4 and evaporated. A white solid was deposited from the residual oil, and was washed with acetone and recrystallized from chloroform as colourless blocks of $N_4P_4Me_4(CH_2Br)_4$. Yield: 1.846 g (60%). M.pt. 155-156°C. Anal. calcd. for $P_4N_4C_8H_{20}Br_4$: C, 15.60; H, 3.27; N, 9.10; Br, 51.91. Found: C, 15.79; H, 3.45; N, 9.07; Br, 51.80.

2.3.4E Preparation of $N_4P_4Me_4(CH_2I)_4$

An excess of iodine (2.839 g, 11.18 mmol) was added to a cold slurry (-78°C) of $N_4P_4Me_4(CH_2Li)_4$ prepared from the reaction of $N_4P_4Me_8$ (0.759 g in 70 ml ether, 2.53 mmol) and n-BuLi (4.40 ml in hexane, 11.18 mmol). The iodine dissolved as the temperature rose. The reaction mixture was stirred at room temperature for sixty-two hours, the ether was distilled off, and the unreacted iodine was removed by titration with aqueous potassium iodide/sodium thiosulphate. The aqueous layer was discarded and the product was precipitated as a white solid on the addition of acetonitrile to the residual red-brown oil. Crystallization of this solid from acetone produced small colourless flakes of $N_4P_4Me_4(CH_2I)_4$. Yield: 0.152 g (14.5%, based on amount of iodine that reacted). M.pt. 158.5-159.5°C. Anal. calcd. for $P_4N_4C_8H_{20}I_4$: C, 11.95; H, 2.51; N, 6.97; I, 63.15. Found: C, 12.12; H, 2.42; N, 6.92; I, 62.89.

2.3.4F Preparation of $N_4P_4Me_4(CH_2AsMe_2)_4$

A pale yellow solution of dimethyliodoarsine (1.436 g, 6.19 mmol) in

60 ml ether was added, over a period of ten minutes, to a cold slurry (-78°C) of $N_4P_4Me_4(CH_2Li)_4$ prepared from the reaction of $N_4P_4Me_8$ (0.465 g in 80 ml ether, 1.55 mmol) and n-BuLi (3.00 ml in hexane, 6.3 mmol). The turbidity of the mixture became less intense following the addition. The mixture was then allowed to reach room temperature overnight, during which time a clear, colourless solution developed. 50 ml aqueous potassium fluoride (0.5 M) was added to precipitate lithium fluoride. The ether layer was separated, washed with 25 ml water, dried over Na_2SO_4 and the solvent removed in vacuo. The residual clear, colourless oil was distilled under reduced pressure to yield pure $N_4P_4Me_4(CH_2AsMe_2)_4$, a viscous, hygroscopic and foul-smelling liquid. Yield: 0.610 g (55%). Anal. calcd. for $N_4P_4C_{16}H_{44}As_4$: C, 26.84; H, 6.19; N, 7.82. Found: C, 27.09; H, 6.11; N, 7.78. A quaternary salt $N_4P_4Me_4(CH_2AsMe_2)_4 \cdot 4MeI$ was prepared by the addition of $N_4P_4Me_4(CH_2AsMe_2)_4$ (0.150 g, 0.21 mmol) to a large excess ($\sim$ 10 ml) of methyl iodide. After three hours of stirring at room temperature, a white solid was filtered off, washed with ether and recrystallized from water as small platelets of a mono-hydrate. It is insoluble in acetonitrile and chloroform. Yield: 0.237 g (88%). M.pt. 280°C (dec). Anal. calcd. for $N_4P_4C_{20}H_{58}As_4I_4O$: C, 18.45; H, 4.49; N, 4.30. Found: C, 18.64; H, 4.53; N, 4.23.

2.3.4G Preparation of $N_4P_4Me_6[CH_2C(O)Ph]_2$

A solution of ethyl benzoate (1.319 g, 8.78 mmol) in 70 ml ether was added, over a period of ten minutes, to a cold slurry (-78°C) of $N_4P_4Me_4(CH_2Li)_4$ prepared from the reaction of $N_4P_4Me_8$ (0.660 g in 75 ml ether, 2.20 mmol) and n-BuLi (4.18 ml in hexane, 8.78 mmol). On slowly warming to room temperature the turbidity gradually decreased, leaving the solution

slightly turbid after five hours of stirring. 50 ml aqueous potassium fluoride (0.5 M) was then added; the organic layer was separated, washed with 50 ml water, dried over Na_2SO_4 and the solvent removed *in vacuo*. Unchanged ethyl benzoate was distilled from the oily residue *in vacuo*. The addition of acetonitrile to the remaining pasty solid yielded a fluffy, white solid, which was purified by repeated crystallization from acetonitrile as white blocks of $N_4P_4Me_6[CH_2C(O)Ph]_2$. Yield: 0.268 g (24%). M.pt. 152.5-156°C. Anal. calcd. for $N_4P_4C_{22}H_{32}O_2$: C, 51.97; H, 6.34; N, 11.02. Found: C, 52.23; H, 6.29; N, 11.06.

CHAPTER 3

PREPARATION OF 1-PYRAZOLYLPHOSPHAZENES

As was mentioned in the introductory chapter, cyclic phosphazenes containing linear and non-aromatic cyclic amino-groups joined by a PN bond are known extensively, and their physical and chemical properties are significantly influenced by exocyclic π-bonding involving the lone pair of electrons on the amino-nitrogen. However, cyclic phosphazenes incorporating aromatic heterocyclic rings joined by a PN bond are little known, yet offer a special interest, in that the lone pair of electrons on the nitrogen atom normally contributes to the aromaticity of the ring. Thus, electronic delocalization into the phosphazene ring in these compounds is expected to be significantly weaker than in the non-aromatic amino-derivatives, and this in turn should be reflected in their structural and chemical properties.

Phosphazenes in which the ring is joined to a pyrazole nucleus have an added feature, in that the pyridine-type nitrogen N(2) (see Figure 3.1)

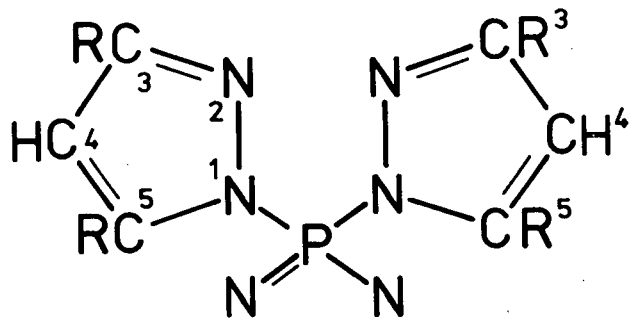

Figure 3.1. Numbering system for 1-pyrazolylphosphazenes.

contains an electron pair that is not formally involved in the aromatic sextet, and consequently, is expected to act as a coordination site[69,101-104]. The potential of 1-pyrazolylphosphazenes to act as donors to transition metal ions is an important part of their chemistry and will be discussed in the following chapter.

The primary concern of this chapter is to describe, in Section 3.1.1, the synthetic methods for preparing 1-pyrazolylphosphazenes $[NP(R^3R^5pz)_2]_n$*, and then to analyze their structural, spectral and chemical properties. The preparation of the partially pyrazolated phosphazenes gem-$N_3P_3Ph_2(Me_2pz)_4$ and gem-$N_3P_3Ph_4(Me_xpz)_2$ (x=1,2) is described in Section 3.2.1 of this chapter. Their usefulness stems from the fact that they contain fewer pyrazole groups than do the fully pyrazolated phosphazenes; they therefore provide simpler models for the study of the coordination chemistry of the pz unit and allow a comparison of the properties of the monomer unit $\{N=P(Me_2pz)_2\}$ in the different compounds. The crystal and molecular structure of $[NP(Me_2pz)_2]_4$ has been determined[104] for a comparison of its structural features with other known tetrameric phosphazenes. The crystal and molecular structures of gem-$N_3P_3Ph_2(Me_2pz)_4$ and gem-$N_3P_3Ph_2(Me_2pz)_4 \cdot ZnCl_2$ have also been determined[62], so as to find the effect of coordination on molecular geometry (see Chapter 5).

---

*The following abbreviations will be used throughout the remainder of this thesis:

$R^3=R^5=H$ ⟶ pz will denote the 1-pyrazolyl group.

$R^3=Me, R^5=H$ ⟶ Mepz will denote the 1-pyrazolyl group with a methyl group on C(3).

$R^3=R^5=Me$ ⟶ Me_2pz will denote the 1-pyrazolyl group with a methyl group on C(3) and C(5).

pzH is pyrazole, MepzH is 3-methylpyrazole and Me_2pzH is 3,5-dimethylpyrazole.

3.1 1-Pyrazolylphosphazenes $[NP(R^3R^5pz)_2]_n$

3.1.1 Preparation of $[NP(R^3R^5pz)_2]_n$

The ammonolysis of PCl_5 is one of the most important reactions in phosphazene chemistry, because it provides suitable quantities of the higher cyclic polymers, from $(NPCl_2)_5$ upwards. Other derivatives of large ring size must therefore be prepared by displacement of the appropriate chloride. In general, substitution reactions can be performed on either the fluoride or the chloride, as illustrated by the known synthetic routes to dimethylaminophosphazenes[26] (Equation 3.1 and 3.2). However, the corresponding pyrazolylphosphazenes have yet to be prepared from the fluorides

$$(NPX_2)_3 + 2Me_2NH \xrightarrow[(X=Cl,F)]{Et_2O} N_3P_3X_5(Me_2N) + Me_2NH\cdot HX \qquad \ldots (3.1)$$

$$(NPF_2)_3 + Me_3MNMe_2 \xrightarrow[\substack{M=Sn}]{\substack{M=Si,\\ \text{no solvent}\\ Et_2O/-78^\circ C}} N_3P_3F_5(NMe_2) + Me_3MF \qquad \ldots (3.2)$$

using similar procedures. Thus, sodium and potassium pyrazolide in THF failed to produce the expected precipitate of alkali fluoride, and only unreacted fluorophosphazene and hydrolyzed Mpz (M=Na,K) were recovered after evaporating the solvent. Trimethylsilylpyrazole (Me_3Sipz) and $(NPF_2)_5$ in a sealed tube did not react, even at 180°C. However, in the case of the more reactive trimethylstannylpyrazole (Me_3Snpz), a precipitate of Me_3SnF was observed in THF (checked by infrared[105]), but no phosphazene containing a pyrazole group was isolated. These results are not surprising in view of the fact that phosphorus trifluoride reacts only with Me_3Snpz and not pzH or Me_3Sipz[77] (Equation 3.3). The lack of reactivity with pzH

$$PF_3 + 3Me_3Snpz \longrightarrow 3Me_3SnF + P(pz)_3 \quad \ldots (3.3)$$

can probably be accounted for by its low base strength (pK_{BH^+} 2.47[66]), since trimethylsilylimidazole (Me_3SiIm) reacts readily with $(NPF_2)_5$[90] (pK_{BH^+}: ImH 6.95[66]), and by the high strength of the PF bond.

When chlorophosphazenes, rather than fluorophosphazenes, are employed, the substitution reactions are more successful, probably because of the weaker P-Cl bond. Thus, the pyrazolylphosphazenes $(NPpz_2)_{3-6}$, $[NP(Mepz)_2]_{3-5}$ and $[NP(Me_2pz)_2]_{3,4}$ have all been prepared from the appropriate chloride and an excess of the pyrazole in THF, triethylamine being used as an acceptor for hydrogen chloride (Equation 3.4). Unfortunately their preparation has met with only limited success; yields are low and the expected products can be equally regarded as by-products.

$$(NPCl_2)_n + 2nR^3R^5pzH \xrightarrow[THF/65°C]{2nEt_3N} [NP(R^3R^5pz)_2]_n + 2nEt_3N\cdot HCl \quad \ldots (3.4)$$

Yields are dependent upon: a) the amount of excess pyrazole and Et_3N, b) the solvent, c) the substituents on the pyrazole ring and d) the size of the phosphazene ring. Unidentified by-products precipitated with $Et_3N\cdot HCl$ in all the reactions. It was found that, although a nearly quantitative amount of $Et_3N\cdot HCl$ was produced in each case, the amount of by-products recovered could be decreased, and in some cases eliminated, if the amount of excess pyrazole and Et_3N was minimized and benzene substituted for THF. Correspondingly, the yields of the expected products also increased (Table 3.1).

Although alkylation of the 3- and/or 5-position of the pyrazole ring increases its basicity (pK_{BH^+}: MepzH 3.56[66], Me_2pzH 4.38[66]), its

Table 3.1. Yields for the reaction $(NPCl_2)_n + 2nR^3R^5pzH \xrightarrow[\text{reflux}]{2nEt_3N}$ $[NP(R^3R^5pz)_2]_n + 2nEt_3N\cdot HCl$

REAGENTS			SOLVENT	PRODUCTS		
$(NPCl_2)_n$ grams	R^3R^5pzH g(%xs)	Et_3N g(%xs)		$[NP(R^3R^5pz)_2]_n$ g(% yield)	$Et_3N\cdot HCl$ g(%yield)	by-products grams
n=3	pzH		THF	$(NPpz_2)_3$		
1.100	1.616(25)	2.113(10)		0.301(18)	2.500(96)	0.820
n=4	pzH		THF	$(NPpz_2)_4$		
1.057	1.863(50)	1.939(5)		0.300(20)	2.302(92)	1.318
n=5	pzH		THF	$(NPpz_2)_5$		
3.889	5.026(10)	7.131(5)		2.705(45)	8.525(92)	1.313
n=6	pzH		THF	$(NPpz_2)_6$		
2.133	3.132(25)	3.911(5)		0.692(21)	4.762(94)	1.021
n=3	MepzH		THF	$[NP(Mepz)_2]_3$		
1.602	2.400(6)	3.077(10)		0.870(30)	3.652(96)	1.412
n=4	MepzH		THF	$[NP(Mepz)_2]_4$		
1.515	2.347(9)	2.910(10)		1.601(59)	3.419(95)	0.387
n=3	Me_2pzH		THF	$[NP(Me_2pz)_2]_3$		
1.656	3.205(17)	3.181(10)		1.960(58)	3.658(93)	0.512
1.772	3.093(5)	3.250(5)	C_6H_6	3.260(91)	4.210(100)	0.000
n=4	Me_2pzH		THF	$[NP(Me_2pz)_2]_4$		
1.863	3.500(13)	3.579(10)		0.303(8)	4.160(94)	0.993
1.791	2.972(0)	3.441(10)	THF	0.621(17)	4.043(95)	0.433

nucleophilicity is partially governed by steric factors. In practice, the reaction of Me_2pzH with either $(NPCl_2)_5$ or $(NPCl_2)_6$ gives nearly theoretical yields of $Et_3N{\cdot}HCl$ but none of the expected product. The residue consists of the usual by-products insoluble in THF or C_6H_6, significant quantities of Me_2pzH, and chloroform insoluble solids that melted > 350°C. The substitution of MepzH for Me_2pzH gave similar results, except that some $[NP(Mepz)_2]_5$ was found, contaminated with large amounts of MepzH. However, the consistently good yields of $Et_3N{\cdot}HCl$ in all the reactions and the relatively high yields of the methylated trimeric pyrazolylphosphazenes suggest that: 1) the reactivity of pyrazole and its methyl derivatives towards chlorophosphazenes parallels its affinity for the hydrogen ion, 2) steric factors are of limited importance and 3) the expected products are formed in all cases but inter- and intra-molecular interactions become more dominant as the size of the phosphazene increases. If steric factors are important then the yields of $Et_3N{\cdot}HCl$ would be expected to decrease with progressive methylation of the pyrazole ring. The greater flexibility of the larger rings and the increase in electron density at the pyridine-type nitrogen N(2) upon methylation would facilitate inter- and intra-molecular interactions, and probably accounts for the unusually large amounts of Me_2pzH and MepzH recovered in the pentameric and hexameric reactions (Figure 3.2). Therefore, yields of the trimeric pyrazolylphosphazenes are primarily controlled by the solvent and the excess pyrazole/Et_3N while those of the larger ring sizes are governed by mainly ring interactions.

The nature of the pyrazolation reactions resembles quite closely that of the reaction between catechol and $(NPCl_2)_3$ in THF[106] (Equation 3.5).

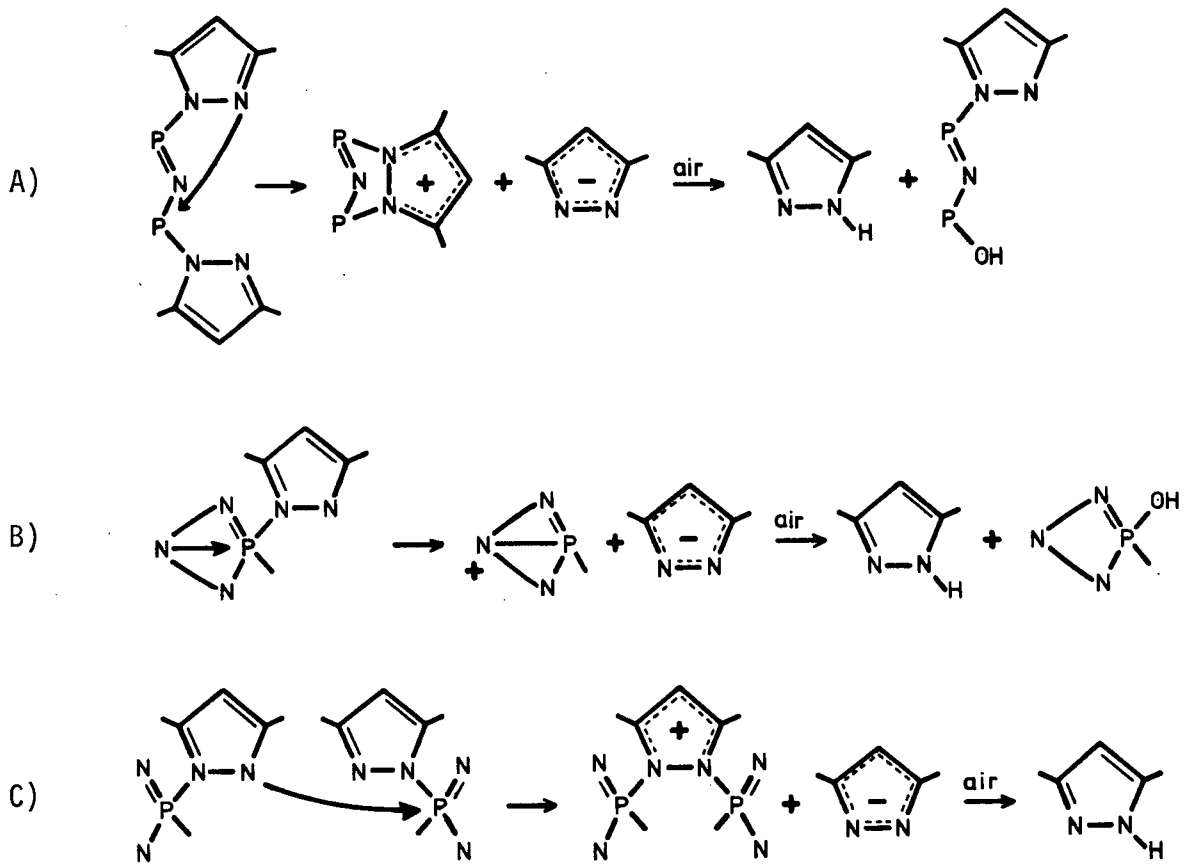

Figure 3.2. Possible intra- and inter-molecular interactions for the production of pyrazole.

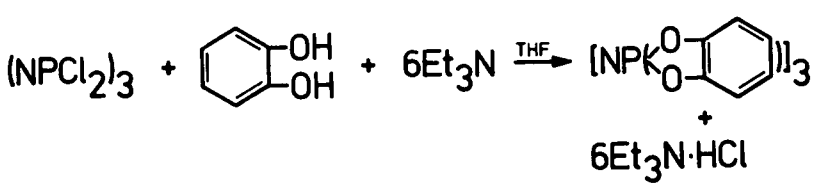

... (3.5)

The products that precipitated with the 90% yield of the $Et_3N \cdot HCl$ were shown to be the expected spirophosphazene as well as a spirophosphorane (Ia-b) resulting from ring degradation by both excess catechol and triethylamine. Furthermore, cross-linked polymers, formed by reactions between different chlorophosphazene molecules, remained soluble in the THF

Ia

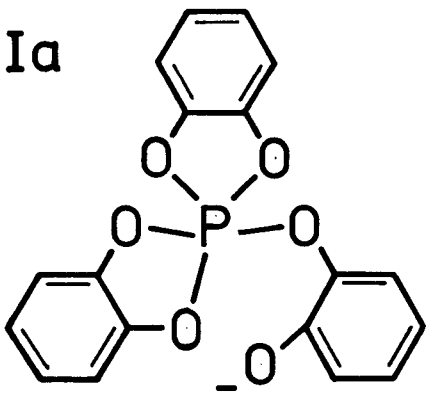

$HNEt_3^+$

Ib

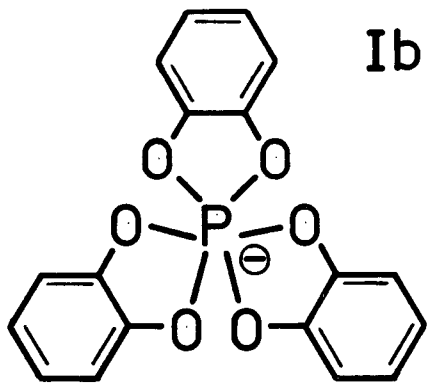

$HNEt_3^+$

filtrate, but became insoluble after evaporation of the solvent and exposure to the atmosphere. More important is the fact that no tetrameric or polymeric derivatives $[NP(O_2C_6H_4)]_{4 \text{ or } n}$ were isolated after reaction with the corresponding chloride, implying that the larger rings are more susceptible to degradative attack.

3.1.2 Structure and Spectra of 1-Pyrazolylphosphazenes

3.1.2A ^1H n.m.r. of $[NP(R^3R^5pz)_2]_n$

Proton n.m.r. spectra indicate that the pyrazole groups on a particular compound are magnetically equivalent and that the 3- and 5-positions on the pyrazole ring are differentiated, but the peak separation is dependent on both solvent and temperature. Spectra run in either CS_2 or CCl_4 at ambient temperature show just a single peak for R^3=R^5=H or Me,

and only give separate resonances on varying the temperature. However, the expected non-equivalence of the 3- and 5-positions is established using chloroform (d^1), toluene (d^8), dimethylsulfoxide (d^6) and nitrobenzene. The bulk of the work in which the solvent and temperature were varied was done on gem-$N_3P_3Ph_2(Me_2pz)_4$ because of its better solubility. The results are presented in Table 3.2. They show that the peak separation at ambient temperature is greatest for the aromatic solvents and varies either directly or inversely with temperature depending on the solvent.

Table 3.2 Variable temperature ^1H n.m.r. data at 100 MHz for gem-$N_3P_3Ph_2(Me_2pz)_4$ in various solvents.

Solvent	$CDCl_3$	$C_6H_5NO_2$	$C_6D_5(CD_3)$	CS_2	CCl_4
Temperature	-30(14) amb(7.0) 55(4.5)	amb(19.5) 50(20.5) 70(21.4) 100(22)	amb(27)	-75(3.3) amb(0)	amb(0) 55(3.2) 70(4.4)

(a) $\Delta(\delta) = \delta Me^5 - \delta Me^3$ is given in brackets and is the peak separation in Hertz between δMe^5 and δMe^3.

These phenomena are similar to those observed in (trimethylsilyl) pyrazoles and in phosphino- and phosphinato-azoles[77]. In the former an intramolecular migration of the $SiMe_3$ group between the two adjacent nitrogens in the pyrazole ring has been suggested to account for the coalescence of the 3- and 5-substituent resonances upon increasing the temperature. However, this type of thermal rearrangement does not appear to be evident in pyrazolylphosphazenes because the coalescence is unsymmetrical in nature and even occurs upon decreasing the temperature in CCl_4. The relatively

large peak separations effected by the aromatic solvents probably is a result of interactions of the induced (secondary) magnetic fields of the solvent and the pyrazole ring.

The assignments of the 3- and 5-positions in N(1) substituted pyrazoles are controversial[109]. However, if R^3=R^5 contain protons which couple to H^4, the peak positions of R^3 and R^5 can be assigned based on the larger coupling constant J(4,5), arising from the greater double bond character of C(4)-C(5). Such is the case for $(NPpz_2)_{3-6}$ (R^3=R^5=H), the more downfield resonance consistently belonging to H^5 (Table 3.3). This pattern is also observed in the spectra of the 1-pyrazolylphosphines (Ppz_3 or $PhPpz_2$)[77], but is reversed in bis-(dimethylamino)1-pyrazolylphosphine ($pzP(NMe_2)_2$)[110], the H^3 resonance being more downfield. The proton coupling constants $J(H^4H^5)$ and $J(H^3H^4)$ are relatively insensitive to ring size, and are similar to those quoted for 1-pyrazolylphosphines[77,110] which also display long range coupling of phosphorus to H^5 (three bonds)[77,110], H^4 (four bonds)[77] and H^3 (four bonds)[77]. However, in the spectra of 1-pyrazolylphosphazenes long range coupling to H^5 is absent, though distant by only three bonds. Hence, the resonance of H^5 is split into a sharp doublet by coupling only to H^4, while those of H^4 and H^3 both appear as broad, unresolved singlets which can only be resolved by ^{31}P-decoupling. The relative peak positions, $H^5 > H^3 > H^4$, in order of decreasing δ, can be further established in these compounds by comparing their ^{31}P-decoupled spectra to those of the methyl analogues (Table 3.3). The methyl signals themselves are less informative; they all appear as sharp singlets, and this lack of coupling, especially if R^3=R^5=Me, hinders their assignments. Thus, the more downfield methyl resonance in $[NP(Me_2pz)_2]_{3,4}$ is arbitrarily designated as Me^5 by analogy with the $(NPpz_2)_n$ system.

Table 3.3. N.m.r. parameters[a], (P=N) stretching frequencies[b], and melting points of the 1-pyrazolylphosphazenes $[NP(R^3R^5pz)_2]_n$.

Compound	M.pt.[f] (°C)	ν(P=N) (cm^{-1})	Proton Shifts δ(ppm) R^5	H(4)[c]	R^3	Coupling Constants (Hz) $J_{3,5}$	$J_{3,4}$	$J_{4,5}$	$-\delta_P$ (ppm)
pzH	67-70		7.61	6.31	7.61		1.9	1.9	
$(NPpz_2)_3$	268-288	1238	8.04	6.37	7.82[c]	-	1.5	2.9	111.9
$(NPpz_2)_4$	361-363	∿1428	8.49	6.28	7.75[c]	∿0.5	1.4	2.8	137.8
$(NPpz_2)_5$	249-285	1425 1447	8.22	6.18	7.56[c]	-	1.5	2.7	137.1
$(NPpz_2)_6$[d]	316-345	1356	8.06 (7.52)	6.21 (6.24)	7.61[c] (7.52)	∿0.7	1.5 (2.1)	2.9 (2.1)	136.9
MepzH	204(b.pt.)		7.48	6.06	2.32			1.7	
$[NP(Mepz)_2]_3$	213-218.5	1234	7.90	6.10	2.22	-	-	2.8	112.8
$[NP(Mepz)_2]_4$	253.5-255	-	8.34	6.02	2.21	-	-	2.7	137.6
$[NP(Mepz)_2]_5$	e	-	8.21	5.98	2.13	-	-	2.6	137.2
Me_2pzH	107.5-108.5		2.21	5.76	2.21				
$[NP(Me_2pz)_2]_3$	253.5-254.5	1228	2.19	5.81	2.09	-	-	-	114.3
$[NP(Me_2pz)_2]_4$	225.5(gels)	-	2.16	5.67	2.02	-	-	-	131.1

(a) From dilute solutions, δ_H(ppm) in $CDCl_3$, reference internal TMS; parameters for pzH, MepzH and Me_2pzH are taken from Elguero, Jacquier, and Tien Duc, Bull. Soc. Chim. Fr., 3727 (1966); δ_P(ppm) in $CDCl_3$, shifts are to high field of external reference P_4O_6. (b) From nujol or hexachlorobutadiene mull spectra; dash means P=N frequency obscured by other vibrations. (c) J(PH) < 1.0 Hz. (d) N.m.r. parameters in brackets in CCl_4; reference internal TMS. (e) Product not isolated pure. (f) $(NPpz_2)_{3-6}$ all decompose.

3.1.2B ^{31}P n.m.r. of $[NP(R^3R^5pz)_2]_n$

Phosphorus n.m.r. in phosphazene chemistry has proved very informative for studying the π-electron distribution within the cyclic PN skeleton. Homogeneously substituted cyclic phosphazenes display only a single peak in their ^{31}P n.m.r. spectra, and these shifts appear to reflect the π-charge density at phosphorus from within the molecule. Generally the electronegativity of the ligand is directly related to the amount of shielding at phosphorus, as it is in phosphine oxides[111]. However, as noted in the previous chapter, anomalies do occur and suggest that angular and steric effects may also influence ^{31}P shifts. For example, the electronegativity of the halogens decreases in the order F > Cl > Br, but the corresponding ^{31}P chemical shifts of the compounds $(NPX_2)_3$ (X=F,Cl,Br) decreases in the order Br(157.9 ppm)[112] > F(103.3 ppm)[113] > Cl(92.7 ppm)[10].

Figure 3.3A shows both the influence of different ligands attached to phosphorus and the effect of ring size within a homologous series on the chemical shifts of phosphorus. The shift to higher field with more electronegative ligands suggests the extent of skeletal nitrogen lone pair delocalization on to phosphorus and the increase in shielding at phosphorus. The pyrazole group is expected to be moderately electronegative, but the anomalously large values of δ_P for 1-pyrazolylphosphazenes (Table 3.3) indicate that angular and steric factors are important. Any appreciable form of conjugative interactions from the pyrazole to the phosphazene ring would tend to concentrate π-electron density, within the phosphazene ring, away from phosphorus as it does in dimethylaminophosphazenes, and thus lower δ_P. Within a series, the progressive increase up to n=5, where diminished ring size effects cause a levelling off after n > 5, is attributed to a widening of the ring angle at nitrogen.

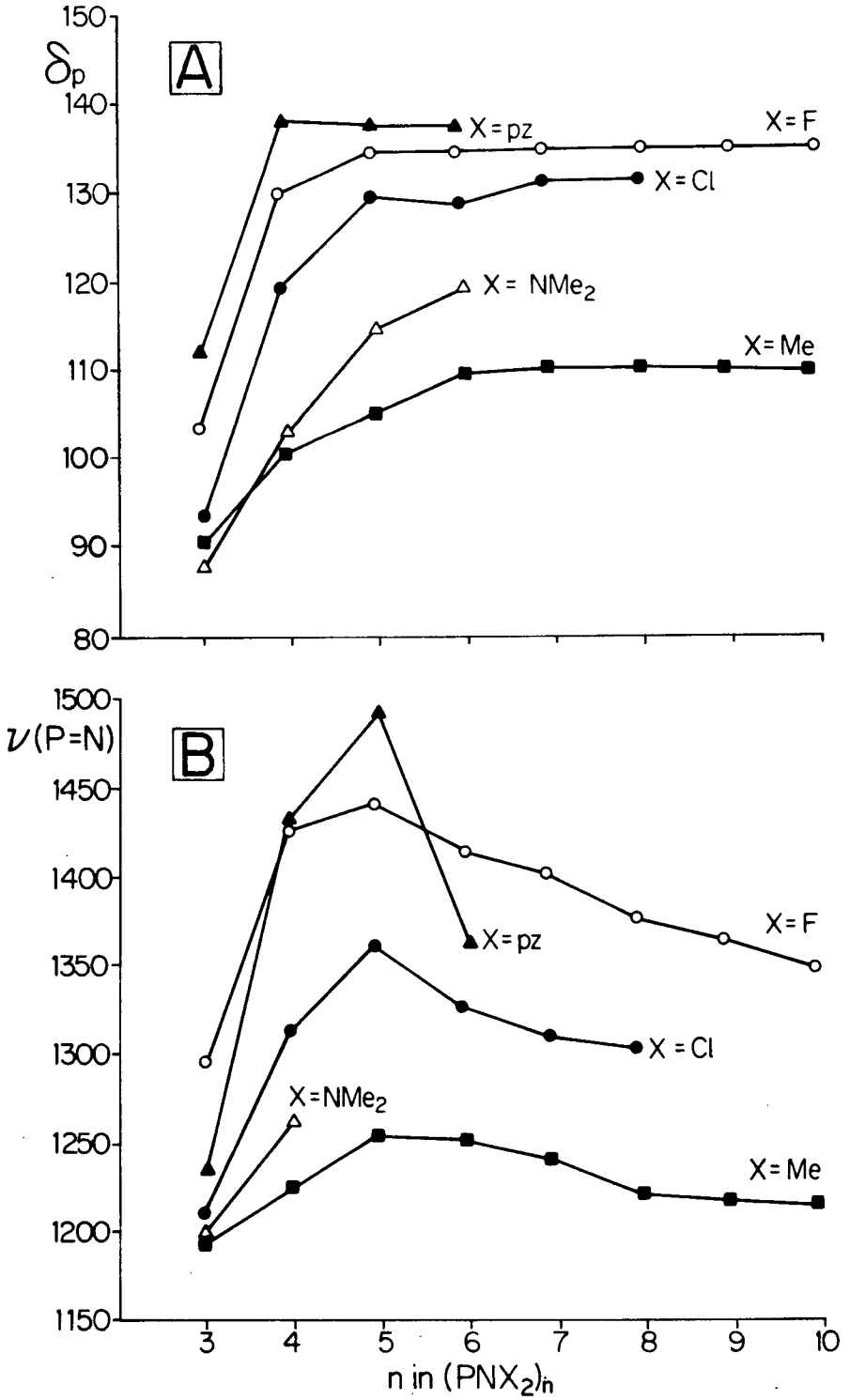

Figure 3.3. (A) ^{31}P chemical shifts (ppm, relative to ext. P_4O_6) and (B) ν(P=N) frequencies (cm^{-1}) of phosphazenes $(NPX_2)_n$ (X = F, pz, Cl, NMe_2, Me) as a function of ring size (n).

3.1.2C Infrared Spectra of $[NP(R^3R^5pz)_2]_n$

The infrared spectra of homogeneously substituted cyclophosphazenes are useful for determining the influence of ligand electronegativity on the character and strength of the P=N bond. The most informative and generally most intense band is the asymmetric stretching vibration $\nu_{asym}(P=N)$ usually found between 1180 and 1400 cm^{-1}, in a region free from most ligand vibrations. However, the PN stretching frequency in the spectra of 1-pyrazolylphosphazenes is quite often obscured by and easily mistaken for ligand vibrations. In most cases this problem is solved by comparing spectra within a homologous series, since they are, broadly speaking, similar with only the PN stretching vibration varying dramatically with ring size. As can be seen from Figure 3.3B, the magnitude of $\nu(P=N)$ varies with the substituent and the size of the ring. The electron attracting fluorine and chlorine groups facilitate a drift of electrons from the lone pair on nitrogen to phosphorus in a π_s-system, thus strengthening the PN bond and increasing $\nu(P=N)$. On the other hand, the electron releasing methyl and dimethylamino groups distribute π-electron density away from phosphorus, thus weakening the PN bond and decreasing $\nu(P=N)$. The values of $\nu(P=N)$ (Table 3.3), as a group, for $(NPpz_2)_n$ resemble those of the more electronegative ligands and, in conjunction with the ^{31}P n.m.r. data, suggest that exocyclic N → P π-bonding is minimal. However, it must be recognized that both $\nu(P=N)$ and δ_P have only limited value, but both show, qualitatively, the electron withdrawing properties of the pz group.

For the same ring size, increasing methylation of the pyrazole ring tends to lower $\nu(P=N)$ slightly, as it should, if the electronegativities decrease in the order pz > Mepz > Me_2pz and steric interactions are minimal.

Within a homologous series, the variation in ν(P=N) with ring size has not been related to a difference in PN bond strength, but instead to the fact that the characteristic ring vibration is a degenerate ring stretching mode and not a vibration of a monomeric unit[99,114].

One of the most discernible ligand vibrations is the pyrazole ring stretching mode which occurs between 1500 and 1600 cm^{-1}. It increases both in frequency and intensity upon progressive methylation of the pyrazole ring yet, within a group, remains relatively invariant upon increase in ring size: $(NPpz_2)_n$ $\sim$ 1520 cm^{-1}, $[NP(Mepz)_2]_n$ $\sim$ 1540 cm^{-1}, $[NP(Me_2pz)_2]_n$ $\sim$ 1570 cm^{-1}.

3.1.2D Mass Spectra of $[NP(R^3R^5pz)_2]_n$

The difficulty in preparing 1-pyrazolylphosphazenes of large ring size is reflected in their mass spectra. Unlike the series of phosphazenes $(NPF_2)_{3-12}$[115] and $(NPMe_2)_{3-12}$[35,80], the stability of the parent ion for $(NPpz_2)_{3-6}$ decreases with increasing ring size, so that, in $(NPpz_2)_6$, the parent ion is not observed. Furthermore, the parent ion for $(NPpz_2)_3$, $[NP(Mepz)_2]_3$ and $[NP(Me_2pz)_2]_3$ is the most abundant species, indicating that the methyl groups cause little, if any, instability in the compounds. This is also in agreement with their relative yields discussed earlier.

The fragmentation process of phosphazenes, in general, is dominated by stepwise loss of the ligand for $n \leq 5$ and by transannular interactions, or both if the phosphorus ligand bond is relatively weak, for $n \geq 6$. Smaller cyclic cations are common products from the degradation of larger rings: $P_6N_6Me_{12}$[80] and $P_6N_6F_{12}$[115] give only P_3N_3 units while $P_7N_7Me_{14}$[80] gives mainly P_4N_4 units. The spectra of $(NPpz_2)_{3-6}$ are all characterized

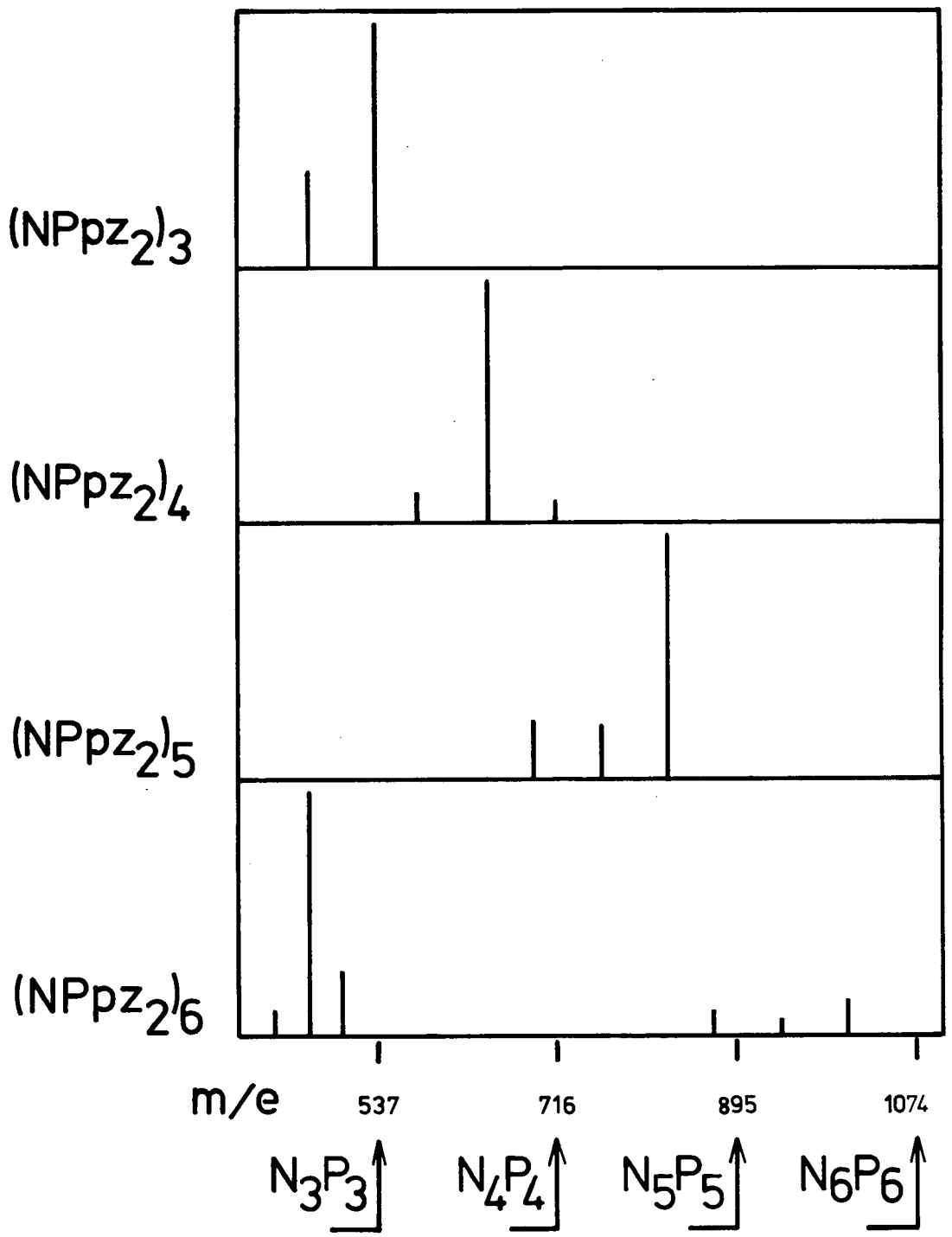

Figure 3.4. The mass spectra of the 1-pyrazolylphosphazenes $(NPpz_2)_{3-6}$. The scales are such that the base peaks of each compound have the same relative intensity. All fragments with an abundance of less than 5% of the base peak are ignored.

by stepwise loss of a pz group and in addition, for $(NPpz_2)_6$, loss of a P_3N_3 unit, the relative abundances of which are shown in Figure 3.4. The appearance of metastable peaks is useful for determining the mode of fragmentation. In all cases loss of a R^3R^5pz group from the parent ion occurs followed by loss of another R^3R^5pz group from the daughter ion, rather than a concerted loss of two R^3R^5pz units from the parent ion.

3.1.2E Structure and Properties of $[NP(R^3R^5pz)_2]_n$

The preparation of 1-pyrazolylphosphazenes now creates a new family of phosphazenes. They are all crystalline solids and, as such, are available sources for precise information concerning ring geometry. Because of the presence of approximately two equivalent π-systems in phosphazenes, efficient π-bonding is not restricted to a particular orientation of successive bonds. Consequently, the conformations found for pyrazolylphosphazenes, like those of $[NP(NMe_2)_2]_n$ (n=4,6,8,3)[46-49] are governed primarily by steric factors.

The crystal and molecular structure of $[NP(Me_2pz)_2]_4$ (see Chapter 5) has been completed[104] and the principal structural parameters are consistent with the presence of inductively withdrawing dimethylpyrazolyl groups on phosphorus. In the series $(NPX_2)_4$ (X=Me[116], Ph[117], Br[118], Cl[119]), the value of L(P=N) decreases uniformly from 1.595Å to 1.565Å (mean), and the ring angle at phosphorus increases from 119.8° to 120.9°. Conjugative electron release from exocyclic dimethylamino groups[46] increases L(P=N) to 1.578Å and decreases the angle at phosphorus to 120.1°. The mean L(P=N) in the pyrazolyl derivative (1.557Å) and the comparatively large ring angle at phosphorus (121.3°) are low and high respectively, showing that the dimethylpyrazolyl group resembles a chlorine rather than a methyl group.

The weakness of conjugative electron release to the phosphazene ring is confirmed qualitatively by the lengthening of the exocyclic P-N bond from 1.652Å in $N_3P_3(NMe_2)_6$[49] and 1.678Å in $N_4P_4(NMe_2)_8$[46] to 1.691Å in the pyrazolyl derivative.

All the pyrazolylphosphazenes have been characterized by elemental analysis and mass, n.m.r. and infrared spectroscopy. They are crystalline, air and moisture stable, white solids that melt above 200°C. At room temperature they are insoluble in acetonitrile and acetone, slightly soluble in THF, diethyl ether, and benzene, and soluble in chloroform, the methylpyrazolyl compounds being more soluble than their unsubstituted analogues.

The chemical effect of exocyclic conjugation in aminophosphazenes is such as to increase the donor properties of the ring nitrogen atoms at the expense of the amino nitrogen atoms. Thus, protonation occurs, in general, at the endocyclic nitrogen. Since exocyclic conjugation is apparently weaker in 1-pyrazolylphosphazenes, the basicity of the N(2) nitrogen in the pyrazolyl group should be greater than that of the ring nitrogen, and therefore protonation should occur on the exocyclic N(2) atom. However, reaction of pyrazolylphosphazenes with dry HCl in benzene yielded, upon workup, chlorophosphazene and pyrazole hydrochloride (Equation 3.6). Protonation at the N(2) nitrogen on the pyrazole ring probably occurs followed by nucleophilic attack of Cl^- at phosphorus, as it does in the corresponding pyrazolylphosphines[78]. The facile cleavage of the exocyclic P-N bond is in accordance with the susceptibility of the exocyclic N-C bond to hydrolysis in N-acetylpyrazole[120],

$$[NP(Mepz)_2]_4 + 16HCl \xrightarrow{C_6H_6} (NPCl_2)_4 + 8MepzH\cdot HCl \qquad \ldots (3.6)$$

mentioned in the introductory chapter. As a comparison, primary alkylaminophosphazenes give simple di- and tri-hydrochloride adducts, but ligand cleavage is characteristic of secondary alkylaminophosphazenes[121] (Equation 3.7). Most likely the more basic dialkyl group allows

$$[NP(HN(CH_2)_4CH_3)_2]_3 + 3HCl \xrightarrow{C_6H_6} [NP(HN(CH_2)_4CH_3)_2]_3 \cdot 3HCl \quad \ldots (3.7)$$

protonation on the amino nitrogen which, in turn, suppresses lone pair delocalization into the phosphazene ring, thereby making phosphorus more susceptible to nucleophilic attack by Cl^-.

3.2 (1-Pyrazolyl)phenylphosphazenes

3.2.1 Preparation of gem-$N_3P_3Ph_n(Me_xpz)_{6-n}$

During the course of the work on the coordination chemistry of $[NP(Me_2pz)_2]_3$, described in the following chapter, problems were encountered in deciding to which nitrogen atoms the metal was binding. The possibilities were numerous and to alleviate the problem a simpler ligand system was needed which contained fewer Me_2pz groups and, most importantly, other substituents attached to phosphorus which would not interfere, either chemically or spectroscopically, with the Me_2pz unit. Accordingly, gem-$N_3P_3Ph_n(Me_2pz)_{6-n}$ (n=2,4) seemed ideal choices, but their preparation requires suitable amounts of gem-$N_3P_3Ph_nCl_{6-n}$ (n=2,4). Fortunately some gem-$N_3P_3Ph_2Cl_4$ was available as its preparation[122] is tedious, and gem-$N_3P_3Ph_4Cl_2$ was synthesized by the method of Schmulbach and Derderian[14].

The progressive geminal replacement of two chlorine ligands by phenyl groups drastically reduces the reactivity of the remaining PCl_2 units towards nucleophiles. Accordingly, the series $N_3P_3Cl_6$ > gem-$N_3P_3Ph_2Cl_4$ > gem-$N_3P_3Ph_4Cl_2$ has been shown to represent a considerable

decline in the reactivity of the phosphazene ring with a particular amine[123]. For example, bubbling an excess of dimethylamine through an ethereal solution of gem-$N_3P_3Ph_4Cl_2$ for several hours displaces only one of the chlorines[80], and replacement of the second chlorine can only be achieved with an excess of $HNMe_2$ at 180°C[123]. Similarly, Me_2pzH and MepzH were also found to substitute chlorine very slowly. At least 8 days in refluxing xylene was required to displace both chlorines in gem-$N_3P_3Ph_4Cl_2$ (Equation 3.8); however, complete substitution of all the chlorines in gem-$N_3P_3Ph_2Cl_4$ was accomplished under relatively milder conditions in refluxing THF (Equation 3.9). The origin of this reactivity

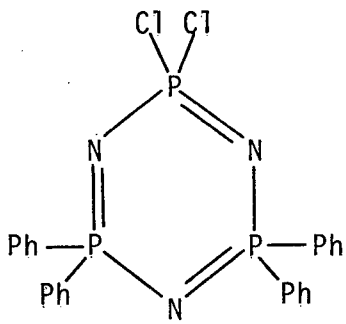

$$\xrightarrow[\text{xylene}]{2Me_xpzH/Et_3N} \text{gem-}N_3P_3Ph_4(Me_xpz)_2 + (x=1,2) + 2Et_3N\cdot HCl \quad \ldots (3.8)$$

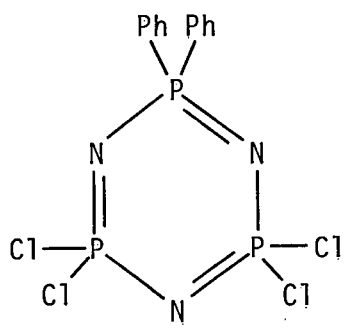

$$\xrightarrow[\text{THF}]{4Me_2pzH/Et_3N} \text{gem-}N_3P_3Ph_2(Me_2pz)_4 + + 4Et_3N\cdot HCl \quad \ldots (3.9)$$

is based upon the electronic properties of the phenyl groups rather than their steric influences. The electron donating phenyl groups and the electron attracting chlorine atoms combine to direct the π-electron density onto the $P(Cl_2)$ phosphorus atoms, thereby effectively reducing the

electrophilic character of phosphorus in the phosphazene. Apart from the longer reaction times required to effect complete substitution, the yields were excellent and by-products absent.

3.2.2 Structure and Spectra of Gem-$N_3P_3Ph_n(Me_xpz)_{6-n}$

The details of the ^1H n.m.r. and infrared spectra are given in Table 3.4. They are very similar to the values given in Table 3.3 for $[NP(Me_xpz)_2]_3$ (x=1,2) except that $J(PH^4)$ and $J(PH^5)$ increase with progressive

Table 3.4. ^1H n.m.r. parameters[a], (P=N) stretching frequencies[b], and melting points of gem-$N_3P_3Ph_n(Me_xpz)_{6-n}$.

Compound	M.pt. (°C)	ν(P=N) (cm^{-1})	Proton Shifts δ(ppm) H^4	Me^3	R^5	Ph
$N_3P_3Ph_2(Me_2pz)_4$	217.5-219	1219,1231	5.77	2.04	2.11	7.25-7.45 7.85-8.15
$N_3P_3Ph_4(Me_2pz)_2$[c]	211-212.5	1214-1224	5.81,d	2.12	2.18	7.30-7.50 7.75-8.00
$N_3P_3Ph_4(Mepz)_2$[d]	203-208	1212,1188	6.04,dd	2.28	7.88,dd	7.30-7.50 7.70-8.00

(a) From dilute solutions, δ_H(ppm) in $CDCl_3$, reference internal TMS.
(b) From nujol mull spectra. (c) $J(PH^4)$ = 2.8 Hz;"d"represents doublet.
(d) $J(PH^4)$ = 2.7 Hz, $J(PH^5)$ = 1.7 Hz, $J(H^4,H^5)$ = 2.7 Hz; "dd" represents doublet of doublets.

phenylation of the phosphazene ring, and are clearly visible in the spectra of gem-$N_3P_3Ph_4(Me_xpz)_2$ (x=1,2). This is believed to be due to the progressive increase in π-electron density (shielding) at the $P(Me_xpz)_2$ phosphorus atoms, the more electronegative pyrazole group being capable of withdrawing π-electron density from the $P(Ph_2)$ phosphorus atoms onto the $P(Me_xpz)_2$

phosphorus atoms. Consistently, an increase in pyrazolation causes a decrease in the shielding of the $P(Ph_2)$ phosphorus atoms. These long range ligand effects on a remote phosphorus, as determined from ^{31}P n.m.r. parameters (see Table 3.5), have been cited as evidence for a delocalized

Table 3.5. ^{31}P n.m.r. chemical shifts[a] and coupling constants[a] of geminally substituted phenylphosphazenes $N_3P_3Ph_{6-2n}X_{2n}$.

n=		0	1	2	3
$X=Me_2pz$	$P(Ph_2)$	98.2[b]	94.1	90.6	-
	$P(Me_2pz)_2$	-	117.5	115.8	114.3
	J(PP)	-	19.9	25.0	-
X=Mepz	$P(Ph_2)$	98.2[b]	93.2	-	-
	$P(Mepz)_2$	-	118.4	-	112.8
	J(PP)	-	19.9	-	-
X=Cl[c]	$P(Ph_2)$	97.3	95.4	93.0	-
	$P(Cl_2)$	-	97.7	95.4	93.2
	J(PP)	-	9.3	12.1	-
X=F[d]	$P(Ph_2)$	98.2[b]	85.2	82.1	-
	$P(F_2)$	-	106.3	100.4	98.6
	J(PP)	-	32.9	86.0	-
$X=NMe_2$[c]	$P(Ph_2)$	97.3	97.0	96.4	-
	$P(NMe_2)_2$	-	91.5	88.4	87.9
	J(PP)	-	16.0	21.9	-

(a) $-\delta$(ppm), relative to external P_4O_6. J(PP) in Hertz. (b) $-\delta$ = 98.2 for $N_3P_3Ph_6$ from H.P. Latscha, Z. Anorg. Allgem. Chem., 382, 7 (1968). (c) R.Keat, R.A.Shaw and M.Woods, J.C.S. Dalton, 1582 (1976). (d) All values except that for $N_3P_3Ph_6$ from C.W.Allen, F.Y.Tsang and T.Moeller, Inorg. Chem., 7,2183 (1968).

π-system in phosphazenes. The ^{31}P n.m.r. spectrum of gem-$N_3P_3Ph_2(Me_2pz)_4$ consists of, as expected, a doublet for the $\underline{P}(Me_2pz)_2$ atoms and a triplet for the $\underline{P}(Ph_2)$ atom, while the reverse is observed in the spectra of gem-$N_3P_3Ph_4(Me_xpz)_2$ (x=1,2). The mass spectra of these compounds, like those

of $[NP(Me_xpz)_2]_3$ (x=1,2) are dominated by stepwise loss of a Me_xpz unit in which the parent ion is also the base peak.

The pyrazolylphenylphosphazenes are white, crystalline solids which are much more soluble in aromatic solvents than the fully substituted pyrazolylphosphazenes. The crystal and molecular structure of gem-$N_3P_3Ph_2(Me_2pz)_4$ confirms the electronic influence of the Ph and Me_2pz groups on the phosphazene skeleton. The mean value of L(P=N) for the $\{(Me_2pz)_2P=N-P(Me_2pz)_2\}$ unit (1.572 Å) is much smaller than the mean value of L(P=N) for the $\{N=P(Ph_2)-N\}$ unit (1.607 Å), consistent with the greater electronegativity of the Me_2pz ligand. A more detailed analysis of this structure will appear in Chapter 5.

3.3 Experimental

The chlorophosphazenes $(NPCl_2)_{3-6}$ (supplied) were each purified by passing a solution in 30-60 petroleum ether through silica gel, and then recrystallizing by slow evaporation of the solvent. Gem-$N_3P_3Ph_2Cl_4$ was supplied but can be made according to the procedure in reference (122). Gem-$N_3P_3Ph_4Cl_2$ was prepared by a ring closure reaction involving the linear phosphazene $[NH_2(Ph_2)PNP(Ph_2)NH_2]^+Cl^-$ and PCl_5 [14]. Pyrazole, 3-methylpyrazole, and 3,5-dimethylpyrazole (Aldrich) were supplied and purified by sublimation or distillation. Anhydrous hydrogen chloride gas (Matheson) was used directly from the lecture bottle. The solvents THF, benzene and xylene were distilled over lithium aluminum hydride before use (THF was also dried by heating under reflux over sodium/benzophenone). Triethylamine was distilled over calcium hydride and stored over 4A molecular sieves. All reactions were done in a streamof dry nitrogen followed by workup in air.

3.3.1 Preparation of $(NPpz_2)_{3-6}$

3.3.1A Preparation of $(NPpz_2)_3$

A solution of pyrazole (1.616 g, 23.73 mmol, 25% xs) and triethylamine (2.113 g, 20.88 mmol, 10% xs) in 50 ml THF was added dropwise to a stirred solution of $(NPCl_2)_3$ (1.100 g, 3.16 mmol) in 60 ml THF. The solution became slightly turbid midway through the addition and eventually discarded a white solid. After heating under reflux for twenty-four hours, a total of 3.320 g of the solid was filtered off, of which 2.500 g was soluble in chloroform and identified as triethylamine hydrochloride (96%). The remaining 0.820 g of residue insoluble in chloroform has not been identified. The THF filtrate was distilled until $\sim$ 20 ml remained. Upon cooling 0.150 g of the product crystallized. The solvent was completely removed and the residual white solid heated at 110°C/0.1 Torr for two hours in order to remove traces of triethylamine hydrochloride and excess pyrazole. Crystallization from acetonitrile yielded a further 0.151 g of $(NPpz_2)_3$, as colourless, prismatic needles. Yield: 0.301 g (18%). M.pt. 268-288°C (dec). Anal. calcd. for $P_3N_{15}C_{18}H_{18}$: C, 40.23; H, 3.38; N, 39.10. Found: C, 40.09; H, 3.31; N, 39.19.

3.3.1B Preparation of $(NPpz_2)_4$

Procedure is the same as above except 1.057 g $(NPCl_2)_4$ (2.28 mmol), 1.939 g triethylamine (19.16 mmol, 5% xs), and 1.863 g pyrazole (27.37 mmol, 50% xs) were used. Reaction was much faster as noted by the immediate precipitation of triethylamine hydrochloride. The product was crystallized from an acetonitrile/1,2-dichloroethane mixture. Yields: $Et_3N{\cdot}HCl$ (2.302g, 92%), by-products insoluble in chloroform and THF (1.318 g), and $(NPpz_2)_4$

(0.300 g, 20%). M.pt. 361-363 (dec). Anal. calcd. for $P_4N_{20}C_{24}H_{24}$: C, 40,23; H, 3.38; N, 39.10. Found: C, 40.60; H, 3.34; N, 39.44.

3.3.1C Preparation of $(NPpz_2)_6$

As above except 2.133 g $(NPCl_2)_6$ (3.07 mmol), 3.132 g pyrazole (46.01 mmol, 25% xs), and 3.911 g triethylamine (38.65 mmol, 5% xs) were used. The product was crystallized from acetonitrile/1,2-dichloroethane. Yields: $Et_3N{\cdot}HCl$ (4.762 g, 94%), by-products (1.021 g), and $(NPpz_2)_6$ (0.692 g, 21%). M.pt. 316-345 (dec). Anal. calcd. for $P_6N_{30}C_{36}H_{36}$: C, 40.23; H, 3.38; N, 39.10. Found: C, 40.43; H, 3.26; N, 38.90.

3.3.1D Preparation of $(NPpz_2)_5$

As above except 3.889 g $(NPCl_2)_5$ (6.71 mmol), 5.026 g pyrazole (73.82 mmol, 10% xs), and 7.131 g triethylamine (70.46 mmol, 5% xs) were used. After filtration of the $Et_3N{\cdot}HCl$ and by-products, the solvent was removed under reduced pressure leaving a clear, colourless oil, which was dissolved in 100 ml 1:1 acetonitrile/toluene and passed through a column of alumina. Slow evaporation of the solvent yielded colourless crystals of $(NPpz_2)_5$. Yields: $Et_3N{\cdot}HCl$ (8.525 g, 92%), by-products (1.313 g), and $(NPpz_2)_5$ (2.705 g, 45%). M.pt. 249-285°C (dec). Anal. calcd. for P_5N_{25}-$C_{30}H_{30}$: C, 40.23; H, 3.38; N, 39.10. Found: C, 40.50; H, 3.39; N, 38.80.

3.3.2 Preparation of $[NP(Mepz)_2]_{3-5}$

3.3.2A Preparation of $[NP(Mepz)_2]_3$

A solution of 3-methylpyrazole (2.400 g, 29.23 mmol, 6% xs) and triethylamine (3.077 g, 30.41 mmol, 10% xs) in 50 ml THF was added dropwise to a stirred solution of $(NPCl_2)_3$ (1.602 g, 4.61 mmol) in 60 ml THF. After

heating under reflux for twenty-four hours, the $Et_3N \cdot HCl$ and by-products were filtered off, and the solvent removed in vacuo. The remaining white semi-solid was washed with acetonitrile and crystallized by slow evaporation from either toluene or an acetonitrile/1,2-dichloroethane mixture, as a microcrystalline mass of $[NP(Mepz)_2]_3$. Some product precipitated with the $Et_3N \cdot HCl$. Yields: $Et_3N \cdot HCl$ (3.652 g, 96%), by-products (1.412 g), and $[NP(Mepz)_2]_3$ (0.870 g, 30%). M.pt. 213-218.5°C. Anal. calcd. for $P_3N_{15}C_{24}H_{30}$: C, 46.38; H, 4.87; N, 33.80. Found: C, 46.69; H, 4.85; N, 33.85.

3.3.2B Preparation of $[NP(Mepz)_2]_4$

As above except 1.515 g $(NPCl_2)_4$ (3.27 mmol), 2.347 g 3-methylpyrazole (28.58 mmol, 9% xs) and 2.910 g triethylamine (58.14 mmol, 10% xs) were used. The product was crystallized from acetonitrile as a microcrystalline mass. Yields: $Et_3N \cdot HCl$ (3.419 g, 95%), by-products (0.387 g), and $[NP(Mepz)_2]_4$ (1.601 g, 59%). M.pt. 253.5-255°C. Anal. calcd. for $P_4N_{20}C_{32}H_{40}$: C, 46.38; H, 4.87; N, 33.80. Found: C, 46.46; H, 4.83; N, 33.50.

3.3.2C Preparation of $[NP(Mepz)_2]_5$

As above except 3.063 g $(NPCl_2)_5$ (5.29 mmol), 4.740 g 3-methylpyrazole (57.73 mmol, 9% xs) and 5.883 g triethylamine (58.14 mmol, 10% xs) were used. Evaporation of the THF filtrate yielded an oil which was dissolved in 170 ml benzene and then passed through a column of alumina. The solvent was removed and the resulting slightly opaque, colourless oil identified by ^1H n.m.r. spectroscopy as a mixture of 3-methylpyrazole and $[NP(Mepz)_2]_5$ ($\sim$ 17:1 mole ratio, respectively). The pure product has not been isolated.

3.3.3 Reaction of $[NP(Mepz)_2]_4$ with HCl

Anhydrous HCl gas was bubbled into a solution of $[NP(Mepz)_2]_4$ (0.121g, 0.15 mmol) in 70 ml benzene for ten minutes. Neither formation of a precipitate nor a change in colour of the solution was noticed. The solution was then heated under reflux for ten minutes, the solvent removed, and the residual white solid identified by ^1H n.m.r. and infrared spectroscopy as a mixture of $(NPCl_2)_4$ and 3-methylpyrazole hydrochloride. Yield: 0.190 g (92%, expect 0.139 g MepzH·HCl and 0.068 g $(NPCl_2)_4$). M.pt. of mixture 113.5-118.5°C (cf M.pt. crude MepzH·HCl 117.5-120.5°C and $(NPCl_2)_4$ 123.5°C).

3.3.4 Preparation of $[NP(Me_2pz)_2]_{3,4}$

3.3.4A Preparation of $[NP(Me_2pz)_2]_3$

A solution of $(NPCl_2)_3$ (1.656 g, 4.76 mmol) in 50 ml THF was added, over a period of ten minutes, to a solution of 3,5-dimethylpyrazole (3.205 g, 33.34 mmol, 17% xs) and triethylamine (3.181 g, 31.43 mmol, 10% xs) in 65 ml THF. The solution became turbid midway through the addition and deposited a white precipitate after the addition was complete. The mixture was heated under reflux for forty-eight hours, filtered, and the filtrate distilled until ∿ 15 ml remained. Upon cooling 1.918 g of a white solid precipitated, which was washed with acetonitrile and crystallized from acetonitrile/1,2-dichloroethane, as colourless blocks of $[NP(Me_2pz)_2]_3$. A further 0.042 g was obtained from the mother liquor. The by-products were separated from $Et_3N·HCl$ by dissolving the latter in chloroform. Yields: $Et_3N·HCl$ (3.658g, 93%), by-products (0.512 g), and $[NP(Me_2pz)_2]_3$ (1.960 g, 58%). M.pt. 253.5-254.5°C. Anal. calcd. for $P_3N_{15}C_{30}H_{42}$: C, 51.06; H, 6.00; N, 29.77. Found: C, 51.10; H, 5.92; N, 29.69. The product can also be prepared in 91% yield

using benzene as the solvent and 5% xs of both triethylamine and 3,5-dimethylpyrazole. In addition no by-products were found.

3.3.4B Preparation of $[NP(Me_2pz)_2]_4$

As above except 1.863 g $(NPCl_2)_4$ (4.02 mmol), 3.500 g 3,5-dimethylpyrazole (36.41 mmol, 13% xs), and 3.579 g triethylamine (35.37 mmol, 10% xs) were used. The white solid that precipitated upon concentrating the THF filtrate contained some 3,5-dimethylpyrazole and $Et_3N{\cdot}HCl$, which were removed by sublimation in vacuo (110°C/0.1 Torr for three hours). The residue was crystallized by slow evaporation from benzene solution as colourless crystals of $[NP(Me_2pz)_2]_4$. Yields: $Et_3N{\cdot}HCl$ (4.160 g, 94%), by-products (0.993 g), and $[NP(Me_2pz)_2]_4$ (0.303 g, 8%). M.pt. 222.5 (gels). Anal. calcd. for $P_4N_{20}C_{40}H_{56}$: C, 51.06; H, 6.00; N, 29.77. Found: C, 51.29; H, 6.05; N, 29.74. The reaction was repeated as above using 0% xs 3,5-dimethylpyrazole and 10% xs triethylamine. Yields: $Et_3N{\cdot}HCl$ (95%), by-products (0.433 g), and $[NP(Me_2pz)_2]_4$ (17%).

3.3.5 Preparation of Gem-$N_3P_3Ph_2(Me_2pz)_4$

A solution of 3,5-dimethylpyrazole (0.854 g, 8.89 mmol, 0.1% xs) and triethylamine (0.988 g, 9.77 mmol, 10% xs) in 50 ml THF was added to a stirred solution of gem-$N_3P_3Ph_2Cl_4$ (0.957 g, 2.22 mmol) in 70 ml THF, and the mixture heated under reflux for eight days. After twenty-four hours the solution was slightly cloudy, after forty-eight hours a white precipitate began to deposit, and after eight days 0.934 g of solely $Et_3N{\cdot}HCl$ (76%) was filtered off. No by-products were found. The filtrate was evaporated under reduced pressure leaving a clear, pale yellow oil, which solidified on standing. The residue was heated at 100°C/0.1 Torr for one hour,

and the sublimate (0.181 g) identified by ^1H n.m.r. spectroscopy as a mixture of $Et_3N \cdot HCl$ and 3,5-dimethylpyrazole. The remaining solid was washed with acetonitrile and crystallized from an acetonitrile/1,2-dichloroethane mixture as colourless needles of gem-$N_3P_3Ph_2(Me_2pz)_4$. Yield: 1.338 g (90%). M.pt. 217.5-219°C. Anal. calcd. for $P_3N_{11}C_{32}H_{38}$: C, 57.40; H, 5.72; N, 23.01. Found: C, 57.10; H, 5.60; N, 22.77.

3.3.6 Preparation of Gem-$N_3P_3Ph_4(Me_2pz)_2$

A solution of 3,5-dimethylpyrazole (0.618 g, 6.42 mmol, 10% xs), triethylamine (0.649 g, 6.42 mmol, 10% xs), and gem-$N_3P_3Ph_4Cl_2$ (1.502 g, 2.92 mmol) in 120 ml xylene was heated under reflux for eight days. During this time the clear, colourless solution became slightly yellow. Also, $Et_3N \cdot HCl$ would crystallize as long needles upon cooling the solution at various stages. After filtering off the $Et_3N \cdot HCl$ (0.582 g, 72%), the solvent was removed in vacuo, leaving a clear, pale yellow oil which eventually solidified. From this solid, 0.161 g 3,5-dimethylpyrazole was removed by sublimation (110°C/0.1 Torr for one hour), which means only 0.457 g or 81% 3,5-dimethylpyrazole reacted. The residual light brown solid was washed with acetonitrile and crystallized from an acetonitrile/1,2-dichloroethane mixture as colourless blocks of gem-$N_3P_3Ph_4(Me_2pz)_2$. Yield: 1.103 g (73% based on the amount of 3,5-dimethylpyrazole that reacted). M.pt. 211-212.5°C. Anal. calcd. for $P_3N_7C_{34}H_{34}$: C, 64.45; H, 5.41; N, 15.47. Found: C, 64.73; H, 5.42; N, 15.53.

3.3.7 Preparation of Gem-$N_3P_3Ph_4(Mepz)_2$

A solution of 3-methylpyrazole (0.304 g, 3.70 mmol, 3.5% xs), triethylamine (> 30% xs), and gem-$N_3P_3Ph_4Cl_2$ (0.920 g, 1.79 mmol) in 80 ml

xylene was heated under reflux for eight days. After filtering off the $Et_3N \cdot HCl$ (0.398 g, 81%), the solvent was removed from the clear, colourless filtrate, and the residual beige solid heated at 85°C/0.1 Torr for one hour. The sublimate collected consisted of 3-methylpyrazole and traces of $Et_3N \cdot HCl$. The remaining solid was washed with acetonitrile and crystallized from this solvent as the acetonitrile adduct. The powdered crystals were heated at 100°C/0.1 Torr for three hours to give gem-$N_3P_3Ph_4(Mepz)_2$. Yield: 0.769 g (71%). M.pt. 203-208°C. Anal. calcd. for $P_3N_7C_{32}H_{30}$: C, 63.47; H, 4.99; N, 16.19. Found: C, 63.35; H, 4.98; N, 15.98.

CHAPTER 4

METAL COMPLEXES OF 1-PYRAZOLYLPHOSPHAZENES

Very few metal complexes of cyclophosphazenes have been made and, in most cases, bonding involves a σ-type overlap between the metal and the lone-pair electrons on the ring nitrogen. Transition metal nitrates and chlorides react with the hexameric dimethylaminophosphazene exclusively at the ring nitrogen[55,124], while reaction of tungsten hexacarbonyl with the tetrameric dimethylaminophosphazene occurs at both a ring nitrogen and an exocyclic amino nitrogen[57,63], an unusual and rare type of bonding pattern.

The coordination chemistry and biological importance of diazole based ligands have attracted considerable attention in recent years. Following a review on pyrazoles in 1972 by Trofimenko[69], much interest has been centered on the synthetic and structural aspects of metal complexes containing the pyrazolyl group. The complexes prepared for this thesis are illustrated in Figure 4.1, and the molecular structures of $N_3P_3(Me_2pz)_6 \cdot 2CoCl_2$ (A), gem-$N_3P_3Ph_2(Me_2pz)_4 \cdot ZnCl_2$ (C) and gem-$N_3P_3Ph_4(Me_2pz)_2 \cdot CoCl_2$ (B) are shown in Figure 4.2. They are all examples of rather rare exocyclic coordination of a phosphazene derivative and, furthermore, show that, at least for zinc and cobalt, that bonding is not restricted to the pyrazolyl groups nor to a unique geometry. In fact, the structure of (A) is an interesting and unique example of a molecule in which cobalt is contained in two different coordination geometries: tetrahedral and trigonal bipyramidal.

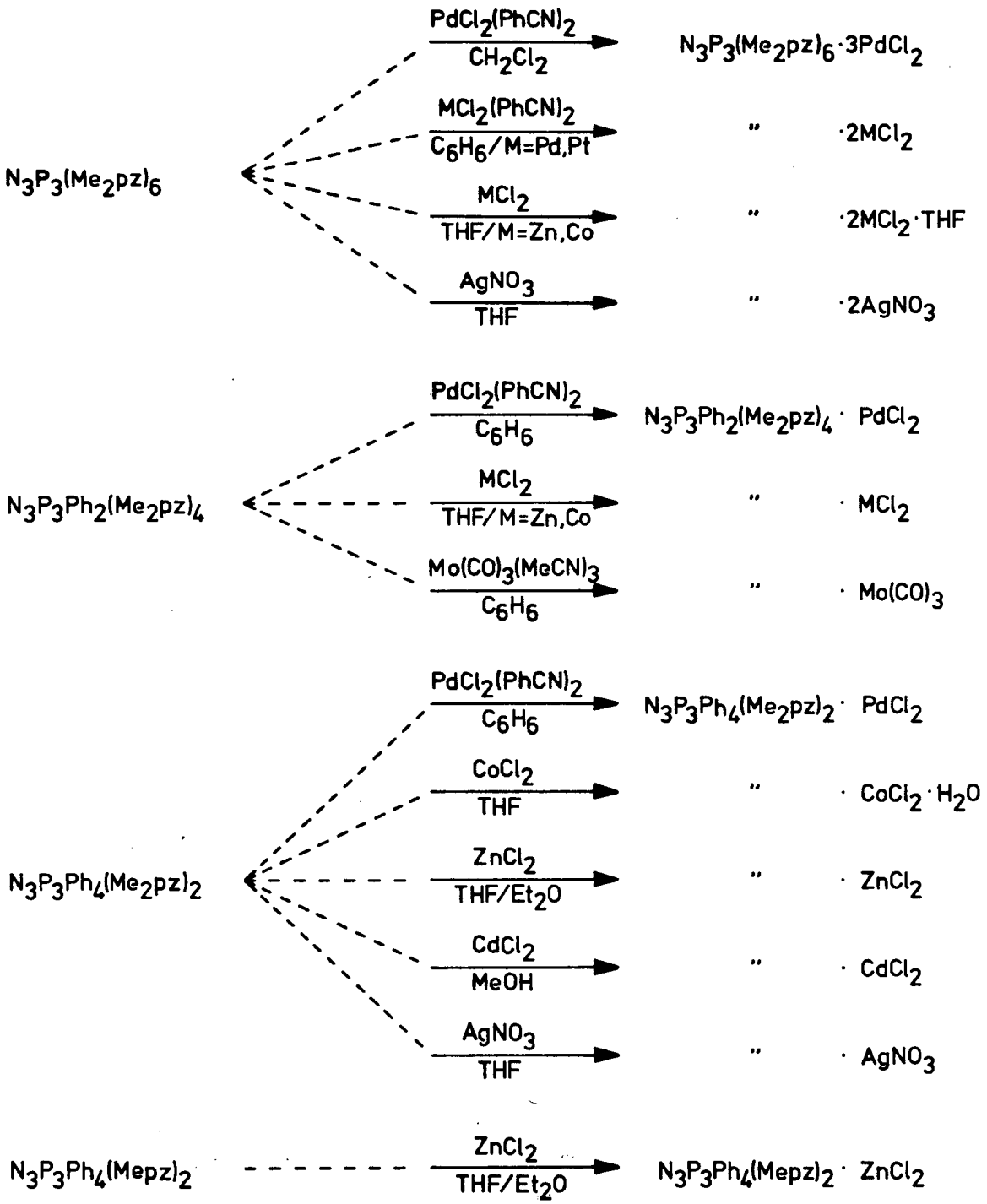

Figure 4.1. Reactions of some transition metal complexes with 1-pyrazolyl-phosphazenes.

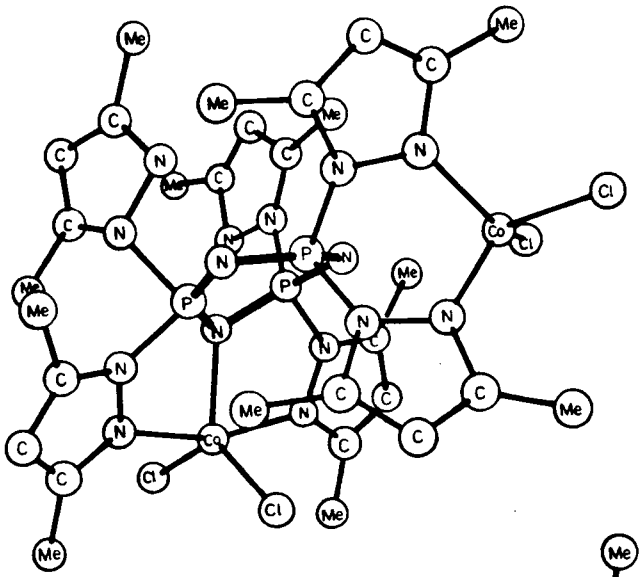

(A)

Co (tetrahedral and TBP)

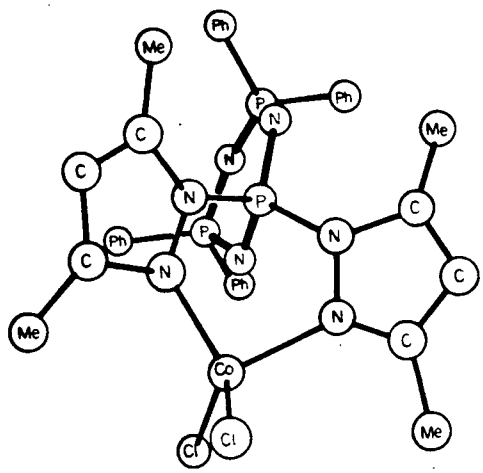

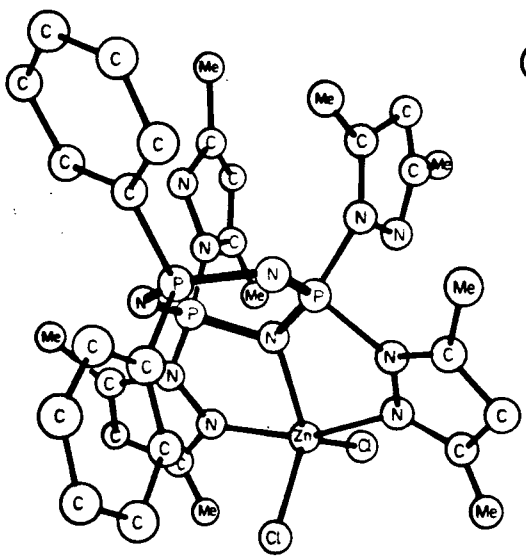

(B)

Co (tetrahedral)

(C)

Zn (trigonal bipyramidal)

Figure 4.2. Molecular structures of $N_3P_3(Me_2pz)_6 \cdot 2CoCl_2$ (A), gem-$N_3P_3Ph_4$-$(Me_2pz)_2 \cdot CoCl_2$ (B), and gem-$N_3P_3Ph_2(Me_2pz)_4 \cdot ZnCl_2$. Coordination geometry of the metal ion is given in parenthesis.

During the course of this work on the coordination chemistry of pyrazolylphosphazenes, it was realized that the stability of the complexes, especially those of cobalt and zinc, towards solvating solvents increased with progressive replacement of a Me_2pz group by a phenyl group. Similarly, although complexes of $N_3P_3(Mepz)_6$ could not be isolated, the influence of the phenyl group has allowed a successful preparation of the tetrahedral zinc chloride complex of gem-$N_3P_3Ph_4(Mepz)_2$, and its properties are discussed with the other zinc compounds in Section 4.1.

The weak π-acceptor qualities of 3,5-dimethylpyrazolyl groups attached to phosphorus have already been noted in the infrared spectra of carbonyl complexes of 3,5-dimethylpyrazolylphosphines[125]. Likewise, the CO frequencies in carbonyl complexes of methylphosphazenes[63] are similar to those in amino complexes, suggesting that there is no interaction of the metal d-orbitals with the π-acceptor levels of the phosphazene ring. Nevertheless, the preparation of a metal carbonyl complex of pyrazolylphosphazenes would be of interest to provide more information about the properties of the ligand, particularly if the phosphazene could coordinate via both the pyrazole and phosphazene ring nitrogens. With this in mind gem-$N_3P_3Ph_2(Me_2pz)_4 \cdot Mo(CO)_3$ was prepared and subsequently shown (Section 4.3) to contain two isomers, both of which, like the zinc compound, may contain the metal atom bonded to a phosphazene ring nitrogen.

Some platinum(II) and palladium(II) chloride derivatives were made and are discussed in Section 4.2. The tendency for these metals to assume square planar and not trigonal bipyramidal coordination geometries suggests that coordination to pyrazolyl groups on different phosphorus atoms is unlikely. This was shown, both experimentally and spectroscopically, to be

the case and, in addition, bonding to the nitrogen in the phosphazene ring is absent. Finally, Section 4.4 of this chapter relates some of the features of the complexes of silver nitrate.

4.1 Cobalt(II), Zinc and Cadmium Complexes

4.1.1 Preparation of Co(II), Zn and Cd Complexes

Reaction of either excess anhydrous cobalt(II)chloride or zinc chloride with a particular pyrazolylphosphazene in THF or THF/Et_2O (Equations 4.1-4.3) precipitated analytically pure samples of the metal complex.

$$N_3P_3(Me_2pz)_6 + MCl_2(>3eq.) \xrightarrow[(M=Zn,Co)]{THF} N_3P_3(Me_2pz)_6\cdot 2MCl_2\cdot THF \quad \ldots (4.1)$$

$$gem\text{-}N_3P_3Ph_2(Me_2pz)_4 + MCl_2(>2eq.) \xrightarrow[(M=Zn,Co)]{THF} gem\text{-}N_3P_3Ph_2(Me_2pz)_4\cdot MCl_2 \quad \ldots (4.2)$$

$$gem\text{-}N_3P_3Ph_4(Me_xpz)_2 + MCl_2(>1eq.) \xrightarrow[\substack{THF\\M=Co,x=2}]{\substack{M=Zn,x=1,2\\THF/Et_2O}} gem\text{-}N_3P_3Ph_4(Me_xpz)_2\cdot MCl_2 \quad \ldots (4.3)$$

THF was found to be the best solvent, especially for the $N_3P_3(Me_2pz)_6$ derivatives, because the reagents are soluble and the products can be filtered pure. Any attempts at recrystallizing the zinc and cobalt complexes of $N_3P_3(Me_2pz)_6$ resulted in variable and irreproducible amounts of coordinated solvent as indicated by the elemental analysis; moreover, the complexes rapidly decomposed in solvating solvents such as water, methanol, acetonitrile and acetone. However, the complexes of the mixed pyrazolylphenylphosphazenes are much more stable in these solvents. For example, $gem\text{-}N_3P_3Ph_4(Me_2pz)_2\cdot CdCl_2$ can be prepared in methanol (Equation 4.4) and

gem-$N_3P_3Ph_2(Me_2pz)_4 \cdot ZnCl_2$ can be crystallized from methanol.

$$\text{gem-}N_3P_3Ph_4(Me_2pz)_2 + CdCl_2(>1\text{eq.}) \xrightarrow{MeOH} \text{gem-}N_3P_3Ph_4(Me_2pz)_2 \cdot CdCl_2 \quad \ldots (4.4)$$

At first sight, the metal complexes of pyrazolylphosphazenes are expected to contain as many metal ions as there are $\{N=P(Me_2pz)_2\}$ units, if an excess of the metal chloride is used, because of the proximity of two pyrazolyl groups attached to the same phosphorus atom. The fact that there are one fewer metal ions than $\{N=P(Me_2pz)_2\}$ units in the derivatives of $N_3P_3(Me_2pz)_6$ and gem-$N_3P_3Ph_2(Me_2pz)_4$ indicates that either solubility is a problem or that the metal ion is not bonding to two pyrazolyl groups on the same phosphorus, and as can be seen from the molecular structures of the cobalt and zinc complexes (Figure 4.2 (A) and (C)), the latter suggestion is correct.

4.1.2 Conductivities of the Co(II) and Zn Complexes

The molar conductivities (Λ_M) ca. 10^{-3}M solutions of the zinc and cobalt(II) complexes in nitromethane at 25°C are given in Table 4.1. Reagent grade nitromethane was purified by heating under reflux over activated charcoal for one hour followed by filtering and predrying over calcium chloride, then distilling over P_2O_5 keeping the fraction that distilled between 101-102°C. This was then passed through a column of dried alumina and stored over molecular sieves (4A). The specific conductivity obtained varied between 2.46×10^{-7} and 52×10^{-7} $ohm^{-1}cm^{-1}$.

The generally accepted range for Λ_M at concentrations ca. 10^{-3}M for 1:1 electrolytes in nitromethane is 75-95 $ohm^{-1}cm^2mole^{-1}$ [126]. The data show that all the complexes are essentially non-conducting in nitromethane

Table 4.1. Molar conductance (Λ_M) data for 1-pyrazolylphosphazene complexes of zinc and cobalt(II) in nitromethane at 25°C.

Compound	Λ_M $cm^2 ohm^{-1} mole^{-1}$	Concentration M x 10^3
$N_3P_3(Me_2pz)_6 \cdot 2CoCl_2 \cdot THF$	26.9[a]	1.417
$N_3P_3(Me_2pz)_6 \cdot 2ZnCl_2 \cdot THF$	26.0	1.104
gem-$N_3P_3Ph_2(Me_2pz)_4 \cdot CoCl_2$	7.3	1.226
gem-$N_3P_3Ph_2(Me_2pz)_4 \cdot ZnCl_2$	6.7	0.670
gem-$N_3P_3Ph_4(Me_2pz)_2 \cdot CoCl_2 \cdot H_2O$	2.5	1.740
gem-$N_3P_3Ph_4(Me_2pz)_2 \cdot ZnCl_2$	2.6	1.325

(a) Λ_M = 0.3 $cm^2 ohm^{-1} mole^{-1}$ in dichloromethane.

and, therefore, formulations for the compounds as ion-pairs of the type $[N_3P_3(Me_2pz)_6M]^{+2}MCl_4^{-2}$ or $[(N_3P_3Ph_2(Me_2pz)_4)_2M]^{+2}MCl_4^{-2}$ can be ruled out. Moreover, the conductivity results indicate that partial dissociation into ionic species is greatest for the $N_3P_3(Me_2pz)_6$ complexes, consistent with the observation that these complexes are rapidly decomposed in solvating solvents such as acetonitrile. Nitromethane, on the other hand, is also a good solvating solvent but a poor donor solvent and, for this reason, decomposes the complexes at a much slower rate. In fact $N_3P_3(Me_2pz)_6 \cdot 2CoCl_2 \cdot$ THF can be recrystallized from nitromethane, without decomposition, if done quickly.

The results of the conductivity measurements lead to the conclusion that all these complexes are present in solution predominantly as non-ionic species. Thus, these will be formulated MCl_2L (M=Zn,Co) where L represents a particular pyrazolylphosphazene.

4.1.3 Mass Spectra of the Co(II) and Zn Complexes

Unlike the spectra of the cobalt complexes, those of the zinc complexes are easy to interpret. The near equivalence in mass of a Me_2pz unit (95 a.m.u.) and a $CoCl^{35}$ unit (94 a.m.u.), and the possibility of proton abstractions both make the detailed interpretation of the fragmentation pattern of the cobalt compound speculative.

The mass spectral data at 70ev are presented in Table 4.2, and indicate the relative strength of the metal-nitrogen bond. In no case is

Table 4.2 Mass spectral fragmentation data for 1-pyrazolylphosphazene complexes of zinc and cobalt(II).

Compound	Probe Temp.(°C)	Positive Fragment Ions[a]
$N_3P_3(Me_2pz)_6 \cdot 2ZnCl_2$	250	M-$2ZnCl_2$ (10)
$N_3P_3(Me_2pz)_6 \cdot 2CoCl_2$	230	M-2HCl (<0.2), M-$CoCl_2$-Cl (0.6)
		M-Me_2pz-2HCl (<0.1)
		M-$2CoCl_2$ or M-Me_2pz-$CoCl_2$-Cl (10.0)
gem-$N_3P_3Ph_2(Me_2pz)_4 \cdot ZnCl_2$	250	M-Cl (<0.1), M-$ZnCl_2$ (10)
gem-$N_3P_3Ph_2(Me_2pz)_4 \cdot CoCl_2$	215	M-Me_2pz (1.4), M-Me_2pz-Me (1.4)
		M-$CoCl_2$ or M-Me_2pz-Cl (10)
gem-$N_3P_3Ph_4(Me_2pz)_2 \cdot ZnCl_2$	250	M-$ZnCl_2$ (10)
gem-$N_3P_3Ph_4(Me_2pz)_2 \cdot CoCl_2$	330	M-Cl (1.1), M-Me_2pz (0.7)
		M-Me_2pz-Me (0.3)
		M-$CoCl_2$ or M-Me_2pz-Cl (10)
gem-$N_3P_3Ph_4(Mepz)_2 \cdot ZnCl_2$	330	M-Cl (2.6), M-$ZnCl_2$ (10)

(a) Only fragment ions containing either Zn or Co are given, in addition to the parent ion of the ligand. The relative intensities on a scale of 0 - 10.0 are given in parenthesis with that of the parent ion of the ligand arbitrarily set at 10.0. If an isotope pattern resulted in a number of peaks for a particular ion then only the peak of maximum intensity is recorded in parenthesis.

a molecular ion observed, and some of the zinc complexes even show no evidence for the Zn-N unit, only peaks due to the phosphazene ligand being apparent. Generally only peaks of weak intensity due to loss of Cl or Me_2pz are evident. It appears that the metal atom is weakly bound to the pyrazolylphosphazene ligand, and more weakly in the zinc than in the cobalt complexes, as expected from the lack of ligand field stabilization and the longer Zn-N bonds in the former.

4.1.4 Electronic Absorption Spectra of the Co(II) Complexes

The electronic spectra of the complexes in the solid and in solution were recorded in the 5000-20,000 cm^{-1} region, and the ligand-field splitting parameters Δ_t and Dq and the Racah parameter B´ were calculated using the equations of Lever[127]. The peak positions, band maxima, spectroscopic assignments and the ligand field parameters are given in Tables 4.3 and 4.4, and the composite drawings of the spectra are displayed in Figures 4.5, 4.6 and 4.7. Where applicable, the tetrahedral T_d model is used to describe the $CoCl_2L$ complexes even though the symmetry is lower. Lever and Nelson[128] have shown that such an approximation does not hinder the model and the parameters calculated will only be compared to similar complexes.

Some information on stereochemistry can be derived from an analysis of the electronic absorption spectra and the magnetic susceptibilities of cobalt(II) complexes (following section). Spin free, octahedral and tetrahedral Co(II) complexes of cubic symmetry can easily be differentiated by their electronic spectra on the basis of their peak positions and intensities. The Orgel diagram for a d^7 configuration in a cubic field is given in Figure 4.3. Octahedral complexes of O_h symmetry (CoX_6 where X

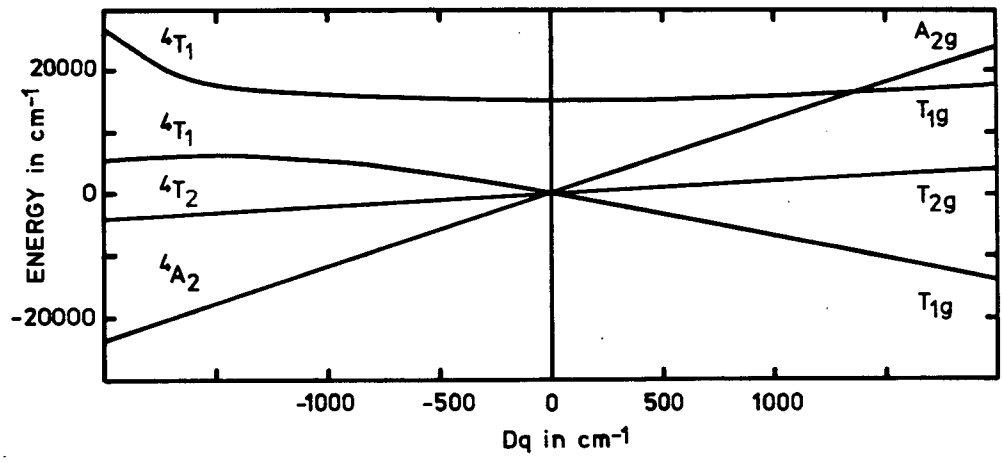

Figure 4.3. Orgel energy diagram for the Co(II) ion. Reference: L.E. Orgel, J. Chem. Phys., 23, 1004 (1955).

refers to six identical donor atoms) have three spin-allowed transitions: $^4T_{1g}(F) \longrightarrow {}^4T_{2g}(F)$ (ν_1), $^4T_{1g}(F) \longrightarrow {}^4A_{2g}(F)$ (ν_2), $^4T_{1g}(F) \longrightarrow {}^4T_{1g}(P)$ (ν_3), all of which are electric dipole forbidden and, therefore, are very low in intensity. The assignments for ν_2 and ν_3 may be interchanged in a strong ligand field. ν_1 is generally observed in the near-infrared region between 8,000-10,000 cm^{-1} and ν_3, the strongest band (molar extinction coefficient of $\varepsilon \sim 5$ $cm^{-1}mole^{-1}\ell$ in $Co(H_2O)_6^{+2}$ [129]), occurs near 20,000 cm^{-1}. ν_2 is a two electron transfer and consequently is expected to be weak in intensity. A reduction from O_h symmetry, either by geometrical distortion or by a non-equivalence of ligand donor atoms, usually increases the extinction coefficient of the bands and causes a splitting of the ν_1 band. On the other hand, the absorptions in the spectra of tetrahedral complexes are much higher in intensity and are displaced to lower energies. The splittings of the ^4F and ^4P states of the Co(II) free ion in a ligand field of T_d symmetry (CoX_4) are shown in the simplified energy level diagram in Figure 4.4. Three transitions from the $^4A_2$ ground state of the

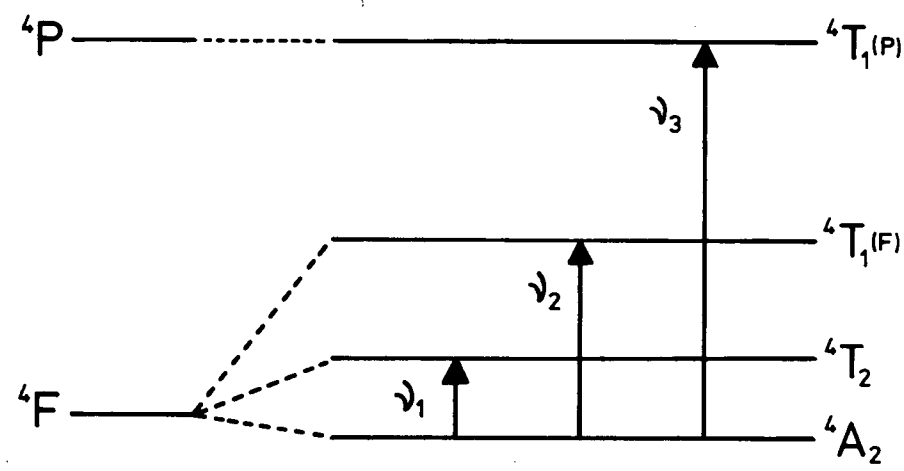

Figure 4.4. Energy level diagram for tetrahedral Co(II) d^7. Reference: "Transition Metal Chemistry", p.7, R.L. Carlin (Ed), Marcel Dekker,Inc., New York, 1965.

cobalt atom are spin-allowed: $^4A_2(F) \longrightarrow {}^4T_2(F)$ (ν_1), $^4A_2(F) \longrightarrow {}^4T_1(F)$ (ν_2), $^4A_2(F) \longrightarrow {}^4T_1(P)$ (ν_3). Only the latter two transitions are electric dipole allowed and occur at about 6300 cm^{-1} ($\varepsilon^{max} \sim 15$ $cm^{-1}mole^{-1}\ell$) and about 15,000 cm^{-1} ($\varepsilon^{max} \sim 600$), respectively, in $(CoCl_4)^{-2}$ [130]. ν_1 has an energy of 10 Dq and since this band occurs in the 3000-5000 cm^{-1} region for most complexes, it is generally not observed. The ν_2 band occurs in the near-infrared region and is usually broad. The ν_3 band is intense, broad and, like the ν_2 band, exhibits a great deal of fine structure, some of which is to be expected as a result of spin-orbit coupling. This band is observed in the visible region between 15,000-20,000 cm^{-1} and is responsible for the blue colour, characteristic of tetrahedral cobalt(II) complexes.

4.1.4A Electronic Spectra of Gem-$N_3P_3Ph_4(Me_2pz)_2 \cdot CoCl_2 \cdot H_2O$

The spectra are given in Table 4.3 and Figure 4.5, and are

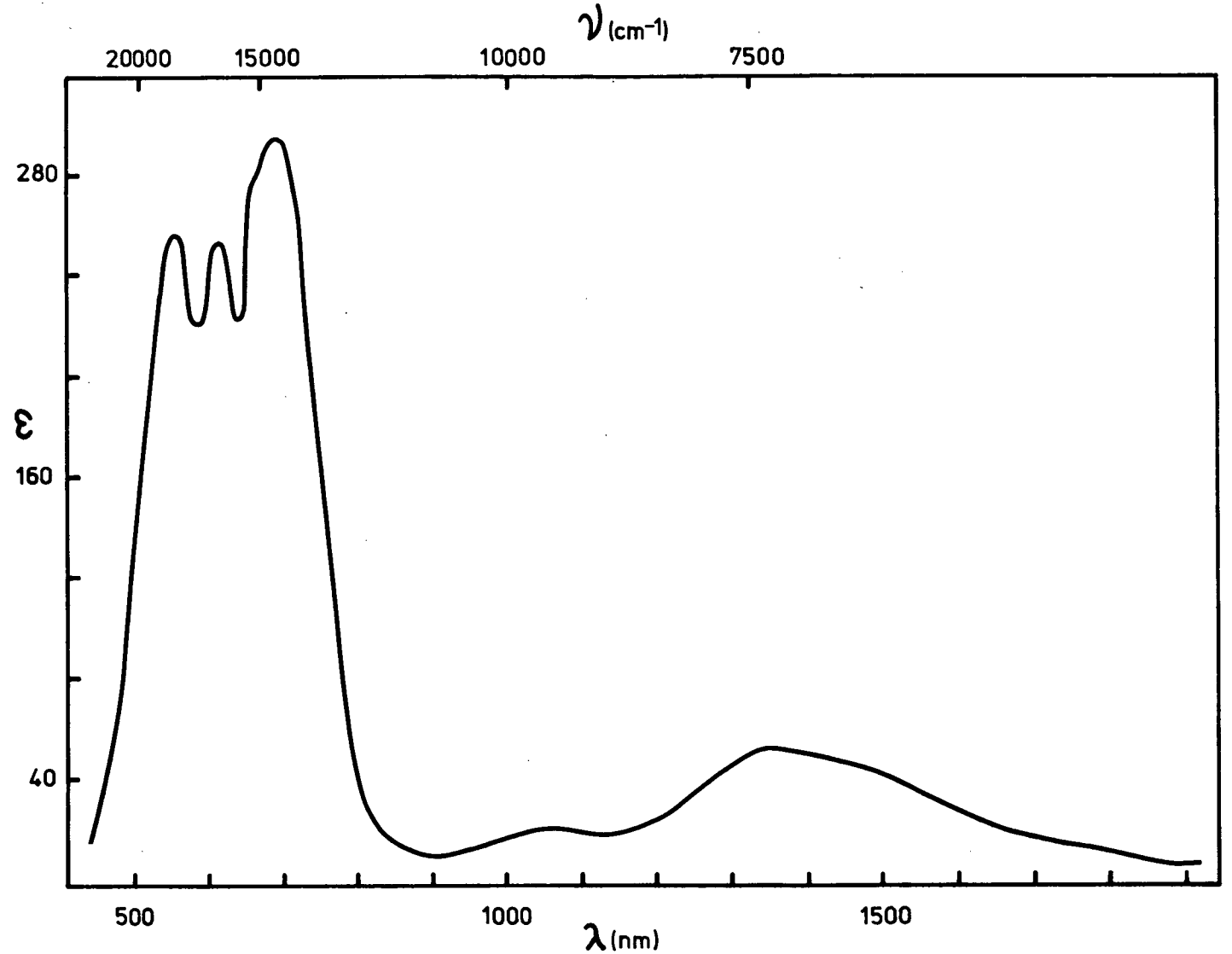

Figure 4.5. Electronic absorption spectrum of gem-$N_3P_3Ph_4(Me_2pz)_2 \cdot CoCl_2 \cdot H_2O$ in CH_2Cl_2. Concentration: 3.583×10^{-3} moles complex/liter.

Table 4.3. Band maxima, spectroscopic assignments and ligand field parameters of $N_3P_3(Me_2pz)_6 \cdot 2CoCl_2 \cdot THF$ and gem-$N_3P_3Ph_4(Me_2pz)_2 \cdot CoCl_2 \cdot H_2O$.

Compound	Medium	Comp. of ν_2^{max} cm^{-1} [a]	ν_2^{avg} cm^{-1} [b]	Comp. of ν_3^{max} cm^{-1} [c]	ν_3^{avg} cm^{-1} [b]	$\nu_1^{calc} = \Delta_t$ [d]	B cm^{-1} [e]
$N_3P_3Ph_4(Me_2pz)_2 \cdot CoCl_2 \cdot H_2O$	Nujol mull	f	-	18083 16584 15385sh 14993	-	-	-
	CH_3NO_2	∿9569(20) ∿7424(54)	7905	18083(256) 16694(252) 15432(279) 15129(299)	16181	4640	678 (.70)
	CH_2Cl_2	∿9634(21) ∿7424(56)	7918	18083(268) 16667(267) 15408sh (∿288) 15106(313)	16181	4650	678 (.70)
$N_3P_3(Me_2pz)_6 \cdot 2CoCl_2 \cdot THF$	Nujol mull	f	-	18051 16367 14993	-	-	-
	CH_3NO_2	∿10010(21) ∿ 7634(39) ∿ 6369(33)	7508	18018(211) 16611(262) 14925(328)	16207	4380	706 (.73)
	CH_2Cl_2	∿ 9901(33) ∿ 7734(52) ∿ 6579(25)	7937	18051(295) 16474(311) 14881(346)	16287	4660	684 (.70)
	CH_3CN	∿11087(16) ∿ 7231(53)	-	19194sh(∿56) 16978(398) 15823sh(308) 14793(462)	-	-	-
$CoCl_2$ in MeCN	CH_3CN	∿ 7220	-	17422 15748sh 16949 14815 16420	-	-	-

(a) $^4A_2(F) \longrightarrow {}^4T_1(F)$ transition. ε^{max}(cm^{-1} $mole^{-1}$ ℓ) in parenthesis. (b) Calculated by taking the center of gravity of the total intensity. (c) $^4A_2(F) \longrightarrow {}^4T_1(P)$ transition. ε^{max} in parenthesis. (d) $^4A_2(F) \longrightarrow {}^4T_2(F)$ transition. (e) β in parenthesis. (f) Peaks in the near-infrared were not discernible due to a poor base line.

Abbreviations: Comp.-components, max-maximum, avg-average, calc-calculated.

characteristic of cobalt in a pseudo tetrahedral environment. The complex is now of the type $CoCl_2X_2$ where X represents two nitrogen atoms. Hence, the site symmetry about the cobalt atom is reduced from T_d to C_{2v}, and the triply degenerate excited states T_2 and T_1 should therefore each split into three transitions: $T_2 \longrightarrow A_1 + B_1 + B_2$ and $T_1 \longrightarrow A_2 + B_1 + B_2$. Although the spectra show that the ν_3 band is split into three intense components, Ferguson[131] has postulated that only the ν_1 and ν_2 transitions are sensitive to changes of the formal symmetry of the ligand field and the peculiar structure of ν_3 bands is mainly a result of coupling to close lying doublet states. The ν_2 band is split into two very broad components of moderate intensity, one of which is asymmetric in appearance and probably contains the third component. Some small splitting of the ν_2 and ν_3 bands is expected from spin-orbit coupling, but certainly cannot account for the 2000-3000 cm^{-1} separation of the highest and lowest energy sub-bands. The features of the ν_2 band are similar to those observed in the spectra of $CoCl_2(imidazole)_2$[132] and $CoCl_2(Me_2pzH)_2$[133] and can probably be ascribed to the lower symmetry (the molecule as a whole has at most a plane of symmetry). In view of this consideration the energies of the ν_2 and ν_3 bands were estimated by taking the center of gravity of the total intensity and were found to be almost virtually identical in CH_2Cl_2, CH_3NO_2 and in the solid state. The calculated values for $\nu_1 = \Delta_t$ (4650 cm^{-1}) and B' (678 cm^{-1}) from solution in CH_2Cl_2 are slightly higher than those calculated for sterically hindered, α-alkyl substituted bis-amino complexes of cobalt(II)chloride $CoCl_2(amine)_2$ (Δ_t = 4280-4473 cm^{-1}, B' = 654-669 cm^{-1}) from solutions in $CHCl_3$, and instead compare very closely to Δ_t (4600-4721 cm^{-1}) and B' (633-643 cm^{-1}) calculated for the complexes of the

unhindered ligands[128]. However, because of the extreme broad nature of the ν_2 bands, no precise energy values can be ascertained from them. Therefore, the absolute values of Δ_t and B' are probably not too significant and only the trends observed will be discussed.

The inter-electron repulsion parameter B' in the complex is lower (678 cm^{-1}) than in the free ion (B=972 cm^{-1}) ($\beta = B'/B = .70$), as expected because of covalency within the complex. Although the ν_1 transition becomes partially electric-dipole allowed under C_{2v} symmetry, it was not observed in the spectral region studied. Moreover, the calculated value of 4650 cm^{-1} lies in a region masked by solvent and ligand vibrations.

4.1.4B Electronic Spectra of Gem-$N_3P_3Ph_2(Me_2pz)_4 \cdot CoCl_2$

The spectrum of this compound in CH_2Cl_2 (Table 4.4 and Figure 4.6) does not resemble those of either octahedral or tetrahedral Co(II) complexes, and especially is different from that of gem-$N_3P_3Ph_4(Me_2pz)_2 \cdot CoCl_2 \cdot H_2O$. More precisely, the intensities of the bands (ε^{max} 23-76 $cm^{-1}mole^{-1}\ell$) are, in general, too low for tetrahedral Co(II) complexes and the positions of the peaks, particularly that of the near-infrared band at 905 nm (11050 cm^{-1}), do not correspond to the area expected for octahedral Co(II) complexes. The crystal structure of the analogous zinc complex shows distorted trigonal bipyramidal coordination of the pyrazolylphosphazene ligand about the zinc atom. Thus, this geometry is also expected to be present in the cobalt complex, and the near equivalence of their infrared peaks (Section 4.1.6) seems to confirm this. Specifically, the spectrum is very similar to those of high-spin Co(II) compounds, to which a distorted trigonal bipyramidal structure has been attributed[134-136] (Table 4.4).

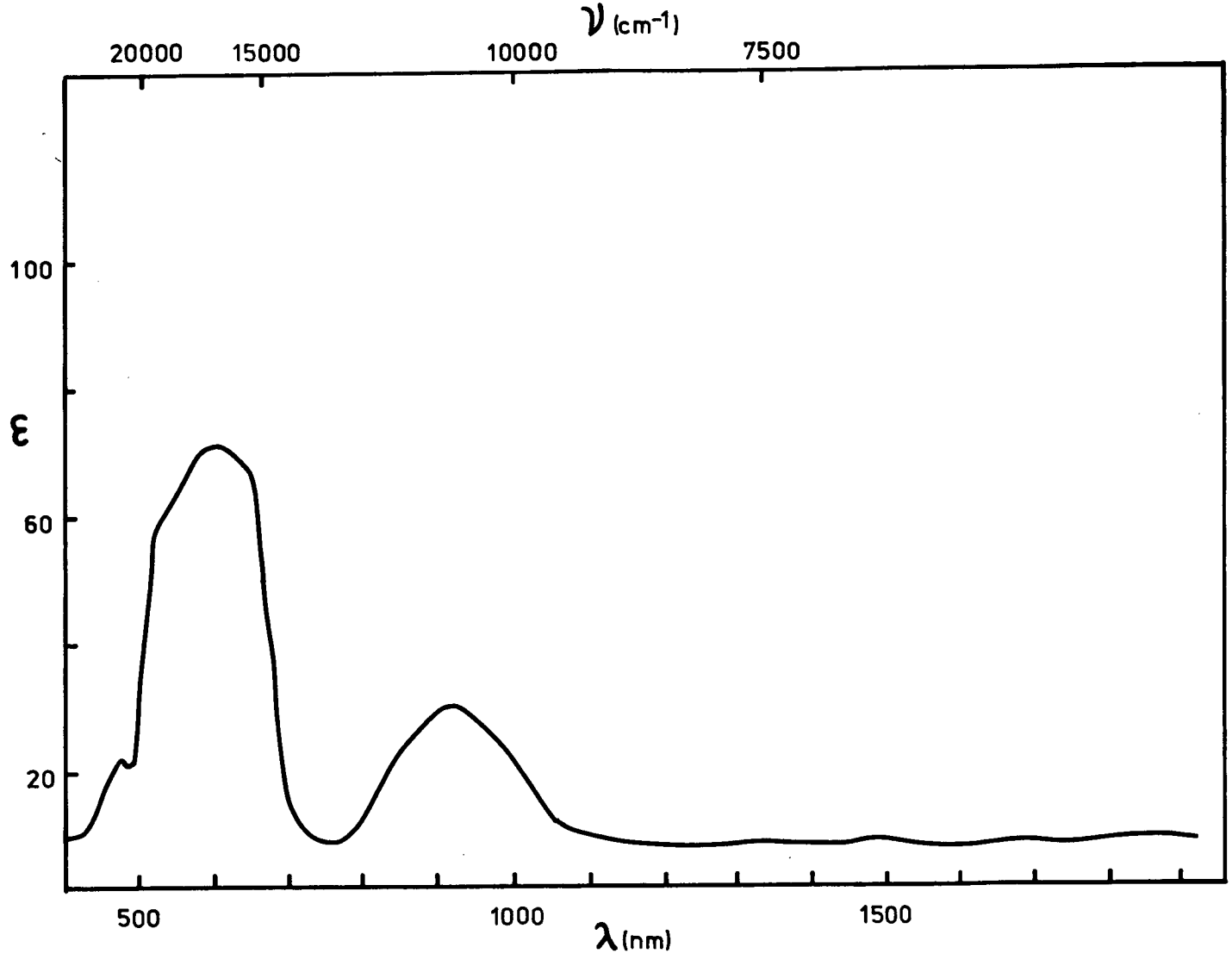

Figure 4.6. Electronic absorption spectrum of gem-$N_3P_3Ph_2(Me_2pz)_4 \cdot CoCl_2$ in CH_2Cl_2. Concentration: 5.979 x 10^{-3} moles complex/liter.

Table 4.4. The maxima and extinction coefficients for the electronic spectra of high-spin, distorted trigonal bipyramidal Co(II) complexes.[a]

Compound	Set of Donor Atoms	Absorption Maxima, cm^{-1} (ε^{max} for solution)	Medium	Ref.
gem-$N_3P_3Ph_2(Me_2pz)_4 \cdot CoCl_2$	N_3Cl_2	∿11050(31), 15504sh(69) 17391sh(71), 16639(76) 18519sh(59) 21277(23)	CH_2Cl_2	-
$CoCl_2$(terpy)	N_3Cl_2	15504, 17544 20000	Solid	136
$CoCl_2(Me_5dien)$	N_3Cl_2	8700sh, 10600(19) 16100(106) 18800(112)	$CHCl_3$	135
$[Co(Me_6tren)Cl]Cl$	N_4Cl	∿5800(32), 12600(30) 15500-16100(87) 20200(118)	$CHCl_3$	134a

(a) Abbreviations:

terpy ⟶ 2,2',2''-terpyridyl 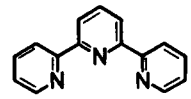

Me_5dien ⟶ bis(2-dimethylaminoethyl)methylamine, $MeN(CH_2CH_2NMe_2)_2$

Me_6tren ⟶ tris(2-dimethylaminoethyl)amine, $N(CH_2CH_2NMe_2)_3$

sh ⟶ shoulder

The energy level diagram for Co(II) in D_{3h} symmetry is shown in Figure 4.8. The triplet T_1 and T_2 terms in cubic symmetry are now split into A and E terms and, as a consequence, more spin-allowed transitions are possible, but only two transitions $^4A_2' \longrightarrow {}^4A_2'' + {}^4A_1''$ and $^4A_2' \longrightarrow {}^4E'$ are (weakly) electric-dipole allowed. Reducing the symmetry even further to C_{2v} splits the E terms into A and B terms of which only the $B_2 \longrightarrow B_1$ transitions are electric-dipole forbidden.

The intrinsic lack of a center of symmetry in trigonal bipyramidal compounds allows better d-p orbital mixing and, therefore, the intensities

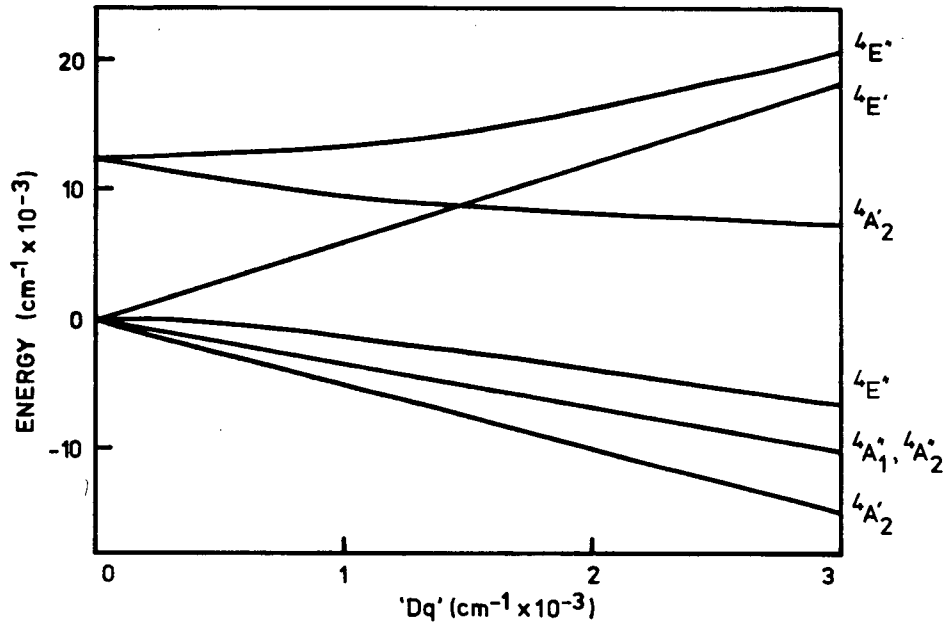

Figure 4.8. Energy level diagram for trigonal bipyramidal complexes of cobalt(II), from reference 137.

of the bands are usually higher than those corresponding to octahedral complexes of O_h symmetry, in which there is a center of symmetry; but lower than those corresponding to tetrahedral complexes. Transitions from the ground state to states arising from the ^4P level of the free ion are usually more intense ($\varepsilon^{max} \sim 100$ $cm^{-1}mole^{-1}\ell$ from Table 4.4) than the bands at lower frequency.

The positions and intensities of the bands in the spectrum of this compound closely parallel those given for the other trigonal bipyramidal Co(II) complexes in Table 4.4. The peak which is present in the spectrum of $[Co(Me_6tren)Cl]Cl$ at 12500 cm^{-1} has been assigned to the transition $^4A_2' \longrightarrow {}^4E'$ by Ciampolini, et al.,[137] and to a spin-forbidden transition $^4A_2' \longrightarrow {}^2E'(G)$ by Wood[138], using D_{3h} symmetry. This band also corresponds to the peaks at 10600 and 8700sh for $CoCl_2(Me_5dien)$[135] and to

the peak at 11050 cm^{-1} for gem-$N_3P_3Ph_2(Me_2pz)_4 \cdot CoCl_2$, and has been shown to be very sensitive to the field strength, very broad, and to split in compounds of low symmetry[139]. Although this band is very broad, and is the only peak present in the near-infrared region, the expected splitting (under C_{2v} symmetry) was not observed. The remaining bands, observed in the visible portion of the spectrum, are broad, flat-topped, and closely spaced. Therefore, making their assignments by comparison to related spectra is difficult.

4.1.4C Electronic Spectra of $N_3P_3(Me_2pz)_6 \cdot 2CoCl_2 \cdot THF$

The spectrum of this compound is expected to be a composite of the spectra of the previous two compounds, since the crystal structure shows that cobalt is situated in both a tetrahedral and trigonal bipyramidal environment. Surprisingly this was not the case, only peaks consistent with a tetrahedral structure being present. Furthermore, the extinction coefficients and band positions are almost identical to those found in the spectrum of gem-$N_3P_3Ph_4(Me_2pz)_2 \cdot CoCl_2 \cdot H_2O$ in the same solvent, except that the third component of the ν_2 band is now discernible at $\sim$6400 cm^{-1} and the shoulder at $\sim$15420 cm^{-1} is absent. At first glance the spectra in CH_3NO_2 and CH_2Cl_2 (Figure 4.7) imply that both cobalt atoms are tetrahedrally coordinated. If this were true then the extinction coefficients, from the spectrum in CH_2Cl_2, should be approximately twice those calculated for gem-$N_3P_3Ph_4(Me_2pz)_2 \cdot CoCl_2 \cdot H_2O$, and as can be seen from Table 4.3 they are instead similar. The similarity between the nujol mull spectrum and the solution spectra in CH_3NO_2 and CH_2Cl_2 indicates that the compound has the same structure both in solution and in the solid state. However, a drastic change due to extensive solvation takes place on dissolution in

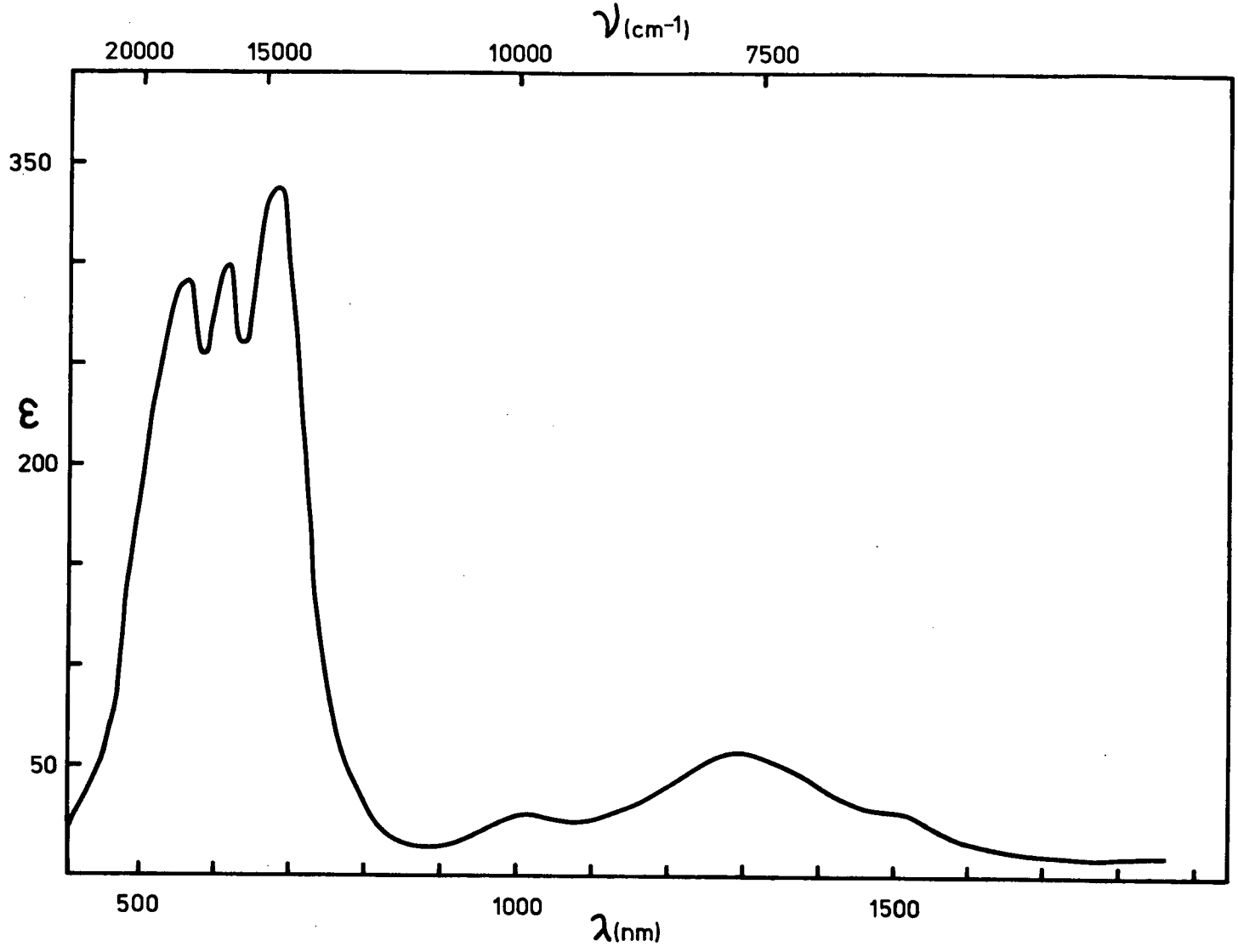

Figure 4.7. Electronic absorption spectrum of $N_3P_3(Me_2pz)_6 \cdot 2CoCl_2 \cdot THF$ in CH_2Cl_2. Concentration: 3.701×10^{-3} moles complex/liter.

CH_3CN and, like the analogous zinc complex, has probably decomposed in this solvent. Some of the peak positions are similar to those in the spectrum of anhydrous $CoCl_2$ dissolved in acetonitrile, but the presence of $CoCl_2(MeCN)_2$ species was not confirmed.

The Δ_t (4660 cm^{-1}) and B' (684 cm^{-1}) values calculated from the spectrum(CH_2Cl_2)for the cobalt atom in the tetrahedral environment are indeed almost identical to the Δ_t (4650 cm^{-1}) and B' (678 cm^{-1}) values calculated for the cobalt in gem-$N_3P_3Ph_4(Me_2pz)_2 \cdot CoCl_2 \cdot H_2O$ in the same solvent. However, dissolution in CH_3NO_2 gives rise to lower extinction coefficients and Δ_t values, and higher B' values, consistent with the conductivity data that the metal-nitrogen bond is more ionic in solvating solvents like nitromethane.

4.1.5 Magnetic Measurements of the Cobalt(II) Complexes

The room temperature magnetic moments are given in Table 4.5, and the values show that the cobalt complexes are all of the high-spin type. Generally when ligands contain donor atoms such as nitrogen or oxygen, the cobalt(II) complexes are high-spin. On the other hand, with ligands such as phosphines and arsines, which contain donor atoms of low electronegativity, the compounds are of the low-spin type.

Magnetic moments of spin-free cobalt(II) complexes are always greater than the spin-only moment of 3.87 B.M. due to a contribution by orbital angular momentum. Octahedral complexes generally have moments much higher than the spin-only value because of the intrinsic orbital angular momentum in the degenerate $^4T_{1g}$ ground state. Thus, there is always a direct orbital contribution and the experimental moments for such compounds around room temperature usually lie in the range 4.7-5.2B.M.

Table 4.5. Magnetic susceptibility data of cobalt(II) complexes of 1-pyrazolylphosphazenes.[a]

Compound	X_m ($\times 10^6$)	Diag corr[b] ($\times 10^6$) (c.g.s.u.)	TIP corr[c] ($\times 10^6$) (c.g.s.u.)	X_m^{corr}[d] ($\times 10^6$) /Co atom	T (^oK)	μ_{eff} B.M.
$N_3P_3(Me_2pz)_6 \cdot 2CoCl_2 \cdot THF$	16589	-486	448	8090	294	4.36
$N_3P_3Ph_2(Me_2pz)_4 \cdot CoCl_2$	8395	-347	-	8742	294	4.53
$N_3P_3Ph_4(Me_2pz)_2 \cdot CoCl_2 \cdot H_2O$	8667	-334	449	8552	292	4.47

(a) The author thanks Mr. John Haynes for measuring the room temperature magnetic susceptibilities by the Faraday method. (b) Corrections for diamagnetism were estimated by summing Pascal's constants and the correction for the N_3P_3 ring was obtained by subtracting 6x the correction for Cl from the diamagnetic susceptibility of $(NPCl_2)_3$. (c) Temperature Independent Paramagnetism (TIP) was calculated from the formula TIP = $^{2.09}/_{\Delta_t}$ where Δ_t is in cm^{-1}. (d) X_m^{corr} means the measured molar susceptibility corrected for both diamagnetism and TIP.

For tetrahedral complexes, the $^4A_2$ ground state has no orbital angular momentum and, therefore, the magnetic moment is expected to be closer to the spin-only value. However, the ground state can acquire orbital angular momentum indirectly through mixing in of the $^4T_2$ state by spin-orbit coupling, and the observed values mostly lie in the range 4.4-4.7 B.M. The values for five-coordinate complexes generally fall within this range also and, as such, magnetic measurements alone cannot distinguish between tetra- and penta-coordination about cobalt. Some values of the magnetic moments of high-spin five coordinate complexes of Co(II) are presented in Table 4.6, and are similar to the value of 4.53 B.M.

Table 4.6. Room temperature magnetic moments of some five-coordinate complexes of cobalt(II).[a]

Complex	Set of donor atoms	Proposed Structure	μ^{eff} (B.M.)	Reference
$[Co(Me_6tren)Cl]Cl$	N_4Cl	TBP	4.45	134a
$Co(Me_5dien)Cl_2$	N_3Cl_2	I	4.60	135
$Co(Et_4dien)Cl_2$	N_3Cl_2	-	4.71	140
$Co(terpy)Cl_2$	N_3Cl_2	TBP	4.97	136
$Co(Mab\text{-}en\text{-}NEt_2)Cl_2$	N_3Cl_2	-	4.82	141

(a) Abbreviations:
TBP ⟶ trigonal bypyramidal
I ⟶ intermediate between TBP and square planar

$Mab\text{-}en\text{-}NEt_2$ ⟶ 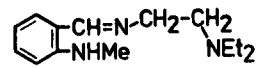

- abbreviations for the other compounds are given in Table 4.4.

obtained for the five-coordinate $gem\text{-}N_3P_3Ph_2(Me_2pz)_4 \cdot CoCl_2$. It follows that the moments for the cobalt(II) complexes of $N_3P_3(Me_2pz)_6$ (4.36) and $gem\text{-}N_3P_3Ph_4(Me_2pz)_2$ (4.47) favor tetrahedral stereochemistry, in accord with the electronic spectral evidence, but the additional trigonal bipyramidal coordination about the other cobalt atom in the former complex could only be determined from the crystal structure.

The effective magnetic moment for tetrahedral cobalt(II) complexes is inversely proportional to Δ_t and is given by the expression $\mu_{eff} = 3.89(1 - 4\lambda'/\Delta_t)$ B.M., where λ' is the spin-orbit coupling constant. Generally the values of λ', like those of B', vary between 60 and 90% of the free ion value ($\lambda = -178$ cm^{-1}) as a result of delocalization of the

d-electrons. However, λ' for gem-$N_3P_3Ph_4(Me_2pz)_2 \cdot CoCl_2 \cdot H_2O$ was calculated to be -173 cm^{-1} (97% of the free ion value) using μ_{eff} = 4.47 B.M. and Δ_t = 4650 cm^{-1}, and confirms that the uncertainties in calculating Δ_t, due to the lower symmetry, are justified.

4.1.6 Infrared Spectra of the Cobalt(II), Zinc and Cadmium Complexes

The infrared spectra of the complexes in nujol mull were recorded in the 200-4000 cm^{-1} region using CsI plates for absorptions above 250 cm^{-1} and polyethylene plates for absorptions less than 250 cm^{-1}. The important stretching frequencies are recorded in Table 4.7 and some are displayed in Figure 4.9.

The general features of the infrared spectra of the Co(II) and Zn complexes with the same pyrazolylphosphazene ligand are very similar. Specifically, the peak positions (to within 5 cm^{-1}) and relative band intensities are identical for all the complexes of $N_3P_3(Me_2pz)_6$, and a similar statement applies to the complexes of gem-$N_3P_3Ph_2(Me_2pz)_4$. They vary somewhat for the complexes of gem-$N_3P_3Ph_4(Me_2pz)_2$. The compounds are therefore assumed to be isostructural.

Apart from the easily identified metal-chloride stretching vibrations between 250 and 350 cm^{-1} (this far-infrared region is completely clear of absorptions by the ligands), the ν(P=N) frequencies are much more difficult to assign. In the case of the ligands containing Me_2pz groups, the ν(P=N) vibration occurs as a broad band between 1210 and 1235 cm^{-1}, and is closely flanked by other sharp ligand vibrations below 1200 cm^{-1}. Upon coordination these sharp peaks broaden and sometimes increase in intensity. Therefore, confusion arises as to whether or not they are components of the ν(P=N) vibration. Some splitting of ν(P=N), especially for the mixed pyrazolyl-

Table 4.7. (P=N), (M-Cl) and pyrazole ring stretching frequencies of the cobalt(II), zinc and cadmium complexes of 1-pyrazolylphosphazenes.[a]

Compound	ν(P=N) (cm^{-1})	ν(M-Cl)[b] (cm^{-1})	ν(Me_xpz ring)[c] (cm^{-1})
$N_3P_3(Me_2pz)_6$	1228	-	1573
" $\cdot 2ZnCl_2 \cdot THF$	1203,1223	310(br)m	1576
" $\cdot 2CoCl_2 \cdot THF$	1224,1201 1182sh	338w,310(br)w 273w	1576
gem-$N_3P_3Ph_2(Me_2pz)_4$	1231,1219	-	1567
" $\cdot ZnCl_2$	1231,1184	306m,276w	1573
" $\cdot CoCl_2$	1231,1182	308m,276w	1577
gem-$N_3P_3Ph_4(Me_2pz)_2$	1214,1224	-	1570
" $\cdot ZnCl_2$	1218	313m,341m	1567
" $\cdot CoCl_2 \cdot H_2O$	1218	300m,336m	1560
" $\cdot CdCl_2 \cdot CHCl_3$	1231	<200	1571
gem-$N_3P_3Ph_4(Mepz)_2$	1212,1188	-	1536
" $\cdot ZnCl_2$	1235,1223 1193,1178	305s,328s	1532

(a) From nujol mull spectra; assignments of ν(P=N) are tentative. M represents either Zn,Co or Cd. (b) Abbreviations: br-broad, w-weak intensity, m-medium intensity, s-strong intensity. (c) x=1 or 2.

phenylphosphazene complexes, is expected because of the low molecular symmetry and the different electronegativities of the substituents attached to phosphorus. Coordination to the nitrogen in the phosphazene ring is also expected to split ν(P=N), as it does for the methylphosphazenium quaternary salts[80,142], and is known to occur in the Zn and Co(II) complexes of $N_3P_3(Me_2pz)_6$ and gem-$N_3P_3Ph_2(Me_2pz)_4$. Generally if the relative intensity of the band system around 1180 cm^{-1} is similar in both the complex and ligand then it was not assigned as a component of ν(P=N). Such

is the case for the complexes of gem-$N_3P_3Ph_4(Me_2pz)_2$ where coordination of the metal to a phosphazene ring nitrogen does not occur. However, it is important to note that an observable splitting of the ν(P=N) vibration, regardless of how much, does not indicate that coordination to a nitrogen in the phosphazene ring is present.

Potentially more informative bands are the metal-chloride stretching frequencies. They are particularly important for the zinc complexes to which the techniques of electronic absorption spectroscopy and magnetism yield no information on the stereochemistry.

Although the symmetry of the isolated complexes is lower, the site symmetry about the metal atom is C_{2v}(Cl_2N_2 or Cl_2N_3 set of donor atoms), and group theory predicts two infrared active stretching modes: A_1 symmetric stretch and B_1 antisymmetric stretch. The values of the two ν(M-Cl) stretching frequencies of medium intensity for the Zn and Co(II) complexes of gem-$N_3P_3Ph_4(Me_xpz)_2$ (x=1,2) (Table 4.7) fall within the range characteristic of tetrahedral compounds of similar symmetry. For example, ν(M-Cl) occurs at 329, 296 cm^{-1} and at 344, 304 cm^{-1} for $ZnCl_2 \cdot 2$pyridine and $CoCl_2 \cdot 2$pyridine, respectively[143]. ν(Cd-Cl) stretching frequencies were neither observed nor expected since they occur at < 200 cm^{-1} for the compound $CdCl_2 \cdot 2$pyridine[143].

The values listed for the five-coordinate complexes of gem-$N_3P_3Ph_2(Me_2pz)_4$ (308, 276 cm^{-1} for Co and 306, 276 cm^{-1} for Zn) are too low to be associated with tetrahedral derivatives and too high to be associated with octahedral derivatives (ν(Co-Cl) has been assigned to the weak peak at 210 cm^{-1} in the spectrum of <u>trans</u>-$CoCl_2 \cdot 4$pyridine[144]). Even though the Zn-Cl and Co-Cl stretching frequencies of five-coordinate complexes

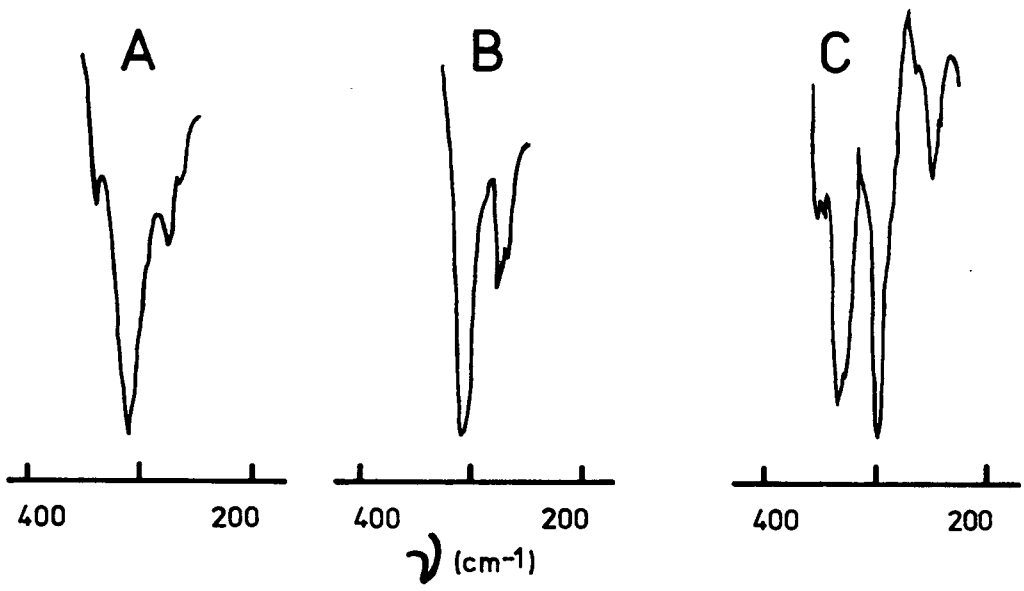

Figure 4.9. Cobalt-chloride stretching frequencies for $N_3P_3(Me_2pz)_6 \cdot 2CoCl_2 \cdot THF$ (A), gem-$N_3P_3Ph_2(Me_2pz)_4 \cdot CoCl_2$ (B) and gem-$N_3P_3Ph_4(Me_2pz)_2 \cdot CoCl_2 \cdot H_2O$ (C).

have not been systematically studied, it seems reasonable to suppose that they would lie intermediate in energy between the values reported for four- and six-coordinate complexes in the same spin state, in accord with the fact that in a change in the stereochemistry with an increase in the coordination number there is a decrease in the frequency values of the metal-halide stretching vibrations.

The far-infrared spectra of the complexes of $N_3P_3(Me_2pz)_6$ are characterized by a broad absorption around 310 cm^{-1}. Some weak satellite peaks at 338 cm^{-1} and 273 cm^{-1} were visible in the spectrum of the cobalt

complex (Figure 4.9), and these are believed to be due to the components of the tetrahedral ν(Co-Cl) and trigonal bipyramidal ν(Co-Cl) stretches, respectively, assuming that there is no coupling between cobalt atoms.

The Me_2pz ring stretching vibration between 1500 and 1600 cm^{-1} are included in Table 4.7 to show that there is little shift in frequency on coordination. Complexation has been known to produce definite positive shifts (as much as 30-40 cm^{-1}) compared to the free ligand in cobalt(II) complexes of α-(3,5-dimethyl-1-pyrazolyl)acetohydrazide[145].

4.1.7 ^1H and ^{31}P n.m.r. Spectra of the Zinc and Cadmium Complexes

The 100 MHz ^1H n.m.r. spectra of the zinc complexes at ambient temperature in deuteriochloroform (Table 4.8) were taken in order to see whether separate sets of resonances for uncoordinated and coordinated pyrazolyl groups could be distinguished. In fact, only one set of time averaged signals was obtained, indicating rapid exchange of the $ZnCl_2$ unit between coordinated and uncoordinated pyrazolyl groups. At -34^oC the rate of exchange was slow enough to observe some separation, but the resulting peaks were very broad, due in part to poor solubility at low temperatures. The compounds are slightly more soluble in CD_2Cl_2, and gem-$N_3P_3Ph_2(Me_2pz)_4 \cdot ZnCl_2$ even remained fluxional, at least down to -60^oC, in this solvent.

Although the spectra of the complexes are all comparatively similar to those of the respective ligands at ambient temperature, certain protons are shifted slightly more downfield on coordination, the shifts being greatest for $N_3P_3(Me_2pz)_6 \cdot 2ZnCl_2 \cdot THF$ and decreasing in the order $N_3P_3(Me_2pz)_6 \cdot 2ZnCl_2 \cdot THF > N_3P_3Ph_2(Me_2pz)_4 \cdot ZnCl_2 > N_3P_3Ph_4(Me_2pz)_2 \cdot ZnCl_2$. The more downfield methyl singlet is tentatively assigned to Me^3 since the proximity to the two chlorines is expected to deshield it more than Me^5.

Table 4.8. ^{1}H and ^{31}P n.m.r. parameters[a] at ambient temperature of the zinc and cadmium complexes of 1-pyrazolylphosphazenes.

Compound	Proton shifts δ(ppm)			Phosphorus shifts δ(ppm)		J(PP)
	Me^3	H^4	R^5	PPh_2	$P(R^3R^5pz)_2$	
$\underline{R^3=R^5=Me}$						
$N_3P_3(Me_2pz)_6$	2.09	5.81br	2.19	-	114.3	-
"·$2ZnCl_2$·THF[b]	2.50br	6.11br	2.20	-	-	-
$\underline{R^3=R^5=Me}$						
gem-$N_3P_3Ph_2(Me_2pz)_4$	2.04	5.77br	2.11	90.6t	115.8d	25.0
" ·$ZnCl_2$[c]	2.33	5.92br	2.02	86.60t	115.1d	19.2
$\underline{R^3=R^5=Me}$						
gem-$N_3P_3Ph_4(Me_2pz)_2$[d]	2.12	5.81d (2.8)	2.18	94.1d	117.5t	19.9
" ·$ZnCl_2$	2.28	5.90d (3.3)	2.12	90.2d	115.9t	13.3
" ·$CdCl_2$·$CHCl_3$	2.42	5.90d (3.9)	2.28	-	-	-
$\underline{R^3=Me,\ R^5=H}$						
gem-$N_3P_3Ph_4(Mepz)_2$[e]	2.28	6.04dd (∿2.7)	7.88dd (∿1.7)	93.2d	118.4t	19.9
" ·$ZnCl_2$	2.68	6.10dd (∿3.1)	7.72dd (∿2.5)	92.8d	120.7t	17.8

(a) From dilute solutions, δ_H(ppm) in $CDCl_3$, reference internal TMS; δ_P(ppm) in $CDCl_3$, shifts are to high field of external P_4O_6. Abbreviations: br-broad, d-doublet, dd-doublet of doublets, t-triplet. (b) δ_H for THF: multiplets at 1.87 and 3.78. At -34°C, δ($\underline{CH_3}$): 2.02,2.13,2.26,2.72; all singlets; δ(H^4): broad multiplet between 5.8 and 6.4. ^{31}P n.m.r. was not taken due to limited solubility. (c) δ($C_6\underline{H_6}$): multiplet between 7.45-7.60 and 7.94-8.20. At -34°C, δ($\underline{CH_3}$): 1.86br, 2.16br, 2.64br; intensity ratio 1:2:1. δ(H^4): 5.88br, 6.06br. (d) J(PH^4), in Hertz, in brackets; δ($C_6\underline{H_6}$): multiplet between 7.4-7.6 and 7.8-8.1 for both Zn and Cd complexes. (e) J(PH^4) and J(PH^5), in Hertz, in brackets; J(H^4H^5): 2.7 Hz for the ligand and 2.6 Hz for the Zn complex.

The assignment of the proton lines of the non-equivalent methyl groups in the 3- and 5-positions for some metal complexes containing the Me_2pz group has also been difficult[146], particularly if no coupling constant data are available. However, some workers have been unambiguously able to distinguish the two resonances by observing the magnitude of the coupling constants between hydrogen and a metal atom of nuclear spin ½, such as ^{195}Pt (natural abundance 33%)[147,148]. If the metal coordinates to N(2) on the pyrazole ring then the metal-proton couplings should be the greatest for Me^3, because the number of intervening bonds to the hydrogens in Me^5 is five compared to four in Me^3. The cadmium (^{111}Cd, spin ½, natural abundance 12.75%; ^{113}Cd, spin ½, natural abundance 12.26%) complex of gem-$N_3P_3Ph_4(Me_2pz)_2$ was made specifically to see if any satellite peaks arising from ^{111}Cd-^1H or ^{113}Cd-^1H coupling could be observed for the low field methyl resonance at 2.42δ. But unfortunately no couplings whatsoever were apparent in the ^1H n.m.r. spectrum. However, the large downfield shift of the Me^3 singlet in the spectrum of gem-$N_3P_3Ph_4(Mepz)_2 \cdot ZnCl_2$ ($\Delta Me^3 = \delta Me^3$ (complex) - δMe^3(ligand) = 0.40δ) is consistent with the Me^3 group, and not the Me^5 group, being assigned to the low field resonance in the spectra of the other complexes.

The ^{31}P n.m.r. spectra of the complexes also resemble those of the respective ligands. This is expected for gem-$N_3P_3Ph_2(Me_2pz)_4 \cdot ZnCl_2$ in which the two $\underline{P}(Me_2pz)_2$ groups still remain equivalent on coordination. On the other hand, if the zinc complexes of gem-$N_3P_3Ph_4(Me_xpz)_2$ (x=1,2) are similar in structure to gem-$N_3P_3Ph_4(Me_2pz)_2 \cdot CoCl_2$, then their ^{31}P n.m.r. spectra should be of the ABX spin-type, the two $\underline{P}Ph_2$ atoms now being distinguished; and not of the A_2X spin-type as in the spectra of the ligands. The fact that an A_2X pattern (doublet for $\underline{P}Ph_2$ and a triplet for $\underline{P}(Me_xpz)_2$ (x=1,2) was

observed indicates that the compounds are stereochemically non-rigid in solution, in agreement with the highly fluxional behaviour of gem-$N_3P_3Ph_2(Me_2pz)_4 \cdot ZnCl_2$ and $N_3P_3(Me_2pz)_6 \cdot 2ZnCl_2 \cdot THF$ in solution (as shown by their proton spectra).

One noteworthy trend in the ^{31}P n.m.r. data is the decrease in the $\underline{P}Ph_2$-$\underline{P}(Me_2pz)_2$ coupling constants on coordination, a feature that has proved useful for assigning phosphorus chemical shifts in the more complicated spectra of the palladium derivatives. Conversely, $J(PH^4)$ and $J(PH^5)$ increase slightly on coordination.

4.2 Palladium and Platinum Complexes

4.2.1 Preparation of Pd(II) and Pt(II) Complexes

Reaction of an excess of trans-bis(benzonitrile)dichloropalladium(II) with a particular pyrazolylphosphazene in benzene precipitated air-stable, orange-yellow solids of the same stoichiometry as those of the corresponding zinc and cobalt(II)chloride complexes (Equations 4.5-4.7). Also yellow crystals of the platinum compound $N_3P_3(Me_2pz)_6 \cdot 2PtCl_2$ were produced in a

$$N_3P_3(Me_2pz)_6 \xrightarrow[M=(Pd;Pt)\ C_6H_6]{MCl_2(PhCN)_2(>3eq.)} N_3P_3(Me_2pz)_6 \cdot 2MCl_2 + 4PhCN \quad \ldots (4.5)$$

$$\text{gem-}N_3P_3Ph_2(Me_2pz)_4 \xrightarrow[C_6H_6]{PdCl_2(PhCN)_2(>2eq.)} \text{gem-}N_3P_3Ph_2(Me_2pz)_4 \cdot PdCl_2 + 2PhCN \quad \ldots (4.6)$$

$$\text{gem-}N_3P_3Ph_4(Me_2pz)_2 \xrightarrow[C_6H_6]{PdCl_2(PhCN)_2(>1eq.)} \text{gem-}N_3P_3Ph_4(Me_2pz)_2 \cdot PdCl_2 + 2PhCN \quad \ldots (4.7)$$

similar but slower reaction with cis-bis(benzonitrile)dichloroplatinum(II). However, the spectroscopic data are not in agreement with trigonal bipyramidal coordination involving two Me_2pz groups on different phosphorus atoms. Therefore, the most likely reason why some Me_2pz groups remained uncoordinated is that the complexes precipitated before complete addition could be achieved. In order to prove this a suitable solvent was required and CH_2Cl_2 was found to be the best. Thus, reaction of three equivalents of $PdCl_2(PhCN)_2$ with $N_3P_3(Me_2pz)_6$ in CH_2Cl_2 gave orange crystals of $N_3P_3(Me_2pz)_6 \cdot 3PdCl_2$ in which all the Me_2pz groups were coordinated (Equation 4.8). Actually CH_2Cl_2 was found to be the best solvent for all the preparations because the reactions are faster and the yields are higher.

$$N_3P_3(Me_2pz)_6 \xrightarrow[CH_2Cl_2]{3PdCl_2(PhCN)_2} N_3P_3(Me_2pz)_6 \cdot 3PdCl_2 + 6PhCN \quad \ldots (4.8)$$

4.2.2 Infrared and N.M.R. Spectra, and Conductivities of the Pd(II) and Pt(II) Complexes

All the spectroscopic parameters and molar conductivities of the complexes appear in Table 4.9: the molar conductivities Λ_M of ca. 10^{-3}M solutions in nitromethane at 25°C are consistent with the expected non-electrolytic behaviour, as in the corresponding Zn and Co(II) complexes; the far-infrared spectra, except for the complexes of $N_3P_3(Me_2pz)_6$, are in agreement with the cis-square planar arrangement about the metal atom demanded by the geometry of the ligand; and the ^1H and ^{31}P n.m.r. spectra show that the complexes are stereochemically rigid in solution, even at 55°C. All of the above evidence, taken together, allows one to assign a gross structure to each compound, the details of which are given below.

Table 4.9. Infrared data[a], ^{1}H and ^{31}P n.m.r. parameters[b], and conductivities[c] of the Pd(II) and Pt(II) complexes of 1-pyrazolylphosphazenes.

Compound	Λ_M	Proton Shifts[d] δ(ppm)		Phosphorus Shifts -δ(ppm)		J(PP)[e] (Hz)	ν(P=N) (cm^{-1})	ν(M-Cl) (cm^{-1})
		H^4	Me	$\underline{P}Ph_2$	$\underline{P}(Me_2pz)_2$			
$N_3P_3Ph_4(Me_2pz)_2 \cdot PdCl_2$ (f)	1.21	5.74d (∿4.0)	2.04 2.68	$1P_A$,93.0d $1P_B$,95.0d	$1P_X$,122.7dd	14.2(AX) 27.3(BX) 0.0(AB)	1230 1197 1180	325,329sp 341
$N_3P_3Ph_2(Me_2pz)_4 \cdot PdCl_2$ (g)	3.41	5.83d (∿4.0) 6.02d (∿4.0)	2.16 2.38 2.70	$1P_X$,91.5dd	$1P_A$,113.8dd $1P_B$,118.1dd	+18.1(AX) +32.7(BX) or -19.3(AX) +33.7(BX) +49.7(AB)	1200 1246	332 347
$N_3P_3(Me_2pz)_6 \cdot 2PdCl_2$	2.26	5.92d (4.8) 5.98d (4.0) 6.03d (4.8)	2.05 2.32 2.35 2.61 2.63 2.72				1212 1225sh	344br
$N_3P_3(Me_2pz)_6 \cdot 2PtCl_2$	1.68	6.02d (5.0) 6.12d (5.0)	2.10,2.27 2.35,2.61 2.63 2.70				1212 1225sh	344br
$N_3P_3(Me_2pz)_6 \cdot 3PdCl_2$ *	-	6.19br	2.52 2.73		3P,123.8		1227	344br

(a) From nujol mull spectra: br-broad, sh-shoulder, sp-split. (b) From $CDCl_3$, *CD_2Cl_2. ^{1}H nmr ref. internal TMS, ^{31}P nmr ref. external P_4O_6. d-doublet, dd-doublet of doublets. (c) ca. $10^{-3}M$ solutions in $MeNO_2$ at 25°C (units of $cm^2 ohm^{-1} mole^{-1}$). (d) J(PH) in brackets. (e) $J(P_AP_X)$=(AX), $J(P_BP_X)$=(BX) and $J(P_AP_B)$=(AB). (f) δ_H(phenyl)=7.35-7.60, 7.80-8.05 and 8.35-8.60. (g) δ_H(phenyl)=7.35-7.55 and 8.15-8.40.

4.2.2A Gem-$N_3P_3Ph_4(Me_2pz)_2 \cdot PdCl_2$

The complex is a yellow, microcrystalline solid which is slightly soluble in acetone, dimethyl sulfoxide (DMSO), chloroform and methylene chloride, and insoluble in methanol. Moreover, n.m.r. indicates that decomposition occurs in DMSO, most likely according to Equation 4.9.

$$gem\text{-}N_3P_3Ph_4(Me_2pz)_2 \cdot PdCl_2 \xrightarrow{DMSO} gem\text{-}N_3P_3Ph_4(Me_2pz)_2 + PdCl_2(DMSO)_2 \quad \ldots (4.9)$$

The cis-configuration of the $PdCl_2$ unit can be determined from the Pd-Cl stretches observed in the far-infrared region. The spectrum has two bands at 325,329 (split) and 341 cm^{-1} corresponding to Pd-Cl symmetric (A_1) and asymmetric (B_1) stretches under C_{2v} symmetry. These are readily assigned by analogy to the Pd-Cl symmetric and asymmetric stretches which appear at 333 and 342 cm^{-1}, respectively, in the spectrum of cis-$PdCl_2(pyridine)_2$[149]. Only one asymmetric stretch (B_{3u} under D_{2h} symmetry) is expected for the trans-configuration. Pd-Cl stretching frequencies have also been tentatively assigned at 339/335 cm^{-1} and at 364/337 cm^{-1} for cis-$PdCl_2(imidazole)_2$[150] and cis-$PdCl_2(Me_2pzH)_2$[148], respectively.

Owing to the number of potential donor nitrogen atoms, several structural possibilities exist, some of which can be distinguished by n.m.r. Palladium can bond to two nitrogens in the phosphazene ring (I), to two Me_2pz groups (II), or to one Me_2pz group and a nitrogen in the phosphazene ring (III). Possibilities I and III can immediately be rejected solely on the basis of the proton n.m.r. spectrum (Figure 4.10A). Only structure II is consistent with the observed equivalence of the two Me_2pz groups, since bonding to the phosphazene ring would differentiate them both chemically

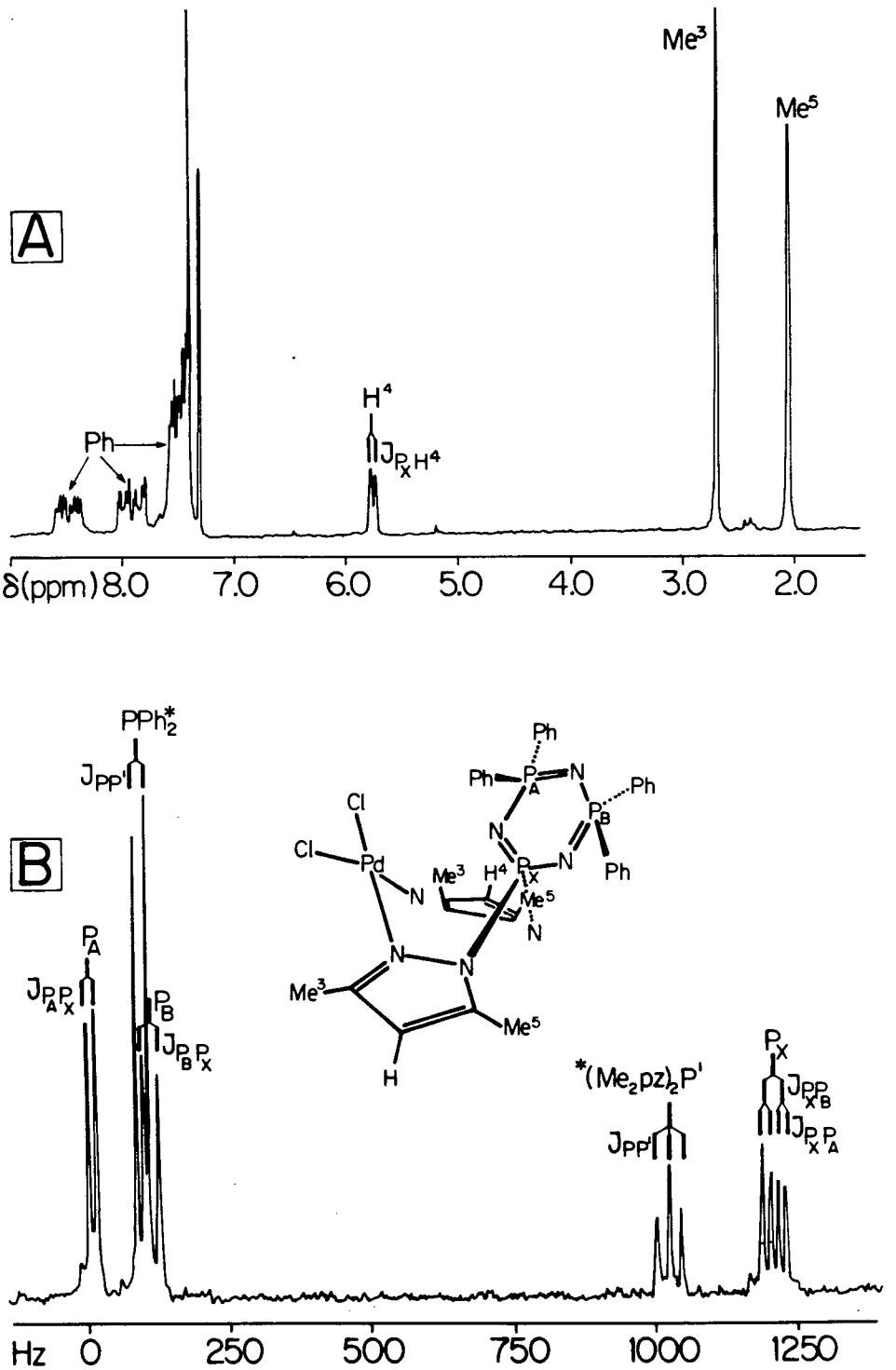

Figure 4.10. 100 MHz ^{1}H n.m.r. spectrum in $CDCl_3$ (A) and ^{1}H-decoupled 40.5 MHz ^{31}P n.m.r. spectrum in DMSO (B) of gem-$N_3P_3Ph_4$-$(Me_2pz)_2 \cdot PdCl_2$. Peaks arising from gem-$N_3P_3Ph_4(Me_2pz)_2$, because of decomposition, are indicated by an asterisk.

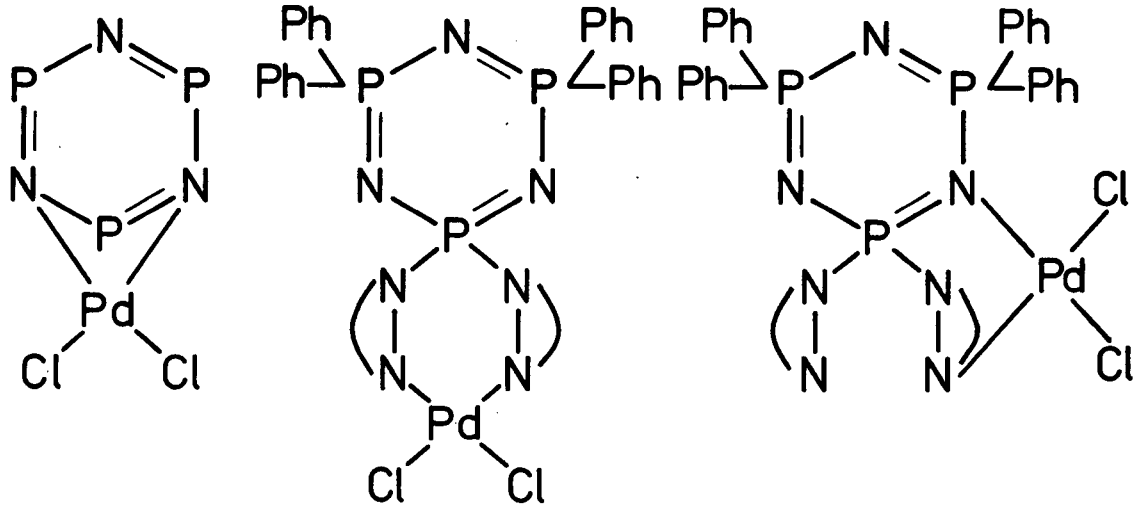

I II III

and magnetically. Furthermore, the ABX pattern present in the ^{31}P n.m.r. spectrum (Figure 4.10B) and the large separation of the resonances of the phenyl protons in the ^{1}H spectrum suggest that the orientation of the $P\{N\text{-}N\}_2PdCl_2$ unit to the phosphazene ring is similar to that observed for the cobalt unit in the structure of gem-$N_3P_3Ph_4(Me_2pz)_2 \cdot CoCl_2$. That is, the six-membered chelate ring (boat conformation) is directed more towards one $\underline{P}Ph_2$ phosphorus atom than the other such that there is no plane of symmetry perpendicular to the plane of the phosphazene ring (see illustration in Figure 4.10B).

In the ^{1}H n.m.r. spectrum of the compound in $CDCl_3$ (Figure 4.10A), the two methyl resonances at 2.04δ and 2.68δ are assigned to the 5-methyl and the 3-methyl group, respectively, in accord with the assignments given at 1.93δ and 2.69δ for $PdCl_2(Me_2PzH)_2$ in the same solvent[148].

The ^{31}P spectrum of the compound in DMSO(d^6) (Figure 4.10B) shows peaks arising from both complex and ligand because of decomposition, the

high field triplet and the low field doublet of highest intensity belonging to the latter. Unlike the A_2X pattern observed for the ligand, the spectrum of the complex is of the ABX type, the two $\underline{P}Ph_2$ phosphorus atoms P_A and P_B now being distinguished. The most downfield $\underline{P}Ph_2$ resonance (93.0δ, doublet) is assigned to the phosphorus atom P_A closest to the $PdCl_2$ unit. It is not surprising that $J(P_AP_B) = 0$ because phosphorus-phosphorus couplings are sometimes not observed if the electronegativity of the substituents attached to phosphorus is low.

4.2.2B $\underline{Gem\text{-}N_3P_3Ph_2(Me_2pz)_4\cdot PdCl_2}$

This palladium complex is an orange crystalline solid considerably more soluble in polar organic solvents than its tetraphenyl analogue.

From a consideration of the molecular structures of the zinc and cobalt(II) complexes, there are only two plausible structures for this derivative: trigonal bipyramidal geometry about the Pd atom incorporating two Me_2pz groups on different phosphorus atoms and a nitrogen in the phosphazene ring (IV), and a four-coordinate structure involving two Me_2pz groups on the same phosphorus (V), of which at least two conformational isomers are possible (Va and Vb).

In the infrared spectrum the two Pd-Cl stretching frequencies occurring at 332 (A_1 symmetric) and 347 cm^{-1} (B_1 asymmetric) lie in the range generally observed for <u>cis</u>-square planar palladium complexes. Although no values for Pd-Cl stretching frequencies were found in the literature for five-coordinate palladium chloride complexes, it seems reasonable to believe that they would lie around 300 cm^{-1}, as in the spectrum of $gem\text{-}N_3P_3Ph_2(Me_2pz)_4\cdot ZnCl_2$. By contrast, the appearance of the P=N region in the two spectra is identical, except for minor frequency differences at 1200,1246cm^{-1}

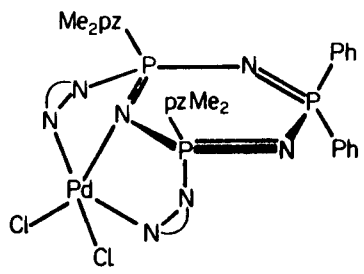

IV

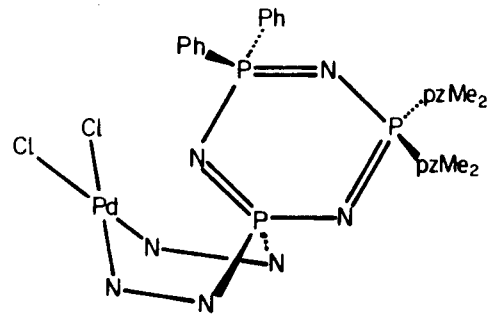

Va

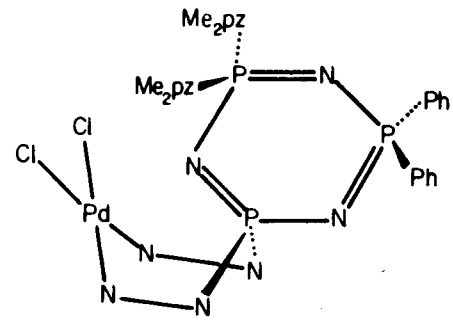

Vb

for the Pd complex and at 1184,1231 for the Zn complex, suggesting that bonding to the nitrogen in the phosphazene ring may be occurring. However, as mentioned previously, a split P=N band is not a reliable indication of bonding to the phosphazene ring.

N.m.r., on the other hand, can unambiguously distinguish between IV and V. Although the proton spectrum (Figure 4.11B) shows two sets of pyrazolyl groups, one coordinated and the other uncoordinated, consistent with both proposed structures, only the ABX pattern observed in the ^{31}P n.m.r. spectrum (Figure 4.11A) supports structure V. The three methyl resonances occurring at 2.16, 2.38 and 2.70δ (relative intensity 2:1:1) in the ^{1}H n.m.r. spectrum are not assigned to particular 3- and 5-methyl groups because of the uncertainties involved. However, the low field H^4 resonance at 6.02δ is expected to belong to the set of coordinated Me_2pz

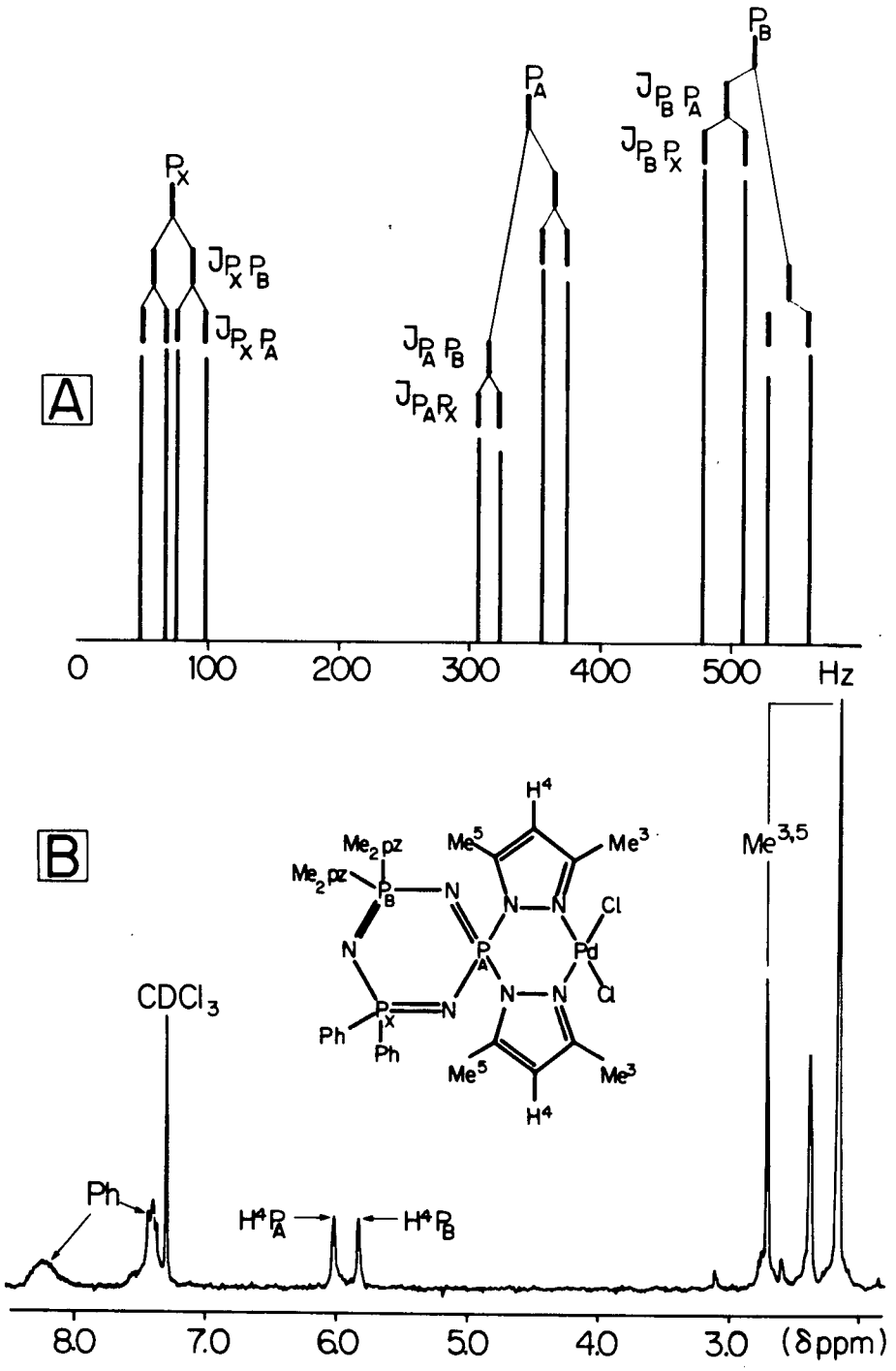

Figure 4.11. ^{31}P-decoupled 100 MHz ^{1}H n.m.r. spectrum (B) and ^{1}H-decoupled 40.5 MHz ^{31}P n.m.r. spectrum (A) of gem-$N_3P_3Ph_2(Me_2pz)_4 \cdot PdCl_2$. Samples in $CDCl_3$ solution.

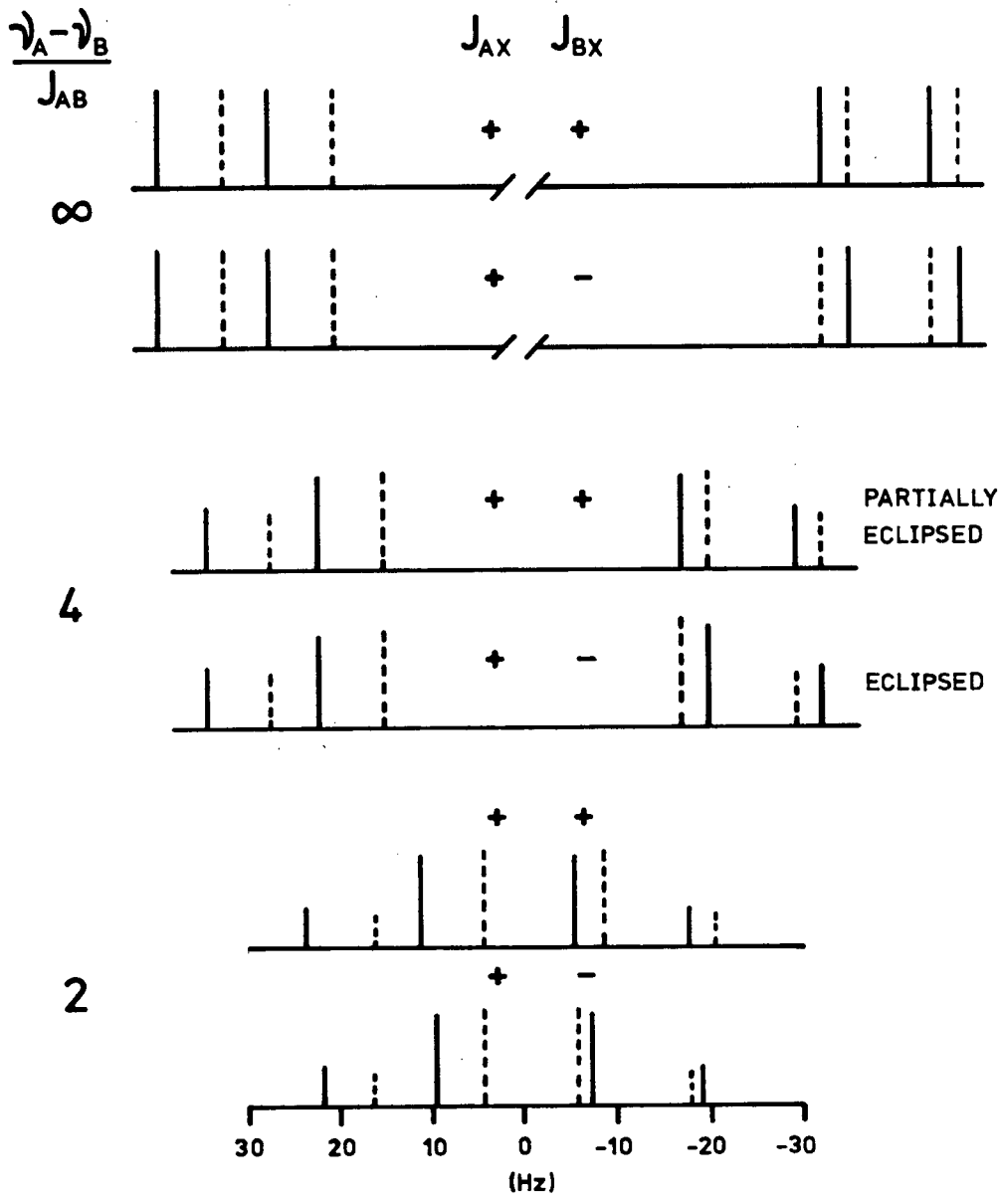

Figure 4.12. The effect of changing the sign of J_{BX} on the AB part of an ABX spectrum. Solid lines: $(ab)_+$ subspectrum; dashed lines: $(ab)_-$ subspectrum. In the totally eclipsed case the $(ab)_-$ subspectrum is contained between the first and fourth lines of the $(ab)_+$ subspectrum. Parameters: J_{AB}=12, J_{AX}=7, J_{BX}=±3Hz; $(\nu_A - \nu_B)/J_{AB}$ indicated in figure. Reference: "High Resolution NMR", E.D. Becker, Academic Press N.Y., 1969, p.159.

groups and is assigned accordingly. Just which isomer, Va or Vb, exists is not certain.

The ABX phosphorus spectrum was analyzed according to the procedure outlined in reference (151). Here $P_A = P_A(Me_2pz)_2$, $P_B = P_B(Me_2pz)_2$ and $P_X = P_XPh_2$. The calculated Larmor frequencies ν_A, ν_B and ν_X (converted to δppm), and coupling constants J_{AB}, J_{BX} and J_{AX} are given in Table 4.9. J_{AB} is arbitrarily chosen to be positive, but the relative signs of J_{AX} and J_{BX} cannot be reliably determined and both sets of values are reported. Generally if $\frac{\nu(A) - \nu(B)}{J(AB)} > \sim 2$ (in this case $\frac{\nu(A) - \nu(B)}{J(AB)} = 3.5$) the correct selection of the two $(ab)_+$ and $(ab)_-$ quartets is sometimes ambiguous (Figure 4.12) and leads only to a reversal of one of the signs of J_{AX} or J_{BX} if an incorrect assignment is made, but can actually lead to the calculation of slightly different magnitudes of these J's as well, if $\frac{\nu(A) - \nu(B)}{J(AB)} < \sim 2$. In this spectrum the two (ab) quartets are either partly eclipsed or totally eclipsed, a distinction which can usually be made by comparing the calculated and observed intensities of the X multiplet. However, both sets of calculations give an intensity ratio of approximately 1:1:1:1 for the four peaks of the X multiplet. The observed ratios are also approximately 1:1:1:1, but vary with each spectrum taken because of background noise. Hence, the sign of J_{AX} is uncertain. The peak at 113.8δ is assigned to the phosphorus atom P_A bonded to the two coordinated Me_2pz groups since $J(\underline{P}Ph_2\text{-}\underline{P}(Me_2pz)_2)$ in the corresponding zinc complex also decreases on coordination, from 25 Hz to 19.2 Hz.

4.2.2C $N_3P_3(Me_2pz)_6 \cdot 2MCl_2$ (M=Pt,Pd)

The yellow platinum and orange palladium complexes are soluble in most organic solvents and exhibit greater stability in solvating solvents,

such as acetonitrile, than do the di-zinc and di-cobalt complexes.

The ^{1}H n.m.r., ^{31}P n.m.r. and infrared spectra of the palladium compound are similar to those of the platinum compound, thus suggesting that they are isostructural. Both compounds display a broad band at 344 cm^{-1} in the infrared spectra corresponding to the metal-chloride stretch. Although this band occurs in the region characteristic of trans-square planar palladium or platinum chloride derivatives, this configuration is geometrically impossible for bidentate ligands. The spectrum of the di-zinc complex also shows only one broad band in the far-infrared region, probably a result of overlapping asymmetric and symmetric stretching frequencies.

The ^{31}P-decoupled ^{1}H n.m.r. spectrum of the palladium complex in $CDCl_3$ (Figure 4.13B) shows six singlets of equal intensity in the methyl region and three singlets of equal intensity in the H^4 region corresponding to three non-equivalent sets containing two Me_2pz groups each. Although the absolute assignments of these resonances cannot be made with certainty, their interpretation in terms of the proposed structure is unambiguous. It was hoped that some ^{195}Pt-^{1}H couplings might be seen in the spectrum of the platinum complex to aid in the assignments, but none was visible.

In conjunction with the observed ABC pattern in the ^{31}P n.m.r. spectrum (Figure 4.13A) only one stereoisomer involving coordination to Me_2pz groups on the same phosphorus atom is possible, if the orientation of the $P(N\text{-}N)_2PdCl_2$ unit is similar to that in the proposed structure of gem-$N_3P_3Ph_4(Me_2pz)_2 \cdot PdCl_2$. An ABC type ^{31}P spectrum can only be realized if the two boat-conformations are not directed towards each other as in VI. If the two boats are symmetrically displaced about the phosphazene ring as in VIIa-b, then the two sets of coordinated Me_2pz groups would be chemically

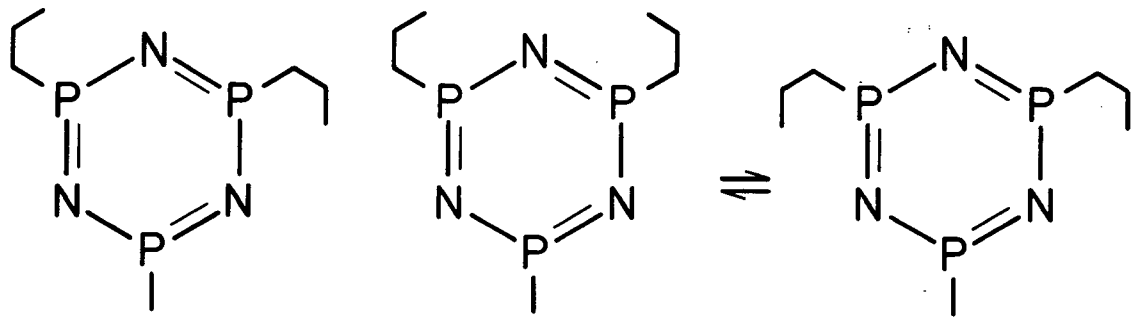

VI VII-a VII-b

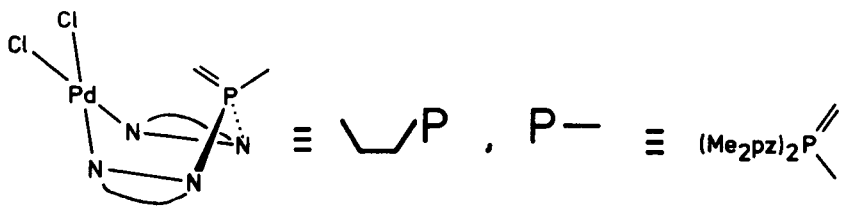

and magnetically equivalent. Thus, only two resonances of intensity ratio 2:1 for H^4 and at most four methyl resonances would be observed in the proton spectrum, and an A_2B or A_2X (doublet for $\underline{P}(Me_2pz)_2$ coordinated and a triplet for $\underline{P}(Me_2pz)_2$ uncoordinated) pattern would be seen in the ^{31}P spectrum. Any form of bonding to the phosphazene ring is disregarded because more than three resonances for H^4 would be expected.

The ABC pattern in the ^{31}P spectrum of the two compounds was determined by the method of Castellano and Waugh[152]. Theoretically fifteen lines can be observed in the case of three non-equivalent spin ½ nuclei, three of which are combination bands. If the twelve lines can be divided into three groups A, B and C each containing four lines such that the following equations hold, then the spectrum is of the ABC spin-type. The spacings are shown on the spectrum in Figure 4.13B; group assignments (A_n, B_n, or C_n) are arbitrary.

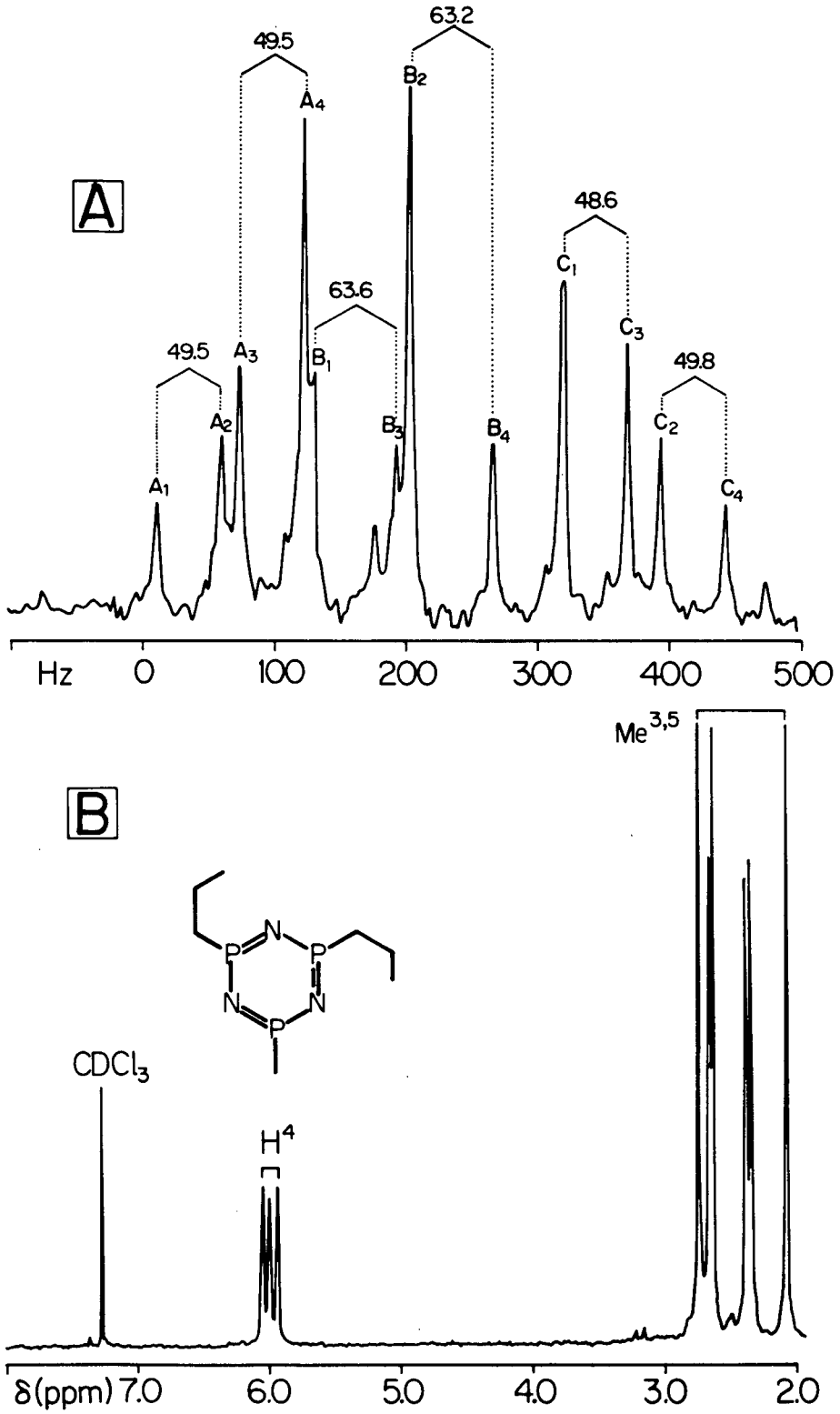

Figure 4.13. ^{31}P-decoupled 100 MHz ^{1}H n.m.r. spectrum (B) and ^{1}H-decoupled 40.5 MHz ^{31}P n.m.r. spectrum (A) of $N_3P_3(Me_2pz)_6 \cdot 2PdCl_2$. Spectra run on samples in $CDCl_3$ solution. See text for explanation of diagram and symbols.

1) $\nu(A_1) - \nu(A_2) = \nu(A_3) - \nu(A_4) = \nu(C_1) - \nu(C_3) = \nu(C_2) - \nu(C_4)$

2) $\nu(A_1) - \nu(A_3) = \nu(A_2) - \nu(A_4) = \nu(B_1) - \nu(B_3) = \nu(B_2) - \nu(B_4)$

3) $\nu(B_1) - \nu(B_2) = \nu(B_3) - \nu(B_4) = \nu(C_1) - \nu(C_2) = \nu(C_3) - \nu(C_4)$

In addition, no ^{195}Pt-^{31}P couplings were noticed in the ^{31}P spectrum of the platinum compound. The complete lack of any platinum couplings is surprising in view of the fact that the proton spectra of most platinum complexes containing pyrazole bonding via the pyridine-type nitrogen to platinum show ^{195}Pt couplings to the protons in the pyrazole ring[147,148].

4.2.2D $N_3P_3(Me_2pz)_6 \cdot 3PdCl_2$

This bright orange solid is insoluble in most organic solvents except methylene chloride. Decreasing solubility upon increasing the number of coordinated metal atoms is a general trend also observed with the zinc and cobalt complexes.

The infrared spectrum is almost identical to that of the ligand, particularly in the 1200 cm^{-1} region where the P=N band remains single, and qualitatively confirms that bonding to the nitrogen in the phosphazene ring is not occurring. The Pd-Cl stretching vibration at 344 cm^{-1} also appears as a broad band in the far-infrared region. The symmetrical nature of the substitution process is confirmed by the simple pair of singlets in the methyl region of the proton spectrum and by the singlet in the ^{31}P spectrum. The H^4 resonance remains as a broad unresolved band, in contrast to the observable phosphorus couplings of $\sim$ 4.0 Hz apparent in the spectra of all the other palladium derivatives.

Introduction of a third $PdCl_2$ unit into the complex $N_3P_3(Me_2pz)_6 \cdot 2PdCl_2$ can occur in two ways, as illustrated in Equation 4.10, but only

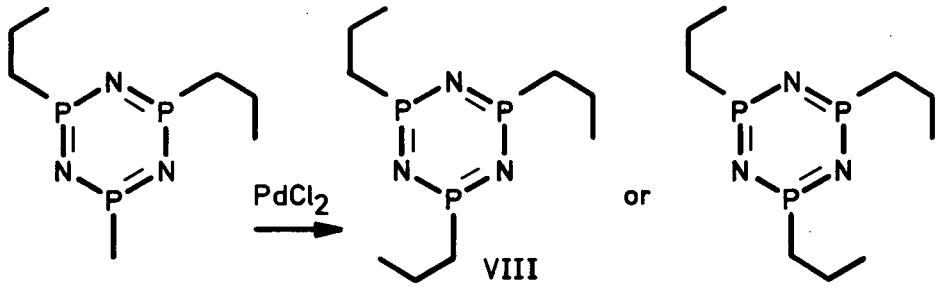

... (4.10)

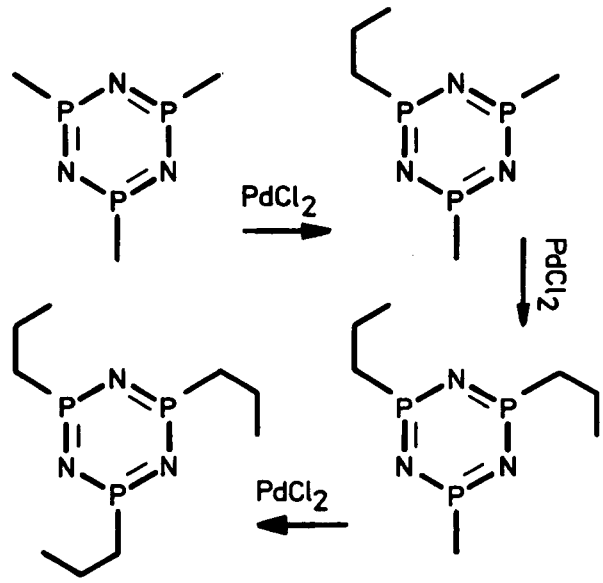

... (4.11)

in VIII are the phosphorus atoms equivalent. Thus, the overall substitution process appears to follow the route shown in Equation 4.11.

4.3 Molybdenum(0)Complexes of Gem-$N_3P_3Ph_2(Me_2pz)_4$

4.3.1 Preparation of the Mo(0) Complexes

The different site selectivities of palladium and zinc towards gem-$N_3P_3Ph_2(Me_2pz)_4$ prompted an interest in making complexes of other metals. Carbonyl complexes of molybdenum were chosen because of the potential information on π-acceptor properties of the ligand. $Mo(CO)_3(CH_3CN)_3$ was used as starting material in accord with the known tridentate nature of the ligand. The site preference of the Mo atom can be similar to Zn or Pd except that the stereochemistry is now octahedral.

However, reaction in benzene yielded not one, but two isomers (hereafter labelled A and B) both of which probably incorporate two Me_2pz groups and a nitrogen atom in the phosphazene ring (Equation 4.12). They can easily be separated by their different solubilities in benzene.

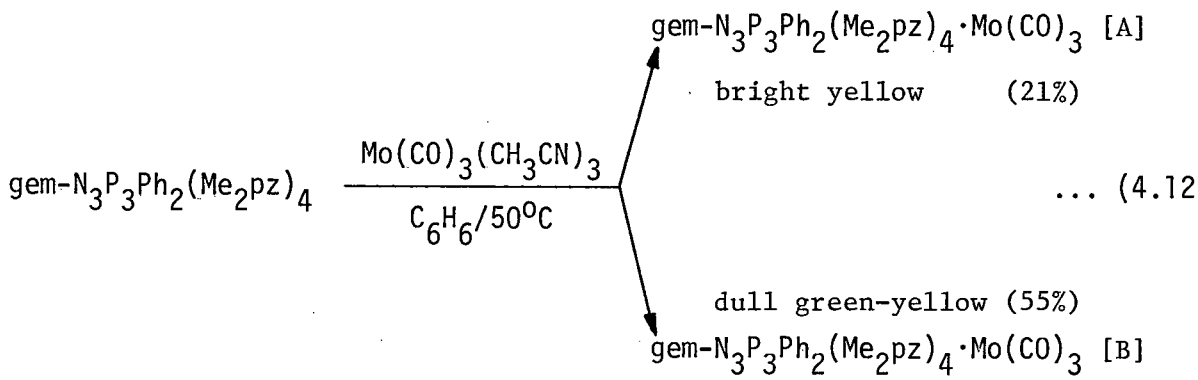

... (4.12)

4.3.2 Physical and Spectroscopic Properties of Gem-$N_3P_3Ph_2(Me_2pz)_4 \cdot Mo(CO)_3$

The two isomers A and B slowly react with chlorinated solvents, such as chloroform, but are stable under nitrogen in benzene. However, both compounds immediately decompose in either solvent in the presence of a high magnetic field. This unique property was discovered when attempting to obtain their ^1H n.m.r. spectra. The yellow solutions of A and the dull green-yellow solutions of B turn bright red in less than one minute after placement in the magnetic field of the 270MHz and 100MHz spectrometers. Decomposition is slower in the 80 MHz spectrometer, occurring after five minutes, and is not observed at 60 MHz. These red solutions gradually become colourless after several days, and only peaks due to the ligand are apparent in their ^1H n.m.r. spectra. Both compounds are stable in an atmosphere of nitrogen, but compound B becomes brown after exposure to air for one week. Compound A is very stable to air.

On the basis of spectroscopic evidence, both species have essentially the same configuration about molybdenum, but probably exist as different

structural isomers. Two geometrical isomers are possible for octahedral complexes of formula $LMo(CO)_3$, where L is a tridentate ligand: 1) the ligands of one type cover one face of the octahedron - facial isomer (IX), or 2) they may span three positions two of which are opposite or trans to each other - meridional isomer (X). The two possibilities are usually

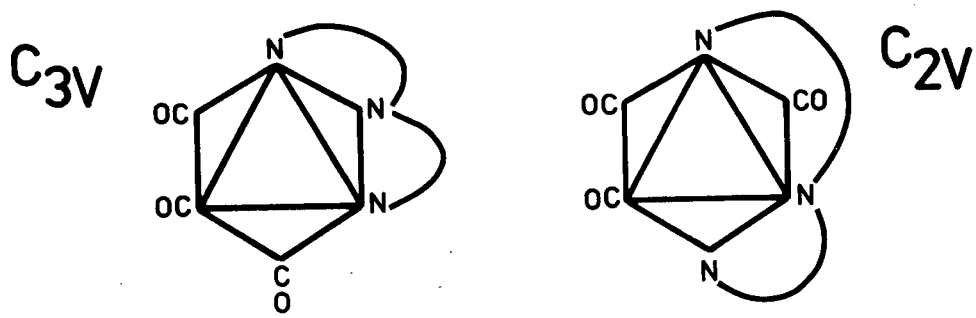

IX X

easy to distinguish by infrared. Compounds containing the facial tricarbonyl group show two CO stretching bands (A_1 and E) if the symmetry is C_{3v} [153]; if lower, the degenerate band may be broadened, as it is in $[(NH_2CH_2CH_2)_2NH]Mo(CO)_3$ [154], or split, as it is in (cycloheptatriene)Mo-$(CO)_3$ [155]. Meridional tricarbonyl isomers, on the other hand, exhibit three CO stretching bands ($A_1(1)$, $A_1(2)$ and B_2 under C_{2v} symmetry) two of which are expected to be about half the intensity of the third [153]. The frequencies of the CO stretching mode are given in Table 4.10 and in Figure 4.14, and are readily interpreted on the basis of an octahedral geometry. Both compounds show two strong bands of similar intensity: a sharp band at 1905 cm^{-1} and a broad or split band at 1770-1790 cm^{-1}, characteristic of pseudo C_{3v} structures. The numerical values are similar to those of the two strong bands in the complexes $PhP(Me_2pz)_2Mo(CO)_3$ (1920, 1805 cm^{-1}) [125] and $N_4P_4Me_8 \cdot Mo(CO)_3$ (1906; 1778, 1755 cm^{-1} broad) [63], and are

Table 4.10. Spectroscopic parameters[a] of gem-$N_3P_3Ph_2(Me_2pz)_4 \cdot Mo(CO)_3$

Compound	Colour	ν(P=N) (cm^{-1})	ν(CO) (cm^{-1}) A_1	ν(CO) (cm^{-1}) E	Proton Shifts δ(ppm) H^4	Proton Shifts δ(ppm) Me	Mass Spectra
A	Bright Yellow	1218 1239	1905[b]	1777 1785sh	5.86 5.90br	6H,1.94 6H,2.16 12H,2.48	M (0.9) M-3CO (5.3) M-Me_2pz-CO (7.4) M-3CO-Mo (10.0)
B	Dull Yellow-Green	1231 1181	1906	1770 1786	5.90br	12H,2.03 6H,2.40 6H,2.51	M-3CO (<1.0) M-3CO-Mo (10.0) M-Me_2pz-CO (<1.0)

(a) Infrared frequencies from nujol mull spectra; sh-shoulder. Mass spectra run at 70eV; probe temperature ∿ 240°C; relative intensities in brackets on a scale from 0-10.0 with the molecular ion of the ligand arbitrarily set at 10.0. ^1H n.m.r. parameters from dilute solutions in $CDCl_3$ at 80 MHz; reference external TMS; br-broad.

(b) 1908; 1765, 1785 cm^{-1} split, from $CHCl_3$ solution.

much lower than those of the phosphine complexes $(F_3P)_3Mo(CO)_3$ (2090,2055 cm^{-1})[156] and $(Me_3P)_3Mo(CO)_3$ (1945, 1854 cm^{-1})[157] in which the carbonyl bonds are strengthened, to different extents, by overlap of the metal d-orbitals with the acceptor orbitals of the ligands. The relatively low frequencies, therefore, suggest that back donation of the molybdenum d-electrons to the π-acceptor orbitals of the pyrazolylphosphazene ligand is weak. Thus, coordination apparently occurs by σ-donation from the nitrogen atoms of the ligand. But just which nitrogen atoms are involved cannot be determined with certainty.

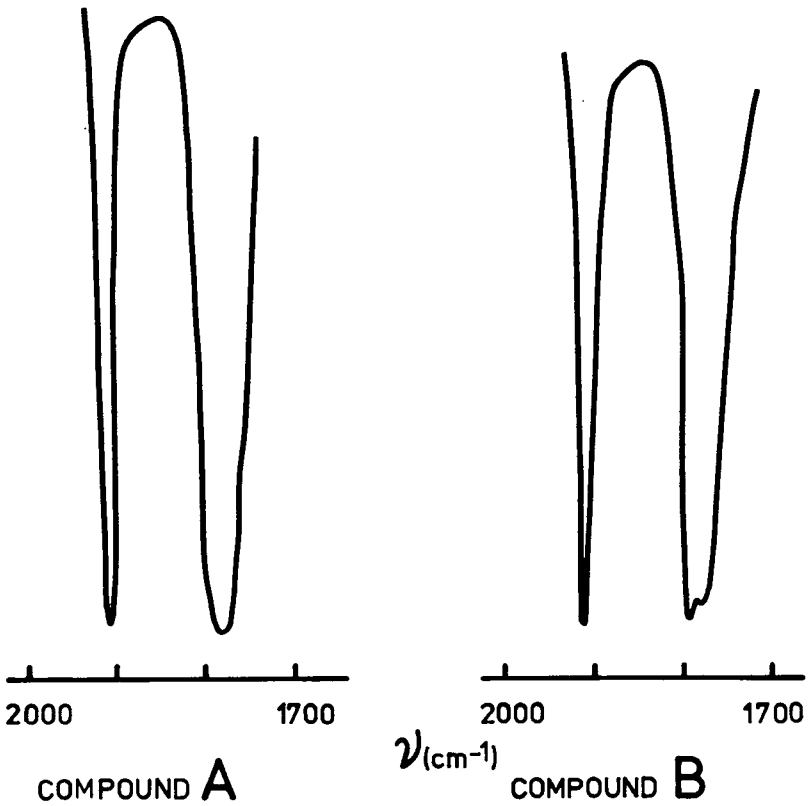

Figure 4.14. Infrared spectra from nujol mull of the carbonyl region. The two isomers of gem-$N_3P_3Ph_2(Me_2pz)_4 \cdot Mo(CO)_3$ are designated in the figure.

There are at least four possible structures for the two isomers, assuming molybdenum attains the stable 18-electron configuration by accepting six electrons from the pyrazolylphosphazene ligand (octahedral coordination geometry about Mo). The metal can coordinate to two Me_2pz groups on the same phosphorus atom (XI and XII) or on adjacent phosphorus atoms (XIII), each incorporating a nitrogen in the phosphazene ring. Finally, the phenyl group can participate as a 2-electron donor (XIV), as it does

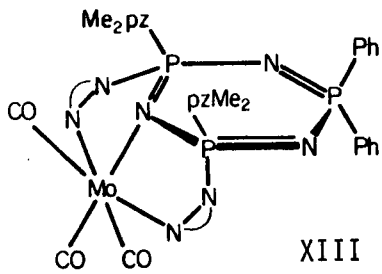

XIII

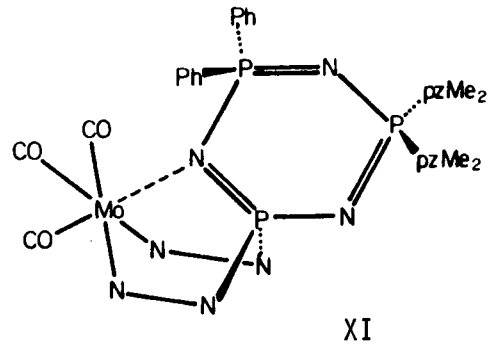

XI

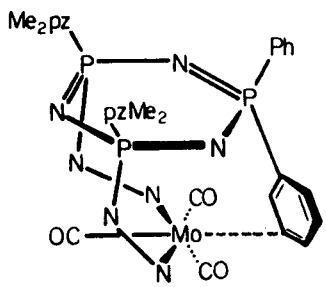

XIV

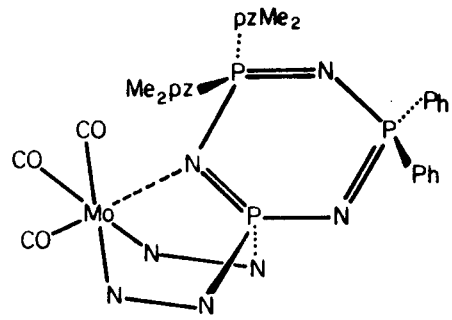

XII

in the complex $PhP(Me_2pz)_2W(CO)_3$[158]. Unfortunately, without the aid of ^{31}P n.m.r. (samples decompose before the spectrum can be run), the structures proposed are only speculative.

The mass spectra of the two isomers suggest that the $Mo(CO)_3$ unit is weakly coordinated in both compounds, and that B is thermodynamically less stable than A even though the yield of B (55%) is almost three times that of A (21%). No parent ion was observed for B only peaks of very low intensity due to loss of three CO groups. The ^1H n.m.r. spectrum of B (Figure 4.15B) is very similar to that of the corresponding palladium complex except that the resonance of H^4 remains as a broad unresolved band. It seems reasonable to believe that A and B correspond to either structure XI or XII, because the $Mo(CO)_3$ unit in the six membered $P\langle N-N\rangle_2Mo$ boat

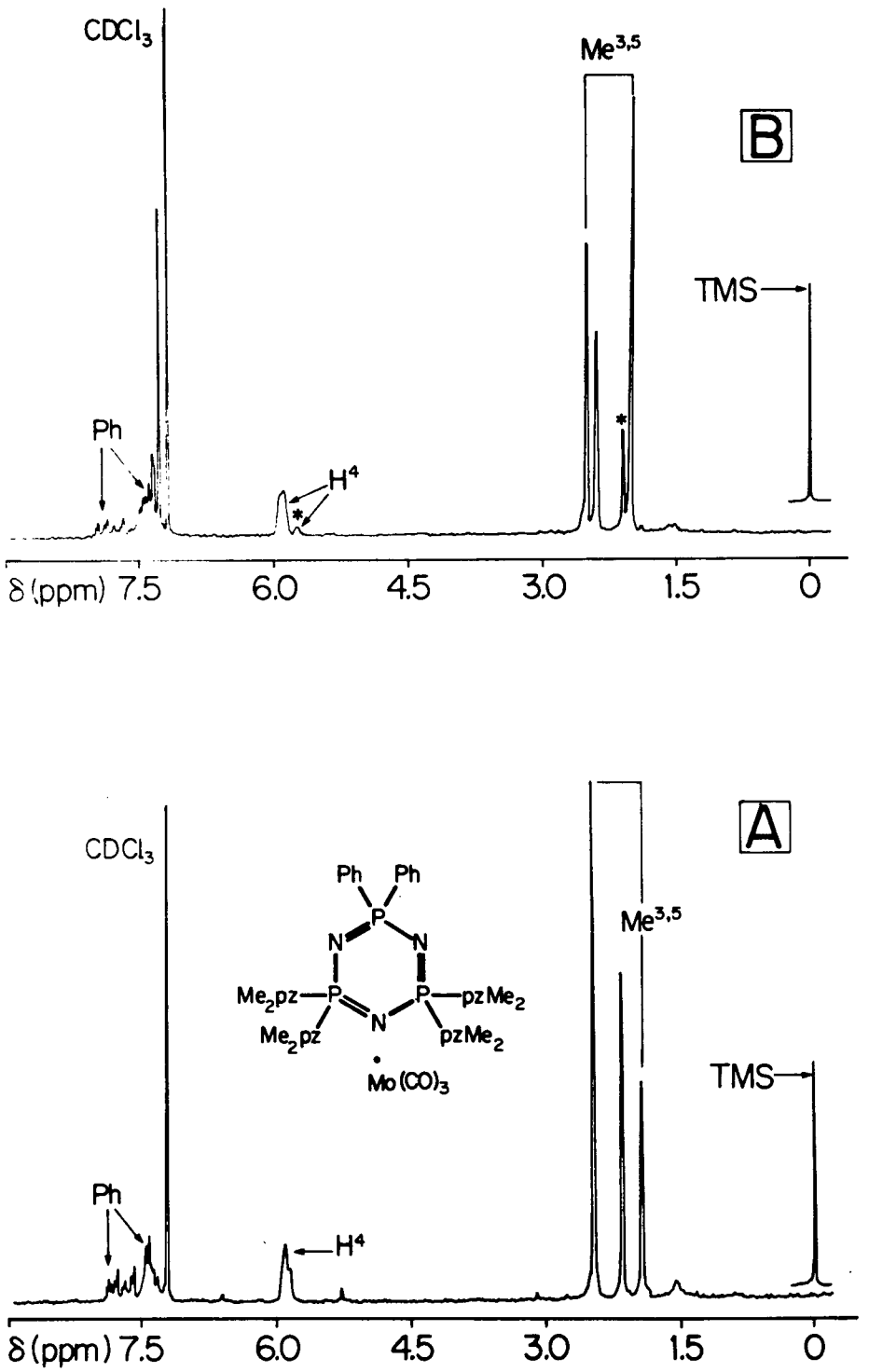

Figure 4.15. 80 MHz ^{1}H n.m.r. spectra of the two isomers of gem-$N_3P_3Ph_2(Me_2pz)_4 \cdot Mo(CO)_3$, A (A) and B (B). Spectra run on samples in $CDCl_3$ solution. The first signs of decomposition are apparent in (B); the peaks due to the ligand are indicated by an asterisk.

conformation would be more sterically congested than in either of the other two metallocycles, thus producing some instability in the molecules. Furthermore, only a steepening of the boat metallocycle is required for Mo to interact with the phosphazene ring nitrogen (see XI or XII), a conformation that is not possible in gem-$N_3P_3Ph_4(Me_2pz)_2 \cdot CoCl_2$ because the tetrahedral arrangement about cobalt places one of the chlorine atoms close to the phosphazene ring (described in Section 5.4). Structures XIII and XIV are also geometrically acceptable for an octahedral configuration about Mo, although a meridional arrangement seems more favorable for XIII.

4.4 Silver(I) Complexes

4.4.1 Preparation of Ag(I) Complexes

Relatively few silver(I) complexes containing pyrazolyl groups have been made. Recently the chemistry of poly(pyrazolyl)borate complexes of the type $Ag^+[HB(Me_2pz)_3]^-$ has received some attention, but the compounds are at best only sparingly soluble in common organic solvents[159]. Poddar et al.[160] have shown that the stabilities of $AgNO_3$ complexes of pyrazoles increase with progressive substitution of a methyl group in the pyrazole ring, a feature opposite to that observed for the analogous cobalt(II) and zinc nitrate complexes[161]. Moreover, the most stable form of $AgNO_3$ complexes of methyl substituted bidentate ligands containing nitrogen donor atoms is the bis type $(AgL_2)^+NO_3^-$, where L is a bidentate ligand such as 4,6,4',6'-tetramethyl-2,2'-bipyridine (tmb). Mono(chelate) complexes have been formed but attempts to purify them by recrystallization resulted in disproportionation to the bis compound[162]. It was thought that this tendency to coordinate a second ligand molecule in the $AgNO_3$ complexes might allow some bis(chelate) complexes of 1-pyrazolylphosphazenes to be isolated. However,

reaction of 1:1 mole ratio of $AgNO_3$ and gem-$N_3P_3Ph_4(Me_2pz)_2$ in THF gave solely the mono(chelate) derivative (Equation 4.13). The bis(silver nitrate) complex of $N_3P_3(Me_2pz)_6$ was also made as a comparison to the other bis(metal) complexes (Equation 4.14).

$$\text{gem-}N_3P_3Ph_4(Me_2pz)_2 + AgNO_3 \xrightarrow{THF} \text{gem-}N_3P_3Ph_4(Me_2pz)_2 \cdot AgNO_3 \quad \ldots (4.13)$$

$$N_3P_3(Me_2pz)_6 + 2AgNO_3 \xrightarrow{THF} N_3P_3(Me_2pz)_6 \cdot 2AgNO_3 \quad \ldots (4.14)$$

4.4.2 Physical and Spectroscopic Properties of the $AgNO_3$ Complexes

Table 4.11. Spectroscopic parameters[a] and conductivities[b] of the $AgNO_3$ complexes of 1-pyrazolylphosphazenes.

Compound	Λ_M	$\delta_H H^4$	$\delta_H Me^3$	$\delta_H Me^5$	$-\delta_P PPh_2$	$-\delta_P P(Me_2pz)_2$	$\nu(P{=}N)$	$\nu(NO_3^-)$
$N_3P_3Ph_4(Me_2pz)_2 \cdot AgNO_3$	52.2	5.86 (3.8)	2.26	2.20	93.4 (18.2)	119.2	1176 1191 1217	1370
$N_3P_3(Me_2pz)_6 \cdot 2AgNO_3$	-	6.09br	2.31	2.21	-	116.9	1234 1227	1379

(a) 100 MHz ^1H n.m.r. parameters, δ_H(ppm) from solutions in $CDCl_3$, reference internal TMS. 40.5 MHz ^{31}P n.m.r. parameters, δ_P(ppm) from solutions in $CDCl_3$, reference external P_4O_6. $J(PH^4)$ and $J(PP)$ are given in parenthesis. Infrared parameters (in units of cm^{-1}) from either nujol or hexachlorobutadiene mull spectra. (b) Molar conductance of ca. 10^{-3}M solutions in nitromethane at 25°C (in units of cm^2 ohm^{-1} $mole^{-1}$).

The two silver complexes are very soluble in common organic solvents, but slowly decompose in chlorinated solvents and in the presence of light. The conductivity of the gem-$N_3P_3Ph_4(Me_2pz)_2$ derivative (52.2 cm^2 ohm^{-1} $mole^{-1}$, Table 4.11), although slightly low for 1:1 electrolytes of ca. 10^{-3}M solutions

in nitromethane (normal range is between 75-95 cm^2 ohm^{-1} $mole^{-1}$), is consistent with the ionic nature of the nitrate group as indicated by the broad, intense band at 1370 cm^{-1} in the infrared spectrum. A similar band at 1379 cm^{-1} in the infrared spectrum of $N_3P_3(Me_2pz)_6 \cdot 2AgNO_3$ also suggests the presence of ionic nitrate groups in this compound.

The infrared spectra of complexes containing uncoordinated nitrate groups (NO_3^-, symmetry D_{3h}) generally show a strong,broad band at about 1360-1380 cm^{-1} arising from the doubly degenerate vibration E'[162,163], and is observed at 1362 cm^{-1} in the spectrum of $AgNO_3$[162]. Coordination through oxygen lowers the symmetry of the ion from D_{3h} to C_{2v} and causes a discernible splitting of this band, thus allowing an easy distinction to be made between ionic and covalent nitrate groups.

The ^1H n.m.r. spectrum of $N_3P_3(Me_2pz)_6 \cdot 2AgNO_3$ in $CDCl_3$ is similar to that of the corresponding di-zinc complex, in which only one set of pyrazolyl proton resonances was observed. Thus, the silver atom is rapidly exchanging between coordinated and uncoordinated Me_2pz groups as it does in the complex $\{Ag[HB(Me_2pz)_3]\}_n$ in the same solvent[159]. The fluxional behaviour also makes the three phosphorus atoms, formally non-equivalent chemically in the solid state, magnetically equivalent as evidenced by the singlet at 116.9δ in the ^{31}P n.m.r. spectrum.

The ^1H n.m.r. and ^{31}P n.m.r. spectra of gem-$N_3P_3Ph_4(Me_2pz)_2 \cdot AgNO_3$ are identical in appearance to those of the ligand, and zinc and cadmium complexes; and, combined with the conductivity data, suggests that silver is bonding to the two Me_2pz groups, thereby achieving a coordination number of two (XV). The fact that no bis(chelate) derivatives of the type $(AgL_2)^+NO_3^-$ were formed may be due to the relatively poorer ability of

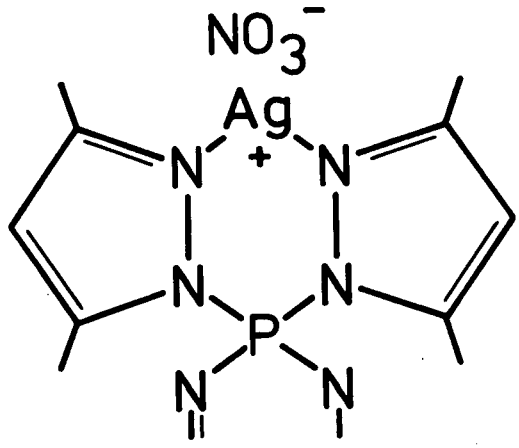

XV

1-pyrazolylphosphazenes to form π bonds than other bidentate ligands such as 1,10-phenanthroline or tmb. In any case these silver(I) compounds are examples of bidentate mono(chelate) complexes.

4.5 Experimental

All reactions were done in an atmosphere of dry nitrogen. Before use, all solvents were distilled from drying agents: THF and diethyl ether from sodium/benzophenone, benzene from $LiAlH_4$, dichloromethane from P_2O_5, acetonitrile from CaH_2, and methanol from molecular sieves (4A) followed by storage over CaH_2. Zinc chloride was dried by heating it in vacuo at 200°C for several hours. Cobalt(II)chloride and cadmium chloride were dehydrated by heating them with thionyl chloride under reflux. Silver nitrate was used as received. Cis-bis(benzonitrile)dichloroplatinum(II)[164], trans-bis(benzonitrile)dichloropalladium(II)[164] and tris(acetonitrile)-molybdenum tricarbonyl[165] were prepared according to published methods. Prior to reactions the pyrazolylphosphazenes were dried at 110°C in an oven for 30 minutes.

4.5.1 Preparation of Co(II), Zn and Cd Complexes

4.5.1A Preparation of $N_3P_3(Me_2pz)_6 \cdot 2ZnCl_2 \cdot THF$

108 mg $ZnCl_2$ (0.79 mmol) was added to a stirred solution of 74.0 mg $N_3P_3(Me_2pz)_6$ (0.11 mmol) in 15 ml hot THF. After heating the solution under reflux for ten minutes a white precipitate appeared. The mixture was heated for a further three hours, and then the solid was filtered and washed with THF. Yield: 110 mg (100%). M.pt. 290-305°C (dec). Anal. calcd. for $P_3N_{15}C_{34}H_{50}Zn_2Cl_4O$: C, 38.88; H, 4.80; N,20.00; Cl,13.50. Found: C,38.79; H,4.87; N,19.98; Cl,13.54.

4.5.1B Reaction of $N_3P_3(Me_2pz)_6 \cdot 2ZnCl_2 \cdot THF$ with CH_3CN

Approximately 5 mg of the zinc complex was dissolved in 2 ml hot CH_3CN. Upon cooling in air white, colourless crystals appeared but later redissolved. Evaporation of the solvent left a white powder which was shown by ^1H n.m.r. and infrared spectroscopy to contain 3,5-dimethylpyrazole. Mass spectrometry indicated complete breakdown of the phosphazene ring: there were no major peaks > $\frac{m}{e}$ 150, and the isotope pattern for $ZnCl_2$ [$\frac{m}{e}$ observed: 134(79%), 136(100%), 137(8.5%), 138(69%), 139(5.7%), 140(25%), 141(6.6%), 142(5.7%)] and the molecular ion for Me_2pzH ($\frac{m}{e}$ 96) were clearly visible. Similar results were observed using methanol in place of acetonitrile.

4.5.1C Preparation of $N_3P_3(Me_2pz)_6 \cdot 2CoCl_2 \cdot THF$

37.1 mg $CoCl_2$ (0.29 mmol) was added to a stirred solution of 73.6 mg $N_3P_3(Me_2pz)_6$ (0.10 mmol) in 15 ml hot THF. Precipitation of a blue-purple solid occurred immediately. After heating the mixture under reflux for three hours the solid was filtered and washed with THF. Yield: 108 mg (100%). M.pt. 315-317°C. Anal. calcd. for $P_3N_{15}C_{34}H_{50}Co_2Cl_4O$: C,39.36;

H,4.86; N,20.25; Cl,13.67. Found: C,39.60; H,4.97; N,20.06; Cl,13.38. Rapid crystallization from nitromethane produced purple platelets suitable for X-ray analysis, but elemental analysis showed the compound to contain variable amounts of solvent.

4.5.1D Preparation of Gem-$N_3P_3Ph_2(Me_2pz)_4 \cdot ZnCl_2$

77.3 mg $N_3P_3Ph_2(Me_2pz)_4$ (0.12 mmol) and 57.2 mg $ZnCl_2$ (0.42 mmol) were dissolved in 25 ml THF. The clear, colourless solution became turbid and discarded a white precipitate immediately upon heating under reflux. The mixture was stirred at 65°C for twenty-four hours, and then the white solid was filtered and washed with THF. Yield: 79.1 mg (85%, product is slightly soluble in THF). M.pt. 295-299°C. Anal. calcd. for $P_3N_{11}C_{32}H_{38}$-$ZnCl_2$: C,47.69; H,4.75; N,19.12; Cl,8.80. Found: C,47.87; H,4.78; N,19.05; Cl,8.73. The complex can be crystallized as small, colourless needles from methanol.

4.5.1E Preparation of Gem-$N_3P_3Ph_2(Me_2pz)_4 \cdot CoCl_2$

44.6 mg $CoCl_2$ (0.34 mmol) was added to a solution of 80.7 mg N_3P_3-$Ph_2(Me_2pz)_4$ (0.12 mmol) in 15 ml THF producing an immediate pale purple precipitate. After heating under reflux for twelve hours, the mixture was filtered and the solid was washed with THF, in which it is slightly soluble. Yield: 77.1 mg (80%). M.pt. 312-313°C (dec). Anal. calcd. for $P_3N_{11}C_{32}H_{38}CoCl_2$: C,48.08; H,4.79; N,19.27; Cl,8.87. Found: C,48.33; H,4.85; N,19.06; Cl,9.04.

4.5.1F Preparation of Gem-$N_3P_3Ph_4(Me_2pz)_2 \cdot ZnCl_2$

53.5 mg $N_3P_3Ph_4(Me_2pz)_2$ (0.08 mmol) was added to a saturated solution

of 27.0 mg $ZnCl_2$ (0.20 mmol) in 4 ml THF / 12 ml Et_2O. The white precipitate which formed was filtered after heating under reflux for three hours, and purified by dissolving it in chloroform and filtering the solution dropwise into a large excess of diethyl ether. Yield: 61.8 mg (95%). M.pt. 247-251.5°C. Anal. calcd. for $P_3N_7C_{34}H_{34}ZnCl_2$: C,53.04; H,4.45; N,12.73; Cl,9.21. Found: C,53.05; H,4.57; N,12.52; Cl,9.26.

4.5.1G Preparation of Gem-$N_3P_3Ph_4(Me_2pz)_2 \cdot CoCl_2 \cdot H_2O$

A stirred solution of 86.0 mg $N_3P_3Ph_4(Me_2pz)_2$ (0.14 mmol) and 27.0 mg $CoCl_2$ (0.21 mmol) in 10 ml THF was heated under reflux for twenty-four hours. The blue solution was evaporated in vacuo yielding a residue which was purified by dissolving it in methylene chloride and filtering dropwise into a large excess of hexane. The blue solid collected was identified as $N_3P_3Ph_4(Me_2pz)_2 \cdot CoCl_2 \cdot H_2O$. Yield: 95.5 mg (90%). M.pt. 141°C (loses H_2O), 300°C (dec). Anal. calcd. for $P_3N_7C_{34}H_{36}OCoCl_2$: C,52.26; H,4.64; N,12.55; Cl,9.07. Found: C,52.34; H,4.50; N,12.44; Cl,8.99. The product can be crystallized either from methylene chloride/diethyl ether as purple needles or from nitromethane/diethyl ether as purple blocks.

4.5.1H Preparation of Gem-$N_3P_3Ph_4(Me_2pz)_2 \cdot CdCl_2 \cdot CHCl_3$

A stirred solution of 73.5 mg $N_3P_3Ph_4(Me_2pz)_2$ (0.12 mmol) and 46.0 mg $CdCl_2$ (0.25 mmol) in 10 ml methanol was heated under reflux for one hour. The solvent was removed in vacuo and the white residue extracted with 2x10 ml hot chloroform. The combined chloroform extracts were slowly allowed to evaporate yielding a white solid which was crystallized twice from chloroform as a microcrystalline mass of $N_3P_3Ph_4(Me_2pz)_2 \cdot$

$CdCl_2 \cdot CHCl_3$. The mother liquor contained some unreacted phosphazene (11.0 mg). Yield: 64.6 mg (70%, based on the amount of phosphazene that reacted). M.pt. 296.5-298.5°C (dec). Anal. calcd. for $P_3N_7C_{35}H_{35}CdCl_5$: C,44.90; H,3.77; N,10.47; Cl,18.93. Found: C,44.96; H,3.74; N,10.70; Cl,18.70.

4.5.1I Preparation of Gem-$N_3P_3Ph_4(Mepz)_2 \cdot ZnCl_2$

68.1 mg $N_3P_3Ph_4(Mepz)_2$ (0.11 mmol) was added to a saturated solution of 28.1 mg $ZnCl_2$ (0.21 mmol) in 4 ml THF / 12 ml Et_2O. The white precipitate which formed was filtered after heating under reflux for ninety minutes, and crystallized from methylene chloride/hexane as colourless crystals of $N_3P_3Ph_4(Mepz)_2 \cdot ZnCl_2$. Yield: 79.3 mg (95%). M.pt. 295-297°C. Anal. calcd. for $P_3N_7C_{32}H_{30}ZnCl_2$: C,51.81; H,4.08; N,13.22; Cl,9.56. Found: C,51.75; H,4.06; N,13.12; Cl,9.40.

4.5.2 Preparation of Pd(II) and Pt(II) Complexes

4.5.2A Preparation of Gem-$N_3P_3Ph_4(Me_2pz)_2 \cdot PdCl_2$

44.8 mg $PdCl_2(PhCN)_2$ (0.12 mmol) in 10 ml methylene chloride was filtered dropwise under a positive pressure of nitrogen into a stirred solution of 70.3 mg gem-$N_3P_3Ph_4(Me_2pz)_2$ (0.11 mmol) in 5 ml methylene chloride. The solution gradually turned from reddish orange to orange and deposited a yellow precipitate during twenty-four hours of stirring at room temperature. The solid was filtered, washed with cold methylene chloride and crystallized from chloroform. More product was obtained from the filtrate. Yield: 81.0 mg (90%). M.pt. 250°C (dec). Anal. calcd. for $P_3N_7C_{34}H_{34}PdCl_2$: C,50.36; N,12.09; H,4.23. Found: C,50.98; N,11.59; H,4.14.

4.5.2B Preparation of Gem-$N_3P_3Ph_2(Me_2pz)_4 \cdot PdCl_2$

163 mg $PdCl_2(PhCN)_2$ (0.42 mmol) in 30 ml benzene was filtered dropwise under a positive pressure of nitrogen into a stirred solution of 117 mg gem-$N_3P_3Ph_2(Me_2pz)_4$ (0.18 mmol) in 10 ml benzene. The solution immediately became a turbid yellow and discarded an orange solid. After stirring for twenty-four hours, the mixture was filtered to give 140 mg of a yellow solid which was extracted with 2x25 ml chloroform. The chloroform extracts and the benzene filtrate were combined and the whole evaporated under vacuum to leave an orange residue which was washed with 5 ml benzene and crystallized from chloroform/benzene as orange needles. Yield: 50.3 mg (34%). M.pt. 225-234°C (dec). Anal. calcd. for $P_3N_{11}C_{32}H_{38}PdCl_2$: C,45.38; H,4.52; N,18.19; Cl,8.37. Found: C,45.23; H,4.41; N,17.94; Cl,8.08.

4.5.2C Preparation of $N_3P_3(Me_2pz)_6 \cdot 2PtCl_2$

203 mg $PtCl_2(PhCN)_2$ (0.43 mmol) in 25 ml benzene was filtered dropwise under a positive pressure of nitrogen into a stirred suspension of 101 mg $N_3P_3(Me_2pz)_6$ (0.14 mmol) in 5 ml benzene. The yellow solution was heated under reflux for one week with the first signs of a precipitate occurring after thirty-six hours. The yellow precipitate was filtered, washed with 50 ml benzene, and crystallized as yellow microcrystals by slow evaporation from chloroform/benzene. Yield: 76.2 mg (43%). M.pt. 275-280°C. Anal. calcd. for $P_3N_{15}C_{30}H_{42}Pt_2Cl_4$: C,29.11; H,3.42; N,16.98. Found: C,29.53; H,3.37; N,15.73 (sample contained traces of benzene which could not be completely removed by heating it in vacuo.

4.5.2D Preparation of $N_3P_3(Me_2pz)_6 \cdot 2PdCl_2$

212 mg $PdCl_2(PhCN)_2$ (0.55 mmol) in 25 ml benzene was filtered drop-

wise under a positive pressure of nitrogen into a stirred suspension of 109 mg $N_3P_3(Me_2pz)_6$ (0.16 mmol) in 5 ml benzene. After two minutes of stirring a fluffy reddish brown precipitate appeared and the supernatant liquid turned from dark red to orange-yellow. After three hours the precipitate was orange-brown, after six hours light orange-brown, and finally after four days dull yellow. The mixture was filtered and the yellow solid washed with 50 ml benzene and crystallized as orange blocks by slow evaporation from chloroform/benzene. Yield: 131 mg (80%). M.pt. 250°C (dec). Anal. calcd. for $P_3N_{15}C_{30}H_{42}Pd_2Cl_4$: C,33.98; H,3.99; N,19.82; Cl,13.37. Found: C,34.10; H,4.84; N,19.47; Cl, 13.77.

Alternative Procedure

146 mg $PdCl_2(PhCN)_2$ (0.38 mmol) was dissolved in 15 ml methylene chloride and the red solution filtered into a solution of 133 mg $N_3P_3(Me_2pz)_6$ (0.19 mmol) in 5 ml methylene chloride. The resulting orange solution was heated under reflux for sixteen hours, concentrated to 5 ml, and added dropwise to a large volume of hexane. The yellow solid produced was filtered and washed with cold benzene. Yield: 198 mg (99%).

4.5.2E Preparation of $N_3P_3(Me_2pz)_6 \cdot 3PdCl_2$

145 mg $PdCl_2(PhCN)_2$ (0.38 mmol) was dissolved in 30 ml methylene chloride and the orange-red solution filtered into a solution of 84.9 mg $N_3P_3(Me_2pz)_6$ (0.12 mmol) in 3 ml methylene chloride. The orange solution was heated under reflux for twenty-four hours, concentrated to 3 ml, and added dropwise to a large volume of hexane. The orange-yellow solid produced was filtered, washed with chloroform, and crystallized from methylene chloride. Yield: 143 mg (96%). M.pt. ca. 250°C (dec). Anal. calcd. for $P_3N_{15}C_{30}H_{42}Pd_3Cl_6$: C,29.12; H,3.42; N,16.98. Found: C,29.89; H,3.82; N,16.57.

4.5.3 Preparation of Gem-$N_3P_3Ph_2(Me_2pz)_4 \cdot Mo(CO)_3$

A solution of 76.1 mg gem-$N_3P_3Ph_2(Me_2pz)_4$ (0.11 mmol) and 34.2 mg $(CH_3CN)_3Mo(CO)_3$ (0.11 mmol) in 15 ml benzene was heated at 50°C for three hours. During this time 20.2 mg of a brownish yellow solid appeared which was filtered and purified by dissolving it in methylene chloride and filtering the solution dropwise into a large excess of hexane. The bright yellow solid (A) was identified as $N_3P_3Ph_2(Me_2pz)_4 \cdot Mo(CO)_3$ and is slightly soluble in benzene. Yield: 21%. M.pt. 230°C (dec). Anal. calcd. for $P_3N_{11}C_{35}H_{38}MoO_3$: C,49.48; H,4.51; N,18.13. Found: C,48.87; H,4.45; N, 17.86. The benzene filtrate was evaporated in vacuo leaving a yellow solid which was crystallized from benzene/hexane as a dull greenish yellow powder (B). Yield: 53.1 mg (55%). M.pt. 200°C (dec). The powder was also identified as $N_3P_3Ph_2(Me_2pz)_4 \cdot Mo(CO)_3$. Anal. found for $P_3N_{11}C_{35}H_{38}MoO_3$: C,48.85; H,4.39; N,17.81.

4.5.4 Preparation of Ag(I) Complexes

4.5.4A Preparation of Gem-$N_3P_3Ph_4(Me_2pz)_2 \cdot AgNO_3$

A solution of 83.8 mg gem-$N_3P_3Ph_4(Me_2pz)_2$ (0.13 mmol) and 22.5 mg $AgNO_3$ (0.13 mmol) in 25 ml THF was heated under reflux for sixteen hours. The clear, colourless solution was evaporated in vacuo and the white residue crystallized from methylene chloride/hexane and identified as gem-$N_3P_3Ph_4(Me_2pz)_2 \cdot AgNO_3$. Yield: 101 mg (95%). M.pt. 229.5-245°C (dec). Anal. calcd. for $P_3N_8H_{34}C_{34}AgO_3$: C,50.83; H,4.27; N,13.95. Found: C,50.86; H,4.10; N,13.97.

4.5.4B Preparation of $N_3P_3(Me_2pz)_6 \cdot 2AgNO_3$

61.6 mg $N_3P_3(Me_2pz)_6$ (0.09 mmol) and 30.0 mg $AgNO_3$ (0.18 mmol) were

dissolved in 15 ml THF and the clear, colourless solution heated under reflux for eighteen hours. The solvent was evaporated in vacuo yielding a white residue which was crystallized twice from THF as white needles. Yield: 63.9 mg (70%). M.pt. 240°C (dec). Anal. calcd. for $P_3N_{17}C_{30}H_{42}$-Ag_2O_6: C,34.47; H,4.05; N,22.78. Found: C,34.55; H,3.90; N,22.64.

4.6 Summary

By the use of ligands such as 1-pyrazolylphosphazenes, having certain steric demands and a number of potential donor atoms, the metal is given the opportunity of selecting its preferred coordination site. Zinc and cobalt prefer to bond to two Me_2pz groups on different phosphorus atoms incorporating a nitrogen in the phosphazene ring to give TBP structures, and will form tetrahedral compounds, using two Me_2pz groups on the same phosphorus, only if the situation demands it. On the other hand, palladium and platinum adopt solely a square planar environment using two Me_2pz groups on the same phosphorus atom. Molybdenum, in the complex gem-$N_3P_3Ph_2(Me_2pz)_4 \cdot Mo(CO)_3$, also prefers one geometry, facial octahedral, but has no single preference for donor sites.

The potential of 1-pyrazolylphosphazenes as ligands in coordination chemistry is virtually unlimited. The ligand $N_3P_3(Me_2pz)_6$ can be an excellent source of mixed metal complexes in which tetra- and penta-coordination numbers are together possible. Making some mixed (1-pyrazolyl)-phenylphosphazenes of the type gem-$N_3P_3Ph_2(pz)_4$ and cis-1,3-$N_3P_3Ph_4(Me_2pz)_2$ can allow a study of five-coordinate TBP MCl_2 complexes, especially of the latter where a TBP geometry is forced. In the former, however, tetra-coordination involving two pz groups on the same phosphorus and hexa-coordination involving two pyrazolylphosphazene ligands are possible, since steric

hindrance is minimized. Unidentate ligands are also possible if just one pyrazolyl group is present in the phosphazene ring. These are just some of the possibilities available for future work on the coordination chemistry of 1-pyrazolylphosphazenes.

CHAPTER 5

STRUCTURES OF PHOSPHAZENES INCORPORATING THE 3,5-DIMETHYLPYRAZOLYL LIGAND

The crystal and molecular structures of five phosphazenes containing 1-pyrazolyl substituents[62] were undertaken in order to compare the geometrical parameters of the uncomplexed ligand with those of other phosphazenes and to gain an insight into the changes in geometry of the phosphazene molecule as a result of coordination to a metal. All the metal complexes incorporate a pyridine-type nitrogen in the pyrazole ring, and in two of the structures, $N_3P_3(Me_2pz)_6 \cdot 2CoCl_2$ and gem-$N_3P_3Ph_2(Me_2pz)_4 \cdot ZnCl_2$, the phosphazene ring is also perturbed by bonding of one of its nitrogen atoms to the metal. Moreover, the coordination geometry about each cobalt atom in the di-cobalt complex is different. Stereoscopic views of the structures are shown in Figure 5.8 and 5.9.

The conformations of the phosphazene ring in 1-pyrazolylphosphazenes, like those in $[NP(NMe_2)_2]_{4,6,8,3}$[46-49], appear to be mainly influenced by steric factors. Because of the duality of the π-system, a particular conformation that is best suited sterically can therefore be adopted without major loss of π-delocalization energy or total π-bond order in the individual PN bonds. If the π_a- and π_s-systems are of equal importance then the total π-bond order is expected to be independent of the dihedral angle, such that, for instance, a decrease in overlap of the $2p_z$ orbital with $d\pi_a$-orbitals (principally d_{xz}) is compensated by an increase in overlap with $d\pi_s$-orbitals (principally $d_{x^2-y^2}$). This flexibility of the phosphazene ring is demonstrated in all five structures, especially in the two

compounds which contain a ring nitrogen coordinated directly to the metal.

5.1 Structure of $N_4P_4(Me_2pz)_8$

Three conformations are generally found for tetrameric phosphazenes: chair (I), tub (II) and saddle (III), the latter two being most common.

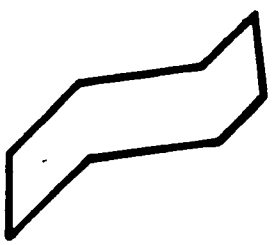

I

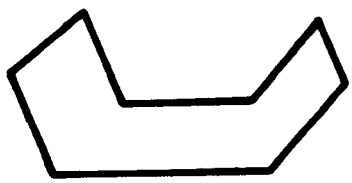

II

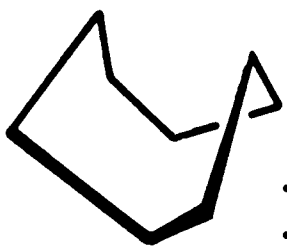

III

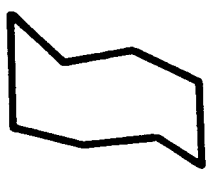

IV

The pure D_{2d} saddle structure, in which the phosphorus atoms are coplanar, has been observed only in $N_4P_4Me_4F_4$ (the trans-geminal isomer)[166]. Most structures are intermediate between tub and saddle, and the molecules $N_4P_4(OMe)_8$ (close to saddle)[168], $N_4P_4(NMe_2)_8$[46], $N_4P_4Me_8$[116], and $N_4P_4Cl_8$-(K)[119b] (close to tub) fall into this class. The C_{2v} chair conformation is found in the other polymorphic form of $N_4P_4Cl_8$(T)[119a].

The conformation of $N_4P_4(Me_2pz)_8$ can best be described as a "long chair" (IV), the two end phosphorus atoms being bent slightly to opposite sides of the plane containing the other ring atoms. The near planarity of the phosphazene ring as a whole is common in tetrameric derivatives with bulky and/or electronegative substituents. The flattening of the ring

in $N_4P_4(NMe_2)_8$ compared to $N_4P_4Me_8$ and $N_4P_4Cl_8$(T) arises from the steric requirements of the electron donating NMe_2 groups[46], while the planarity of $N_4P_4F_8$ is a consequence of the strongly electronegative fluorine atoms[169].

Although the direct strengthening effect of the PN ring by an electronegative substituent can be regarded as established, other factors have an important effect on the structural parameters. The 1-pyrazolyl group is both electronegative and bulky, and its size induces geometrical changes through changes in σ-hybridization. The geometrical trends summarized in Section 3.1.2E for the $N_4P_4(Me_2pz)_8$ molecule, like the anomalously high values of δ_P for the $(NPpz_2)_{3-6}$ series, can therefore be due to a combination of a π-effect, arising from the electronegativity of the Me_2pz group, and a σ-effect, arising from the steric requirements of the Me_2pz group. Generally the former is dominant.

The unit cell of $N_4P_4(Me_2pz)_8$ contains two independent but closely related molecules on centers of symmetry; a stereoscopic view of one of them is shown in Figure 5.8. The relative orientation of the two pyrazolyl groups attached to each phosphorus appear to be sterically acceptable, the mean exocyclic $\widehat{NPN}$ angle being 102.4°.

5.2 Structure of Gem-$N_3P_3Ph_2(Me_2pz)_4$

The mean distances and angles of chemically equivalent bonds in gem-$N_3P_3Ph_2(Me_2pz)_4$ are given in Figure 5.1. The conformation of the phosphazene ring ("flat chair") is the same as that found in gem-$N_3P_3Ph_2Cl_4$, and the main structural features are also similar[50], showing that the electronic properties of the Me_2pz group resemble those of a chlorine atom. Both molecules show the same type of variation in the PN bond lengths, a

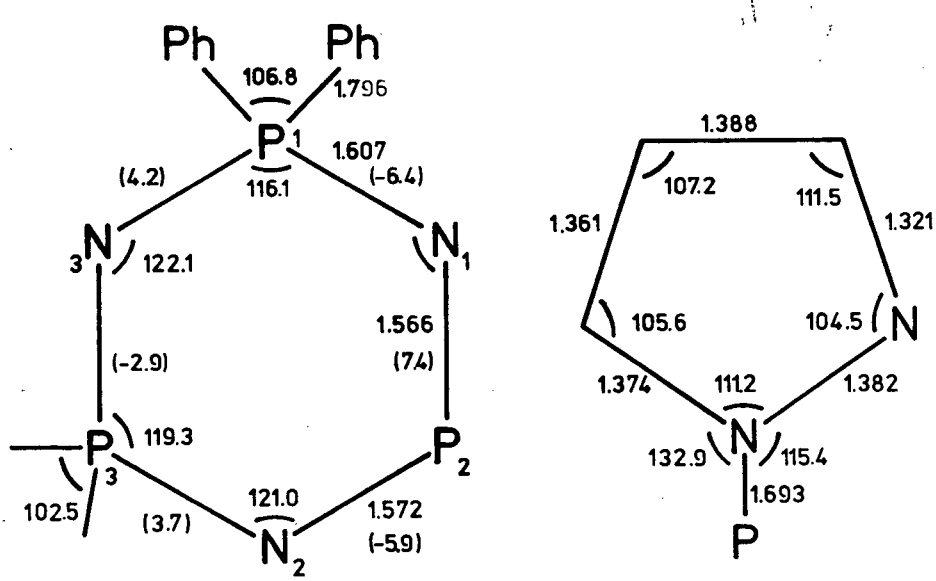

Figure 5.1. Mean values of the bond lengths (angstroms) and bond angles (degrees) in gem-$N_3P_3Ph_2(Me_2pz)_4$. Dihedral angles are given in brackets.

consequence of the perturbation at the $P(Ph_2)$ phosphorus atom by the less electronegative phenyl group. The two bonds nearest to the perturbed atom are the longest, the adjacent pair are the shortest and the remote pair are intermediate in length. The mean values of successive PN bond lengths from $\underline{P}(Ph_2)$ are 1.607, 1.566 and 1.572 Å in $N_3P_3Ph_2(Me_2pz)_4$, and 1.615, 1.555 and 1.578 Å in $N_3P_3Ph_2Cl_4$. This alternation in bond length is predicted by HMO theory, and therefore stresses the importance of π-effects in phosphazenes. For a pure σ-inductive effect a steady change away from the perturbed atom would be expected.

Regarding the endocyclic angles, the largest $\hat{NPN}$ angle occurs at the $\underline{P}(Me_2pz)_2$ atoms (119.3°, mean) consistent with the greater electron

density in the PN bonds meeting at these phosphorus atoms, and hence greater interbond repulsion. The $\hat{PNP}$ angles are almost identical and average to 121.7°.

The mean exocyclic PN bond length of 1.693 Å is longer than that found in $N_3P_3(NMe_2)_6$, where exocyclic conjugation lowers the value to 1.652 Å[49]. Thus, conjugative electron release to the phosphazene ring is minimal, as it is in $N_4P_4(Me_2pz)_8$ (mean exocyclic PN bond length is 1.691 Å).

The bond lengths and bond angles found for the Me_2pz and Ph ligands are normal. The rings are also planar to within experimental error.

5.3 Structure of Gem-$N_3P_3Ph_2(Me_2pz)_4 \cdot ZnCl_2$

In this complex the pyrazolylphosphazene ligand is donating to the metal through three nitrogen atoms (one from each of the two $P(Me_2pz)_2$ units and one from the phosphazene ring) to form two five-membered rings which are fused by the Zn-N(2) (phosphazene nitrogen) bond, and, together with the two bound pyrazolyl groups, constitute a nearly planar arrangement of four fused, five-membered rings. The two chlorine atoms are above and below the plane, respectively. The $ZnCl_2$ unit is situated well below the phosphazene ring so avoiding steric hindrance from the remaining non-bonded Me_2pz groups. The bond angles and bond lengths involving the zinc atom are given in Figure 5.2 (the numbering of the atoms is the same as for $N_3P_3Ph_2(Me_2pz)_4$), and different perspectives of the complex can be seen in Figures 4.2 and 5.8. The coordination geometry about the zinc atom is a distorted trigonal bipyramid, the chlorine atoms and the nitrogen in the phosphazene ring N(2) occupying the equatorial positions, since the equatorial angles are close to 120°. The axial bonds are bent back decreasing

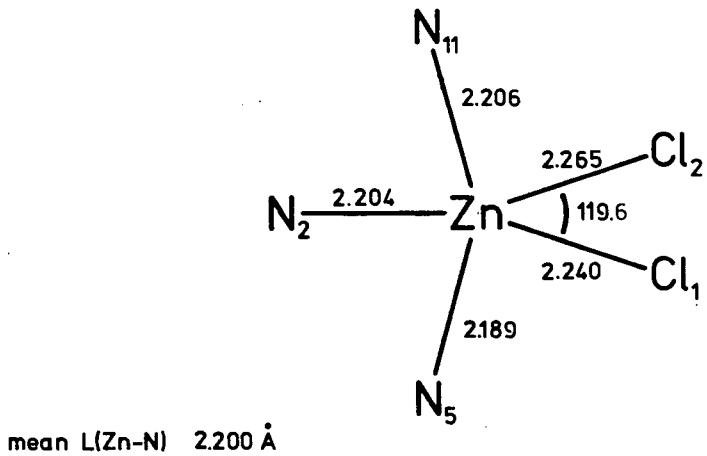

Figure 5.2. Structural parameters of the atoms bonded to zinc in gem-$N_3P_3Ph_2(Me_2pz)_4 \cdot ZnCl_2$.

the angle between them from 180°, in an ideal trigonal bipyramidal geometry, to 153.9°. This type of distortion from TBP geometry is also found in terpyridylzinc chloride, where the angle between the axial bonds (NẐnN) is decreased to 151°[170].

The Zn-Cl bond lengths (2.253 Å, mean) are consistent with covalently bound chlorine atoms. All the Zn-N bonds are similar in length (2.200 Å, mean) and lie in a plane at right angles to the plane of the Zn-Cl bonds, such that the coordination sphere about the zinc atom has two planes of symmetry intersecting in a two-fold axis which bisects the ClẐnCl angle (C_{2v} symmetry).

Bonding of the zinc atom to the nitrogen atom in the PN ring results in significant changes in the geometry of the ring itself. Not only

is the conformation different but the bond angles and bond lengths are altered, especially near the perturbed nitrogen (Figure 5.3). Coordination localizes the lone-pair electrons on N(2), thereby partially removing them from the π_s-system and weakening the endocyclic PN bonds meeting at this nitrogen atom. The resulting increase in the electronegativity of the adjacent phosphorus atoms is compensated by increased donation from the other two nitrogen atoms, N(1) and N(3), in the phosphazene ring. The mean values of chemically equivalent bonds from N(2) are 1.602, 1.560 and 1.611 Å, and can be compared to the corresponding values of 1.572, 1.566 and 1.607 Å found in $N_3P_3Ph_2(Me_2pz)_4$. Although the differences (+0.030, -0.006 and +0.004, respectively) are small (the second and third are insignificant), they are in the expected direction, and are similar to those observed in other phosphazenes when the ring nitrogen is coordinated to a metal. For example, in $(N_4P_4Me_8H)CuCl_3$[61] and $N_4P_4(NMe_2)_8 \cdot W(CO)_4$[57] the mean PN bond length of the two bonds involving the coordinated nitrogen is increased from 1.596(5) Å in the parent compound, $N_4P_4Me_8$[116], to 1.635 Å (Δ = +0.038 Å) in the former; and from 1.578(10) Å in $N_4P_4(NMe_2)_8$[46] to 1.63(2) Å (Δ = +0.052 Å) in the latter. The changes are greater than that for gem-$N_3P_3Ph_2(Me_2pz)_4 \cdot ZnCl_2$ (Δ = +0.030 Å), and parallel the basicities* of the parent compounds: gem-$N_3P_3Ph_2Cl_4$ < $N_4P_4Me_8$ < $N_4P_4(NMe_2)_8$, assuming the basicity of gem-$N_3P_3Ph_2Cl_4$ is similar to gem-$N_3P_3Ph_2(Me_2pz)_4$; the better the availability of the lone-pair electrons, the greater the extent of localization.

---

*pK_{BH^+} is < -6.0 for gem-$N_3P_3Ph_2Cl_4$ in nitrobenzene at 25°C[171], 5.72 for $N_4P_4Me_8$ in H_2O[142] and 8.3 for $N_4P_4(NMe_2)_8$ in nitrobenzene at 25°C[172]. As a comparison for the values in different solvents, the pK_{BH^+} of $N_4P_4Et_8$ at 25°C is 6.45 in H_2O and 7.60 in nitrobenzene[173].

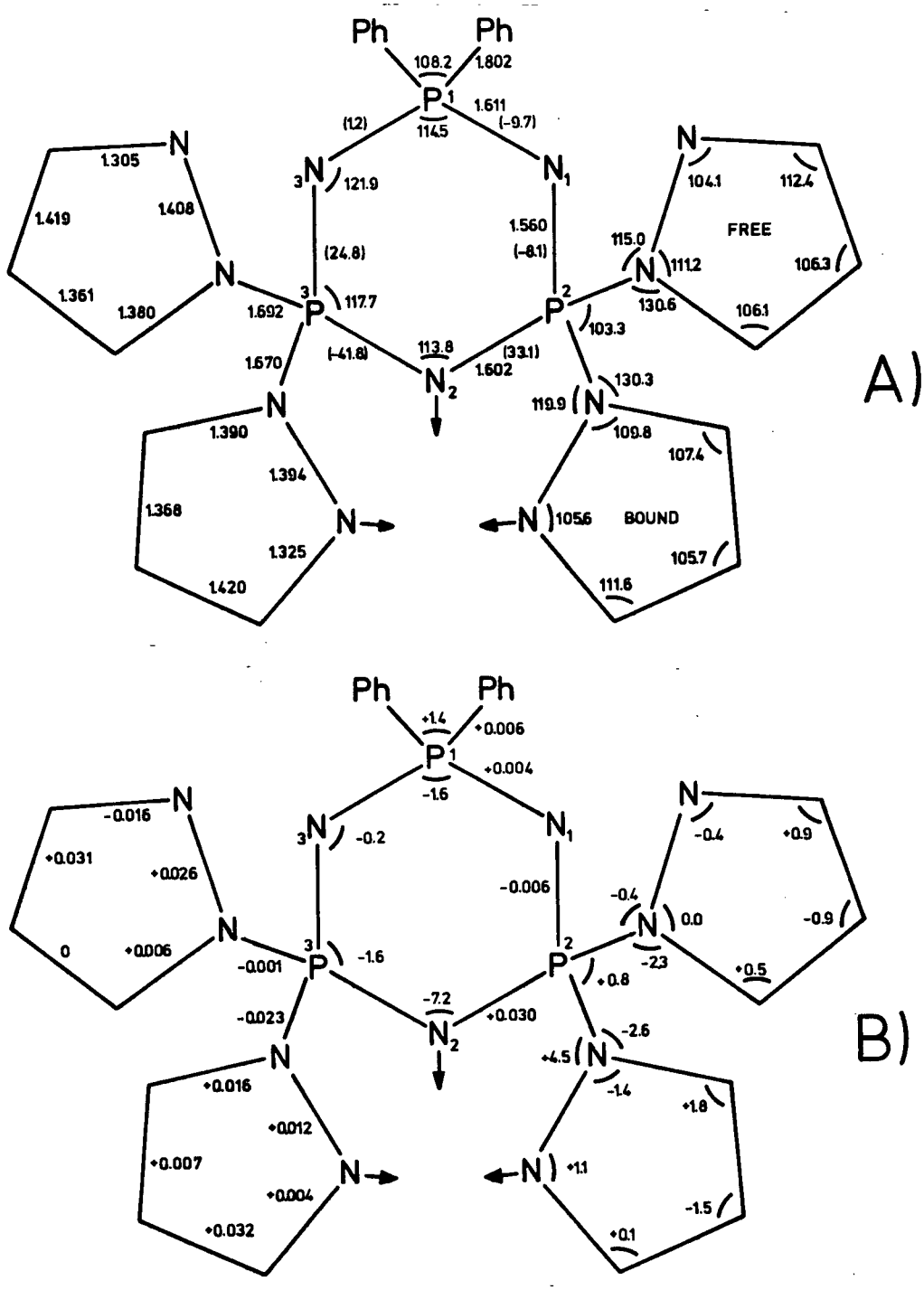

Figure 5.3. Mean structural parameters of the coordinated ligand in the complex gem-$N_3P_3Ph_2(Me_2pz)_4 \cdot ZnCl_2$ (A), and the deviations from the free ligand (B). A positive deviation corresponds to longer bonds and larger angles in the complex. Dihedral angles are given in brackets.

All the mean bond angles in the phosphazene ring are decreased from those in the free ligand. The greatest change occurs at N(2) (Δ = -7.2°) where the lone-pair electrons are localized. The large decrease is not unusual as it is also observed at the nitrogen coordinated to Cu in $(N_4P_4Me_8H)CuCl_3$ (Δ = -8.8°)[61] and to W in $N_4P_4(NMe_2)_8 \cdot W(CO)_4$ (Δ = -8.6°)[57], and is attributed to less interbond repulsion as a result of localization of the lone-pair electrons.

In order to accommodate the $ZnCl_2$ unit in a manner most sterically acceptable, one of the nitrogen atoms in the PN ring must bend considerably from the mean plane containing the other five atoms. The conformation thus becomes a distorted boat, the portion nearest the zinc atom being much steeper, as illustrated by the larger dihedral angles.

Most of the other parameters are not greatly affected by the perturbation at the three nitrogens when averaged values are considered. The mean exocyclic PN bond length of 1.692 Å for the free Me_2pz groups and 1.670 Å for the bound groups are similar to the value of 1.693 Å found in $N_3P_3Ph_2(Me_2pz)_4$, and the mean exocyclic $\hat{NPN}$ angle is slightly increased from 102.5° to 103.3°. The Me_2pz and Ph groups also retain their planarity. All the structural deviations from the free ligand are given in Figure 5.3B.

5.4 Structure of Gem-$N_3P_3Ph_4(Me_2pz)_2 \cdot CoCl_2$

The coordination geometry about the cobalt atom in this complex is a distorted tetrahedron, incorporating one nitrogen atom from each of the two Me_2pz groups (see Figures 4.2 and 5.9). The cobalt atom, the four nitrogen atoms and the phosphorus atom form a six-membered ring with a boat conformation, a form commonly found in complexes of pyrazolylborate[69]

and pyrazolylgallate ligands[102,103]. The boat arrangement places the $CoCl_2$ unit closer to one $P(Ph_2)$ group than the other, and, combined with the proximity of the phosphazene ring to one of the chlorine atoms, confines the cobalt atom in approximately the same plane as the four nitrogen atoms (shallow boat). The phosphorus end of the boat is, however, much steeper.

Each of the six angles around the central cobalt atom deviates significantly from 109.5° (Figure 5.4), for a regular tetrahedral geometry.

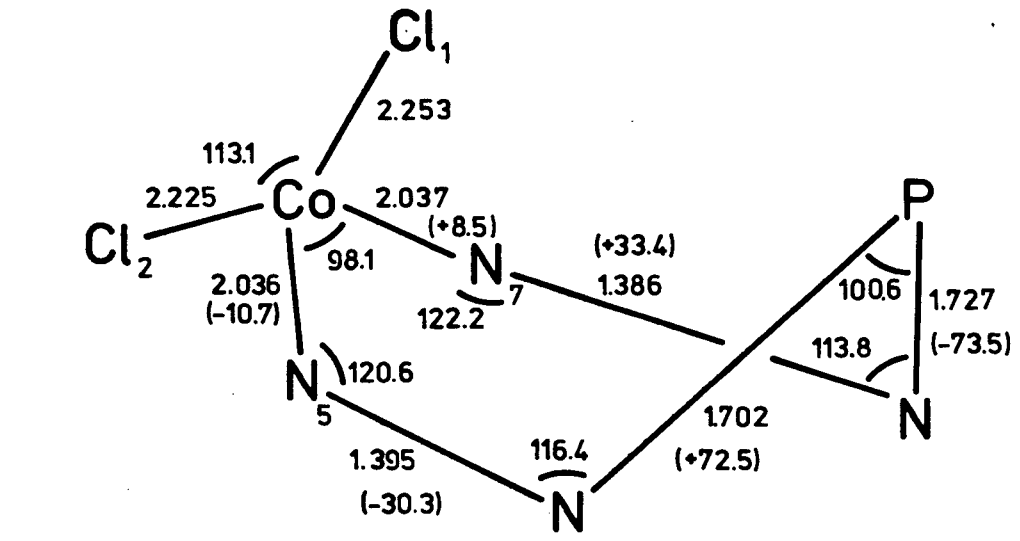

mean L(Co-Cl)	2.239 Å
mean L(Co-N)	2.037 Å
mean L(P-N)	1.715 Å

N(7)$\hat{C}$oCl(1)	118.3°
N(7)$\hat{C}$oCl(2)	104.2°
N(5)$\hat{C}$oCl(1)	118.1°
N(5)$\hat{C}$oCl(2)	102.7°

Figure 5.4. Structural parameters of the boat conformation present in the complex gem-$N_3P_3Ph_4(Me_2pz)_2 \cdot CoCl_2$. Dihedral angles are given in brackets.

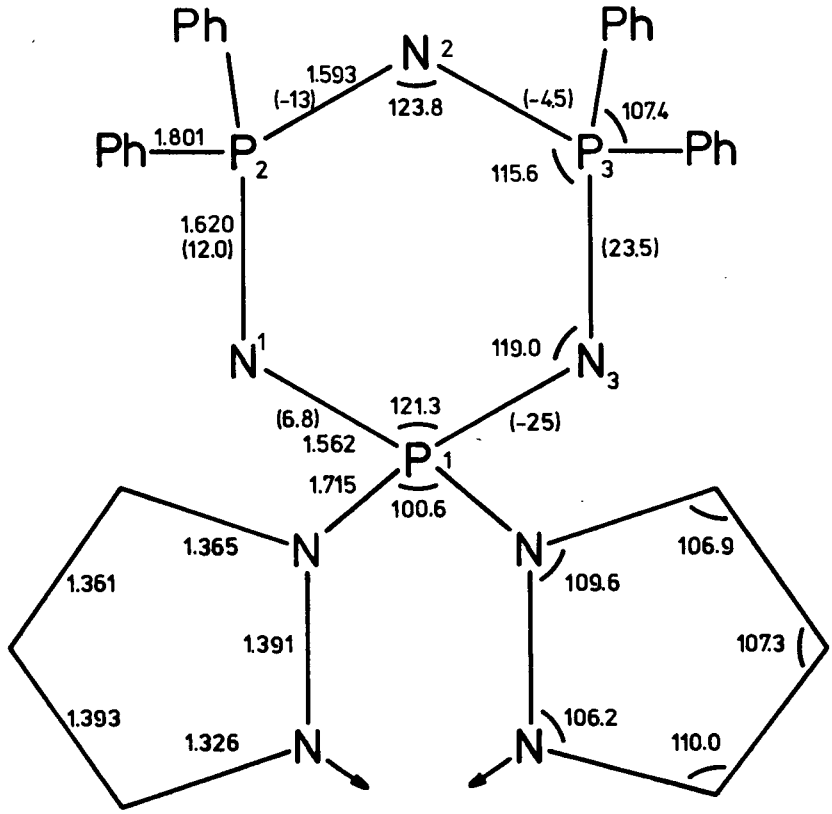

Figure 5.5. Mean structural parameters of the coordinated ligand in the complex gem-$N_3P_3Ph_4(Me_2pz)_2 \cdot CoCl_2$. Dihedral angles are given in brackets.

The Co-Cl bonds are approximately coplanar with the phosphazene ring, and are of the length (mean, 2.239 Å) expected for covalently bonded chlorine.

The exocyclic $\hat{NPN}$ angle of 100.6° is slightly decreased from the values of 102.4 and 102.5° found in $N_4P_4(Me_2pz)_8$ and gem-$N_3P_3Ph_2(Me_2pz)_4$, respectively, and is similar to the $\hat{NPN}$ angle of 101(2)° observed in $[Re(CO)_3(P(Me_2pz)_2C_6H_5)Br]$ where the $P\langle N\text{-}N\rangle_2Re$ metallocycle is also present

in a boat conformation[158]. The exocyclic PN bonds are also of similar length (1.715 Å compared to 1.705 Å in the Re complex, mean values).

The phosphazene ring is definitely non-planar, the $\underline{P}(Ph_2)$ atom and the nitrogen atom closest to the $CoCl_2$ unit deviating the most from the mean plane. The average values of successive PN bonds from the $\underline{P}(Me_2pz)_2$ atom (1.562, 1.620 and 1.593 Å, respectively) are similar to those in gem-$N_3P_3Ph_4Cl_2$ (1.555, 1.609 and 1.578 Å from the $\underline{P}Cl_2$ atom, respectively[174]). Moreover, the alternating pattern of short, long and short bonds is consistent with the inductive effects of the groups attached to phosphorus. The structural parameters are given in Figure 5.5.

5.5 Structure of $N_3P_3(Me_2pz)_6 \cdot 2CoCl_2$

The structure of this complex consists of one cobalt atom in a tetrahedral environment and the other cobalt atom in a TBP environment (see Figures 4.2, 5.6 and 5.9). The structural parameters are really a composite of those found in the former two complexes. A comparison is given in Table 5.1.

The TBP cobalt atom, like the zinc atom in gem-$N_3P_3Ph_2(Me_2pz)_4$, is situated well below the plane of the phosphazene ring, while the tetrahedral cobalt atom is again located approximately in the plane of the PN ring. The Co-Cl and the Co-N bond lengths of the latter are both shorter (mean, 2.219 and 2.047 Å, respectively) than those of the former (mean, 2.276 and 2.137 Å, respectively) as expected for a smaller coordination number.

The exocyclic $\hat{NPN}$ angles are slightly increased (mean, 104.0°) when cobalt bonds to two Me_2pz groups on different phosphorus atoms (TBP), and slightly decreased (101.4°) when cobalt coordinates to one $P(Me_2pz)_2$

Table 5.1. Comparison of some of the structural features observed in $N_3P_3(Me_2pz)_6 \cdot 2CoCl_2$ (Co_2), gem-$N_3P_3Ph_2(Me_2pz)_4 \cdot ZnCl_2$ (Zn) and gem-$N_3P_3Ph_4(Me_2pz)_2 \cdot CoCl_2$ (Co).

Mean Structural[a] Parameters	Tetrahedral Metal Atom	TBP Metal Atom	Compound
L(M-Cl)	2.219	2.276	Co_2
	2.239		Co
		2.253	Zn
L(M-N)	2.047	2.137	Co_2
	2.037		Co
		2.200	Zn
exo-L(P-N)	1.696	1.668(free),1.675(bound)	Co_2
	1.715		Co
		1.692(free),1.670(bound)	Zn
exo-$\hat{NPN}$	101.4	104.0	Co_2
	100.6		Co
		103.3	Zn
$\hat{NCoN}$ [b]	95.5	159.9	Co_2
	98.1		Co
		153.9	Zn
L(Cl···N) [c]	3.570	3.676	Co_2
	3.716		Co
		3.806	Zn
L(Cl···Me^3) [d]	3.499,3.538	3.618,3.686	Co_2
	3.601,3.639		Co
		3.723,3.763	Zn

(a) Bond lengths in angstroms and bond angles in degrees. (b) Angle between the two axial bonds in the TBP geometry. (c) Shortest non-bonded distance between a chlorine atom and the phosphazene ring. (d) Non-bonded distances between the two 3-methyl groups on the coordinated pyrazole rings and the nearest chlorine atom.

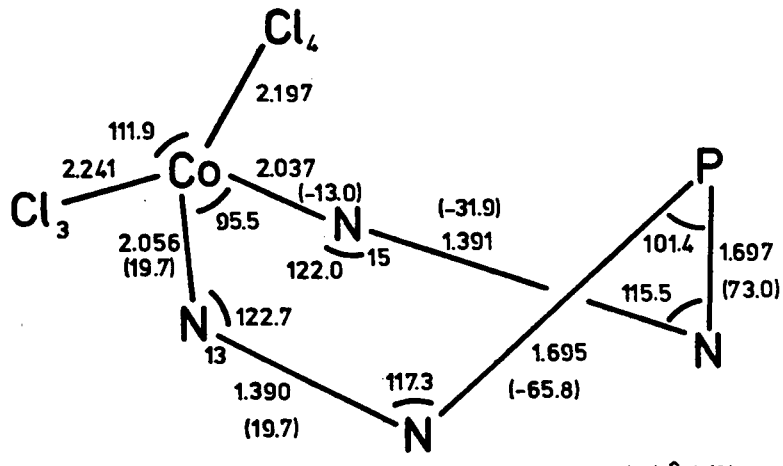

A)

mean L(Co-Cl) 2.219 Å
mean L(Co-N) 2.047 Å
mean L(P-N) 1.696 Å

N(13)ĈoCl(3) 107.1°
N(13)ĈoCl(4) 118.6°
N(15)ĈoCl(3) 106.5°
N(15)ĈoCl(4) 115.5°

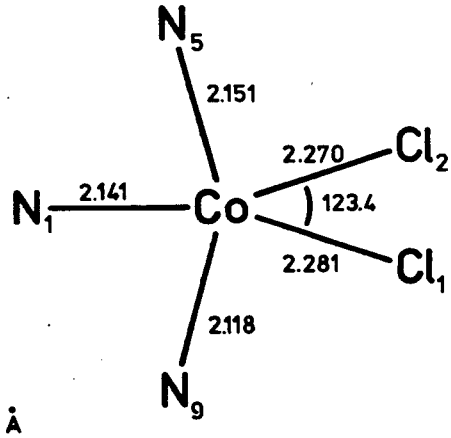

B)

mean L(Co-N) 2.137 Å
mean L(Co-Cl) 2.276 Å

N(1)ĈoCl(1) 112.4°
N(1)ĈoCl(2) 124.2°
Cl(1)ĈoCl(2) 123.4°
mean 120.0°

N(5)ĈoN(9) 159.3°

Figure 5.6. Structural parameters of the boat conformation (A) and the atoms bonded to the TBP cobalt atom (B), present in the complex $N_3P_3(Me_2pz)_6 \cdot 2CoCl_2$. Dihedral angles are given in brackets.

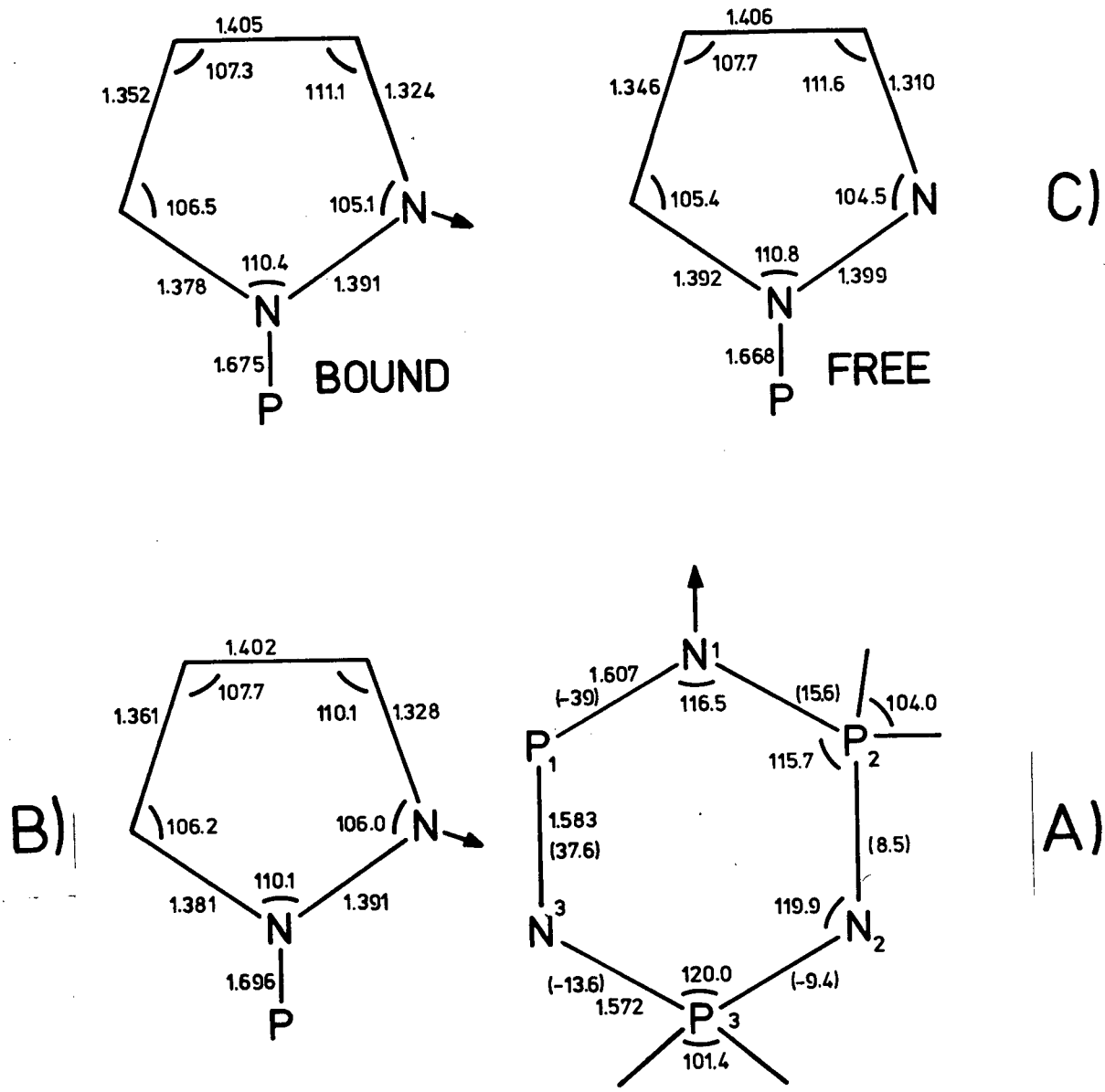

Figure 5.7. Mean structural parameters of the phosphazene ring (A), and the $P(Me_2pz)_2$ units coordinated to the tetrahedral cobalt atom (B) and to the TBP cobalt atom (C). Dihedral angles are given in brackets.

unit (tetrahedral), if 102.4°, found in $N_4P_4(Me_2pz)_8$, can be accepted as the value in the free ligand. This trend is also apparent in $N_3P_3Ph_2(Me_2pz)_4 \cdot ZnCl_2$ and $N_3P_3Ph_4(Me_2pz)_2 \cdot CoCl_2$. The exocyclic PN bonds are all similar in length, 1.679 Å being the mean value, compared to 1.693 Å in $N_3P_3Ph_2(Me_2pz)_4$ and 1.691 Å in $N_4P_4(Me_2pz)_8$. However, the PN bonds in the $P\{N\text{-}N\}_2Co$ ring are slightly longer (mean, 1.696 Å) than those in $P(Me_2pz)_2$ units bonded to the TBP cobalt (mean, 1.668 Å in the free Me_2pz groups and 1.675 Å in the bound groups). Since the electronegativity of the phosphorus atoms adjacent to the coordinated nitrogen in the PN ring is increased, some competitive electron donation from the pyrazolyl groups attached to these phosphorus atoms may be occurring, thus shortening these exocyclic PN bonds. This decrease in the length of the exocyclic PN bonds upon coordination to a phosphazene nitrogen is also noted in the zinc complex, and in $[N_6P_6(NMe_2)_{12}CoCl]^+[Co_2Cl_6]^{-2}$ and $[N_6P_6(NMe_2)_{12}CuCl]^+[CuCl_3]^-$, where the lengths of the exocyclic PN bonds at the phosphorus atoms nearest to the coordinated nitrogens are lowered from 1.699(10) Å in $N_6P_6(NMe_2)_{12}$[47] to 1.637(5) Å (mean) in the Co complex[175] and to 1.631 Å (mean) in the Cu complex[55]. The decrease is least in the pyrazolyl complex because of the aromaticity of the pyrazole ring.

The phosphazene ring is considerably distorted as a result of the bonding of one of its nitrogen atoms to cobalt. As expected, the bonds meeting at the perturbed nitrogen are the longest (mean, 1.607 Å) and the endocyclic $P\hat{N}P$ angle at this atom is the smallest angle at nitrogen (116.5°). Consistent with less electron density in this region of the PN ring, the two endocyclic $N\hat{P}N$ angles nearest to the coordinated nitrogen (116.3 and 115.0°) are the smallest angles at phosphorus. The structural details concerning the ligand are given in Figure 5.7.

5.6 Discussion

From an analysis of the structures of these compounds we can understand why bonding by $CoCl_2$ and $ZnCl_2$ to two Me_2pz groups on different phosphorus atoms, in a TBP arrangement, is more favorable, even though the proximity of two Me_2pz groups on the same phosphorus atom would suggest solely a tetrahedral coordination geometry. From the point of view of the ligand, it requires less reorganization of the Me_2pz groups to orient themselves for the TBP geometry about the metal atom than for the tetrahedral geometry. Furthermore, the TBP arrangement provides less steric congestion within the molecule. For example, in $N_3P_3(Me_2pz)_6 \cdot 2CoCl_2$, the shortest non-bonded distance between the PN ring and the nearest chlorine atom is the smallest when the $CoCl_2$ unit is bonded tetrahedrally to two Me_2pz groups on the same phosphorus atom (3.570 Å compared to 3.676 Å in the TBP geometry). In addition, the 3-methyl groups on the coordinated pyrazole rings are situated much closer to one of the chlorine atoms in this type of bonding (3.499 and 3.538 Å, tetrahedral; 3.618 and 3.686 Å, TBP). The corresponding distances are all longer in $N_3P_3Ph_2(Me_2pz)_4 \cdot ZnCl_2$ and $N_3P_3Ph_4(Me_2pz)_2 \cdot CoCl_2$ (see Table 5.1) showing that the steric requirements are greater when two metals coordinate to the same ligand.

A tetrahedral coordination geometry involving two Me_2pz groups on different phosphorus atoms is not observed because either the M-N bond lengths would be too long, the $\hat{NMN}$ angle too large or the exocyclic $\hat{NPN}$ angles too large. An increase in the exocyclic $\hat{NPN}$ angles is generally observed upon coordination to two Me_2pz groups on different phosphorus atoms, but any further increase would be compensated by a decrease in the endocyclic $\hat{NPN}$ angles, thus constricting the PN ring.

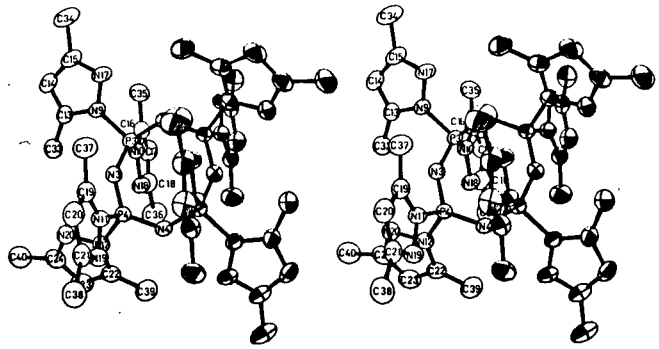

A)

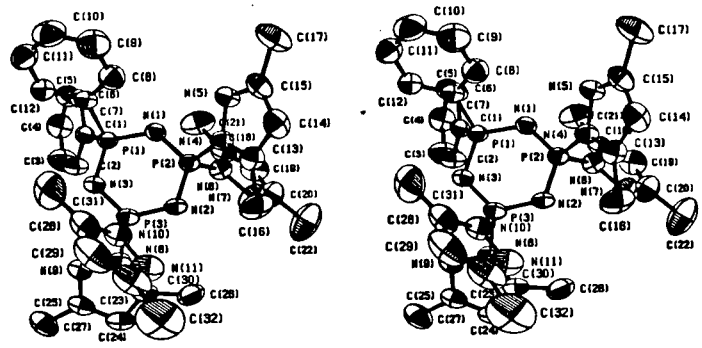

B)

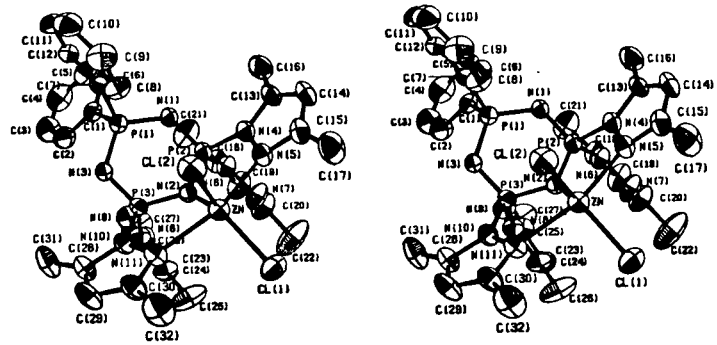

C)

Figure 5.8. Stereoscopic views of $N_4P_4(Me_2pz)_8$ (A), gem-$N_3P_3Ph_2(Me_2pz)_4$ (B) and gem-$N_3P_3Ph_2(Me_2pz)_4 \cdot ZnCl_2$ (C).

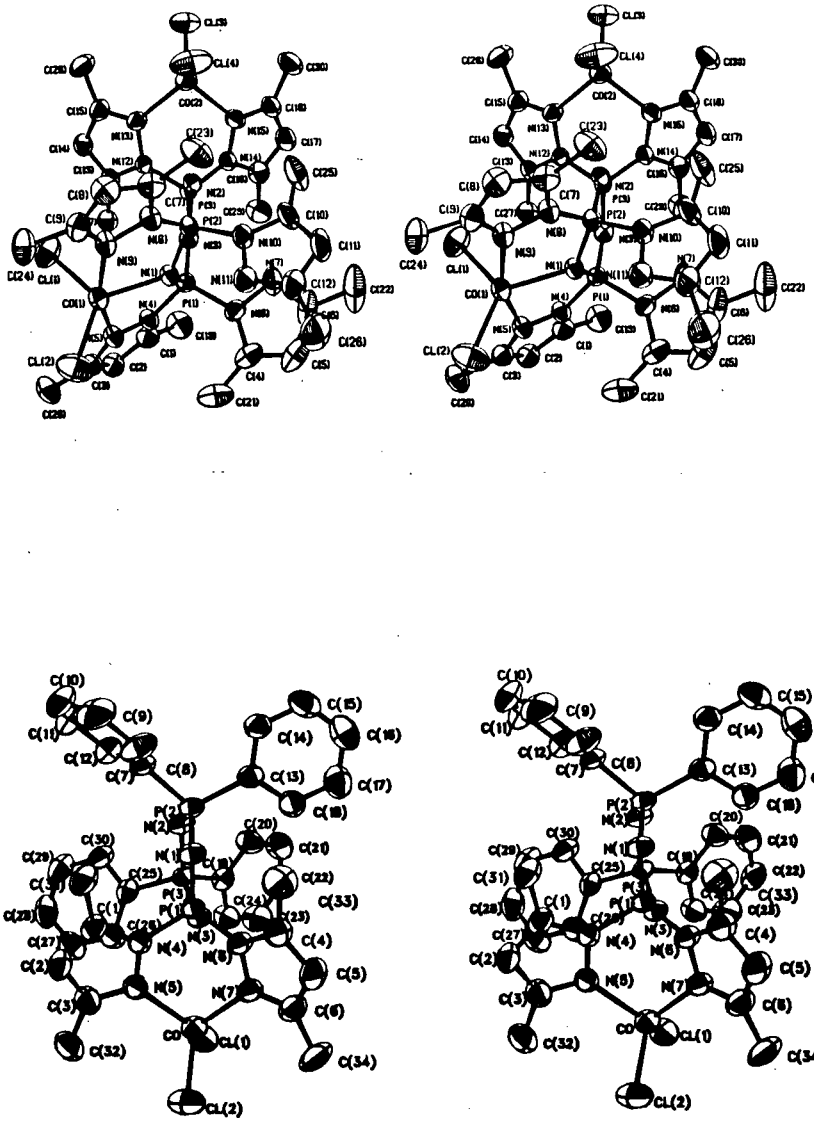

Figure 5.9. Stereoscopic views of $N_3P_3(Me_2pz)_6 \cdot 2CoCl_2$ (A) and gem-$N_3P_3Ph_4(Me_2pz)_2 \cdot CoCl_2$ (B).

REFERENCES

1) L.F. Audrieth, R. Steinman, and A.D.F. Toy, Chem. Rev., 32, 109 (1943).

2) H. Rose, Ann. Chem., 11, 131 (1834).

3) R. Schenck and G. Römer, Chem. Ber., 57B, 1343 (1924).

4) H.T. Searle, Proc. Chem. Soc., 7 (1959).

5) A.J. Bilbo, Z. Naturforschung, 15B, 330 (1960).

6) C.B. Haber, D.L. Herring, and E.A. Lawton, J. Amer. Chem. Soc., 80, 2116 (1958).

7) I.I. Bezman and J.H. Smalley, Chem. Ind., 839 (1960).

8) R.A. Shaw and C. Stratton, J. Chem. Soc., 5004 (1962).

9) H.R. Allcock, "Phosphorus-Nitrogen Compounds", Academic Press, N.Y. 1972.

10) L.G. Lund, N.L. Paddock, J.E. Proctor, and H.T. Searle, J. Chem. Soc., 2542 (1960).

11) M. Becke-Goehring and G. Koch, Chem. Ber., 92, 1188 (1959).

12) R.T. Oakley and N.L. Paddock, Can. J. Chem., 53, 3038 (1975).

13) R. Appel and G. Saleh, Chem. Ber., 106, 3455 (1973).

14) C.D. Schmulbach and C. Derderian, J. Inorg. Nucl. Chem., 25, 1395 (1963).

15) D.L. Herring and C.M. Douglas, Inorg. Chem., 3, 428 (1964).

16) K.D. Gallicano, R.T. Oakley, and N.L. Paddock, J. Inorg. Nucl. Chem., 42, 923 (1980).

17) J. Emsley, Ph.D. Thesis, University of Manchester, 1963.

18) F. Seel and J. Langer, Angew. Chem., 68, 461 (1956); Z. Anorg. Allg. Chem., 295, 317 (1958).

19) G. Allen, M. Barnard, J. Emsley, N.L. Paddock, and R.F.M. White, Chem. Ind. (London), 952 (1963).

20) O. Schmitz-Dumont and A. Braschos, Z. Anorg. Allg. Chem., 243, 113 (1939).

21) J. Emsley and N.L. Paddock, J. Chem. Soc., A, 2590 (1968).

22) B. Green and D.B. Sowerby, Chem. Commun., 628 (1969); J. Chem. Soc., A, 987 (1970); Inorg. Nucl. Chem. Lett., 5, 989 (1969).

23) G. Ottman, H. Agahigian, H. Hooks, G.D. Vickers, E. Kober, and R. Rätz, Inorg. Chem., 3, 753 (1964).

24) A.A. Kropacheva and N.M. Kashnikova, J. Gen. Chem. USSR, 32, 645 (1962); 33, 1036 (1963); 35, 1978 (1965).

25) E.T. McBee, P. Johncock, S.E. French, and H.P. Braendlin, U.S. Govt. Tech. Serv. Res. Rep., AD 254,985, 36, no.1, 14 (1961).

26) T. Chivers, R.T. Oakley, and N.L. Paddock, J. Chem. Soc., A, 2324 (1970).

27) R.A. Shaw and F.B.G. Wells, Chem. Ind. (London), 1189 (1959).

28) H. Bode and H. Bach, Chem. Ber., 75B, 215 (1942).

29) E.T. McBee, H.R. Allcock, R. Caputo, A. Kalmus, C.W. Roberts, and L. Brinkmann, U.S. Govt. Res. Rep. AD 209,668 (1959).

30) M. Biddlestone and R.A. Shaw, Chem. Commun., 407 (1968); J. Chem. Soc., A, 178 (1968).

31) J.E. Brown, M.Sc. Thesis, Penn. State University, 1969.

32) N.L. Paddock, T.N. Ranganathan, and S.M. Todd, unpublished results.

33) N.L. Paddock, T.N. Ranganathan, and S.M. Todd, Can. J. Chem., 49, 164 (1971); Inorg. Chem., 12, 316 (1973).

34) K.D. Gallicano, R.T. Oakley, N.L. Paddock, S.J. Rettig, and J. Trotter, Can. J. Chem., 55, 304 (1977).

35) R.T. Oakley, unpublished results.

36) D.P. Craig and N.L. Paddock, Nature (London), 181, 1052 (1958); J. Chem. Soc. (London), 4118 (1962).

37) D.W.J. Cruickshank, J. Chem. Soc. (London), 5486 (1961).

38) M.J.S. Dewar, E.A.C. Lucken, and M.A. Whitehead, J. Chem. Soc. (London), 2423 (1960).

39) D. Feakins, W.A. Last, N. Neemuchwala, and R.A. Shaw, J. Chem. Soc., 2804 (1965).

40) D.P. Craig and N.L. Paddock, J. Chem. Soc., 4118 (1962).

41) C.E. Brion, D.J. Oldfield, and N.L. Paddock, Chem. Commun., 226 (1966).

42) E. Hobbs, D.E. Corbridge, and B. Raistrick, Acta Cryst., 6, 621 (1953); D.W.J. Cruickshank, Acta Cryst., 17, 671 (1964).

43) B. Berking and D. Mootz, Acta Cryst., B27, 740 (1971).

44) H.P. Calhoun and J. Trotter, J. Chem. Soc. (Dalton), 377 (1974).

45) B. Bak, L. Hansen-Nygaard, and J. Rastrup-Anderson, J. Mol. Spectry., 2, 361 (1958); C. Rérat, Acta Cryst., 15, 427 (1962).

46) G.J. Bullen, J. Chem. Soc., 3193 (1962).

47) A.J. Wagner and A. Vos, Acta Cryst., B24, 1423 (1968).

48) H.P. Calhoun, N.L. Paddock, and J. Trotter, J. Chem. Soc. (Dalton), 38 (1976).

49) S.J. Rettig and J. Trotter, Can. J. Chem., 51, 1295 (1973).

50) N.V. Mani, F.R. Ahmed, and W.H. Barnes, Acta Cryst., 19, 693 (1965).

51) C.W. Allen, J.B. Faught, T. Moeller, and I.C. Paul, Inorg. Chem., 8, 1719 (1969).

52) T. Chivers and N.L. Paddock, Chem. Commun., 704 (1968); Inorg. Chem., 11, 848 (1972).

53) N.V. Mani and A.J. Wagner, Acta Cryst., B27, 51 (1971).

54) R.W. Allen, J.P. O'Brien, and H.R. Allcock, J. Amer. Chem. Soc., 99, 3987 (1977).

55) a) W.C. Marsh, N.L. Paddock, C.J. Stewart, and J. Trotter, Chem. Commun., 1190 (1970); b) W.C. Marsh and J. Trotter, J. Chem. Soc., A, 1482 (1971).

56) J.N. Rapko and G.R. Feistel, Chem. Commun., 474 (1968); Inorg. Chem., 9, 1401 (1970).

57) H.P. Calhoun, N.L. Paddock, and J. Trotter, J. Chem. Soc. (Dalton), 2708 (1973).

58) L.F. Lappert and G. Srivastava, J. Chem. Soc., A, 210 (1966).

59) T.W.J. Mah, M.Sc. Thesis, U. of British Columbia, 1974.

60) J. Dyson, Ph.D. Thesis, U. of Manchester, 1964; J. Trotter and S.H. Whitlow, J. Chem. Soc., A, 460 (1970).

61) J. Trotter and S.H. Whitlow, J. Chem. Soc., A, 455 (1970).

62) S.J. Rettig, unpublished results.

63) N.L. Paddock, T.N. Ranganathan, and J.N. Wingfield, J. Chem. Soc. (Dalton), 1578 (1972); F.A. Cotton and A. Shaver, Inorg. Chem., 10, 2362 (1971).

64) N.K. Hota and R.O. Harris, Chem. Commun., 407 (1972).

65) H.P. Calhoun, R.H. Lindstrom, R.T. Oakley, N.L. Paddock, and S.M. Todd, Chem. Commun., 343 (1975); R.T. Oakley, Ph.D. Thesis, U. of British Columbia, 1976.

66) A. Albert, in "Physical Methods in Heterocyclic Chemistry", Vol. 1, p. 97; Academic Press, N.Y., 1963.

67) R. Fusco, in "Heterocyclic Compounds", Vol. 22, p. 3; Interscience Publishers, N.Y., 1967.

68) T.L. Jacobs, in "Heterocyclic Compounds", Vol. 5, p. 45; John Wiley and Sons, Inc., N.Y., 1957.

69) S. Trofimenko, Chem. Rev., 72, 497 (1972).

70) G.S. Hartley, "Phosphoric Esters and Related Compounds", Chem. Soc. Spec. Publ. No. 8, p. 33 (1957).

71) J. Boutagy and R. Thomas, Chem. Rev., 74, 87 (1974).

72) E.J. Corey and J.I. Shulman, J. Org. Chem., 35, 777 (1970).

73) R.D. Clark, L.G. Kozar, and C.H. Heathcock, Synth., 635 (1975).

74) E.J. Corey and G.T. Kwiatkowski, J. Amer. Chem. Soc., 88, 5652, 5653 (1966); 90, 6816 (1968).

75) E.J. Corey and D.E. Cane, J. Org. Chem., 34, 3053 (1969).

76) J.R. Richards and C.V. Banks, J. Org. Chem. 28, 123 (1963).

77) S. Fischer, L.K. Peterson, and J.F. Nixon, Can. J. Chem., 52, 3981 (1974).

78) S. Fischer, J. Hoyano, and L.K. Peterson, Can. J. Chem., 54, 2710 (1976).

79) J. Högel and A. Schmidpeter, Z. Anorg. Allg. Chem., 458, 168 (1979).

80) R.T. Oakley, Ph.D. Thesis, U. of British Columbia, 1976.

81) M. Bermann and K. Utvary, J. Inorg. Nucl. Chem., 31, 271 (1969).

82) A. Schmidpeter and J. Ebeling, Z. Anorg. Allg. Chem., 394, 171 (1972).

83) H.N. Rydon and B.L. Tonge, J. Chem. Soc., 3043 (1956).

84) R.T. Oakley and N.L. Paddock, Can. J. Chem., 55, 3651 (1977).

85) A. Schmidpeter and H. Eiletz, Chem. Ber., 109, 2340 (1976).

86) R.D. Sharma, unpublished results.

87) S.C. Cohen, M.L.N. Reddy, D.M. Roe, A.J. Tomlinson, and A.G. Massey, J. Organomet. Chem., 14, 241 (1968).

88) M. Schmeisser, N. Wessel, and M. Weidenbruch, Chem. Ber., 101, 1897 (1968).

89) A.K. Barbour, M.W. Buxton, P.L. Coe, R. Stevens, and J.C. Tatlow, J. Chem. Soc., 808 (1961).

90) R.D. Sharma, private communication.

91) H.P. Calhoun, R.T. Oakley, N.L. Paddock, and J. Trotter, Can. J. Chem., 53, 2413 (1975).

92) G. Chioccola and J.J. Daly, J. Chem. Soc., A, 568 (1968).

93) J.G. Dupont and C.W. Allen, Inorg. Chem., 16, 2964 (1977).

94) J.K. Brown and N. Sheppard, Proc. Roy. Soc. (London), A231, 555 (1955).

95) L.J. Bellamy and R.L. Williams, Trans. Faraday Soc., 55, 14 (1959).

96) C.W. Davies and C.B. Monk, J. Chem. Soc., 413 (1949).

97) B. Topley, Quart. Rev., 3, 345 (1949).

98) R.T. Wragg, Tetrahedron Letters, 56, 4959 (1969).

99) D.P. Craig and N.L. Paddock, in "Nonbenzenoid Aromatics", Vol. 2, p. 273; Academic Press, N.Y., 1971.

99a) G.W. Parshall, Org. Synth., 45, 102 (1965).

100) E. Roberts, E.E. Turner, and F.W. Bury, J. Chem. Soc., 1443 (1926).

101) A. Shaver, J. Organomet. Chem. Library, 3, 157 (1976).

102) D.F. Rendle, A. Storr, and J. Trotter, J. Chem. Soc. (Dalton), 2252 (1973); 176 (1975).

103) D.J. Patmore, D.F. Rendle, A. Storr, and J. Trotter, J. Chem. Soc., (Dalton), 718 (1975).

104) K.D. Gallicano, N.L. Paddock, S.J. Rettig, and J. Trotter, Inorg. Nucl. Chem. Letters, 15, 417 (1979).

105) H. Kriegsmann, Z. Anorg. Chem., 294, 113 (1958).

106) H.R. Allcock, J. Amer. Chem. Soc., 86, 2595 (1964).

107) D.H. O'Brien and Chang-Po Hrung, J. Organomet. Chem., 27, 185 (1971).

108) V.N. Torocheshnikov, N.M. Sergeyev, N.A. Viktorov, G.S. Goldin, V.G. Poddubny, and A.N. Koltsova, J. Organomet. Chem., 70, 347 (1974).

109) T.J. Batterham, in "N.M.R. Spectra of Simple Heterocycles", p. 165; E.C. Taylor and A. Weissberger, (Eds.), John Wiley and Sons, N.Y., 1973.

110) J. Elguero and R. Wolf, Compt. Rend., Series C, 265, 1507 (1967).

111) J.R. Van Wazer and J.H. Letcher, Topics in Phosphorus Chem., 5, p. 190.

112) G. Engelhardt, E. Steger, and R. Stahlberg, Z. Naturforsch., 21B, 586 (1966).

113) T. Moeller and F.Y. Tsang, Chem. Commun., 361 (1962); C.W. Allen, T. Moeller, and F.Y. Tsang, Inorg. Chem., 7, 2183 (1968).

114) A.C. Chapman, N.L. Paddock, D.H. Paine, H.T. Searle, and D.R. Smith, J. Chem. Soc., 3608 (1960).

115) C.E. Brion and N.L. Paddock, J. Chem. Soc., A, 392 (1968).

116) M.W. Dougill, J. Chem. Soc., 5471 (1961).

117) M.J. Begley, D.B. Sowerby, and R.J. Tillott, J. Chem. Soc. (Dalton), 2527 (1974).

118) H. Zoer and A.J. Wagner, Acta Cryst., B28, 252 (1972).

119) a) R. Hazekamp, T. Migchelsen, and A. Vos, Acta Cryst., 15, 539 (1962); b) A.J. Wagner and A. Vos, Acta Cryst., B24, 707 (1968).

120) H.A. Staab, Angew, Chem. Int. Ed., 1, 351 (1962).

121) K. Denny and S. Lanoux, J. Inorg. Nucl. Chem., 31, 1531 (1969).

122) E.T. McBee, K. Okuhara, and C.J. Morton, Inorg. Chem., 4, 1672 (1965).

123) K. Hills and R.A. Shaw, J. Chem. Soc. (London), 130 (1964).

124) H.P. Calhoun, N.L. Paddock, and J.N. Wingfield, Can. J. Chem., 53, 1765 (1975).

125) H.B. Davis, J.K. Hoyano, P.Y. Leung, L.K. Peterson, and B. Wolstenholme, Can. J. Chem., 58, 151 (1980).

126) W.J. Geary, Coord. Chem. Rev., 7, 81-122 (1971).

127) A.B.P. Lever, J. Chem. Ed., 45, 711 (1968).

128) A.B.P. Lever and S.M. Nelson, J. Chem. Soc., A, 859 (1966).

129) C.J. Ballhausen and C.K. Jorgensen, Acta Chem. Scand., 9, 397 (1955).

130) L.E. Orgel, J. Chem. Phys., 23, 1004 (1955).

131) J. Ferguson, J. Chem. Phys., 32, 528 (1960).

132) W.J. Eilbeck, F. Holmes, and A.E. Underhill, J. Chem. Soc., A, 757 (1967); C.E. Taylor and A.E. Underhill, J. Chem. Soc., A, 368 (1969).

133) M.J. Bagley, D. Nicholls, and B.A. Warburton, J. Chem. Soc., A, 2694 (1970).

134) a) M. Ciampolini and N. Nardi, Inorg. Chem., 5, 41 (1966); b) Inorg. Chem., 6, 445 (1967).

135) M. Ciampolini and G.P. Speroni, Inorg. Chem., 5, 45 (1966).

136) C.M. Harris, T.N. Lockyer, R.L. Martin, H.R.H. Patil, E. Sinn, and I.M. Stewart, Aust. J. Chem., 22, 2105 (1969).

137) M. Ciampolini, N. Nardi, and G. Speroni, Coord. Chem. Rev., 1, 222 (1966).

138) J.S. Wood, Inorg. Chem., 7, 852 (1968).

139) M. Ciampolini, Structure and Bonding, 6, 71 (1969).

140) Z. Dori and H.B. Gray, J. Amer. Chem. Soc., 88, 1394 (1966).

141) L. Sacconi, I. Bertini, and R. Morassi, Inorg. Chem., 6, 1548 (1967).

142) H.T. Searle, J. Dyson, T.N. Ranganathan, and N.L. Paddock, J. Chem. Soc. (Dalton), 203 (1975).

143) R.J.H. Clark and C.S. Williams, Inorg. Chem., 4, 350 (1965).

144) M. Goldstein and W.D. Unsworth, Spectrochim. Acta, 28A, 1297 (1972).

145) N. Saha and D. Bhattacharyya, Indian J. Chem., 16A, 812 (1978).

146) E.E. Zaev, V.K. Voronov, M.S. Shvartsberg, S.F. Vasilevsky, Yu. N. Molin, and I.L. Kotljarevsky, Tetra. Letters, 5, 617 (1968).

147) G. Minghetti, G. Banditelli, and F. Bonati, J. Chem. Soc. (Dalton), 1851 (1979).

148) F. Coletta, R. Ettorre, and A. Gambaro, J. Inorg. Nucl. Chem., 37, 314 (1975).

149) J.R. Durig, R. Layton, D.W. Sink, and B.R. Mitchell, Spectrochim. Acta, 21, 1367 (1965).

150) J. Reedijk and J.K. de Ridder, Inorg. Nucl. Chem. Letters, 12, 585 (1976).

151) R.A. Hoffman, S. Forsén, and B. Gestblom, in "NMR, Basic Principles and Progress", Vol. 5, p. 70; Springer-Verlag, N.Y., 1971.

152) S. Castellano and J.S. Waugh, J. Chem. Phys., 34, 295 (1961).

153) P.S. Braterman, in "Metal Carbonyl Spectra", p. 44; Academic Press, N.Y., 1975.

154) E.W. Abel, M.A. Bennett, and G. Wilkinson, J. Chem. Soc., 2323 (1959).

155) E.W. Abel, M.A. Bennett, R. Burton, and G. Wilkinson, J. Chem. Soc., 4559 (1958).

156) R. Schmutzler, quoted by F.A. Cotton, Inorg. Chem., 3, 702 (1964).

157) R. Poilblanc and M. Bigorgne, Bull. Soc. Chim. France, 1301 (1962).

158) R.E. Cobbledick, L.R.J. Dowdell, F.W.B. Einstein, J.K. Hoyano, and L.K. Peterson, Can. J. Chem., 57, 2285 (1979).

159) M.I. Bruce and J.D. Walsh, Aust. J. Chem., 32, 2753 (1979).

160) S.N. Poddar, S. Ghosh, S.M. Bhattacharyya, and S.R. Chaudhuri, J. Inorg. Nucl. Chem., 39, 739 (1977).

161) B. Lenarcik and J. Kulig, Polish J. Chem., 52, 2089 (1978).

162) C.C. Addison and B.M. Gatehouse, J. Chem. Soc., 613 (1960).

163) B.M. Gatehouse, S.E. Livingstone, and R.S. Nyholm, J. Chem. Soc., 4222 (1957).

164) F.R. Hartley, Organomet. Chem. Rev., A, 6, 119 (1970).

165) D.P. Tate, W.R. Knipple, and J.M. Augl, Inorg. Chem., 1, 433 (1972).

166) W.C. Marsh, T.N. Ranganathan, J. Trotter, andN.L. Paddock, Chem. Commun., 815 (1970).

168) G.B. Ansell and G.J. Bullen, Chem. Commun., 430 (1966).

169) H. McD. McGeachin and F.R. Tromans, J. Chem. Soc., 4777 (1961).

170) D.E.C. Corbridge and E.G. Cox, J. Chem. Soc., 594 (1956).

171) D. Feakins, W.A. Last, S.N. Nabi, R.A. Shaw, and P. Watson, J. Chem. Soc., A, 196 (1969).

172) D. Feakins, W.A. Last, and R.A. Shaw, J. Chem. Soc., 4464 (1964).

173) D. Feakins, W.A. Last, N. Neemuchwala, and R.A. Shaw, Chem. Ind. (London), 164 (1963); J. Chem. Soc. (London), 2804 (1965).

174) N.V. Mani, F.R. Ahmed, and W.H. Barnes, Acta Cryst., 21, 375 (1965).

175) W. Harrison, N.L. Paddock, J. Trotter, and J.N. Wingfield, Chem. Commun., 23 (1972); W. Harrison and J. Trotter, J. Chem. Soc. (Dalton), 61 (1973).

176) B.N. Figgis and J. Lewis, in "Modern Coordination Chemistry", J. Lewis and R.G. Wilkins, Ed., Interscience, N.Y., pp. 400-454, 1960.

177) D.P. Craig, M.L. Heffernan, R. Mason, and N.L. Paddock, J. Chem. Soc., 1376 (1961).

APPENDIX

Details of the instruments used for recording the various types of spectra and physical measurements are given below.

i) Infrared Spectra: These were recorded on a Perkin-Elmer 457 grating spectrophotometer for wavenumbers between 250-4000 cm^{-1}, using cesium iodide plates; and a Perkin-Elmer 225 grating spectrophotometer for wavenumbers < 250 cm^{-1}, using polyethylene plates. Unless otherwise indicated, all spectra were recorded on samples in nujol (and hexachlorobutadiene) mulls, and calibrated against a standard polystyrene spectrum. Solution spectra were taken using cells with potassium bromide windows.

ii) Raman Spectra: These were recorded on a Spex Ramalog 5 spectrophotometer equipped with an argon ion laser (514.5 nm). No depolarization measurements were taken.

iii) Mass Spectra: These were all recorded at 70 ev on a Varian (Atlas) CH 4-B mass spectrometer, and on a Kratos AEI MS-902 mass spectrometer for compounds with molecular weights > 1000.

iv) N.m.r. Spectra: ^{1}H n.m.r. spectra were run at 60 MHz on a Varian T-60 n.m.r. spectrometer, at 80 MHz on a WP-80 n.m.r. spectrometer, at 100 MHz on either a Varian XL-100 or HA-100 n.m.r. spectrometer, at 270 MHz on a Nicolet-Oxford H-270 n.m.r. spectrometer, and at 400 MHz on a Bruker WH-400 n.m.r. spectrometer. ^{31}P n.m.r. spectra were recorded at 40.5 MHz on a Varian XL-100 n.m.r. spectrometer. $^{31}P-^{1}H$ decoupling experiments were carried out using a double resonance technique (see L.D. Hall and R. Burton, Can. J. Chem., 48, 59 (1970).

v) Electronic Absorption Spectra: These were all recorded on a Cary Model 17 spectrophotometer, using quartz cells with a path length of 1 cm for solution spectra. Solid mull spectra were obtained using nujol mulls between quartz windows; light scattering was compensated by placing a nujol-soaked filter paper in the reference beam.

vi) Conductivity Measurements: These were all measured at 25°C with a Wayne Kerr Universal Conductivity Bridge, Model B221A. Λ_M was calculated according to the formula $\Lambda_M = \frac{1000 \cdot k}{M \cdot R}$ where $\underline{k}$ is the cell constant (cm^{-1}), $\underline{M}$ is the molar concentration (moles cm^{-3}), and $\underline{R}$ is the resistance (ohm).

vii) Magnetic Susceptibility Measurements: These were done on powdered samples by the Faraday method, using an Alpha Model 9500 6" water-cooled electromagnet with Heyding pole design to provide constant field gradients of 253, 526 and 869 $T^2\ cm^{-1}$. The sample was placed in a quartz bucket suspended from a Cahn Rg electrobalance, and measurements were made with the sample in an atmosphere of nitrogen. The effective magnetic moment of the metal ion, μ_{eff}, was calculated using the equation

$$\mu_{eff} = 2.828(X_m^{corr} \cdot T)^{\frac{1}{2}}$$

where $\underline{T}$ is the absolute temperature and X_m^{corr} is the measured molar susceptibility corrected for diamagnetism, and where necessary, temperature independent paramagnetism (tip). The diamagnetic corrections used in the present study were estimated by summing Pascal's constants[176] and the correction for the N_3P_3 ring (-38.3×10^{-6} c.g.s. units) was obtained by subtracting 6x the correction for Cl from the diamagnetic susceptibility of $(NPCl_2)_3$[177]. A c.g.s. unit is $cm^3\ mole^{-1}$.

viii) Melting Point Measurements: Melting points or decomposition temperatures < 280°C were determined using a Thomas Hoover capillary melting point apparatus in which both the sample (in an open capillary tube) and the thermometer bulb were heated in an oil bath. For temperatures > 280°C a Gallenkamp melting point apparatus was used. The melting points are reported uncorrected.